T

TAFONE

Originally used to describe unusual weathering features found in Corsica, tafone (or tafoni, plural) has become established as the generic name for a type of cavernous weathering characterized by the existence of hollows or cavities that range in size from a few centimeters to a meter or more in diameter. Depth is variable, the cavities commonly being nearly hemispherical. The shape and orientation are strongly influenced by the rock fabric, causing the hollows to be elongated in the direction of foliation of bedding planes. Coalescence of the cavities produces mushroomlike shapes, natural arches, and other unusual sculptured forms. Eventually the outcrop surface may be destroyed by this process of expansion. When numerous small cavities occur, the resulting spongelike texture is termed honeycomb weathering. Both honeycomb weathering and tafone may occur independently, but often the two forms coexist and seem to originate from a similar process. Tafone occurs commonly in granitic rocks and in sandstone, but has also been observed in many other rocks. The rate of development may be rapid, cavities having formed in stone seawalls built less than a century ago.

Tafoni are abundant in the polar regions of Victoria Land, Antarctica, but they also occur in deserts of Australia, Africa, central Asia, and South America as well as in such humid regions as Hong Kong and the island of Aruba, West Indies. In North America, tafoni occurs in such diverse areas as the deserts of New Mexico, Utah, Arizona, and the coast of Washington state (Figure T1), and at mid-continent locations in Wisconsin and Illinois (Bryan, 1928; Blackwelder, 1929; Mustoe, 1982).

Tafoni are commonly found in outcrops having a hardened surface layer caused by precipitation of iron hydroxides or other compounds derived during weathering of the interior rock. The cementing action of these oxides produces a resistant rind. Any form of erosion that attacks the outcrop in a localized fashion will produce cavities, since penetration of the protective layer leads to rapid destruction of the weaker interior rock. Differential attack of the surface might result from variations in lithology, the presence of fissures or zones of high porosity that allow water to penetrate, or localized attack by organisms such as lichens. Because the formation of the protective ring requires moisture, this explanation is consistent with the observation that tafone seldom occurs in extremely dry environments, being more common along the margins of deserts than in the arid central regions. In many locations, tafoni occur mainly as coastal features presumably owing to the existence of a favorable microclimate, since even in extremely arid regions sea winds may cause the coastline to be relatively humid. The existence of a protective rind is most favored by an environment where some moisture is present but where periods of dryness allow evaporation to occur at the rock surface.

Tafoni typically form as a result of salt weathering, where evaporation of saline water triggers physical and chemical attack of the rock surface (Evans, 1970; Young, 1987; Rodriguez-Navarro and Doehne, 1999). In general, the distribution of tafone throughout the world correlates well with environments where salt crystallization occurs. In arid zones, salt weathering is concentrated where moisture is retained along the base of cliffs and undersides of boulders, where shadow weathering (tafone) may often be found. Along the coast, cavities are presumed to form by salt crystallization as wave-splash evaporates. Because salt weathering may attack in a relatively selective fashion, being controlled by variations in moisture or exposure to salt spray, tafoni might be formed even on outcrops where a hardened surface layer is absent, though the development of cavities would be enhanced when such a rind is present. Early explanations of tafoni invoking erosion by wind

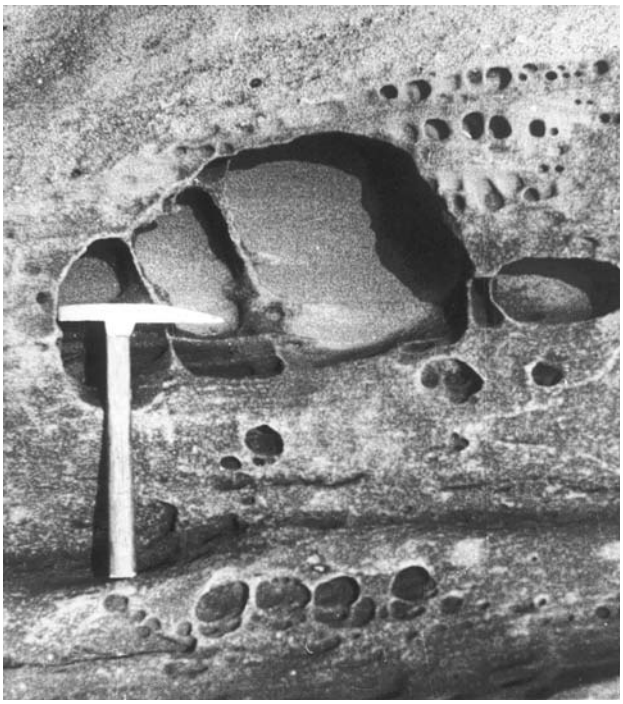

Figure T1 Tafone in arkosic sandstone, Larrabee State Park, near Bellingham, Washington USA (Photo, George Mustoe).

action, temperature fluctuation, or frost wedging have largely been abandoned owing to lack of substantiating evidence.

George Mustoe

Bibliography

Blackwelder, E., 1929. Cavernous rock surfaces of the desert. *American Journal of Science*, **17**: 393–399.
Bryan, K., 1928. Niches and other cavities in sandstone at Chaco Canyon, New Mexico. *Zeitschrift fur Geomorphologie*, **3**: 125–140.
Evans, I.S., 1970. Salt crystallization and rock weathering: a review. *Revue De Géomorphologie Dynamique*, **19**: 153–177.
Mustoe, G.E., 1982. Cavernous weathering in the Capitol Reef desert. Utah. *Earth Surface Processes and Landforms*, **8**: 517–526.
Rodriguez-Navarro, C., and Doehne, E., 1999. Salt weathering: influence of evaporation rate, supersaturation and crystallization. *Earth Surface Processes and Landforms*, **24**: 191–209.
Young, A.R.M., 1987. Salt as an agent in the development of cavernous weathering. *Geology*, **15**: 962–966.

Cross-references

Bioerosion
Cliffs, Lithology versus Erosion Rates
Coastal Climate
Coastal Hoodoos
Coastal Wind Effect
Desert Coasts
Honeycomb Weathering
Notches
Shore Platforms
Weathering in the Coastal Zone

TECTONICS AND NEOTECTONICS

Introduction

Rock deformation caused by the structure of the earth (e.g., folds, faults, joints, cleavage) is often the only kind of tectonic deformation considered by geological manuals, giving the impression that areas devoid of such type of deformation are "tectonically stable." However, according to the American Geological Institute (1960), "tectonic" is defined as "designating the rock structure and external forms resulting from the deformation of the earth crust." This definition implies that all processes which modify the external form of the crust, also when they result from forces external to the earth, have to be considered tectonic. This is the case, for example, for unidirectional vertical movements produced by earth surface processes of weathering and erosion (sedimento-isostasy), and also for rise and fall of the solid earth surface, especially in coastal areas, caused by external factors such as climate change (glacio-isostasy, hydro-isostasy) or eventually, at a smaller timescale, by the attraction of the sun and the moon (earth tides).

The term "neotectonics," ignored by most geological dictionaries or glossaries, was introduced by geodesists, geophysicists, and quaternarists during the last decades and defined in 1978 by the Board of the Neotectonic Commission of the International Association for Quaternary Research (INQUA) as "any active earth movement or deformation of the geodetic reference level, their mechanisms, their geological background (how old it ever may be), their implication for various practical purposes and their future extrapolation." This definition shows care not to isolate crustal movements from their geodynamic inheritance. Therefore, neotectonics has a wider scope than "active tectonics" (Wallace, 1986), which is defined as "tectonic movements that are expected to occur within a future time span of concern to society" and no real boundary back in time. It includes all timescales of movements, from instantaneous (seismic), 10–10^2 yr (geodetic), 10^2–10^4 yr (Holocene studies), 10^4–10^6 yr (Pleistocene studies), up to about 10^7 yr, if it is necessary to enable us to understand the origins of recorded movements (Mörner, 1980). The difference between former tectonics and neotectonics is therefore not far from that existing between an extinct fossil and a still living organism. Among the distinctive attributes of neotectonic studies listed by Stewart and Hancock (1994) are: (1) A wide range of methodologies and a variety of experts are commonly involved in a comprehensive study of the neotectonic history of a region, whereas paleotectonic structures are often investigated by structural geologists working on their own. (2) The neotectonician has the ability to compare inferences drawn from field observations with geophysical and geodetic data about rates and mechanisms of present-day processes. (3) Neotectonic displacement histories can be established with greater precision than paleotectonic ones, because Quaternary dating techniques allow relatively short time intervals to be detected. However, the approach by Stewart and Hancock (1994) mainly refers to active fault ruptures which are indeed privileged indicators of neotectonic displacements, but remains limited to boundaries of deformed crustal blocks, which may also remain obscured, without reaching the earth surface, or become obliterated by recent erosion or sedimentation processes.

In the following, various possible processes of tectonic/ neotectonic deformation in coastal areas are briefly reviewed, with special attention to vertical displacements which may be related to sea level. Significant examples of tectonic displacements are provided and rates of vertical movements are assessed. Some developments are partly inspired from ideas already discussed by Pirazzoli (1995).

Present-day and fossil coasts

The coastal outline has undergone major changes during the earth history. Some 300 Myr ago, when all continents are believed to have formed a single, huge landmass, Pangea, marine coasts could only exist along the perimeter of such a landmass. This supercontinent started to split apart about 200 Myr ago, first into two parts, Laurasia at the north and Gondwana near the South Pole, separated by a sea, Tethys. Subsequently Laurasia split out into North America, Europe, and North Asia, whereas Gondwana fragmentated into South America, Africa, Arabia, Madagascar, India, Australia, New Zealand, and Antarctica. Lastly, a slow drift has brought the various continents or continental fragments to their present state.

The reconstruction of the positions of the continents during the splitting or at the time of their coming together, during their migration, as well as the mechanisms of plate tectonics, make possible a comprehensive view of present-day and fossil coastal areas, with some marks of the latter now perched also near the top of mountain chains.

When the separation of two continents had been caused by the opening of a rift, continental margins are usually characterized by a low seismicity and a weak orogeny; in these structurally passive continental margins, which are devoid of an oceanic trench, the continental and the oceanic crust, which belong to the same plate, are joined. Such margins are frequent around the Atlantic Ocean and characterized by a well-developed continental shelf and a relative structural-tectonic stability (though they may be affected by important vertical deformation of isostatic origin).

On the other hand, where subduction processes occur, tectonics of continental margins are structurally active and show high seismicity and relief. Such margins, typical of Pacific coasts, correspond to areas where an oceanic plate is underthrusting beneath a continental plate. The continental shelf if present is very narrow, or even absent. Coastal California corresponds to a variant, with a sliding motion between the Pacific oceanic plate and the continental North-American plate along the San Andreas Fault.

In accretion zones, two continental plates are colliding. These active continental margins with strong seismicity and orogeny are generally located inside continents, far away from present-day coasts. However, at the first stages of collision, wide marine and coastal areas can be affected. This is the case in the present time of the Mediterranean region. Lastly, the coasts of epicontinental seas (bordering oceanic depths) form a special case, because the greater part of these shallow seas extending above continental shelves usually disappear during low sea-level periods and are therefore affected by significant hydro-isostatic vertical deformation.

Processes

Thermo-isostatic and volcano-isostatic tectonics

It is now generally accepted that plate tectonics modify, slowly but continuously, the shape of the oceanic basins. The rock of oceanic plates is formed by lava extrusions along oceanic ridges. After its formation, the oceanic crust moves slowly away and crosses the ocean, to be later destroyed in a subduction trench. When the crust spreads away from the ridges, it cools and thickens, thereby increasing in density. As a result the seafloor subsides isostatically, gradually submerging oceanic islands as they are carried laterally. Over several million years, thermo-isostatic

subsidence will be on the order of kilometers. This can be verified easily in any world atlas, where the ocean depth is shown to increase gradually from 2,000–3,000 m above submarine ridges to 5,000–6,000 m or more above oceanic trenches. In tropical waters, the rate of thermo-isostatic subsidence is increased by the load of coral reefs, which have to grow vertically to maintain their sea-level position. The normal vertical evolution of an oceanic island in intraplate areas, when eustatic fluctuations of sea level are disregarded, would therefore be a gradual submergence, accompanied by relatively rapid erosion of exposed rocks by subaerial weathering and wave action. The existence of such general oceanic subsidence was first observed by Darwin, who used it to explain the different types of coral reefs by evolution from fringing reefs, to barrier reefs, and to atolls. Darwin did not know what the cause of subsidence was, but his theory was correct. We know today that oceanic intraplate subsidence is due to thermo-isostasy.

If an intraplate oceanic island is not subsiding, it is anomalous and requires explanation. Two main kinds of anomalies have been recognized: thermal rejuvenation and volcano-isostasy.

When the oceanic crust approaches a hot spot, which normally corresponds to an asthenospheric bump above a more or less fixed mantle melting anomaly, the normal cooling process is reversed, so that the crust is heated, becomes less dense and thinner, and thus rises (thermal rejuvenation process). Moving away from the hot spot area, cooling and subsidence predominate again.

Near hot spots, lava eruptions often occur. Their load produces on the lithosphere an isostatic depression under the volcanic mass and a peripheral raised rim at some distance (volcano-isostasy). According to empirical observations made around oceanic islands, the radius of the depressed area is generally less than 150 km from the load barycenter, whereas the peripheral rim develops at a distance of between some 150 and 300 or 330 km. When the translation movement of an oceanic plate over a hot spot has produced a line of islands, and two or more thermal rejuvenation spots form an alignment in the direction of plate movement, interaction between isostatically depressed areas and uplifted rims of nearby islands is possible and may produce complicated sequences of vertical deformation, with repeated phases of uplift and sinking.

Example of Quaternary thermo-isostatic uplift: Rurutu Island (South Pacific). Rurutu (22°30′S–151°20′W) is a basaltic island of the Austral–Cook island chain, approximately halfway between the hot spot near the active undersea Mac Donald volcano and the northernmost atoll of the Cook Islands (Palmerston). The volcanic basement of Rurutu has been dated 10.5 ± 2 Ma, whereas the age of the surrounding seafloor lies in the range of 40–90 Ma. The age of the volcanic basement of Rurutu is therefore consistent with the migration rate (10–11 cm/yr) of the Austral–Cook lithosphere with respect to the hot spot reference frame and the distance of about 1,350 km from Mac Donald. There is, however, a second hot spot along the Austral–Cook island chain, which generated some Cook Islands (Mauke, Atiu, Aitutaki) during the last 10 Myr. This second hot spot or plume is located near the present position of Rurutu (Dickinson, 1998). During the Quaternary, Rurutu entered the uplifting side of the hot spot swell. No new lava extrusion seems to have occurred, but gradual uplift took place, so that today the volcanic basement of Rurutu is surrounded by raised limestone tabular blocks, dated less than 1.85 Ma, reaching about 100 m in altitude. The limestone blocks finish in high vertical cliffs facing the ocean. Variations in the water table associated with Quaternary sea-level changes superimposed on gradual uplift have provoked karstic dissolution in the limestone at several levels (Figure T2). Dated remnants of the Last Interglacial coastline are now at +8–10 m in elevation; marks of Holocene sea stands have been identified at +1.7, +1.2, and +0.6 m (Pirazzoli and Salvat, 1992). The available evidence indicates that thermo-isostatic deformation has uplifted Rurutu Island at the average rate of 0.05–0.10 mm/yr since the early Pleistocene and at about 0.17 mm/yr in the Holocene.

Example of historical rapid thermo-isostatic deformation: "Temple of Serapis," Pozzuoli (Italy). This site demonstrates repeated rapid up and down displacements in the Phlegraean Fields caldera, near Naples. Burrows of *Lithophaga* mollusca in the three columns still left standing of the "Temple" (a Roman market probably built in the 2nd century BC near the Pozzuoli Harbor), clearly show that the ruins had subsided under sea level and then been gradually uplifted (Figure T3). Geomorphological, archaeological, historical, and radiometric data suggest a complex relative sea-level history. After the "Temple" was constructed, a subsidence of about 12 m took place. Elevated marine fossils indicate two submersion peaks, between the 5th and the 7th century AD, then again in the 13th to 14th century AD (Morhange *et al.*, 1999). An uplift of about 7 m followed, culminating in the Monte Nuovo volcanic eruption in AD 1538, and further subsidence. More recently, tide-gauge data from the Pozzuoli Harbor show two brief periods (1970–73 and 1982–84) of rapid uplift reaching a total of 3.2 m

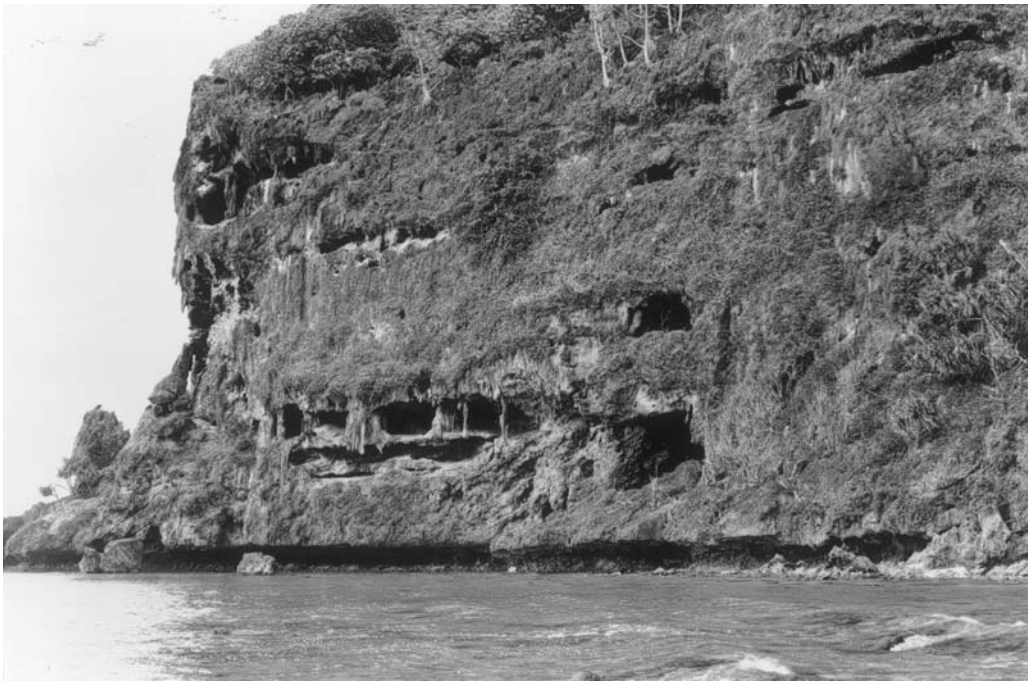

Figure T2 The outer limestone cliff of Rurutu (Austral Islands, South Pacific) appears cut by networks of caves at several levels, remnants of karstic drainage corresponding to higher relative sea-level positions. The lowest line of caves, with the floor at +8–10 m, contains marine material which has been dated from the Last Interglacial. The cliff is also undercut by a slightly elevated deep notch dating from the Late Holocene (Photo 5743, April 1980).

Figure T3 The "Temple of Serapis" in Pozzuoli (Italy). Note the dark band on the columns produced by molluscan borings (the upper limit of which is slightly less than 6 m above the paving of the "Temple," which is partly flooded by a few centimeters of water) (Photo D388, October 1991). The same floor appears more submerged in photos taken in 1982–83 (Vita-Finzi, 1986, p. 10).

between 1968 and 1984, followed by slight renewed subsidence, still going on. Such vertical movements are understood as being of thermo-isostatic origin, with uplift corresponding to rock expansion under the action of heat beneath the caldera, and subsidence to contraction on cooling.

Vertical tectonic deformation near plate boundaries

When oceanic crust approaches the end of its travel, near a trench or a continental margin, the arrival of its mass in a subduction or a collision zone produces high seismicity and vertical tectonic movements become more complex.

In a subduction zone, the underthrusting side, which will be destroyed by plunging into the earth mantle, has a relatively simple tectonic behavior, differing notably from that of the overthrusting side. Before being submerged, the oceanic plate is generally subjected to arching phenomena, in order to make possible the change from a horizontal translation to a plunging beneath the overriding plate. This arching implies a wave-like flexuring of the lithosphere, with first a gradual uplift, as in the case of an oceanic island approaching a hot spot, than a gradual subsidence at accelerating rates. Case studies of such arching phenomena have been reported from Christmas Island, 200 km southwest of the Sunda Trench, from the Daito (Borodino) Islands, 150 km east of the Ryukyu Trench, and from the Loyalty Islands, at varying distances west of the New Hebrides Trench.

On the overthrusting side, various local or regional structural geodynamic factors may be superimposed. Here uplift is frequent and may be caused by: (1) piling up above the oceanic plate, on the inner side of the trench, of sediments too light to be subducted, which will raise the overthrusting edge isostatically; (2) elastic rebound phenomena linked to subduction faulting; (3) tilting of lithosphere blocks or other structural tectonic processes; and (4) volcanic activities. Subsidence in structural basins may also be significant.

Where subduction processes are prevented by the occurrence of a transform fault or by continental lithosphere on both sides of a plate boundary, collision or transform processes will occur with vertical movements which can become highly irregular. The best-known example of a transform fault crossing a coastal area is probably that of the San Andreas Fault, which extends south to north over a distance of about 1,300 km between the Gulf of California and the Mendocino Fracture Zone. South of the Mendocino triple junction, strike slip predominates along a broad and braided system of faults with a roughly northwesterly strike; blocks between faults are warped, folded, uplifted, depressed, and rotated. Farther northwestwards, vertical movements predominate (Crowell, 1986). In several areas along the San Andreas Fault evidence of uplift is missing, however, and aseismic uplift has also been reported from southern California.

The superimposed effects of long-term gradual uplift and of eustatic sea-level fluctuations often produce sequences of stepped marine terraces.

Example of stepped marine terraces in the Santa Cruz area, California. Six marine terraces, in which raised shell beds were first described by Darwin, indent a 60 km stretch of coastal topography. These terraces seem to have been raised by repeated slip earthquakes on the San Andreas Fault, with a return time of three to six centuries, uplifting the terraces at average rates between 0.13 and 0.35 mm/yr (Lajoie, 1986; Valensise and Ward, 1991).

Seismic displacements

In many seismic areas, vertical displacements of land may appear gradual in the long term, but in the short term they can consist of sudden vertical movements, separated by more or less long periods of quiescence or of gradual movement (Figure T4). The sudden movements usually take place at the time of great-magnitude earthquakes, which are often accompanied by surface faulting or folding and ground deformation. Land displacements occurring spasmodically at the time of an earthquake are called *coseismic*. Gradual displacements, often in opposition to the coseismic ones, may occur during the few years or decades preceding (*preseismic*) or following (*postseismic*) the coseismic event. The duration of the time interval between two coseismic events (*interseismic* period) is not perfectly regular and depends on the variability of the local tectonic stress accumulation. It may tend, however, to be repetitive statistically, with a return time which can vary, according to the seismotectonic area considered, from a few centuries to over ten thousand years. In coastal seismic areas, investigation and dating of former shorelines different from the present ones may be used to determine the age, distribution, and succession of vertical displacements. Of special interest for seismic prediction is the identification of the preseismic movements which may indicate the imminence of a great-magnitude earthquake.

Certain coseismic movements can be impressive. In Crete (Greece), a jerk of coseismic uplift raised the southwestern most part of the island as much as 9 m, probably on July 21, AD 365 (Pirazzoli *et al.*, 1996); in

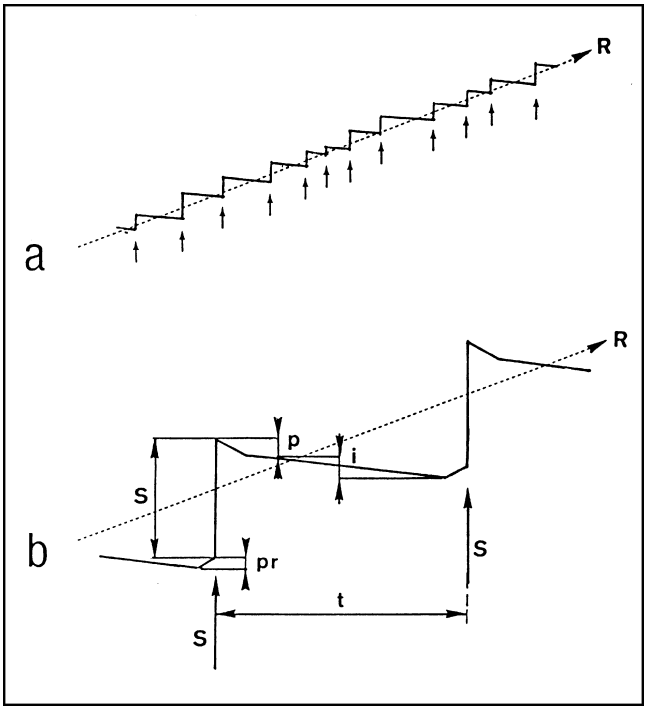

Figure T4 In uplifting seismic regions, the raising trend, though apparently gradual over the long term, may consist in the short term of sudden uplifting movements accompanying great earthquakes, separated by more or less long periods of seismic quiescence and gradual subsidence. pr, preseismic; S, coseismic; p, postseismic; i, interseismic; t, return period.

Alaska, the great earthquake of March 27, 1964 (magnitude ≥8.4) was accompanied by uplift reaching 10 m on land in Montague Island and more than 15 m offshore (Plafker, 1965).

Example of repeated Holocene coseismic deformation: Hatay (Turkey). On the Hatay coasts, clear evidence of uplifted Quaternary coastlines near the Orontes Delta have been recognized up to at least 140 m in elevation. The lower evidence, between 35 and 8 m above present sea level, consists of stepped, elevated, deltaic sedimentary surfaces, suggesting that the Orontes River has built here intermittent delta formations since at least the late mid-Pleistocene. Detailed study of late Holocene marine notches (Figure T5) and bioconstructed rims made of vermetids, oysters, and calcareous algae, have demonstrated that uplift has been episodic rather than gradual (Pirazzoli *et al*., 1992). Two rapid land movements, probably of seismic origin, have been identified. The first movement, which occurred about 2,500 ± 100 years BP, was the strongest one and caused a local vertical displacement of about 1.7 m. The second movement (an uplift of 0.7–0.8 m) occurred around 1,400 years BP, probably at the time of the great earthquake followed by tsunami waves of May AD 526, which caused devastating damage in Antioch and prevented further use of its harbor Seleucia Pieria. The long-term trend of uplift in this coastal area can be ascribed to episodic reactivation of local fault lines, probably in connection with movements on the East Anatolian Fault system.

Glacio-isostatic and hydro-isostatic neotectonics

Transfers of ice or water masses between ice sheets and the ocean produce load displacements and therefore isostatic phenomena. The load of an ice sheet deforms the earth's crust. The resulting subsidence beneath the ice makes deeper material flow away, and raises an uplifted rim at a certain distance. When the ice sheet melts, an unloading occurs, resulting in uplift beneath the melted ice; the marginal rim will consequently tend to subside and move towards the center of the vanishing load. Part of these glacio- isostatic movements are elastic, and thus contemporaneous with loading and unloading. Due to the viscosity of the earth material, however, part of the movement will continue for several thousand years after the loading or unloading has stopped. Although most of the ice in Canada and Fennoscandia had disappeared between about 8,000 and

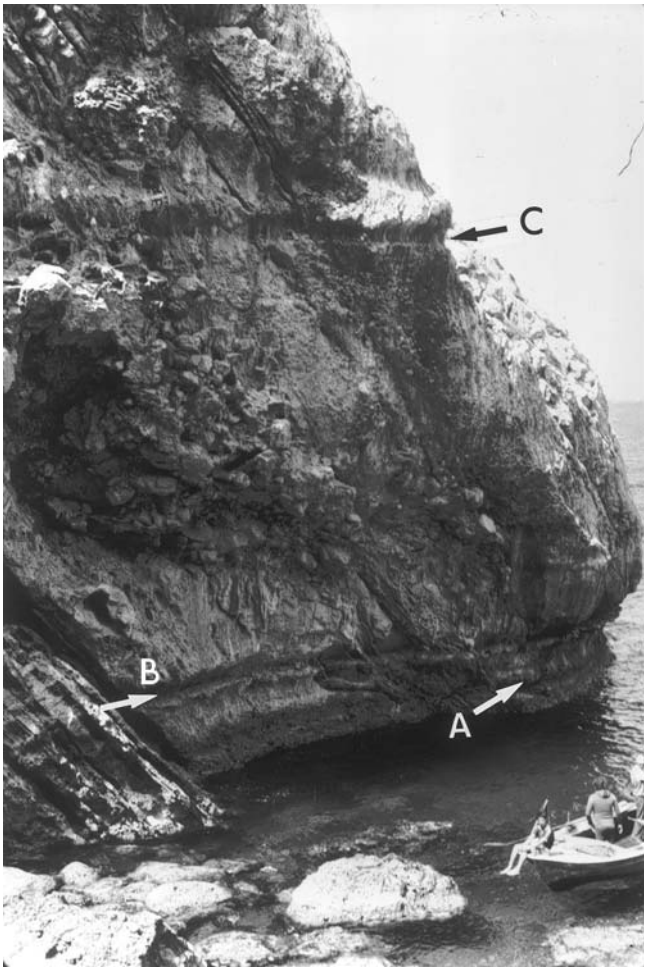

Figure T5 Two continuous notches cut into the limestone cliff at about (A) +0.7 m and (B) +2.0 m, mark the sea-level positions before two coseismic uplift movements which occurred some 1,500 and 2,500 years ago. (C) A similar undated notch at +12.3 m, may correspond to a Late-Pleistocene shoreline. South of the Orontes Delta, near the Turkish–Syrian boundary (Photo A739, May 1988).

6,000 years BP, large vertical movements of uplift and subsidence continue in these areas today.

It was during the second half of the 19th century, when the postglacial coastal record in Fennoscandia became accurate enough to yield a persuasive description of dome-like uplift, that the concept of glacio-isostasy could be asserted by De Geer, as had been done at about the same time for Lake Bonneville, in the United States, by Gilbert. During deglaciation, meltwater from ice sheets produces a considerable load on the ocean floor (on the order of 100 t/m^2 for a sea-level rise of 100 m), so that the sea bottom subsides (hydro-isostasy). In the upper part of gently sloping continental shelves, or in shallow seas where the postglacial water depth is less than the global change in sea level, the meltwater load will vary according to the local topography and bathymetry, generally increasing gradually towards the open sea. In this case, the hydro-isostatic constraints will produce a lithospheric flexure with a typical seaward tilting.

Small islands which rise steeply from the deep ocean floor are often considered as potentially good place to measure eustatic changes because, as discussed by Bloom (1971, p. 371) they "will be warped downward by the water load around them, but because the entire deep ocean floor is depressed, the volume of the ocean basin increases and sea level with reference to an island, or to a hypothetical buoy moored in deep water, should not change because of the isostatic deformation." In equatorial and tropical regions remote from the ice sheets, hydro-isostatic subsidence may be partly compensated by "equatorial ocean siphoning" (Mitrovica and Peltier, 1991). This mechanism, driven by the subsidence of those portions of the glacial forebulges which exist over oceanic regions, acts to draw water away from most equatorial and

tropical regions, in order that the oceans maintain hydrostatic equilibrium, making some emergence possible. For this reason, slight Holocene emergence is frequent in tropical oceanic islands. This is the case, for example, for most Pacific atolls (Figure T6) in spite of their long-term trend towards thermo-isostatic subsidence.

Some geophysical models, based on the mathematical analysis of the deformation of a viscoelastic earth produced by surface loads, have been developed during the last two decades. They have been able to mimic, with an accuracy on the order of a few meters, sea-level changes reported from the field in various areas. These models, which assume a simplified earth structure and a melting history for all the continental ice loads which existed at the time of the last glacial maximum, have demonstrated that the rate, direction, and magnitude of crustal movements must have varied from place to place and, therefore, that no region can be considered as tectonically stable. Though they cannot replace field observation, these models have also been useful in providing a first-order approximation of the deglacial and postglacial sea-level history in areas where no field data are available.

Sediment-isostatic neotectonics

Weathering and gravitational forces cause continuous transfers of sediments in a one-way direction, from the continents to the oceans. This implies isostatic adjustments, with predominant uplift on the continents and subsidence in nearshore basins affected by rapid sedimentation. At the mouth of great rivers, when the rate of fluvial input overtakes the rate of sea-level change, deltaic sequences may tend to accumulate, especially on microtidal coasts. Recent sediment accumulation is affected by compaction, which produces subsidence, but is also expected to form on the lithosphere surface an isostatic depression under the load and a marginal rim slightly rising at some distance. However, remaining in an area where general subsidence predominates, such rims may only appear as an area of lesser sinking. Lateral displacement of major delta branches have often occurred during the late Holocene; they imply, after some time, also a migration if their isostatic peripheral bulge.

The purely isostatic component is generally difficult to estimate, because observed rates of lowering include also sediment compaction, possible faulting, and for the past millennium also anthropogenic influences, such as conversion of wetlands to agricultural fields, river channelization, pumping, and withdrawal of water and diversion of water flow for irrigation. What can be measured is only the total amount of vertical displacement that has occurred during the Holocene delta formation, that is, since the postglacial sea-level rise began to decelerate, generally from about 8,000 to 6,500 years BP (Stanley and Warne, 1994). This vertical displacement varies locally, usually reaching a maximum on the outer delta plain close to the present coast.

Figure T6 Late-Holocene *scleractinian* corals have been left emerged in growth position, at the top of a pinnacle in the lagoon of Takapoto Atoll (Tuamotus), by a slight fall in the relative sealevel of probable hydro-isostatic origin (Pirazzoli and Montaggioni, 1988) (Photo 5478, March 1980).

Structural faulting and folding

Faults (and folds, which can develop ahead of blind faults propagating from depth towards the surface) are generally the main object of study for most structural tectonicians. In coastal areas, however, at least for vertical displacements, the most important neotectonic indicator is sea level. With high-tide shoreline marks, sea level leaves evidence of an altimetric datum all along the coast. An active fault may cross a rocky coast, leaving recognizable displaced high-tide shorelines on both sides (Figure T7). Such an occurrence is precious, because it may enable one to measure very precisely the vertical displacement between the footwall and the hanging wall of the fault, that is, the maximum amount of displacement when we are dealing with a tilted crustal block. In even more favorable cases former high-tide shorelines may be preserved, at least over a certain distance, at various levels on the fault plane; it will then be sufficient to map them along the coast to reconstruct tilting patterns and, if the high-tide shorelines can be dated, vertical displacement rates. Some caution is necessary, however; high coastal cliffs which are abnormally straight or gently curved are commonly suspected of being fault scarps. When uplifted evidence of former high-tide shorelines is missing from the cliff, the footwall of the fault may be underwater, concealed by sediments, or eroded, and this makes estimations of vertical movements hypothetical. But straight high cliffs may also result from differential erosion having removed a weaker seaward rock formation, without any tectonic implication. Many mappable faults may also have been formed by geologically ancient deformations, under tectonic regimes and stress situations long abandoned.

In most cases, active faults do not cut the coastline, but remain at a certain distance from it, on land or offshore; marks of uplift or subsidence indicated by former high-tide shorelines are therefore likely to indicate a lesser vertical displacement than at the fault scarp and a more complete survey is necessary before interpreting the vertical displacement observed.

Example of a paleotectonic coastal scarp: northernmost Chile. Between Arica and Iquique, except locally, an exceptionally high cliff directly drops into the sea, and is still retreating under wave action. In the surroundings of the Cerro Punta Madrid (18°57′S, 70°18′W) it reaches a height of about 1,000 m. This cliff derives from a large system of north–south oriented, *en échelons*, normal faults which formed at the end of the Oligocene epoch and whose scarps retreated under marine erosion during a Middle to Upper Miocene transgression. South of Iquique, the scarp is an abandoned cliff no longer receding under wave action; at its foot lies a shore platform, sometimes wider than 1 km, which has been uplifted to 50 m above present sea level (Paskoff, 1996).

Example of a neotectonic coastal scarp: southwestern Calabria (Italy). Calabria has been affected by strong uplift movements during the Quaternary. At least 12 Pleistocene levels of marine terraces have been identified, reaching as much as 1,350 m in altitude. Near Reggio Calabria, Last Interglacial marine deposits with the guide fossil *Strombus bubonius* at 157 m suggest that the average uplift rate exceeded 1 mm/yr during the last 125 ka. Near Palmi, the steepness of the coastal relief (Figure T8) and the narrowness (only a few hundred meters) of the continental shelf can be ascribed to active faulting, which is leaving abrupt scarps on the gneissic rock formations.

Example of neotectonic coastal folding. Along the southernmost coast of Taiwan (Hengchung Peninsula), the inner edge of the mid-Holocene

Figure T7 The surface of Late Pleistocene raised marine terraces has been displaced by a recent fault near Kupang, West Timor, Indonesia (photo B266, August 1988).

Figure T8 The active fault scarp near Palmi (Calabria, Italy) (photo E722, April 1996).

marine terrace is 10–15 m high, but its elevation gradually increases westwards, deformed by undulation movements. Its altitude ranges from 5 to 36 m along a distance of less than 10 km (Liew and Lin, 1987).

Rates of vertical neotectonic movements

Because of the various potential tectonic processes, rates of vertical movements in coastal areas have varied much in space and time.

Over the long term (10^6–10^5 yr), structural tectonics is indeed the predominant factor, with rates reaching several millimeters per year reported from tectonically very active areas such as near Ventura, California, where Pleistocene marine terraces have been uplifted at average rates exceeding 8 mm/yr (Lajoie, 1986), with even much higher rates reported from the land interior (about 10–15 mm/yr estimated for the crest of the Ventura anticline during the last few hundred thousand years (Wallace, 1986, p. 7)). At Huon Peninsula, Papua New Guinea, uplift of up to 3 mm/yr during the last 124 ka has been demonstrated by Chappell (1974). Evidence of well-preserved Quaternary shorelines is, however, rare in areas of rapid uplift, because strong erosion rates most often effaced most ancient marine marks. At the same timescale, volcano-isostatic factors can be estimated to have been on the order of a few millimeters per year for subsidence and one order of magnitude less for arching uplift; thermo-isostatic vertical displacement rates usually remain limited to the order of a fraction of millimeters per year: average subsidence rates have been estimated at 0.2 mm/yr during the last 60 Myr in the Marshall Islands and 0.12 mm/yr since the Pliocene in Mururoa Atoll (Tuamotus). Glacio- and hydro-isostatic factors cannot be assessed at the timescale of 10^6–10^5 yr.

During the last 20 kyr, the most important vertical displacements have been of glacio-isostatic origin; near the center of the former Fennnoscandian ice sheet, uplift since the last glacial maximum has been estimated at about 800–850 m, that is, at 40–42 mm/yr on average (Mörner, 1979); since the beginning of the Holocene, uplift has been about 284 m, that is, 28 mm/yr on average, decreasing exponentially from over 50 mm/yr at that time to about 9 mm/yr at the present time (Pirazzoli, 1991). Residual present-day uplift is therefore almost 1 m/century. In Canada, with a marine limit close to 300 m in elevation near the eastern part of Hudson Bay (Andrews, 1989) maximum uplift values are probably of the same order as in Fennoscandia.

Hydro-isostatic displacements are also significant over the timescale of 10^4 yr. They can be estimated on the order of about one-third of the sea-level change, that is, some 40 m in deep-sea areas for an eustatic change of 120 m (i.e., 2 mm/yr on average since the last glacial maximum) and less in shallow coastal areas.

At the timescale of 10^4 yr, structurally tectonic displacements can be in some cases on the same order as glacio-isostatic ones: on the east coast of Taiwan, marine evidence suggests an average uplift rate of about 8 mm/yr since 14 kyr ago near Tulan (Pirazzoli *et al*., 1993) as well as since 4,000–3,000 kyr ago near Hualien (Konishi *et al*., 1968) (Figure T9). Because the amount of glacio- and hydro-isostatic displacements has been decreasing exponentially with time after complete melting of the

Figure T9 *In situ* coral reefs about 3 kyr old, uplifted up to 25 m above sea level, are visible (arrows) above a cliff at Hualien, east coast of Taiwan (photo B805, January 1990).

ice caps, movements of structurally tectonic origin have become predominant and easily recognizable in several areas during the last few thousand years. Very rapid rates of vertical displacement of thermo-isostatic origin can be reached in volcanic areas during relatively short periods. The most spectacular example is probably Iwo (Sulphur) Island, a volcano situated 1,200 km south of Tokyo, where over 20 steps of marine terraces occupying nearly the whole area of the island (used as military airstrips by the Japanese during the last world war) have been recognized up to 120 m above sea level. The average uplift rate was here of more than 100 mm/yr over the last several centuries, reaching 200 mm/yr in some parts of the island (Kaizuka, 1992). In the case of the Pozzuoli area mentioned above, average vertical displacement rates have reached even faster peaks, such as the uplift rate of up to 800 mm/yr recorded between 1968 and 1984.

Rates of subsidence in delta areas induced by sediment compaction and sedimento-isostasy is often significant over the long term. At the shelf edge of the eastern Mississippi delta, for example, the long-term averaged subsidence rate since the last glacial period has been estimated to at least 1 mm/yr (Stanley *et al*., 1996). For the four largest modern depocenters in the Mediterranean, long-term mean lowering rates have been reported of 4–5 mm/yr from the Ebro Delta, >7 mm/yr at the mouth of the Grand Rhône Delta, possibly from 1 to 3 mm/yr from the Po Delta, and 4–5 mm/yr from the Nile Delta (Stanley, 1997). The best-known example of land subsidence produced by sediment compaction, accelerated by man-induced drainage during the last centuries, is indeed that of the Netherlands, where the soil level may be as low as 6 m below sea level. More recently, man-induced land subsidence following oil and natural gas extraction or groundwater exploitation has taken place during the last century in many coastal plains of estuarine, delta, or lagoonal areas: the greatest measured land subsidence (a maximum of 4.6 m) is probably that reported from the Tokyo Lowland region, where an area of about 70 km^2, supporting more than half a million inhabitants, is below mean sea level. Significant amounts of land subsidence have been reported also from the Po Delta (3.2 m), Houston-Galveston (3.0 m from 1906 to 1987), Shanghai (2.7 m), Tianjin (2.5 m), the southwestern part of Taiwan (2.4 m), Taipei (1.9 m), and Bangkok (1.6 m). In several big cities built in coastal plains of developing countries (Jakarta, Hanoi, Haiphong, Rangoon), where detailed measurements are lacking, the probable occurrence of land subsidence is revealed by increasing difficulties in drainage which produce more frequent flooding.

Among the many possible causes of coastal change and evolution, tectonics and neotectonics have been indeed major controlling factors, virtually at all timescales. For the present time, however, a new tectonic cause—man-induced land subsidence—is becoming significant in many densely populated or industrial coastal areas, with short-term impacts which may exceed those of all other natural causes occurring in the same area.

Paolo A. Pirazzoli

Bibliography

American Geological Institute, 1960. *Glossary of Geology and Related Sciences*, 2nd edn. Washington DC: National Academy of Sciences.

Andrews, J.T., 1989. Postglacial emergence and submergence. In Fulton, R.J. (ed.), *Quaternary Geology of Canada and Greenland.* Geology of Canada no. 1. Geological Survey of Canada.

Bloom, A.L., 1971. Glacial-eustatic and isostatic controls of sea level since the last glaciation. In Turekian, K.K. (ed.), *The Late Cenozoic Glacial Ages*. New Haven and London: Yale University Press, pp. 355–379.

Chappell, J., 1974. Geology of coral terraces, Huon Peninsula, New Guinea: a study of Quaternary tectonic movements and sea-level changes. *Geological Society of America Bulletin*, **85**: 553–570.

Crowell, J.C., 1986. Active tectonics along the western continental margin of the conterminous United States. In Wallace, R.E. (panel chairman), *Active Tectonics*. Studies in Geophysics. Washington DC: National Academy Press, pp. 20–29.

Dickinson, W.R., 1998. Geomorphology and geodynamics of the Cook–Austral island-seamount chain in the South Pacific Ocean: implications for hotspots and plumes. *International Geology Review*, **40**: 1039–1075.

Kaizuka, S., 1992. Coastal evolution of a rapidly uplifting volcanic island: Iwo-Jima, western Pacific Ocean. *Quaternary International*, **15/16**: 7–16.

Konishi, K., Omura, A., and Kimura, T., 1968. 234^{U}-230^{Th} dating of some Late Quaternary coralline limestones from southern Taiwan (Formosa). *Geology and Palaeontology of Southeast Asia*, **5**: 211–224.

Lajoie, K.R., 1986. Coastal tectonics. In Wallace, R.E. (panel chairman), *Active Tectonics*. Studies in Geophysics, Washington DC: National Academics Press, pp. 95–124.

Liew, P.M., and Lin, C.F., 1987. Holocene tectonic activity of the Hengchun Peninsula as evidenced by the deformation of marine terraces. *Memoir of the Geological Society of China*, **9**: 241–259.

Mitrovica, J.X., and Peltier, W.R., 1991. On postglacial geoid subsidence over the equatorial oceans. *Journal of Geophysical Research*, **96**(B12): 20053–20071.

Morhange, C., Bourcier, M., Laborel, J., Giallanella, C., Goiran, J.P., Crimaco, L., and Vecchi, L., 1999. New data on historical relative sea level movements in Pozzuoli, Plaegrean Fields, southern Italy. *Physics and Chemistry of the Earth*, A, **24**(4): 349–354.
Mörner, N.A., 1979. The Fennoscandian uplift and Late Cenozoic geodynamics: geological evidence. *Geojournal*, **3**: 287–318.
Mörner, N.-A., 1980. The INQUA Neotectonic Commission. *Bulletin INQUA Neotectonic Commission*, **3**: 1.
Paskoff, R., 1996. *Atlas de Las Formas de Relieve de Chile*. Instituto Geografico Militar de Chile.
Pirazzoli, P.A., 1991. *World Atlas of Holocene Sea-Level Changes*. Amsterdam: Elsevier.
Pirazzoli, P.A., 1995. Tectonic shorelines. In Carter, R.G.W., and Woodroffe, C.D. (eds.), *Coastal Evolution: Late Quater- nary Shoreline Morphodynamics*. Cambridge University Press, pp. 451–476.
Pirazzoli, P.A., Arnold, M., Giresse, P., Hsieh, M.L., and Liew, P.M., 1993. Marine deposits of late glacial times exposed by tectonic uplift on the east coast of Taiwan. *Marine Geology*, **110**: 1–6.
Pirazzoli, P.A., Laborel, J., Saliège, J.F., Erol, O., Kayan, I., and Person, A., 1992. Holocene raised shorelines on the Hatay coasts (Turkey): palaeoecological and tectonic implications. *Marine Geology*, **96**: 295–311.
Pirazzoli, P.A., Laborel, J., and Stiros, S.C., 1996. Earthquake clustering in the Eastern Mediterranean during historical times. *Journal of Geophysical Research*, **101**(B3): 6083–6097.
Pirazzoli, P.A., and Montaggioni, L.F., 1988. Holocene sea-level changes in French Polynesia. *Palaeogeography, Palaeoclimatology, Palaeoecology*, **68**: 153–175.
Pirazzoli, P.A., and Salvat, B., 1992. Ancient shorelines and Quaternary vertical movements on Rurutu and Tubuai (Austral Isles, French Polynesia). *Zeits, Geomorphol.*, **36**: 431–451.
Plafker, G., 1965. Tectonic deformation associated with the 1964 Alaska Earthquake. *Science*, **148**(3678): 1675–1687.
Stanley, D.J., 1997. Mediterranean deltas: subsidence as a majpr control of relative sea-level rise. In Briand, F., and Maldonado, A. (eds.), *Transformations and Evolution of the Mediterranean Coastline*. Monaco, CIESM Science Series No, 3, pp. 35–62.
Stanley, D.J., and Warne, A.G., 1994. Worldwide initiation of Holocene marine deltas by deceleration of sea-level rise. *Science*, **265**: 228–231.
Stanley, D.J., Warne, A.G., and Dunbar, J.B., 1996. Eastern Mississippi delta: late Wisconsin unconformity, overlying transgressive facies, sea level and subsidence. *Engineering Geology*, **45**: 359–381.
Stewart, I.S., and Hancock, P.L., 1994. Neotectonics. In Hancock, P.L. (ed.), *Continental Deformation*. Tarrytown: Pergamon Press, pp. 370–409.
Valensise, G., and Ward, S.N., 1991. Long-term uplift of the Santa Cruz coastline in response to repeated earthquakes along the San Andreas Fault. *Bulletin of the Seismological Society of America*, **81**: 1–11.
Vita-Finzi, C., 1986. *Recent Earth Movements: An Introduction to Neotectonics*. London, Academic Press, 226 p.
Wallace, R.E. (panel chairman), 1986. *Active Tectonics*. Studies in Geophysics, Washington DC: National Academy Press.

Cross-references

Changing Sea Levels
Coastal Subsidence
Coastline Changes
Faulted Coasts
Isostasy
Physical Models
Seismic Displacement
Submerging Coasts
Uplift Coasts

THALASSOSTATIC TERRACES

A term derived from Greek roots, the expression "Thalassostatic" obtains its prefix from "thalassic," having to do with the sea, and its suffix "static" referring to its equilibrium state. A fluvial terrace is said to be thalassostatic when it is the product of a former sea level that caused flood-stage sediment load to accumulate as an alluvial surface. Its seaward limit is usually determined by a beachridge or beachridge plain.

The actual term itself was coined by Zeuner (1945), who saw that an estuary created by downcutting during a Pleistocene low sea-level state would become aggraded during a following interglacial phase. Even earlier, Ramsay (1931) pointed out that alluvial terraces of this sort would provide clearer evidence of former eustatic levels than strictly marine terraces that are more liable to erosion or other factors. Clayton (in Fairbridge, 1968, p. 142) mentions the actualistic evidence of modern aggradation behind dams. This filling will extend only a short distancer upstream where the gradient is changed. Zeuner believed that gravel terraces of the lower Thames in England must be solifluction products of glacial-phase stream loading, thus having nothing to do with thalassostatic events.

In the classic work of de Lamothe (1918) on the Somme Valley in northern France, the concept of eustatic control was first presented, but erroneously extended to the entire fluvial terrace system. The Dutch worker, Brouwer (1956) considered the question of thalassostatic terraces in general and showed that only the lowest sectors were appropriately so-named. Earlier, Pleistocene examples would be largely obliterated by erosion.

In the world's major deltas like the Mississippi and the Rhine, a quasi-stable tectonic fulcrum develops, with subsidence on the seaward side, uplift on the landward side. Thus the fluvial terraces are stacked progressively lower and in stratigraphic sequence downstream. On the Mississippi the fulcrum area is above Baton Rouge, on the Rhine about at Nijmegen. However, the exact fulcrum point shifts up- or downstream depending upon the current eustatic level. A problem develops, however, with these large rivers in their propensity to major flood events, their discharge being greatly amplified by the large area and multiple sources of their drainage basins. Such events are likely to overtop levees in the deltaic regions. These so-called "avulsion" breaks are commonly matched by the drying out of other distributary channels, so that a rather complex stratigraphy develops (Törnquist, 1994; Berendsen, 1995). Nevertheless, a strongly cyclical pattern is discernible.

Where an extensive data source has been provided by detailed geophysical transects, as in the Mississippi delta, it can be seen that layers of Holocene transgressive facies are alternating with regressive events when channels deepen and their outlets shift seawards. In contrast, the transgressive intervals are marked by sandy chenier ridges (sand from longshore sources) that form distinctive markers in the otherwise muddy or peaty deltaic facies. Compaction of these water-saturated substrates leads to areas of accelerated subsidence, as shown by very variable tide-gauge evidence, that can be misleading for the delta as a whole, which has a very modest subsidence rate. With each transgression the thalassostatic terrace building shifts upstream, but with the renewed downcutting after avulsion an entirely new delta-lobe is likely to evolve (Lowrie and Hamiter, 1995).

A pioneering attempt to relate thalassostatic eustasy to the rivers of Borneo (Kalimantan) was made by Smit Sibinga (1953). A detailed glacial-age drainage network extends over much of the Sunda Shelf according to the submarine mapping by Molengraaff and referred to as the "Molengraaff River System" by Umbgrove (1947). With each successive eustatic rise thalassostatic terrace deposits must have lined these former waterways. The eustatic curve is not a sine-wave, however, but is a strongly fluctuating one, so that there are extended intervals of pause or reversal, during which there would have been accelerated thalassostatic sedimentation.

Best known and well dated of these interruptions was the Younger Dryas event which lasted approximately 1,000 yr, 11,740–10,740 cal. BP, with abrupt transitions, both at its commencement and terminations. Eustatic sea level at that time fell to about 30 m below present mean sea level. Its coastline is particularly well marked by the presence, in the warmer latitudes and along the more stable coasts, of an abrupt line of reefs or distinctive beach deposits. A wave-resistant beachrock facies is a distinctive marker where carbonate sands permit rapid lithification. In some sectors carbonate sands led to the development of littoral dunes, which also become rapidly lithified to form "eolianites." Today these eolianites form reefs that are well known to fishermen (e.g., "Twelve Fathom Reefs" of Western Australia).

Other sea-level fluctuations were marked in the deep ocean by the "Heinrich events" (at 3–7 kyr intervals) which mark iceberg distribution in the N.W. Atlantic. Heinrich events are marked by climatic extremes, both positive and negative, thus raising the chicken-and-egg problem. Analogous eustatic fluctuations are indicated by the thalassostatic data. Sudden warming of the water around Greenland, such as occurred in AD 1912, accelerates iceberg calving (with disastrous effect on RMS *Titanic*). In this case, however, it was not so much climatic, as tidal, because 1912 marked the largest lunisolar tidal extremes in over 500 years (Wood, 2001).

Thalassostatic terrace building (and its erosion) thus relates to movement of relative sea level (RSL). The bed of a river on reaching the sea is nicely adjusted to velocity and bed-load, which dictate the equilibrium water depth at the river mouth, subject to tidal characteristics and seasonal changes such as storminess and monsoonal shifts.

The equilibrium status may be modified by one or more of several processes: (a) Tectonic, which may be sudden as a result of an earthquake, such as the historic shifts in 1855 and 1931, of Wairapa (Wellington) or Napier in New Zealand or the subsidence of parts of Yokohama in Japan. It may also be secular as a result, for example, of glacioisostatic rebound such as observed today at Stockholm in Sweden (at 5 mm/yr) or at Great Whale River in Quebec (at 8 mm/yr). (b) Eustatic and/or climatic; these are related but partly independent, although not easily distinguished. When a dominant wind system changes, it affects also RSL as observed, for example, in the Hudson Bay, in the Gulf of California and in the eastern Gulf of Mexico, all being partly related to the 11 yr sunspot cycle and the 18.6 yr lunar cycle (Fairbridge, 1992). It is also observed on a 6-month basis in the Red Sea and Arabian Sea and Bay of Bengal, a consequence of the Asiatic monsoon reversal. Longer cycles, of the order of 45, 90, and more years are observed in the arctic and subarctic latitudes, relating in part to the polar anticyclone and the magnetic pole in its periodic shifts from the longitude of Greenland to that of eastern Siberia, and back again.

For whatever reason, a fall in RSL leads to a shallowing of the debouching river mouths. Two possibilities ensue. If the fluvial discharge is linked, as it usually is, to climate fluctuation, a decreased discharge coinciding with a shallowing of the stream beds, then the result will be a "siltation" of local harbors. Around the Mediterranean in Roman times (1st century AD) there was widespread siltation and as a result many Roman docks, harbor facilities, and fish tanks had to be re-engineered. Some harbors, as in Turkey and farther afield in India (entrance of the Narbada River) were abandoned altogether, or the city shifted somewhat downstream (Kayan, 1997).

The opposite condition is associated with a systematic rise in RSL. This occurred, for example, in the post-Carolingian (after Charlemagne) global warming that persisted until about AD 1300. River courses were backed up and deepened. Roman-era dock or defensive facilities were drowned. An example of the latter can be seen at Portchester in the south of England.

Rhodes W. Fairbridge

Bibliography

Berendsen, H.J.A., 1995. Holocene fluvial cycles in the Rhine delta? *Journal of Coastal Research*, **17**(Special issue): 103–108.

Brouwer, A., 1956. Thalassostatic terraces and Pleistocene chronology. *Leidse Geologische Mededelingen*, **20**: 22–33.

De Lamothe, Gen., 1918. Les anciennes nappes alluviales et lignes de rivage du bassin de la Somme et leur rapports avec celles de la Méditerranée occidentale. *Bulletin de la Societe Géologique de France*, **18**(4): 3–58.

Fairbridge, R.W., 1968. *The Encyclopedia of Geomorphology*. New York: Van Nostrand Reinhold.

Fairbridge, R.W., 1992. Holocene marine coastal evolution of the United States. *S.E.P.M.. Publication*, **48**: 9–20.

Kayan, I., 1997. Bronze Age regression and change of sedimentation on the Aegean coastal plain of Anatolia (Turkey). In Dalfes, H.N. *et al*. (eds.), *Third Millennium BC Climate Change and Old World Collapse* Berlin: Springer, NATO-ASI series 1, Global Environment Change **49**: 431–450.

Lowrie, A., and Hamiter, R., 1995. Fifth and sixth order eustatic events during Holocene (fourth order) high stand influencing Mississippi delta-lobe switching. *Journal of Coastal Research*, **17**(Special issue).

Ramsay, W., 1931. Changes of sea-level resulting from the increase and decrease of glaciation. *Fennia*, **52**(5): 1–62.

Smit Sibinga, G.L., 1953. Pleistocene eustasy and glacial chronology in Borneo. *Geologie en Mijnbouw*, **15**: 365–383.

Törnquist, T.E., 1994. Middle and Late Holocene avulsion history of the River Rhine (Rhine-Meuse delta, Netherlands). *Geology*, **22**: 711–714.

Umbgrove, J.H.F., 1947. *The Pulse of the Earth*. The Hague: Nyhoff.

Wood, F.J., 2001. *Tidal Dynamics*, Vol. 2. *Journal of Coastal Research*, Special Issue 31.

Zeuner, F.E. (1945). *The Pleistocene Period*. London: Ray Society.

Cross-references

Archaeological Site Location, Effect of Sea-Level Changes
Beach Ridges
Cheniers
Eolian Processes
Late Quaternary Marine Transgression
Offshore Sand Banks and Linear Sand Ridges

THALASSOTHERAPY—See HEALTH BENEFITS

TIDAL CREEKS

Is a tidal creek an estuary? Stamp (1966) in his *Glossary of Geographical Terms* quotes the OED definition of creek as, "*a narrow recess or inlet in the coastline of the sea, or the tidal estuary of a river; an armlet of the sea which runs inland in a comparatively narrow channel* …." The *Dictionary of Geological Terms* published by the American Geological Institute (1976) defines a creek as, "*a small inlet, narrow bay, or arm of the sea, longer than it is wide, and narrower and extending farther into the land than a cove*."

Figure T10 Tidal creek in mangroves showing the narrow shallow channel and low hydrodynamic energy conditions.

Geomorphically, the essential characteristics of a tidal creek are that they are relatively long and narrow, are shallow, and exhibit tidal water level fluctuations and weak tidal currents. They are relatively small-scale landforms with a low hydrodynamic energy environment without significant wave action or strong current action (Figure T10). Typically along its banks the tidal creek is well vegetated. The friction from the banks and the length of the creek ensure that the tidal wave within the creek is hyposynchronous (reducing tidal range upstream). Such conditions facilitate sediment deposition, so tidal creeks exhibit active deposition and infilling over a time frame of decades. Tidal creeks may drain to the open coast of an enclosed coastal sea or bay, or may be part of a larger estuary or delta system. They also occur at the distal ends of arms of drowned river valley (ria) harbors where tidal creeks drain sectors of mangrove stands and/or salt marsh. In tropical areas, tidal creeks and distributaries create a dense network of small-scale drainage through the mangrove forests, while a similar reticulated plexus of creeks occurs in temperate salt marsh (Guilcher, 1958). Pethick (1984) notes that salt marsh creek systems have a very high ratio of total creek length to drainage area—on the order of 40 km/km^2. Tidal creeks also occur in sinuous meandering forms draining extensive intertidal mudflats. However, tidal creeks do not tend to occur draining to open coast high-energy sandy beaches.

Often the creeks extend as the headwaters of a large estuary into the surrounding drainage basin, and on occasion carry freshwater discharges and episodic floodwaters from surrounding catchments. Thus the tidal creeks are frequently the mixing zones of fresh and saline tidal water, and exhibit an enhanced vertical salinity structure due to the low-energy conditions. Accordingly, they are also favored zones for flocculation processes, so that deposition of muds is typical and ongoing within tidal creeks. Unfortunately, tidal creeks often tend to become a receptacle for human waste and rubbish, and are frequently reclaimed.

Terry R. Healy

Bibliography

American Geological Institute, 1976. Dictionary of Geological Terms. Garden City, NY: Anchor Press.
Guilcher, A., 1958. *Coastal and Submarine Morphology*. London: Methuen.
Pethick, J., 1984. *An Introduction to Coastal Geomorphology*. London: Edward Arnold.
Stamp, L.D., 1966. Glossary of Geological Terms. London: Longmans.

Cross-references

Estuaries
Mangroves, Ecology
Mangroves, Geomorphology
Muddy Coasts
Ria
Salt Marsh
Tidal Flats
Vegetated Coasts

TIDAL DATUMS

Introduction

A sea-level datum is a surface constructible statistically from sea-level observations that is used as a reference for measuring and describing vertical positions near the earth's surface. At official intervals, the elevations of sea-level datums are revised to reestablish their relationship to a new mean water level. A multitude of sea-level datums are in use. Each has its own advantages and disadvantages with no universally superior choice. Preferences depend on location, purpose, and past practices. Focus here will be on tidal datums defined at different phases of the tide; for example, high water and low water (Figure T11). Discussion of tidal datums illustrates some of the uses, practices, and limitations common to the broader class of vertical datums.

Scope

Details in the operational definitions of tidal datums evolved as concepts matured, needs for precision increased, field methodologies improved, and new legal issues arose. In this discussion of broad tidal datum issues, operational details may be sacrificed to provide an overall understanding of the basics, at least as understood by a coastal morphologist limited in practice to North America. Specific details continue to evolve with advances in measurement technology and changing society needs. Prescriptions of such details are left to official documents.

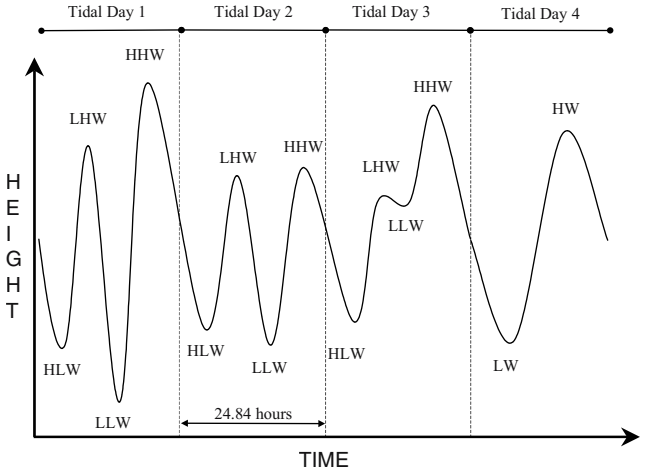

Figure T11 Tide phases labeled on a stylized tide curve. When two high-tide phases can be distinguished in the tide curve during a single tidal day (24.82 h), the higher of the two is called higher high water (HHW) and the other lower high water (LHW). When two low-tide phases are discernable in one day, the higher of the two lows is called higher low water (HLW) and the other lower low water (LLW). When only one high and one low-tide phase appear (e.g., Tidal Day 4), the high phase is called high water (HW) and the low is called low water. The record from sites that usually have only a single high and low per day will periodically transition in and out of multiple-cycles-per-day episodes that can have distinctly different phases like Tidal Day 2 or less distinct phases, more like Tidal Day 3 above.

Historical developments

The astronomical tide causes sea level to vary on daily, monthly, and longer cycles. These deterministic cycles are superimposed on more random water level fluctuations related primarily to weather. Normally, the reference point for repeated measurements should be stable, that is, anchored to the system containing the objects measured. What factors explain widespread adoption of a continually fluctuating water surface as a vertical reference? Early communities developed at sea ports where knowledge of the water depths in navigable channels was vital for the economy and defense. Soil productivity [EBH1] was another fundamental concern related to height above water because of altitudinal climate gradients if not more directly through frequencies of flooding. Referencing elevations to water levels was, therefore, of keen interest to early civilizations. Sea level also provided a common reference elevation applicable widely throughout the world. It could be reestablished with little loss of accuracy near coasts and without the need for long-distance surveys or recover of any destructible marker (e.g., benchmark). Fluctuations of the sea surface (and hence the zero reference) were probably small relative to the precision required to make decisions, especially for civilizations developing around the Mediterranean Sea where the range of tidal fluctuations is small compared with a typical range in the ocean. As coastal property ownership disputes increased, navigation clearances tightened, and tidal fluctuations became recognized (though not yet understood), comparison of elevations with respect to different sets of sea- level observations became more problematic. Later recognition of a broad spectrum of sea-level changes required further adjustments to allow tidal datums to persist as widely used references. Continuing advantages of referencing to sea level, instead of a fixed datum, include: conveniences related to historical precedence, natural differences in human use of property above and below sea level, lateral continuity (at least along coasts), apparent simplicity, lack of geographic bias in definition, and the greater relevance of mean water levels over any truly level surface for most hydrologic and navigation considerations.

Because concerns of navigation and coastal engineering are closely tied to sea level, the reference point in these fields should change with long-term changes in mean sea level. For endeavors in which sea level is

irrelevant, a stable nontidal datum may be preferable. For this reason, and to better understand tidal datums themselves, some discussion of nontidal datums is included.

The name of the organization having responsibility for official datum and charting standards within the United States changed with time from the Survey of the Coast, to the Coast Survey, Coast and Geodetic Survey, National Ocean Survey and, now, the National Ocean Service (NOS). The NOS's authoritative references on present and historic coastal boundary determinations are Reed (2000) and Shalowitz (1962, 1964). Kraus and Rosati (1997) summarize procedures for determining shoreline positions for coastal engineering. Prescription for US Army Corps of Engineer surveys of waterways and additional guidance on tidal datums can be found in USACE (2002). All five references can be found on the World Wide Web (www).

Methods of tidal datum determination

Statistically averaging sea-level measurements is the process by which an unsteady surface is fixed to serve as an unambiguous and repeatable datum. There are a number of ways to average sea level, giving rise to a number of different tidal datums. For an unambiguous datum definition, the frequency of the measurements and the time span over which they are to be averaged must be specified. For any tidal datum, the manner of relating the measurements to a clearly defined tidal phase (Figure T11) must also be specified. Breakdown in any one of these fundamental requirements, causes problems as we shall see.

Astronomical cycles and the tidal response

Astronomical tides are the sea's response to gravitational forces of the moon and sun (and to a lesser extent other celestial bodies) that vary over the earth's surface. These forces also vary with time as relative astronomical positions continually change over a wide spectrum of cycles. Procedures to calculate the local elevation of each of six standard tidal datums (upper portion of Table T1) follow similar official algorithms regardless of which of the six is selected. Selection would typically be based on location and purpose, for example, whether it involves resolving legal disputes, promoting navigation, assessing environmental resources, or analyzing geophysical phenomena.

The longest cycle conventionally damped by tidal averaging (the Metonic cycle) has a period of about 18.61 years. The NOS selects a specific 19-year time interval, called the *National Tidal Datum Epoch*, as the official span over which tide measurements are averaged to obtain the current tidal datum elevations throughout North America.

Gauges

The NOS presently maintains about 189 *primary tide gauges* where hourly water levels have been recorded continuously for more than 19 years. *Tidal benchmarks* are physical monuments maintained along the coast and to which tidal datum elevations have been surveyed (see *Geodesy*). Three to five bench marks are tied to NOS tide gauges by precise surveying and monitored to detect possible gauge disturbances.

Elevations are established at a larger set of *secondary gauges* by comparing their shorter tidal records (less than 19 years, but more than one year) with simultaneous measurements from nearby primary stations. Tidal datums can be reestablished by leveling short distances from tidal benchmarks. Numerical modeling of the tide can be used to extend datums longer distances between gauge sites including inland across the continent.

The elevation of water levels (and, therefore, tidal datums) in estuaries and coastal lagoons is typically higher than along adjacent open coasts. This super elevation is primarily due to freshwater flowing into the bay and nonlinear friction in tidal currents. Adjacent to inlets, the transition is smooth, but relatively steep. Therefore, primary gauges are often located away from their immediate vicinity (see *Tide Gauges*).

Table T1 A few North American vertical datums used by coastal engineers and scientists

Acronym	Name and definition	Origin, use or advantages
Tidal datums (based on gauge records)		
MHHW	Mean higher high water Mean of all higher high waters[a, b, c]	
MHW	Mean high water Mean of all high water heights (i.e., HW, HHW, and LWH, see Figure T11)[a, b, c]	Frequently used boundary separating private from state lands. See text. Landward limit for US Corps of Engineers jurisdiction over navigable waters.
MTL	Mean tide level Mean of MHW and MLW datums[a,b,c,d]	More descriptively called half-tide level.
MSL	Mean sea level Mean of hourly water surface heights[c]	Maintained US-wide by the National Geodetic Survey as "the most practicable and stable datum for general engineering," Shalowitz (1962).
MLW	Mean low water Mean of all low water heights (i.e., LW, LLW, and HLWs, see Figure T11)[a, c, d]	Use of the synonymous term, mean low tide, is discouraged by NOS.
MLLW	Mean lower low water Mean of all lower low water heights[a, c, d]	Principal chart datum for all of U.S. since 1981. Used by six states as boundary separating private and state lands.
Orthometric vertical datums (based on topographic surveying)		
NGVD 29	National Geodetic Vertical Datum 1929	Earlier standard geodetic datum. Based on first order survey nets of the United States and Canada fit to MSL at 26 tide gauges.
NAVD 88	North American Vertical Datum 1988	Official vertical datum for all of North America since June 24, 1993. An upgrade of NGVD 1928 based on more measurements over a larger area and independent of any tide gauge measurements.
Three-dimensional datums (based on measurements from space)		
NAD 83	North American Datum 1983	An upgrade using space-based measurements of the previous standard, NAD27.
WGS 84	World Geodetic System 1984	US Defense Mapping Agency equivalent of NOAA's NAD 83.

[a] Each stage of the tide in the time series to be averaged must, by official convention, differ by at least a "0.10 ft" and "2.0 h" from the adjacent measurements in the series. The series usually extend over a specified National Tidal Datum Epoch, but sometimes over a shorter stated duration.
[b] A high water is a maximum in a tide curve reached by a rising tide. The higher of two unequal high waters during the same day (24 h 50 min = the period of the M_1 tidal component) is the higher high water. The other high water is the lower high water.
[c] Definitions from US Department of Commerce Tide and Current Glossary (Hicks, 1989).
[d] A low water is a minimum in the tide curve that is reached by a falling tide. The lower of two unequal low tides during the same day is the lower low water. The other is the higher low water.

Tidal datum elevation algorithms

To calculate the elevations of a particular tidal datum at a primary tide gauge site, select the elevation measurements associated with the chosen tide phase (e.g., high tide) from the set of hourly data that covers the current National Tidal Datum Epoch. Official rules specify which hourly readings are associated with the chosen phase of the astronomical tide, but other factors (primarily weather) contributed to the water level measured at that time. Arguments have been made, especially for regions where the wind is strong, to loosen the required association between astronomical tidal phases and selection of which observations to average. Following the official rules (more details in next major section and in Table T1), a single daily high (or low) water elevation was traditionally selected at stations where the tide is classified as being *diurnal* (displaying a single cycle with one high and low per day, Figure T11, Tidal Day 4); elevations of two high (or low) waters are selected daily at stations classified as *semidiurnal* or *mixed* (displaying two cycles per day, Figure T11, Tidal Days 1, 2, and 3). Sum the selected observations and divide by the number selected. By thus averaging long series of data, the shorter cyclic variations (astronomical tide) and the random (weather-related) variations are damped. Including the full 19th year avoids biasing related to the strong annual cycle. Significant longer term (>19-year) variations arise from astronomical forces, thermal expansion (contraction) of the oceans, crustal movement, glacial melting, etc. These longer-term changes (see *Eustasy* and *Changing Sea Levels*) are compensated for, as needed at irregular intervals, by adopting evermore recent 19-year periods (Epochs) as the National Tidal Datum Epoch. For North America, the current Epoch is 1960–78; previous Epochs include 1941–59 and 1924–42. Agencies responsible for datum definitions elsewhere agree that tidal epochs should span complete 19-year periods, but they do not all use the same 19-year periods.

Spaced-based measurements

After a period of improvement and acceptance, spaced-based measurements derived from the NAVSTAR Global Positioning System (GPS) are now widely used not only as a convenient way to reestablish local datum elevations near benchmarks, but also in defining new coordinate systems (lowest portion of Table T1). Numerical models can introduce tidal datums into these three-dimensional coordinate systems based on idealized reference ellipsoids rather than tidal data. This approach is now quicker and less expensive than collecting tidal measurements or leveling from local tidal datum benchmarks. In the future, direct measurement of sea surface elevations from space may become accurate enough to establish tidal datum elevations essentially continuously along the coast in an iterative blend of observation and tidal dynamic modeling.

Limitations and precautions in applications

Temporal and spatial variations

The difference between successive high and low waters, *tide range*, is neither uniform nor constant. The phases of the moon and the inclination of its orbital plane with respect to the plane of the earth's orbit around the sun (*declination*) are two of the factors contributing to daily variations in tide range on approximately 28-day and 14-day cycles, respectively. In contrast to the elegant theory explaining temporal variations in the astronomical tide, its spatial variations are complex. Tidal dynamics vary with location on the earth, outline of the coast, bathymetry of the seafloor, and such factors as wind, salinity, and river discharge. Each tidal component is characterized by an amplitude and frequency (see *Tides*). The bathymetry and outline of the coast (*basin shape*) modulates sea-level response to the total gravitational force in a manner somewhat analogous to the way the material properties and shape of a poorly tuned musical instrument distorts chords. Some frequencies resonate and are amplified. Others are out of tune with the basin (instrument) and are damped (muffled). Furthermore, frequency-dependent nodes (antinodes) may exist within the basin where responses are maximized (minimized).

Nonuniform height differences between datums

Complexities of tidal propagation cause the mean differences among tidal datums to vary spatially, for example, the difference between MLW and MLLW varies along shore. The mean tide range varies around the world being about 10 m at Anchorage, Alaska; 1 m at San Diego, California; 0.1 m at Galveston, Texas; and less than a centimeter at Chicago, Illinois, on Lake Michigan.

Advent of the www improved the availability and dissemination of the empirically determined elevation differences among tidal datums in the form of tables issued by federal organizations throughout the world (e.g., http://co-ops.nos.noaa.gov/bench. html). Many of these tables also report the highest and lowest observed sea levels. Some sea-level datums (e.g., the British chart datum, Lowest Astronomical Tide) are based on extremes.

Type of tide

The range and timing of the tide goes through cycles as lunar and solar declinations change. They also vary spatially over the earth's surface. The type of tide varies spatially and temporally as well. The type of tide is predominately *semidiurnal* (two similar, semi-sinusoidal cycles per day with little difference between the two lows or the two highs) over most of the US East Coast and *mixed* (two lows and two highs per day that are unequal in elevation) along most of the US West Coast. Along the Gulf of Mexico, the type of tide is not so uniform, but at most locations it is *diurnal* (only one high and one low per day). Figure T11 shows a mixed type during Tidal Day 1 and Tidal Day 3. Tidal Day 2 is semidiurnal and Tidal Day 4 is diurnal. A real tide curve would transition between these types more gradually (see *Tides*).

The most common type of tide throughout the world is semidiurnal. Figure T12 depicts regional variations in type of tide along the north shore of the Gulf of Mexico and a portion of the Atlantic. The basin shapes in Tampa Bay and Charlotte Harbor, on the west coast of Florida, are tuned to diurnal tidal forces. Therefore, the tide type in these estuaries is predominately diurnal even though the open Gulf beaches of west Florida are predominately mixed. *Predominately* means that the type of tide is as designated for more than half of the time at that particular site. Along the Mediterranean Sea, stretches of coast that are predominately semidiurnal alternate with reaches that are predominately mixed. Tides are predominately semidiurnal around most of England, mixed around most of Australia, and diurnal along much of southeast Asia, Japan, and northeast Siberia.

Analysis procedures and datum elevations were established in the Gulf of Mexico prior to a full appreciation of these complex changes in type of tide (Hicks *et al*., 1988). With the benefit of longer term and spatially denser measurements, it became apparent that some initial datum calculation procedures (as well as inconstancies in terminology) were causing problems. One of the problems was that the MHW and MLW datums had abrupt breaks (*jump discontinuities*) in elevation as one moved alongshore. The global continuity of sea level was a prime feature promoting the widespread adoption of tidal datums. MHW and MLW discontinuities arose because, traditionally, their official definitions included provisions that where the tide was classified as predominately diurnal, only one high (or low) would be included daily in the 19-year series for datum determination. Where the tide was predominately semidiurnal or mixed, both lows and both highs were traditional (and still are) included in these calculations. There are times during the monthly lunar cycle when diurnal forces are small relative to semidiurnal forces. During these times, the tide signal (even at sites where the tide is classified as diurnal) may take on mixed-type characteristics briefly (i.e., exhibit a second daily high and/or low). Likewise at sites that are mixed-type, the second daily high and/or low may become indiscernible for a few days during the month. Tide type is unambiguously classified according to a ratio of amplitude terms for the major tidal constituents. The shape of tide curves vary smoothly along the shore with transition zones between areas with different types of tide. Discontinuities arose

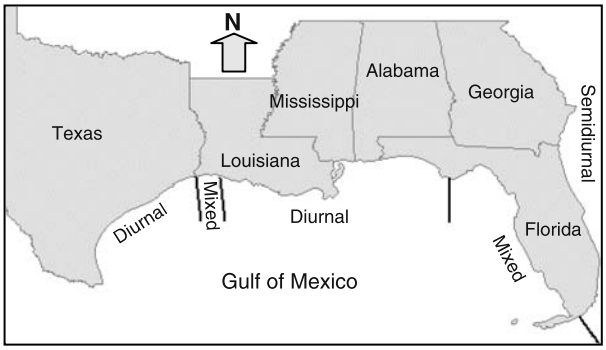

Figure T12 Regional variations in type of tide (modified from Hicks *et al.,* 1988).

from the traditional definitions of MHW and MLW being dependent on tide type. Resulting problems were especially acute in the case of MHW because of its role as a legal state boundary.

Through a series of carefully planned and well-coordinated moves that began as early as the 1970s, the procedures for defining MHW and MLW and the inconsistent naming practices that had crept in at some Gulf sites were changed. Table T1 follows the revised, uniform NOS definitions. Another half dozen modifications were collected into one endeavor that unified analysis, created a single uniform chart datum (MLLW), freed MHW and MLW definitions from dependence on tide type, updated the National Tidal Datum Epoch, moved private–state property boundary seaward along certain reaches, and eliminated all datum discontinuities (Hicks *et al*., 1988). Though announced much earlier, this comprehensive corrective action officially took effect on November 28, 1980. Complete updating of charts and NOS's Coast Pilot actually proceeded incrementally over the following decade. Tide tables predicting tidal heights for East Coast of North and South America switched chart datum from MLW to MLLW starting with the 1989 volume (making it consistent with NOS tables for other regions). This correction (The National Tidal Datum Convention of 1980) thus simplified standards for tidal datums throughout the Americas.

Nontidal datums

The *geopotential elevation* of tidal datums vary spatially (i.e., the potential energy of a unit mass at a given elevation with respect to each datum varies geographically). For long periods, a tidal datum can deviate on the order of a meter from an *equipotential surface* (surface of constant specific potential energy) due to prevailing atmospheric pressure, temperature, wind, currents, and salinity differences (see *Altimeter Surveys, Coastal Tides and Shelf Circulation*). For example, the geopotential elevation of sea level rises (falls) generally northward along the west (east) coast of the United States. For certain applications (e.g., long-distance pumping, ballistics) it is desirable that the elevation of an equipotential surface be spatially invariant. In such cases, a nontidal datum is clearly required (lower portion of Table T1).

The latest geodetic datum (NAVD 88, middle of Table T1) is not parallel to any tidal datum or to the geodetic datum it replaced (NGVD 29). The NGVD 29 was defined so that it approximated the MSL datum. The new NAVD 88 is on the order of a meter above the MSL datum on the West Coast and 0.1–0.5 m below the MSL datum on the East Coast (Figure T13) and is independent of sea level.

Shorelines

Conceptually, the intersection of any tidal datum with the beach rigorously defines a shoreline. The acronym for this shoreline is obtained by appending an "L" to the acronym for the selected tidal datum. In the United States, the mean high water line (MHWL) was adopted by most states as the boundary between private and public land. Six northeastern states allow private ownership down to the mean lower low water line (MLLWL). In Texas, private ownership has, at least in certain cases, been restricted to being above the mean higher high water line (MHHWL). Federal submerged lands, exclusive fishing zones, and national economic zones are related back to the MLLWL by their legal definitions.

In practice, charted shorelines are sometimes inferred from rectified aerial photographs taken at specific phases of the tide. Such mapped shorelines only approximate the rigorously defined tidal-datum shorelines, but are much easier to establish. Unfortunately, imprecise usage often results in them being labeled MHWL or MLWL. Even less-accurate approximations of tidal-datum shorelines are inferred from the wetted bound on the beach, berm line, and toe of the dune as identified in aerial photographs. These charted shorelines may be unlabeled or mislabeled.

Figure T13 Height in centimeters of MSL datum above NAVD88 (redrawn from USACE, 2002).

Statements like "this chart uses the MLLW datum," do not imply that the shoreline is the MLLWL or any other tidal datum, only that printed soundings are referenced to MLLW. The shoreline could be the water's edge at an arbitrary height of the tide, a high water mark, or follow a geomorphic feature like a berm or toe of dune. Caution is advised not to infer too much from shoreline labels without consulting the description of the procedures used in production of that specific chart. Increased use of digital maps may exacerbate problems because chart developers can no longer anticipate the scale to which the user will take measurements from these zoomable products.

The label "HWL" (for high water line as distinct from MHWL) specifically acknowledges that the shoreline has been located less precisely than tidal-datum shorelines. Nevertheless, the HWL does approximate the MHWL, and is therefore considered "of primary importance in distinguishing the upland from the shore on charts" (Shalowitz, 1964). For practical reasons of determination, however, the surveyed HWL is based on observed physical features in the field (such as berm crest). Thus, the HWL stands above the MHWL by an uncertain distance related to wave runup and surveyor judgment.

Concluding guidance

Tidal datums are listed in Table T1 in the order of decreasing elevation from top to bottom. The vertical offset of orthometric and three-dimensional datums (lower portions of Table T1) from tidal datums varies spatially (e.g., Figure T13). Chart depths usually refer to a tidal datum (MLLW is the official chart datum to which depths are referred in the United States). Elevations on maps usually refer to an orthometric or a three-dimensional datum (NAVD 88 or NAD 83 for older maps in the United States). By convention, elevations are positive above datum; depths are positive below datum (i.e., an object 10 m below the water has an elevation of -10 m and a depth of $+10$ m).

In the 1990s, proliferation of personal computer software made it easy to convert between reference systems (see *Geographic Information Systems*). Caution is advised, however, when analyzing measurements made to different references. For example, the effectiveness of coastal erosion mitigation is often assessed by analyzing the difference between variable rates of shoreline change after project completion and a series of measurements made before project initiation. Consider a scrabbled mixture of HWLs and MHWLs. Early shorelines exist only as HWLs. The ratio of HWLs to MHWLs would tend to decrease as aerial surveying and GPS technology became pervasive. The horizontal distance separating a HWL from a MHWL is not recoverable after the HWL survey. Because shoreline positions based on tidal and orthometric datums are more precisely defined than the HWL, MHWL positions may appear more reliable (for analyzing shoreline change rates) than the HWLs that only approximate them. For just the years that have both a HWL and a MHWL, it might seem desirable to delete the less precise of the two measurements, but this would tend to bias the post-construction period and produce the appearance of unwarranted erosion reduction (i.e., deletion the HWLs would tend to displace the shoreline landward more frequently during later years). In most such cases, the more precisely located MHWLs might well be ignored to obtain an unbiased (though imprecise) estimate of changes in the rate of shore retreat.

Adoption of a new National Tidal Datum Epoch is pending. Previous updates have raised datums (reduced the elevations of benchmarks above tidal datums) by amounts that varied with the particular epoch transition, gauge location, and datum selection. For the MHW datum, an increase on the order of 0.25 m would not be unusual from one Epoch to the next. In areas of subsidence (Louisiana, the Netherlands, and portions of Texas, see *Coastal Subsidence*) or crustal uplift (e.g., Alaska, see *Changing Sea Levels*), datums could be raised or lowered on the order of a meter. Comparisons of shoreline positions documented during different Epochs can, therefore, be problematic. Adjustments can be made to estimate the shoreline positions for a common Epoch based on the vertical shift in tidal datum between two Epochs and the slope of the beach at these elevations. The adjusted results would only be as good as the knowledge of the beach slope used to translate the vertical shift into a shoreline displacement, but the results could be useful. Beaches (including the dune, berm, and longshore bars) generally migrate upward with the historic long-term rise of sea level. So, comparing unadjusted shorelines, referred to datums that

shifted between epochs, can also be valid from the perspective of quantifying how the volume of beach sand changes in concert with sea-level changes. Whether to accept the inter-Epoch shoreline displacement or adjust the shorelines would depend on the time span, magnitude of sea-level change, and knowledge of slope changes. Analysis from both perspectives can be useful. For example, along a 50 km reach of Lake Michigan, the average shore retreat of 17.9 m (over a specific six years during which the mean lake level rose persistently) was decomposed into 14.5 m (at a fixed datum elevation) due to erosion and recession of the profile and 3.4 m due to submergence under a 0.39 m higher mean lake level (Figure 11, Hands, 1979).

For accuracy, charts and tables should clearly state the method of determining elevations and shorelines, coordinate systems, units of measurement, and any coordinate transform procedures employed. To maintain accuracies on the order of 0.1 m or better, be certain of and document which particular Epoch was used in the tidal datum definition.

Edward B. Hands

Bibliography

Hands, E.B., 1979. Changes in rates of shore retreat, Lake Michigan, 1967–76. *CERC TP 79-4*, Vicksburg, MS: US Army Engineer Research and Development Laboratory.

Hicks, S.D., 1989. *Tide and Current Glossary*. Washington, DC: US Department of Commerce.

Hicks, S.D., Hull, W.V., Weir, J.P., Long, E.E., and Hickman, L.E., Jr., 1988. The national tidal datum convention of 1980—the final push. *Proceeding, 3rd Biennial National Ocean Service International Hydrographic Conference*, Washington, DC: National Ocean Service/NOAA. pp. 121–128.

Kraus, N.C., and Rosati, J.D., 1997. Interpretation of shoreline-position data for coastal engineering analysis. *Coastal Engineering Technical Note II-39*, Vicksburg, MS: US Army Engineer Research and Development Laboratory.

Reed, M., 2000. *Shore and Sea Boundaries*, Vol. 3; *The Development of International Maritime Boundary Principles through United States Practice*. Washington, DC: US Department of Commerce.

Shalowitz, A.L., 1962. *Shore and Sea boundaries;* Vol. 1; *Boundary problems Associated with the Submerged Lands Cases and the Submerged Lands Acts*. Washington, DC: US Department of Commerce.

Shalowitz, A.L., 1964. *Shore and Sea Boundaries*; Vol. 2; *Interpretation and use of Coast and Geodetic Survey data*. Washington: US Department of Commerce.

USACE, 2002. *Hydrographic Surveying*, Engineer Manual 1110-2-1003, especially Chapter 5, *Tidal Datums*, Sections 5–7 through 5–9. Washington, DC: US Army Corps of Engineers.

Cross-references

Altimeter Surveys, Coastal Tides and Shelf Circulation
Changing Sea Levels
Coastal Changes, Gradual
Coastal Subsidence
Eustasy
Geodesy
Geographic Information Systems
Sea-Level Change During the Last Millennium
Tide Gauges
Tides

TIDAL ENVIRONMENTS

Definitions

A tidal environment is that part of a marine shore which is regularly submerged and exposed in the course of the rise and fall of the tide. Such environments exhibit particular physical and biological characteristics which, among others, play an important role in coastal dynamics, coastal ecology, coastal protection and engineering works, and integrated coastal zone management.

The coastal area affected by the ocean tides is known as the intertidal or eulittoral zone. Being a long-period wave, the tidal water level oscillates about a mean water level, which usually corresponds to the mean sea level. The vertical distance covered by the tide is known as the tidal range, whereas the part above or below the mean tide level is the tidal amplitude, which can hence have a positive or negative sign. In practice, a number of critical tide levels are distinguished on the basis of longer-term averages. Proceeding from high to low water levels, these are: MEHWS, mean equinoxial high water springs (highest astronomical tide); MHWS, mean high water springs; MHWN, mean high water neaps; MWL, mean water level (commonly mean sea level); MLWN, mean low water neaps; MLWS, mean low water springs; and MELWS, mean equinoxial low water springs (lowest astronomical tide). These mean tide levels are well correlated with various morphological and biological characteristics of tidal environments.

Besides the astronomical modulations, instantaneous tidal elevations can, in the short term, be substantially modified by water-level fluctuations induced by wind and/or wave set-up or set-down. The degree of wave and wind exposure can thus have a substantial influence on the nature of a tidal shore. Where such secondary and irregular fluctuations in coastal water levels are so frequent and strong that they completely mask the tidal signal, the coast is considered to be nontidal (e.g., the Baltic Sea).

In summary, tidal shores are highly variable environments which are not only influenced by the astronomically induced periodic rise and fall of the sea level, but also by numerous secondary processes. In combination, these factors define the local physical nature of a tidal environment (e.g., Davies, 1980; Allen and Pye, 1992; Allen, 1997; French, 1997).

Tidal forcing factors

The tides are essentially produced by the interactive forces exerted on the oceans by the sun and the moon. Since the motions of the sun and the earth–moon system are known with great precision, the tide-generating potential can be mathematically resolved into strictly periodic components. These components vary over time as the position of the sun and the moon relative to the position and orientation of the earth changes. The sum of all the tractive forces at any one time defines the total instantaneous potential. Doodson (1922) computed no less than 390 such harmonic components, of which about 100 are long period, 160 diurnal, 115 semidiurnal, and 14 one-third diurnal. Of these, only seven (i.e., four semidiurnal and three diurnal components) are of practical importance (e.g., McLellan, 1975). Indeed, only four of these are used to define the character of the tides around the globe (Figure T14), in which semidiurnal, diurnal, and two mixed tidal types, comprising a predominantly semidiurnal and a predominantly diurnal one, are distinguished (cf. Table T2). Since the tidal type has an important influence on the physical nature of tidal environments, the global distribution of these four types are illustrated in Figure T15.

As the sun, the earth, and the moon move along their elliptical orbits, they continually change their positions relative to each other. As a result, the total potential defining the height of the astronomical tide is modulated as a function of geographic location in the course of a day, a month, a year, and also on longer timescales. The most prominent tidal period is the fortnightly spring–neap cycle (synodic tide). Thus, spring tides coincide with full moon and new moon, whereas neap tides occur at the corresponding half-moon phases. These tidal ranges are further modulated in the course of a lunar month (anomalistic tides), the highest spring tides occurring when the moon is closest to the earth (perigee), the lowest when the moon is furthest away from the earth (apogee), the difference in distance amounting to roughly 13%. The solar component varies in similar manner between perihelion (currently coinciding with the winter solstice) and aphelion (currently coinciding with the summer solstice), the difference in distance between the two amounting to about 4%.

Another important astronomical feature influencing tidal environments on short timescales is the daily inequality of the tide (declinational tide). This feature results from the inclination of the earth's axis relative to the plane of the ecliptic, and hence the tidal bulge. As the earth rotates around its axis, the position of a geographic locality continually changes relative to the tidal bulge, alternating between a maximum and a minimum tidal elevation every 12.42 h, a feature which affects the elevations of both successive high tides and low tides. On this, the declination of the moon is superimposed which, in turn, causes a progressive change in the daily inequality over time. Thus, with the moon over the equator, successive tides are equal in height (equatorial tides), whereas towards the position of maximum declination successive tides become progressively more unequal in height, dividing into a "large tide" and a "half tide" (tropical tides). The solar tide shows a similar inequality, being zero at the equinoxes (spring and autumn) and largest at the solstices (summer and winter).

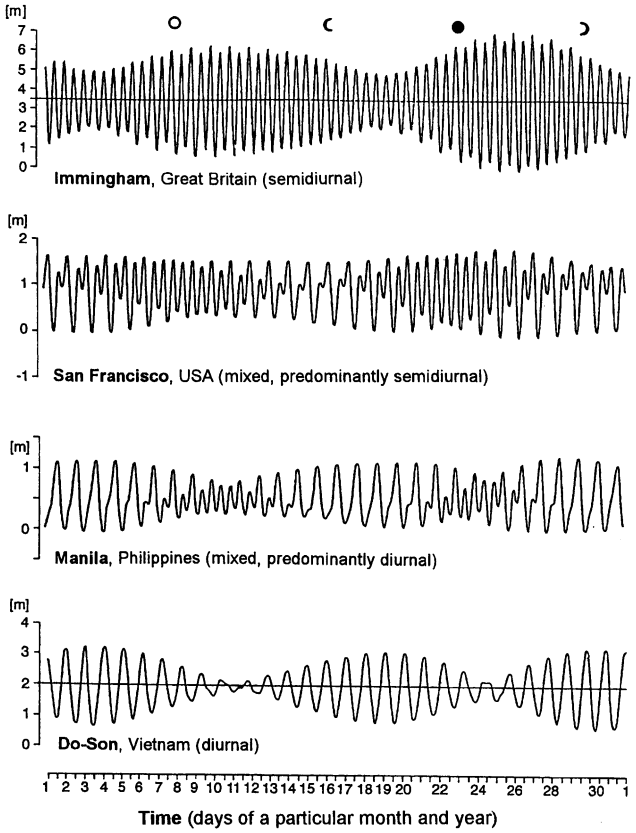

Figure T14 Selected examples of tidal curves from different geographic locations illustrating the main tidal types (adapted from Dietrich *et al.*, 1975). (A) semi-diurnal tides (e.g., Immingham, Great Britain); (B) mixed, predominantly semidiurnal (e.g., San Francisco, USA); (C) mixed, predominantly diurnal (e.g., Manila, Philippines); (D) diurnal (e.g., Do-Son, Vietnam).

The largest astronomical tides, that is, the greatest spring and lowest neap tides, in the course of a year occur at the vernal and autumnal equinoxes when the orbital path of the earth–moon system crosses the plane of the celestial equator (nodal points), that is, when the total potential of the tide-generating forces is largest because of their closest alignment.

In addition to these short-period astronomical cycles, the tide is also modulated by longer period phenomena which need to be considered when analyzing ancient tidal deposits (e.g., Archer *et al.*, 1991; Williams, 1991; Oost *et al.*, 1993; de Boer and Smith, 1994). Among these are the nutational motion or nodal cycle (≈18.6-year cycle) caused by the oscillation of the earth's axis about its mean position, the precessional motion (≈23,000-year cycle) of the earth's axis, the obliquity (≈41,000-year cycle) which defines the angle of inclination of the earth's axis between 22° and 24.8° (currently 23.5°), and the eccentricity (≈100,000-year cycle) controlling the rate of change in the elliptical radius of the earth's orbit around the sun. In addition, it has been shown that the length of the year has decreased from 420 to currently 365 days, while the length of the day has increased from 21 to currently 24 h in the course of the last 500 million years or so (e.g., Williams, 1991).

Besides the geographic variation in tidal type and tidal range resulting from astronomical modulations, the physical nature of a tidal environment is also influenced by numerous secondary factors. Among the more important of these are variations in tidal range with distance from the amphidromic point around which the tidal wave rotates, the Coriolis effect as a function of geographic location, the rate of change in water depth, the coastline configuration (plan shape and slope angle), as well as resonant effects resulting from the shape and depth of a tidal basin. Thus, at the center of an amphidrome the tidal range is considered to be zero, but it progressively increases in height with distance along the axis of the two opposing tidal bulges which rotate around the center offset by 180° or 6 h (tidal phases). The Coriolis force, in turn, forces the tidal wave to rotate clockwise in the Southern Hemisphere and anticlockwise in the Northern Hemisphere, but this principle can be upset near the Equator. The direction in which the tidal wave propagates along a shore thus depends entirely on the geographic location of the coast. Where tidal waves rotating around neighboring amphidromes meet, the tidal water motion can even be perpendicular to the coast.

Table T2 The tidal character (F) as defined on the basis of the ratio between the sum of the lunisolar diurnal (K_1) and principle lunar diurnal (O_1) and the sum of the principle lunar semidiurnal (M_2) and principle solar semidiurnal (S_2) tidal components

$F = K_1 + O_1/M_2 + S_2$	Tidal character
0–0.25	Semidiurnal tides
0.25–1.5	Mixed, predominantly semidiurnal tides
1.5–3.0	Mixed, predominantly diurnal tides
>3.0	Diurnal tides

Source: Dietrich *et al.* (1975).

In addition, the amplification of the tidal wave and the tidal type are strongly influenced by the configuration of the coastline and the rate of shoaling, the effect of this interaction being illustrated in Figures T15 and T16. With decreasing water depth (h) the length of the tidal wave (λ) progressively decreases proportionally in the form $\lambda \propto h^{0.5}$. When propagating into funnel-shaped estuarine water bodies, the initial increase in tidal range due to convergence of the opposite shores is eventually compensated for by friction along the seabed as a result of which the tidal wave gradually decreases in height. This interplay between friction and convergence is proportionally related in the form $a_0 \propto b^{-0.5} * h^{-0.25}$ where a_0 is the amplitude of the tidal wave (m), b is the width (m), and h is the water depth (m) at a particular location along the estuary. This relationship can take on complicated patterns and in nature three basic modes of tidal wave propagation can be distinguished. Thus, in the case where friction dominates over convergence the tidal range progressively decreases in height up-estuary (hypersynchronic mode). In the opposite case, the tidal range increases in height (hyposynchronic mode), and where friction and convergence are in balance the tidal range remains constant (synchronic mode). Even neighboring estuaries will exhibit quite different modes of tidal wave propagation if they differ in shape and water depth (e.g., Borrego *et al.*, 1995). In many estuarine environments a combination of two or even all three modes can be observed.

In some cases, the entrance channel of an estuary or lagoon is so narrow and shallow that the propagation of the tidal wave is "choked" with the effect that the tidal range is dramatically reduced. This filtering mechanism, expressed by the so-called coefficient of repletion (K), has the numerical form of $K = (T/2a_0\pi) * (A_c/A_b) * [2a_0 g/(1 + 2gln^2 r^{-4/3})]^{0.5}$ where T is the tidal period, $2a_0$ is the tidal range (a_0 being the tidal amplitude), l is the length of the entrance channel, A_c is the cross-sectional channel area, A_b is the surface area of the water body, r is the hydraulic radius of the channel, g is the gravitational acceleration, and n is the Manning's friction (0.01–0.10 s $m^{-1/3}$). This coefficient of repletion controls reductions in tidal range, phase shifts between ocean and lagoonal tides, non-sinusoidal variations of the lagoonal tides, and flow exchanges between the ocean and the estuarine or lagoonal water bodies (e.g., Kjerfve and Magill, 1989).

A final forcing factor which may affect the behavior of tidal waves in shallow water is resonance, a feature associated with standing waves. Clearly, a standing wave superimposed on a normal tidal wave would dramatically affect the physical nature of a tidal environment. In this context, we distinguish two types. In the case of a half-wave oscillator or seiche, the length of the water body is half the wavelength of the standing wave. The fundamental period (T) of a seiche is defined as $T = 2l/(gh)^{0.5}$ where l is the length of the water body, h is the water depth, and g is the gravitational acceleration. Seiches are particularly common in lakes and marginal seas, where they are forced by wind stress, and hence of less importance in tidal environments. However, quarter-wave oscillators come into operation where the lengths of open-ended elongate gulfs or deep estuaries together with adjacent bays correspond to a quarter of the tidal wavelength ($l = 0.25\mathrm{T} * (gh)^{0.5}$). In this case, the period $T = 4l/(gh)^{0.5}$ with notations as above. If this condition is fulfilled, or nearly so, tidal amplification can be quite considerable (e.g., Bay of Fundy, Canada).

Coastal classification by tidal type and range

Besides classifying the world's coastline according to tidal type (Figure T15), coastal tidal environments are also classified on the basis of tidal range, the scheme of Davies (1964, 1980) having been the most

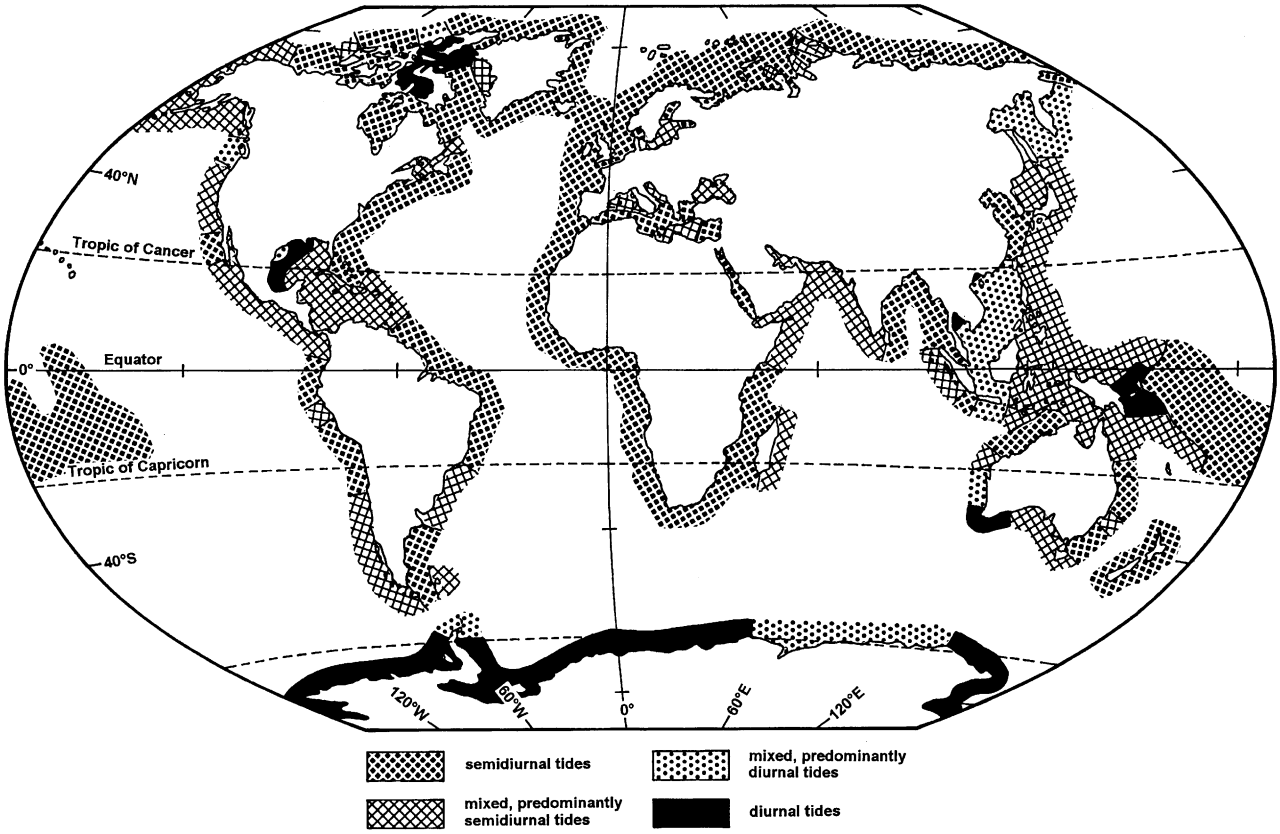

Figure T15 Global distribution of the main tidal types (adapted from Davies, 1980). Note that the transitions between semidiurnal and diurnal tidal types (here represented by so-called mixed tides) are progressive and not abrupt.

Table T3 Contrasting two existing classification schemes of tidal shores on the basis of tidal range

Davies (1964)		Hayes (1979)	
Tidal range (m)	Class name	Tidal range (m)	Class name
<2.0	Microtidal	<1.0	Microtidal
2.0–4.0	Mesotidal	1.0–2.0	Lower mesotidal
>4.0	Macrotidal	2.0–3.5	Upper mesotidal
		3.5–5.5	Lower macrotidal
		>5.5	Upper macrotidal

widely applied to date (Table T3). However, with only three subdivisions, this rather arbitrary approach prevents differentiation where it is most needed, that is, near the lower and upper limits of the potential tidal regime. For example, the Gulf of Mexico coast with an average tidal range of only 0.5 m is very different in character from the west coast of southern Africa where the tidal range averages at 1.6 m, yet both are classified as microtidal. In contrast to this, a more pragmatic classification, comprising five subdivisions (see Table T2), has been proposed by Hayes (1979). This latter scheme takes distinct, process-related geomorphic features into consideration, for example, the upper limit of barrier island occurrence at a tidal range of 3.5 m, which hence marks the transition between upper mesotidal and lower macrotidal regimes in this classification. To contrast the two classification schemes, the global pattern of coastal subdivision using the latter scheme is presented here for the first time (Figure T16).

Rocky versus sandy and muddy tidal environments

The coastlines of the world can be divided into four basic types, namely rocky shores, sandy shores, muddy shores, and bio-shores. In all cases, the character of a particular shore reflects the interaction between the substrate, the local wave climate, the tides, and the biology (e.g., Newell, 1979; Davies, 1980; Raffaeli and Hawkins, 1996). Geographic location, which controls climatic influences and biological species composition (e.g., Chapman, 1974), and the Holocene evolution of a coast (e.g., Bird and Schwartz, 1985) being important additional factors to consider. Rocky shores occupy the smallest overall area because the intertidal zone is commonly narrow as compared with the other shore types. Shore processes have received considerable attention by engineers for constructional purposes (e.g., Horikawa, 1989), whereas biologists have long been intrigued by the distinct faunal and floral zonation patterns along tidal gradients which evidently reflect high degrees of adaptation to the intertidal environment and the overprinting effects of competition between specific organisms (e.g., Lewis, 1972; Raffaeli and Hawkins, 1996). However, the interplay between biological and physical factors in defining zonation patterns is still not well enough understood to allow accurate predictions to be made (e.g., Delafontaine and Flemming, 1989). Different tidal environments are also characterized by different biogeochemical processes due to different climates, substrates, and biological community structures (Alongi, 1998).

The biological zonation pattern observed along the rocky shores of Great Britain as a function of tidal gradient and the degree of exposure to wave action is illustrated in Figure T17 (adapted from Lewis, 1972; Raffaeli and Hawkins, 1996). This basic scheme can be applied to most rocky shores of the world, the only difference being the species composition and distribution, a good example from subtropical Bermuda being shown in Thomas (1985). Important to note here is that the tidal gradient in Figure T17 is relative, expanding or contracting proportional to the tidal range.

In contrast to rocky shores, into which bio-shores can also be included, sandy and muddy tidal shores can attain shore normal extensions of many kilometers (e.g., Davis, 1994; Flemming and Hertweck, 1994). French (1997) distinguishes no less than seven intertidal coastal types based mainly on morphology and facies successions. The final transition between land and sea along sheltered coasts is characterized by sharp boundaries separating different floral zones, the typical pattern observed along the barrier island shore of the southern North Sea being illustrated in Figure T18 (adapted from Streif, 1990).

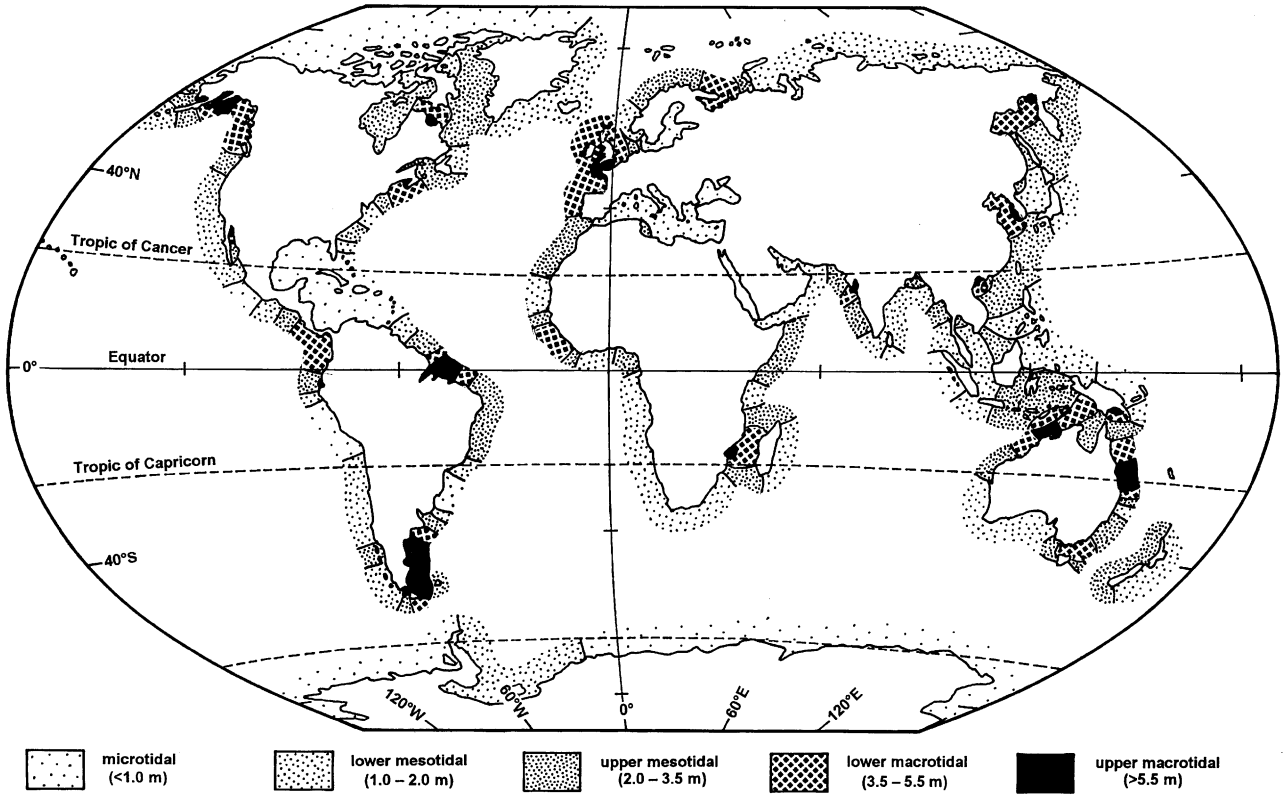

Figure T16 Global distribution of tidal shores based on tidal range according to the classification scheme of Hayes (1979).

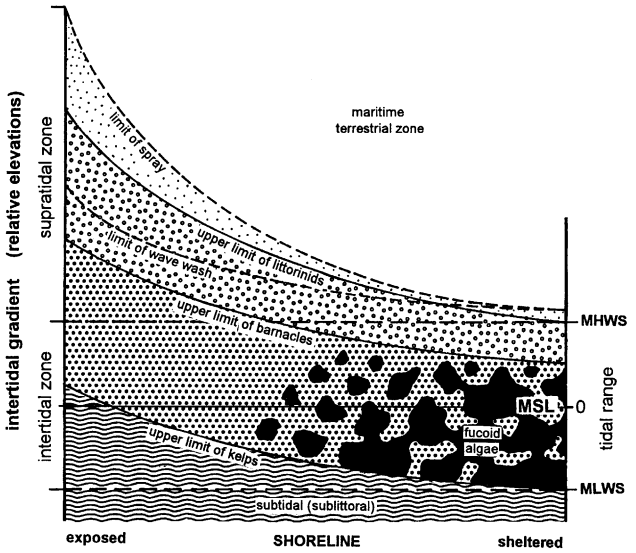

Figure T17 Zonation patterns along rocky tidal shores as a function of exposure to wave action (adapted from Lewis, 1972; Raffaeli and Hawkins, 1996). Note that the scaling is relative to any particular observed tidal gradient.

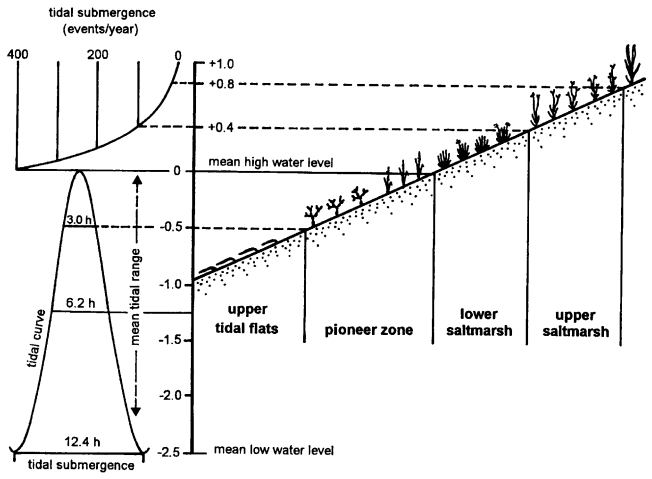

Figure T18 Floral zonation pattern observed at the transition between upper intertidal flats and the terrestrial environment of the Wadden Sea (southern North Sea) as a function of tidal elevation and the frequency of tidal submergence in the course of a year (adapted from Streif, 1990).

In this example the zones are separated by the frequency of tidal submergence in the course of the year which is controlled by the elevation along the tidal gradient. In principle, this basic pattern should be applicable the world over, individual transition levels being dependent on local floral associations, the tidal range, the seasonal wave climate, and the difference in elevation between mean high tide levels at spring and neap tide (e.g., Chapman, 1974; Lugo and Snedaker, 1974). A systematic investigation of the factors controlling the upper and lower limits of occurrence of *Spartina anglica* relative to mean sea level along the coast of the United Kingdom has generated quantitative relationships between the spring tidal range, the fetch available for wave generation and propagation, the area of the tidal basin, and in the case of the upper limit also the geographic location (Gray, 1992). Thus, the lower limit (L_l) is defined as $L_l = -0.805 + 0.366R_s + 0.053F + 0.135 * \log_e A_b$, where R_s is the spring tidal range (m), F is the fetch in the direction of the transect (km), and A_b is the area of the tidal basin (km^2). The upper limit, by contrast, is defined as $L_u = 4.74 + 0.483R_s + 0.068F - 0.199L°$, where $L°$ is the degree North Latitude expressed as a decimal. The correlation coefficients of $r = 0.97$ for L_l and $r = 0.95$ for L_u demonstrate the predictive potential of this approach.

A comprehensive overview of physical and biological processes active along sandy tidal shores is provided in McLachlan and Erasmus (1983).

Outlook

Many features of tidal environments are still poorly understood. Among these are the quasi-periodic, decadal to subdecadal fluctuations in the elevation of mean high tide and mean low tide levels. Being a worldwide phenomenon, one might assume that they result from variations in the astronomical factors defining the tidal potential. A clear correlation, however, is still lacking. As far as sandy tidal environments are concerned, accurate sediment budgets and transport pathways have remained elusive problems whose solution becomes more pressing in view of the predicted acceleration in sea-level rise. The distinction between strictly local features and others of global relevance requires more attention. A number of other unresolved issues have been addressed in the text.

B. W. Flemming

Bibliography

Allen, J.R.L., and Pye, K. (eds.), 1992. *Salt marshes, Morphodynamics, Conservation and Engineering Significance*. Cambridge: University Press.

Allen, P.A., 1997. *Earth Surface Processes*. Oxford: Blackwell Science.

Alongi, D.M., 1998. *Coastal Ecosystem Processes*. Boca Raton: CRC Press.

Archer, A.W., Kvale, E.P., and Johnson, H.R., 1991. Analysis of modern equatorial tidal periodicities as a test of information encoded in ancient tidal rhythmites. In Smith, D.G., Reinson, G.E., Zaitlin, B.A., and Rahmani, R.A. (eds.), Clastic tidal sedimentology. *Canadian Society of Petroleum Geologist, Memoirs,* **16**: 189–196.

Bird, E.C., and Schwartz, M.L. (eds.), 1985. *The World's Coastline*. New York: Van Nostrand Reinhold.

Borrego, J., Morales, J.A., and Pendon, J.G., 1995. Holocene estuarine facies along the mesotidal coast of Huelva, south-western Spain. In Flemming, B.W., and Bartholomä, A. (eds.), *Tidal Signatures in Modern and Ancient Sediments*. Oxford: Blackwell Science. *Special Publication International Association of Sedimentologists*, **24**: 151–170.

Chapman, V.J., 1974. *Salt Marshes and Salt Deserts of the World*, 2nd edn. Lehre (Germany): Cramer.

Davies, J.L., 1964. A morphogenetic approach to world shorelines. *Zeitschrift für Geomorphologie*, **8**: 127–142.

Davies, J.L., 1980. *Geographical Variation in Coastal Development*. Geomorphology Texts 4. London: Longman.

Davis, R.A., Jr. (ed.), 1994. *Geology of Holocene Barrier Island Systems*. Berlin: Springer.

de Boer, P.L., and Smith, D.G. (eds.), 1994. *Orbital Forcing and Cyclic Sequences*. Spec. Publ. Int. Ass. Sediment. No. 19. Oxford: Blackwell Science.

Delafontaine, M.T., and Flemming, B.W., 1989. Physical factors in barnacle community structure: a conceptual model. In Ros, J.D. (ed.), *Topics in Marine Biology. Scientia Marina*, **53**: 405–410.

Dietrich, G., Kalle, K., Krauss, W., and Siedler, G., 1975. *Introductory Oceanography*, 3rd edn. in German. Berlin: Gebr. Borntraeger.

Doodson, A.T., 1922. The harmonic development of the tide-generating potential. *Proceedings of the Royal Society of London*, **A100**: 305–329.

Flemming, B.W., and Hertweck, G. (eds.), 1994. Tidal flats and barrier systems of continental Europe: a selective overview. *Senckenbergiana maritima*, **24**: 1–209.

French, P.W., 1997. *Coastal and Estuarine Management*. London: Routledge.

Gray, A.J., 1992. Salt marsh plant ecology: zonation and succession revisited. In Allen, J.R.L., and Pye, K. (eds.), *Salt Marshes*. Cambridge: Cambridge University Press, pp. 63–79.

Hayes, M.O., 1979. Barrier island morphology as a function of tidal and wave regime. In Leatherman, S.P. (ed.), *Barrier Islands*. New York: Academic Press, pp. 1–27.

Horikawa, 1989. *Nearshore Dynamics and Coastal Processes: Theory, Measurement, and Predictive Models*. Tokyo: University of Tokyo Press.

Kjerfve, B., and Magill, K.E., 1989. Geographic and hydrodynamic characteristics of shallow coastal lagoons. *Marine Geology*, **88**: 197–199.

Lewis, J.R., 1972. *The Ecology of Rocky Shores*. London: The English University Press.

Lugo, A.E., and Snedaker, S.C., 1974. The ecology of mangroves. *Annual Review of the Ecology and Systematics*, **5**: 39–64.

McLachlan, A., and Erasmus, T. (eds.), 1983. *Sandy Beaches as Ecosystems*. Developments in Hydrobiology 19. The Hague: Dr. W. Junk Publishers.

McLellan, H.J., 1975. *Elements of Physical Oceanography*. Oxford: Pergamon Press.

Newell, R.C., 1979. *Biology of Intertidal Animals*. Faversham (UK): Marine Ecological Surveys Ltd.

Oost, A.P., de Haas, H., Ijnsen, F., van den Boogert, J.M., and de Boer, P.L., 1993. The 18.6 year nodal cycle and its impact on tidal sedimentation. *Sedimentary Geology*, **87**: 1–11.

Raffaeli, D., and Hawkins, S., 1996. *Intertidal Ecology*. London: Chapman & Hall.

Streif, H., 1990. *The East Frisian Coast. North Sea, Islands, Wadden Sea, and Marshes* (in German). Berlin: Borntraeger.

Thomas, M.L.H., 1985. Littoral community structure and zonation on the rocky shores of Bermuda. *Bulletin of Marine Science*, **37**: 857–870.

Williams, G.E., 1991. Upper Proterozoic tidal rhythmites, South Australia: sedimentary features, deposition, and implications for the earth's paleorotation. In Smith, D.G., Reinson, G.E., Zaitlin, B.A., and Rahmani, R.A. (eds.), Clastic Tidal Sedimentology. *Canadian Society of Petroleum Geologists, Memoir,* **16**: 161–178.

Cross-references

Barrier Islands
Beach Processes
Bioerosion
Classification of Coasts (see Holocene Coastal Geomorphology)
Estuaries
Littoral
Microtidal Coasts
Rock Coast Processes
Sandy Coasts
Tidal Flats
Tides
Wave-Dominated Coasts

TIDAL INLETS

Introduction

Tidal inlets are found along barrier coastlines throughout the world. They provide a pathway for ships and small boats to travel between the open ocean to sheltered waters. Along many coasts, including much of the East and Gulf Coasts of the United States, the only safe harborages, including some major ports, are found behind barrier islands. The importance of inlets in providing navigation routes to these harbors is demonstrated by the large number of improvements that are performed at the entrance to inlets such as the construction of jetties and breakwaters, dredging of channels, and the operation of sand bypassing facilities.

Diversity in the morphology, hydraulic signature, and sediment transport patterns of tidal inlets attests to the complexity of their processes. The variability in oceanographic, meteorologic, and geologic parameters, such as tidal range, wave energy, sediment supply, storm magnitude, and frequency, freshwater influx, and geologic controls, and the interactions of these factors, are responsible for this wide range in tidal inlet settings.

What is a tidal inlet

A tidal inlet is defined as an opening in the shore through which water penetrates the land thereby proving a connection between the ocean and bays, lagoons, and marsh and tidal creek systems. Tidal currents maintain the main channel of a tidal inlet.

The second half of this definition distinguishes tidal inlets from large, open embayments or passageways along rocky coasts. Tidal currents at inlets are responsible for the continual removal of sediment dumped into the main channel by wave action. Thus, according to this definition, tidal inlets occur along sandy or sand and gravel barrier coastlines, although one side may abut a bedrock headland. Some tidal inlets coincide with the mouths of rivers (estuaries) but in these cases inlet dimensions and sediment transport trends are still governed, to a large extent, by the volume of water exchanged at the inlet mouth and the reversing tidal currents, respectively.

At most inlets over the long term, the volume of water entering the inlet during the flooding tide equals the volume of water leaving the inlet during the ebbing cycle. This volume is referred to as the tidal prism. The tidal prism is a function of the open water area and tidal range in the backbarrier as well as frictional factors, which govern the ease of flow through the inlet.

Inlet morphology

A tidal inlet is specifically the area between two barriers or between the barrier and the adjacent bedrock or glacial headland. Commonly, the recurved ridges of spits, consisting of sand that was transported toward the backbarrier by refracted waves and flood-tidal currents form the sides of the inlet. The deepest part of an inlet, the inlet throat, is located normally where spit accretion of one or both of the bordering barriers constricts the inlet channel to a minimum width and minimum cross- sectional area. Here, tidal currents normally reach their maximum velocity. Commonly, the strength of the currents at the throat causes sand to be removed from the channel floor leaving behind a lag deposit consisting of gravel or shells or in some locations exposed bedrock or indurated sediments.

Tidal deltas

Closely associated with tidal inlets are sand shoals and tidal channels located on the landward and seaward sides of the inlets. Flood-tidal currents deposit sand landward of the inlet forming flood-tidal deltas and ebb-tidal currents deposit sand on the seaward side forming an ebb-tidal delta.

Flood-tidal delta. Their presence or absence, size, and development are related to a region's tidal range, wave energy, sediment supply, and backbarrier setting. Tidal inlets that are backed by a system of tidal channels and salt marsh (mixed-energy coast) usually contain a single horseshoe-shaped flood-tidal delta (i.e., Essex River Inlet, Massachusetts; Figure T19). Contrastingly, inlets that are backed by large shallow bays may contain multiple flood-tidal deltas. Along some microtidal coasts, such as in Rhode Island, flood deltas form at the end of narrow inlet channels cut through the barrier. Changes in the locus of deposition at these deltas produce a multi-lobate morphology resembling a lobate river delta (Boothrdyd *et al*., 1985). Flood delta size commonly increases as the amount of open water area in the backbarrier increases. In some regions, flood deltas have become colonized and altered by marsh growth, and are no longer recognizable as former flood-tidal deltas. At other sites, portions of flood-tidal deltas are dredged to provide navigable waterways and thus are highly modified.

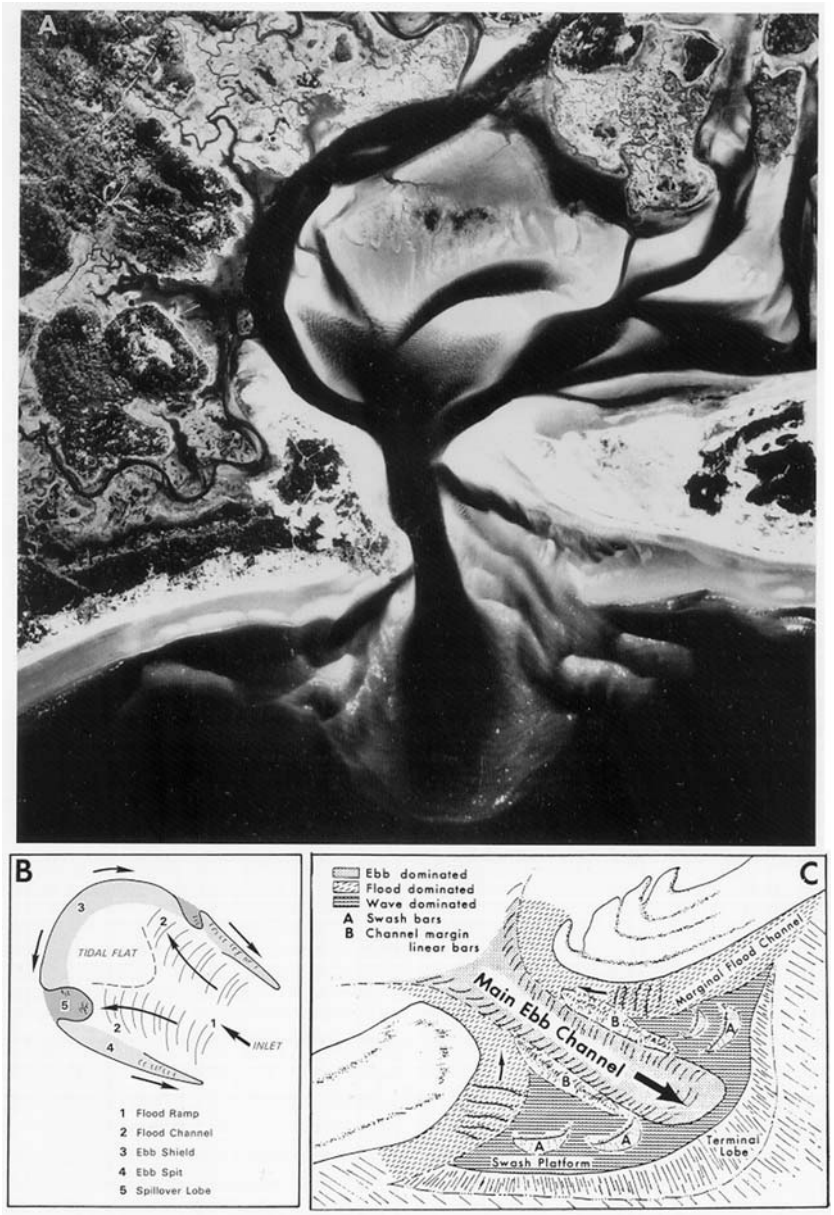

Figure T19 (A) Vertical aerial photograph of Essex River Inlet, Massachusetts with well-developed flood- and ebb-tidal deltas. (B) Flood-tidal delta model (after Hayes, 1975). (C) Ebb-tidal delta model (after Hayes, 1975).

Flood-tidal deltas are best revealed in areas with moderate to large tidal ranges (1.5–3.0 m) because in these regions they are well exposed at low tide. As tidal range decreases, flood deltas become largely subtidal shoals. Most flood-tidal deltas have similar morphologies consisting of the following components (Hayes, 1975, 1979).

1. *Flood ramp*. This is a landward shallowing channel that slopes upward toward the intertidal portion of the delta. Strong flood-tidal currents and landward sand transport in the form of landward-oriented sandwaves dominate the ramp.
2. *Flood channels*. The flood ramp splits into two shallow flood channels. Like the flood ramp, these channels are dominated by flood-tidal currents and flood-oriented sand waves. Sand is delivered through these channels onto the flood delta.
3. *Ebb shield*. It defines the highest and landwardmost part of the flood delta and may be partly covered by marsh vegetation. It shields the rest of the delta from the effects of the ebb-tidal currents.
4. *Ebb spits*. These spits extend from the ebb shield toward the inlet. They form from sand that is eroded from the ebb shield and transported back toward the inlet by ebb-tidal currents.
5. *Spillover lobes*. These are lobes of sand that form where the ebb currents have breached through the ebb spits or ebb shield depositing sand in the interior of the delta.

Through time, some flood-tidal deltas accrete vertically and/or grow in size. This is evidenced by an increase in areal extent of marsh grasses, which require a certain elevation above mean low water to exist. At migrating inlets new flood-tidal deltas are formed as the inlet moves along the coast and encounters new open water areas in the backbarrier. At most stable inlets, however, sand comprising the flood delta is simply recirculated. The transport of sand on flood deltas is controlled by the elevation of the tide and the strength and direction of the tidal currents. During the rising tide, flood currents reach their strongest velocities near high tide when the entire flood-tidal delta is covered by water. Hence, there is a net transport of sand up the flood ramp, through the flood channels and onto the ebb shield. Some of the sand is moved across the ebb shield and into the surrounding tidal channel. During the falling tide, the strongest ebb currents occur near mid to low water. At this time, the ebb shield is out of the water and diverts the currents around the delta. The ebb currents erode sand from the landward face of the ebb shield and transport it along the ebb spits and eventually into the inlet channel where once again it will be moved onto the flood ramp thus completing the sand gyre.

Ebb-tidal delta. This is an accumulation of sand that has been deposited by the ebb-tidal currents and which has been subsequently modified by waves and tidal currents. Ebb deltas exhibit a variety of forms dependent on the relative magnitude of wave and tidal energy of the region as well as geological controls. Along mixed energy coasts, most ebb-tidal deltas contain the same general features including:

1. *Main ebb channel*. This is a seaward shallowing channel that is scoured into the ebb-tidal delta sands. It is dominated by ebb-tidal currents.
2. *Terminal lobe*. Sediment transported out the main ebb channel is deposited in a lobe of sand forming the terminal lobe. The deposit slopes relatively steeply on its seaward side. The outline of the terminal lobe is well defined by breaking waves during storms or periods of large wave swell at low tide.
3. *Swash platform*. This is a broad shallow sand platform located on both sides of the main ebb channel, defining the general extent of the ebb delta.
4. *Channel margin linear bars*. These are bars that border the main ebb channel and sit atop the swash platform. These bars tend to confine the ebb flow and are partially exposed at low tide.
5. *Swash bars*. Waves breaking over the terminal lobe and across the swash platform form arcuate-shaped swash bars that migrate onshore. The bars are usually 50–150 m long, 50 m wide, and 1–2 m in height.
6. *Marginal-flood channels*. These are shallow channels 0–2 m deep at mean low water located between the channel margin linear bars and the onshore beaches. The channels are dominated by flood-tidal currents.

Ebb-tidal delta morphology

The general shape of an ebb-tidal delta and the distribution of its sand bodies tell us about the relative magnitude of different sand transport processes operating at a tidal inlet. Ebb-tidal deltas that are elongate with a main ebb channel and channel margin linear bars that extend far offshore are tide-dominated inlets. Wave-generated sand transport plays a secondary role in modifying delta shape at these inlets. Because most sand movement is in onshore–offshore direction, the ebb-tidal overlaps a relatively small length of inlet shore. This has important implications concerning the extent to which the inlet shore undergoes erosional and depositional changes.

Wave-dominated inlets tend to be small relative to tide-dominated inlets. Their ebb-tidal deltas are driven onshore, close to the inlet mouth by the dominant wave processes. Commonly, the terminal lobe and/or swash bars form a small arc outlying the periphery of the delta. In many cases, the ebb-tidal delta of these inlets is entirely subtidal. In other instances, sand bodies clog the entrance to the inlet leading to the formation of several major and minor tidal channels.

At mixed energy tidal inlets the shape of the delta is the result of tidal and wave processes. These deltas have a well-formed main ebb channel, which is a product of ebb-tidal currents, their swash platform and sand bodies substantially overlap the inlet shore many times the width of the inlet throat due to wave processes and flood-tidal currents.

Ebb-tidal deltas may also be highly asymmetric such that the main ebb channel and its associated sand bodies are positioned primarily along one of the inlet shores. This configuration normally occurs when the major backbarrier channel approaches the inlet at an oblique angle or when preferential accumulation of sand on the updrift side of the ebb delta causes a deflection of the main ebb channel along the downdrift barrier shore.

Tidal inlet formation

The formation of a tidal inlet requires the presence of an embayment and the development of barriers. In coastal plain settings, the embayment or backbarrier was often created through the construction of the barriers themselves, like much of the East Coast of the United States or the Friesian Island coast along the North Sea. In other instances, the embayment was formed due to rising sea level inundating an irregular shore during the late Holocene. The embayed or indented shore may have been a rocky coast such as that of northern New England and California or it may have been an irregular unconsolidated sediment coast such as that of Cape Cod in Massachusetts or parts of the Oregon coast. The flooding of former river valleys has also produced embayments associated with tidal inlet development.

Breaching of a barrier

Rising sea level, exhausted sediment supplies, and human influences have led to thin barriers that are vulnerable to breaching. The breaching process normally occurs during storms after waves have destroyed the foredune ridge and storm waves have overwashed the barrier depositing sand aprons (washovers) along the backside of the barrier. Even though this process may produce a shallow overwash channel, seldom are barriers cut from their seaward side. In most instances, the breaching of a barrier is the result of the storm surge heightening waters in the backbarrier bay. When the level of the ocean tide falls, the elevated bay waters flow across the barrier toward the ocean gradually incising the barrier and cutting a channel. If subsequent tidal exchange between the ocean and bay is able to maintain the channel, a tidal inlet is established. The breaching process is enhanced when offshore winds accompany the falling tide and if an overwash channel is present to facilitate drainage across the barrier (Fisher, 1962). Many tidal inlets that are formed by this process are ephemeral and may exist for less than a year, especially if stable inlets are located nearby. Barriers most susceptible to breaching are long and thin and wave-dominated.

Spit building across a bay

The development of a tidal inlet by spit construction across an embayment usually occurs early in the evolution of a coast. The sediment to form these spits may have come from erosion of the nearby headlands, discharge from rivers, or from the landward movement of sand from inner shelf deposits. Most barriers along the coast of the United States and elsewhere in the world are 3,000–5,000 years old coinciding with a deceleration of rising sea level. It was then that spits began enclosing portions of the irregular rocky coast of New England, the West Coast, parts of Australia, and many other regions of the world. As a spit builds across a bay, the opening to the bay gradually decreases in width and in cross-sectional area. It may also deepen. Coincident with the decrease in size of the opening is a corresponding increase in tidal flow. The tidal prism of the bay remains approximately constant, so as the opening gets

smaller, the current velocities must increase. A tidal inlet is formed as the spit reaches a stable configuration.

Drowned river valleys

Tidal inlets have formed at the entrance to drowned river valleys due to the growth of spits and the development of barrier islands which have served to narrow the mouths of the estuaries. It has been shown through stratigraphic studies, particularly along the East Coast of the United States, that in addition to drowned river valleys, many tidal inlets are positioned in paleo river valleys in which there is no river leading to this site today (Halsey, 1979). These are old river courses that were active during the Pleistocene when sea level was lower and they were migrating across the exposed continental shelf. Tidal inlet become situated in these valleys because tidal currents easily remove the sediment filling the valleys.

Tidal inlet migration

Some tidal inlets have been stable since their formation, whereas others have migrated long distances along the shore. In New England and along other glaciated coasts, stable inlets are commonly anchored next to bedrock outcrops or resistant glacial deposits. Along the California coast most tidal inlets have formed by spit construction across an embayment with the inlet becoming stabilized adjacent to a bedrock headland. In coastal plain settings, stable inlets are commonly positioned in former river valleys. One factor that appears to separate migrating inlets from stable is the depth to which the inlet throat has eroded. Deeper inlets are often situated in consolidated sediments that resist erosion. The channels of shallow migrating inlets are eroded into sand.

Although the vast majority of tidal inlets migrate in the direction of dominant longshore transport, there are some inlets that migrate updrift (Aubrey and Speer, 1984). In these cases, the drainage of backbarrier tidal creeks control flow through the inlet. When a major backbarrier tidal channel approaches the inlet at an oblique angle, the ebb-tidal currents coming from this channel are directed toward the margin of the inlet throat. If this is the updrift side of the main channel, then the inlet will migrate in that direction. This is similar to a river where strong currents are focused along the outside of a meander bend causing erosion and channel migration. Inlets that migrate updrift are usually small to moderately sized and occur along coasts with small to moderate net sand longshore transport rates.

Tidal inlet relationships

Tidal inlets throughout the world exhibit several consistent relationships that have allowed coastal engineers and marine geologists to formulate predictive models: (1) Inlet throat cross-sectional area is closely related to tidal prism, and (2) Ebb-tidal delta volume is a function of tidal prism.

Inlet throat area–tidal prism relationship

The size of a tidal inlet is tied closely to the volume of water going through it (Figure T20(A); O'Brien, 1931, 1969). Although inlet size is primarily a function of tidal prism, to a lesser degree inlet cross-sectional area is also affected by the delivery of sand to the inlet channel. For example, at jettied inlets tidal currents can more effectively scour sand from the inlet channel and therefore they maintain a larger throat cross section than would be predicted by the O'Brien Relationship.

Similarly, for a given tidal prism, Gulf Coast inlets have larger throat cross sections than Pacific Coast inlets. This is explained by the fact that wave energy is greater along the West Coast and therefore the delivery of sand to these inlets is higher than at Gulf Coast inlets. Jarrett (1976) has improved the tidal prism-inlet cross-sectional area regression equation for US inlets, separating, into three classes the low-energy Gulf Coast inlets, moderate-energy East Coast inlets, and higher-energy West Coast inlets. Even better correlations are achieved when structured inlets are distinguished from natural inlet.

Variability. It is important to understand that the dimensions of the inlet channel are not static but rather the inlet channel enlarges and contracts slightly over relatively short-time periods (<1 year) in response to changes in tidal prism, variations in wave energy, effects of storms, and other factors. For instance, the inlet tidal prism can vary by more than 30% from neap to spring tides due to increasing tidal ranges. Consequently, the size of the inlet varies as a function of tidal phases. Along the southern Atlantic Coast of the United States water temperatures may fluctuate seasonally by 35–40°F. This and other factors cause the surface coastal waters to expand, raising mean sea level by 30 cm or more. In the summer and early fall, when mean sea level reaches its highest seasonal

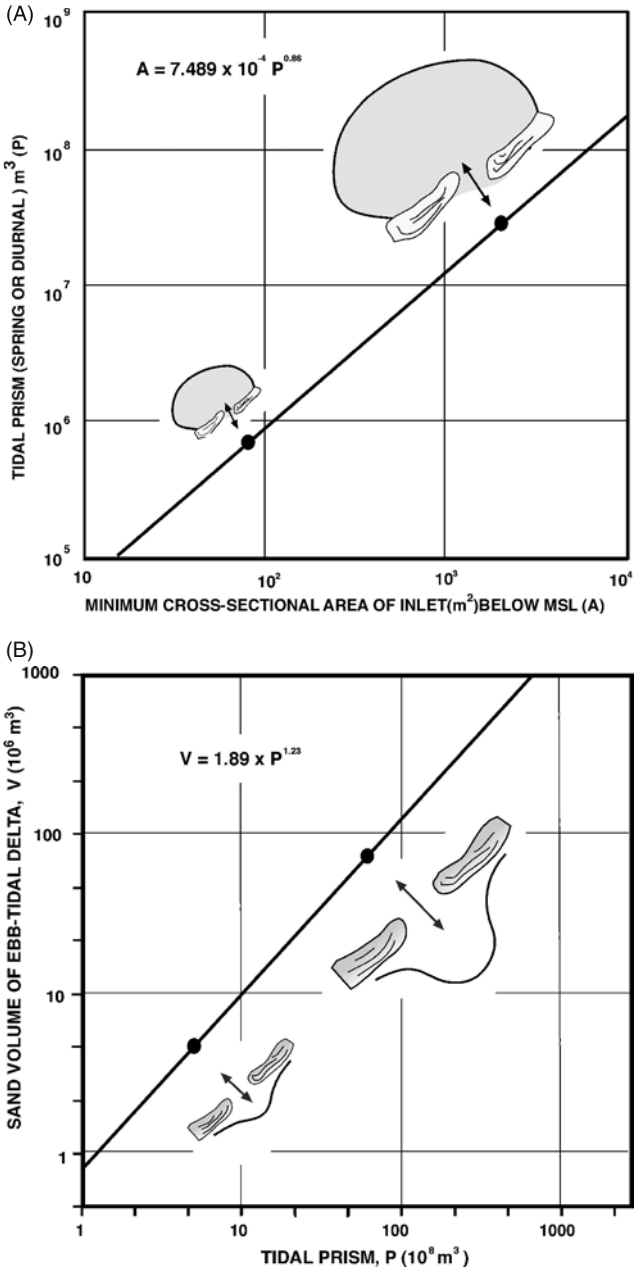

Figure T20 (A) Graph depicting relationship between tidal prism and inlet throat cross-sectional area (data after O'Brien, 1969). (B) Graph showing correspondence between tidal prism and volume of the ebb-tidal delta (data after Walton and Adams, 1976).

elevation, spring tides may flood backbarrier surfaces that normally are above tidal inundation. This produces larger tidal prisms, stronger tidal currents, increased channel scour, and larger inlet cross-sectional areas. At some Virginia inlets this condition increases the inlet throat by 5–15% (Byrne *et al.*, 1975). Longer-term (>1 year) changes in the cross section of inlets are related to inlet migration, sedimentation in the backbarrier, morphological changes of the ebb-tidal delta, and human influences.

Ebb-tidal delta volume–tidal prism relationship

In the mid-1970s, Walton and Adams (1976) showed that the volume of sand contained in the ebb-tidal delta is closely related to the tidal prism (Figure T20(B)). Walton and Adams also showed that the relationship was improved slightly when wave energy was taken into account in a manner similar to Jarrett's divisions. Waves are responsible for transporting sand back onshore thereby reducing the volume of the ebb-tidal

delta. Therefore, for a given tidal prism, ebb-tidal deltas along the West Coast contain less sand than do equal sized inlets along the Gulf or East Coast.

Variability. The Walton and Adams Relationship works well for inlets all over the world. However, field studies have shown that the volume of sand comprising ebb-tidal deltas changes through time due to the effects of storms, changes in tidal prism, or processes of inlet sediment bypassing (FitzGerald *et al*., 1984). When sand is moved past a tidal inlet, it is commonly achieved by large bar complexes migrating from the ebb delta and attaching to the landward inlet shoreline. These large bars may contain more than 300,000 m^3 of sand and represent more than 10% of sediment volume of the ebb-tidal delta (FitzGerald, 1988; Gaudiano and Kana, 2000).

Sand transport patterns

The movement of sand at a tidal inlet is complex due to reversing tidal currents, effects of storms, and interaction with the longshore transport system. The inlet contains short- and long-term reservoirs of sand varying from the relatively small sandwaves flooring the inlet channel that migrate meters each tidal cycle to the large flood-tidal delta shoals where some sand is recirculated but the entire deposit may remain stable for hundreds or even thousands of years. Sand dispersal at tidal inlets is complicated because in addition to the onshore–offshore movement of sand produced by tidal and wave-generated currents, there is constant delivery of sand to the inlet and transport of sand away from the inlet produced by the longshore transport system. In the discussion below the patterns of sand movement at inlets are described including how sand is moved past a tidal inlet.

General sand dispersal trends

The ebb-tidal delta has segregated areas of landward versus seaward sediment transport that are controlled primarily by the way water enters and discharges from the inlet as well as the effects of wave-generated currents. During the ebbing cycle the tidal flow leaving the backbarrier is constricted at the inlet throat causing the currents to accelerate in a seaward direction. Once out of the confines of the inlet, the ebb flow expands laterally and the velocity slows. Sediment in the main ebb channel is transported in a net seaward direction and eventually deposited on the terminal lobe due to this decrease in current velocity. One response to this seaward movement of sand is the formation of ebb-oriented sandwaves having heights of 1–2 m.

In the beginning of the flood cycle, the ocean tide rises while water in the main ebb channel continues to flow seaward as a result of momentum. Due to this phenomenon, water initially enters the inlet through the marginal flood channels, which are the pathways of least resistance. The flood channels are dominated by landward sediment transport and are floored by flood-oriented bedforms. On both sides of the main ebb channel, the swash platform is most affected by landward flow produced by the flood-tidal currents and breaking waves. As waves shoal and break, they generate landward flow, which augments the flood-tidal currents but retards the ebb-tidal currents. The interaction of these forces acts to transport sediment in net landward direction across the swash platform. In summary, at many inlets there is a general trend of seaward sand transport in the main ebb channel, which is countered by landward sand transport in the marginal flood channels and across the swash platform.

Inlet sediment bypassing

Along most open coasts, particularly in coastal plain settings, angular wave approach causes a net movement of sediment, which along much of the East Coast of the United States varies from 100 to 200,000 m^3/yr. The manner whereby sand moves past tidal inlets and is transferred to the downdrift shore is called inlet sediment bypassing. The primary mechanisms of sand bypassing natural inlets include: (l) Stable inlet processes, (2) Ebb-tidal delta breaching, and (3) Inlet migration and spit breaching. One of the end products in all the different mechanisms is the landward migration and attachment of large bar complexes to the inlet shore. Discussion of this topic can be found in FitzGerald (1982) and FitzGerald *et al*. (2000).

Stable inlet processes. This mechanism of sediment bypassing occurs at inlets that do not migrate and whose main ebb channels remain approximately in the same position. Sand enters the inlet by: (1) wave action along the beach, (2) flood-tidal and wave-generated currents through the marginal flood channel, and (3) waves breaking across the channel margin linear bars. Most of the sand that is dumped into the main channel is transported seaward by the dominant ebb-tidal currents and deposited on the terminal lobe.

At lower tidal elevations waves breaking on the terminal lobe transport sand along the periphery of the delta toward the landward beaches in much the same way as sand is moved in the surf and breaker zones along beaches. At higher tidal elevations waves breaking over the terminal lobe create swash bars on both sides of the main ebb channel. The swash bars (50–150 m long, 50 m wide) migrate onshore due to the dominance of landward flow across the swash platform. Eventually, they attach to channel margin linear bars forming large bar complexes. Bar complexes tend to parallel the beach and may be more than a kilometer in length. They are fronted by a slipface (25–33 degrees), which may be up to 3 m in height.

The stacking and coalescence of swash bars to form a bar complex is the result of the bars slowing their onshore migration as they move up the nearshore ramp. As the bars gain a greater intertidal exposure, the wave bores, which cause their migration onshore, act over an increasingly shorter period of the tidal cycle. Thus, their rate of movement onshore decreases. Eventually the entire bar complex migrates onshore and welds to the upper beach. When a bar complex attaches to the downdrift inlet shore, some of this newly accreted sand is then gradually transported by wave action to the downdrift beaches, thus completing the inlet sediment bypassing process. It should be noted that some sand bypasses the inlet independent of the bar complex. In addition, some of the sand comprising the bar reenters the inlet via the marginal flood channel and along the inlet shoreline.

Ebb-tidal delta breaching. This means of sediment bypassing occurs at inlets with a stable throat position, but whose main ebb channels migrate through their ebb-tidal deltas like the wag of a dog's tail. Sand enters the inlet in the same manner as described above for *Stable inlet processes*. However, at these inlets the delivery of sediment by longshore transport produces a preferential accumulation of sand on the updrift side of the ebb-tidal delta. The deposition of this sand causes a deflection of the main ebb channel until it nearly parallels the downdrift inlet shore. This circuitous configuration of the main channel results in inefficient tidal flow through the inlet, ultimately leading to a breaching of a new channel through the ebb-tidal delta. The process normally occurs during spring tides or periods of storm surge when the tidal prism is very large. In this state the ebb discharge piles up water at the entrance to the inlet where the channel bends toward the downdrift inlet shoreline. This causes some of the tidal waters to exit through the marginal flood channel or flow across low regions on the channel margin linear bar. Gradually over several weeks or convulsively during a single large storm, this process cuts a new channel through the ebb delta thereby providing a more direct pathway for tidal exchange through the inlet. As more and more of the tidal prism is diverted through the new main ebb channel, tidal discharge through the former channel decreases causing it to fill with sand.

The sand that was once on the updrift side of the ebb-tidal delta and which is now on the downdrift side of the new main channel is moved onshore by wave-generated and flood-tidal currents. Initially, some of this sand aids in filling the former channel while the rest forms a large bar complex that eventually migrates onshore and attaches to the downdrift inlet shore. The ebb-tidal breaching process results in a large packet of sand bypassing the inlet. Similar to the stable inlets discussed above, some sand bypasses these inlets in a less dramatic fashion, grain by grain on a continual basis.

It is noteworthy that at some tidal inlets the entire main ebb channel is involved in the ebb-tidal delta breaching process, whereas at others just the outer portion of main ebb channel is deflected. In both cases, the end product of the breaching process is a channel realignment that more efficiently conveys water through the inlet, as well as sand being bypassed in the form of a bar.

Inlet migration and spit breaching. A final method of inlet sediment bypassing occurs at migrating inlets. In this situation, an abundant sand supply and a dominant longshore transport direction cause spit building at the end of the barrier. To accommodate spit construction, the inlet migrates by eroding the downdrift barrier shore. Along many coasts as the inlet is displaced further along the downdrift shore, the inlet channel to the backbarrier lengthens retarding the exchange of water between the ocean and backbarrier. This condition leads to large water level differences between the ocean and bay, making the barrier highly susceptible to breaching, particularly during storms. Ultimately, when the barrier spit is breached and a new inlet is formed in a hydraulically more favorable position, the tidal prism is diverted to the new inlet and the old inlet closes. When this happens, the sand

comprising the ebb-tidal delta of the former inlet is transported onshore by wave action commonly taking the form of a landward migrating bar complex. It should be noted that when the inlet shifts to a new position along the updrift shore a large quantity of sand, has effectively bypassed the inlet. The frequency of this inlet sediment bypassing process is dependent on inlet size, rate of migration, storm history, and backbarrier dynamics.

Bar complexes. Depending on the size of the inlet, the rate of sand delivery to the inlet, the effects of storms, and other factors, the entire process of bar formation, its landward migration, and its attachment to the downdrift shore may take from 6 to 10 years. The volume of sand bypassed can range from 100,000 to over 1,000,000 m^3. The bulge in the shore that is formed by the attachment of a bar complex is gradually eroded and smoothed as sand is dispersed to the downdrift shore and transported back toward the inlet.

In some instances, a landward migrating bar complex forms a salt water pond as the tips of the arcuate bar weld to the beach stabilizing its onshore movement. Although the general shape of the bar and pond may be modified by overwash and dune building activity, the overall shore morphology is frequently preserved. Lenticular-shaped coastal ponds or marshy swales become diagnostic of bar migration processes and are common features at many inlets.

Tidal inlet effects on adjacent shorelines

In addition to the direct consequences of spit, accretion and inlet migration are the effects of volume changes in the size of ebb-tidal deltas, sand losses to the backbarrier, processes of inlet sediment bypassing, and wave sheltering of the ebb-tidal delta shoals (FitzGerald, 1988).

Number and size of tidal inlets

The degree to which barrier shore are influenced by tidal inlet processes is dependent on their size and number. As the O'Brien Relationship demonstrates, the size or cross-sectional area of an inlet is governed by its tidal prism. This concept can be expanded to include an entire barrier chain in which the size and number of inlets along a chain are primarily dependent on the amount of open water area behind the barrier and the tidal range of the region. In turn, these parameters are a function of other geological and physical oceanographic factors. Wave-dominated, microtidal coasts tend to have long barrier islands and few tidal inlets and mixed energy coasts have short stubby barriers and numerous tidal inlets (Hayes, 1975, 1979). Presumably, the mesotidal conditions produce larger tidal prisms than along microtidal coasts, which necessitate more holes in the barrier chain to let the water into and out of the backbarrier. Many coastlines follow this general trend but there are many exceptions due to the influence of sediment supply, large versus small bay areas, and other geological controls (Davis and Hayes, 1984).

Tidal inlets as sediment sinks

Tidal inlets not only trap sand temporarily on their ebb-tidal deltas, but they also are responsible for the longer-term loss of sediment moved into the backbarrier. At inlets dominated by flood-tidal currents, sand is continuously transported landward enlarging flood-tidal deltas and building bars in tidal creeks. Sand can also be transported into the backbarrier of ebb-dominated tidal inlets during severe storms. During these periods increased wave energy produces greater sand transport to the inlet channel. At the same time the accompanying storm surge increases the water surface slope at the inlet resulting in stronger than normal flood tidal currents. The strength of the flood currents coupled with the high rate of sand delivery to the inlet results in landward sediment transport into the backbarrier. Along the Malpeque barrier system in the Gulf of St. Lawrence, New Brunswick it has been determined that during a 33 year period 90% of the sand transferred to the backbarrier took place at tidal inlets and at former inlet locations along the barrier (Armon, 1979).

Sediment may also be lost at migrating inlets when sand is deposited as channel fill. If the channel scours below the base of the barrier sands, then the beach sand, which fills this channel, will not be replaced entirely by the deposits excavated on the eroding portion of the channel. Because up to 40% of the length of barriers is underlain by tidal inlet fill deposits ranging in thickness from 2 to 10 m (Moslow and Heron, 1978; Moslow and Tye, 1985) this volume represents a large, long-term loss of sand from the coastal sediment budget. Another major process producing sand loss at migrating inlets is associated with the construction of recurved spits that build into the backbarrier. For example, along the East Friesian Islands recurved spit development has caused the lengthening of barriers along this chain by 3–11 km since 1650. During this stage of barrier evolution the large size of the tidal inlets permitted ocean waves to transport large quantities of sand around the end of the barrier forming recurves that extend far into the backbarrier. Due to the size of the recurves and the length of barrier extension, this process has been one of the chief natural mechanisms of bay infilling (FitzGerald and Penland, 1987).

Changes in ebb-tidal delta volume

Ebb-tidal deltas represent huge reservoirs of sand that may be comparable in volume to that of the adjacent barrier islands along mixed-energy coasts (i.e., northern East and West Friesian Islands, Massachusetts, southern New Jersey, Virginia, South Carolina, and Georgia). For instance, the ebb-tidal delta volume of Stono and North Edisto Inlets in South Carolina is 197×10^6 m^3 and the intervening Seabrook-Kiawah Island barrier complex contains 252×10^6 m^3 of sand (Hayes *et al.*, 1976). In this case, the deltas comprise 44% of the sand in the combined inlet-barrier system. The magnitude of sand contained in ebb-tidal deltas suggests that small changes in their volume dramatically affect the sand supply to the landward shorelines.

A transfer of sand from the barrier to the ebb-tidal delta takes place when a new tidal inlet is opened, such as the formation of Ocean City Inlet when Assateague Island, Maryland was breached during the 1933 Hurricane. Initially, the inlet was only 3 m deep and 60 m across but quickly widened to 335 m when it was stabilized with jetties in 1935. Since the inlet formed more than 14 million cubic meters of sand have been deposited on the ebb-tidal delta. Trapping the southerly longshore movement of sand by the north jetty and growth of the ebb-tidal delta have led to serious erosion along the downdrift beaches. The northern end of Assateague Island has been retreating at an average rate of 11 m per year. The rate of erosion lessened when the ebb tidal delta reached an equilibrium volume and the inlet began to bypass sand (Stauble and Cialone, 1996).

In contrast to the cases discussed above, the historical decrease in the inlet tidal prisms along the East Friesian Islands has had a beneficial effect on this barrier coast. From 1650 to 1960 the reclamation of tidal flats and marshlands bordering the German mainland as well as natural processes, such as the building and landward extension of recurved spits, decreased the size of the backbarrier by 80%. In turn, the reduction in bay area decreased the inlet tidal prisms, which led to smaller sized inlets, longer barrier islands, and smaller ebb-tidal deltas. Wave action transported ebb-tidal delta sands onshore as tidal discharge decreased. This process increased the supply of sand to the beaches and aided in lengthening of the barriers (FitzGerald *et al.*, 1984).

Wave sheltering

The shallow character of ebb-tidal deltas provides a natural breakwater for the landward shore. This is especially true during lower tidal elevations when most of the wave energy is dissipated along the terminal lobe. During higher tidal stages intertidal and subtidal bars cause waves to break offshore expending much of their energy before reaching the beaches onshore. The sheltering effect is most pronounced along mixed-energy coast where tidal inlets have well-developed ebb-tidal deltas.

The influence of ebb shoals is particularly well illustrated by the history of Morris Island, South Carolina that forms the southern border of Charleston Harbor. Before human modification, the entrance channel to the harbor paralleled Morris Island and was fronted by an extensive shoal system. In the late 1800s jetties were constructed at the harbor entrance to straighten, deepen, and stabilize the main channel. During the period prior to jetty construction (1849–80) Morris Island had been eroding at an average rate of 3.5 m/yr. After the jetties were in place the shoals eroded and gradually diminished in size, so did the protection they afforded Morris Island, especially during storms. From 1900 to 1973 Morris Island receded 500 m at its northeast end increasing to 1,100 m at its southeast end, a rate three times what it had been prior to jetty construction (FitzGerald, 1988).

Effects of inlet pediment bypassing

Tidal inlets interrupt the wave-induced longshore transport of sediment along the coast, affecting both the supply of sand to the downdrift beaches and the position and mechanisms whereby sand is transferred to the downdrift shores. The effects of these processes are exhibited well along the Copper River Delta barriers in the Gulf of Alaska. From east to west along the barrier chain the width of the tidal inlets increases as

does the size of the ebb-tidal deltas (Hayes, 1979). In this case, the width of the inlet can be used as a proxy for the inlet's cross-sectional area. These trends reflect an increase in tidal prism along the chain, which is caused by an increase in bay area from east to west while tidal range remains constant. Also quite noticeable along this coast is the greater downdrift offset of the inlet shore in a westerly direction. This morphology is coincident with an increase in the degree of overlap of the ebb-tidal delta along the downdrift inlet shoreline. The offset of the inlet shore and bulbous shape of the barriers are produced by sand being trapped at the eastern, updrift end of the barrier. The amount of shore progradation (build out) is a function of inlet size and extent of its ebb-tidal delta. What we learn from the sedimentation processes along the Copper River Delta barriers is that tidal inlets can impart a very important signature on the form of the barriers (FitzGerald, 1996).

Drumstick barrier model. In an investigation of barrier islands shores in mixed energy settings throughout the world, Hayes (1979) noted that many barriers exhibit a drumstick barrier island shape. In this model, the meaty portion of the drumstick barrier is attributed to waves bending around the ebb-tidal delta producing a reversal in the longshore transport direction. This process reduces the rate at which sediment bypasses the inlet, resulting in a broad zone of sand accumulation along the updrift end of the barrier. The downdrift, or thin part of the drumstick, is formed through spit accretion. Later studies demonstrated that landward-migrating bar complexes from the ebb-tidal delta determine barrier island morphology and overall shore erosional–depositional trends, particularly in mixed energy settings.

Studies of the Friesian Islands demonstrate that inlet processes exert a strong influence on the dispersal of sand and in doing so dictate barrier form (FitzGerald *et al*., 1984). In addition to drumsticks, the East Friesian Islands exhibit many other shapes. Inlet sediment bypassing along this barrier chain occurs, in part, through the landward migration of large swash bars (>1 km in length) that deliver up to 300,000 m^3 of sand when they weld to the beach. In fact, it is the position where the bar complexes attach to the shore that determines the form of the barrier along this coast. If the ebb-tidal delta greatly overlaps the downdrift barrier, then the bar complexes may build up the barrier shore some distance from the tidal inlet, forming *humpbacked barriers*. If the downdrift barrier is short and the ebb-tidal delta fronts a large portion of the downdrift barrier, then bar complexes weld to the downdrift end of the barrier forming *downdrift bulbous barriers*.

Human influences

Dramatic changes to inlet beaches can also result from human influences including the obvious consequences of jetty construction that reconfigures an inlet shore. By preventing or greatly reducing an inlet's ability to bypass sand, the updrift beach progrades while the downdrift beach, whose sand supply has been diminished or completely cut off, erodes. There can also be more subtle human impacts that can equally affect inlet shores, especially those associated with changes in inlet tidal prism, sediment supply, and the longshore transport system. Nowhere are these types of impacts better demonstrated than along the central Gulf Coast of Florida where development has resulted in the construction of causeways, extensive backbarrier filling and dredging projects, and the building of numerous engineering structures along the coast. A detailed study of this region by Barnard and Davis (1999) has revealed that since the late-1980s 17 inlets have closed along this coast and at least five closures can be traced to human influences caused primarily by changes in inlet tidal prism. For example, access to several barriers has been achieved through the construction of causeways that extend from the mainland across the shallow bays. Along most of their lengths the causeways are dike-like structures that partition the bays, thereby changing bay areas and inlet tidal prisms. In some instances, tidal prisms were reduced to a critical value causing inlet closure. At these sites, the tidal currents were unable to remove the sand dumped into the inlet channel by wave action. Similarly, when the Intracoastal Waterway was constructed along the central Gulf Coast of Florida in the early 1960s, the dredged waterway served to connect adjacent backbarrier bays thereby changing the volume of water that was exchanged through the connecting inlets. The Intracoastal Waterway lessened the flow going through some inlets while at the same time increased the tidal discharge of others. This resulted in the closure of some inlets and the enlargement of others (Barnard and Davis, 1999).

Duncan M. FitzGerald

Bibliography

Armon, J.W., 1979. Landward sediment transfers in a transgressive barrier island system, Canada. In Leatherman, S.P. (ed.), *Barrier Islands: From the Gulf of St. Lawrence to the Gulf of Mexico*. New York: Academic Press, pp. 65–80.

Aubrey, D.G., and Speer, P.E., 1984. Updrift migration of tidal inlets. *Journal of Geology*, **92**: 531–546.

Barnard, P.L., and Davis, R.A., 1999. Anthropogenic versus natural influences on inlet evolution: West-Central Florida. *Proceedings, Coastal Sediments '99, ASCE*, pp. 1489–1504.

Boothroyd, J.C., Friedrich, N.E., and McGinn, S.R., 1985. Geology of microtidal coastal lagoons, RI. In Oertel, G.F., and Leatherman, S.P. (ed.), *Barrier Islands. Marine Geology*, **63**: 35–76.

Byrne, R.J., Bullock, P., and Taylor, D.G., 1975. Response characteristics of a tidal inlet: a case study. In Cronin, L.E. (ed.), *Estuarine Research*, Vol. 2. New York: Academic Press, pp. 201–216.

Davis, R.A., Jr., and Hayes, M.O., 1984. What is a wave-dominated coast? *Marine Geology,* **60**: 313–329.

Fisher, J.J., 1962. Geomorphic expression of former inlets along the Outer Banks of North Carolina, unpub. Masters thesis. Chapel Hill: University of North Carolina.

FitzGerald, D.M., 1982. Sediment bypassing at mixed energy tidal inlets. *Proceedings 18th Coastal Engineering Conference*, *ASCE*, pp. 1094–1118.

FitzGerald, D.M., 1988. Shoreline erosional–depositional processes associated with tidal inlets. In Aubrey, D.G., and Weishar, L. (eds.), *Hydrodynamics and Sediment Dynamics of Tidal Inlets.* Berlin: Springer, pp. 186–225.

FitzGerald, D.M., 1996. Geomorphic variability and morphologic and sedimentological controls on tidal inlets. In Mehta, A.J. (ed.), *Understanding Physical Proc.* at Tidal Inlets. *Journal of Coastal Research* (Special Issue), **23**: 47–71.

FitzGerald, D.M., Kraus, N.C., and Hands, E.B., 2000. Natural mechanisms of sediment bypassing at tidal inlets, ERDC/CHL-IV-Vicksburg, MS: US Army Engineer Research and Development Center.

FitzGerald, D.M., and Penland, S., 1987. Backbarrier dynamics of the East Friesian Island. *Journal of Sedimentary Petrology,* **57**: 746–754.

FitzGerald, D.M., Penland, S., and Nummedal, D., 1984. Control of barrier island shape by inlet sediment bypassing: East Friesian Islands, West Germany. *Marine Geology*, **60**: 355–376.

Gaudiano, D.J., and Kana, T.W., 2000. Shoal bypassing in South Carolina tidal inlets: geomorphic variables and empirical predictions for nine mesoscale inlets. *Journal of Coastal Research*, **17**: 280–291.

Halsey, S., 1979. Nexius: a new model of barrier island development. In Leatherman, S.P. (ed.), *Barrier Islands: From the Gulf of St. Lawrence to the Gulf of Mexico*. New York: Academic Press, pp. 185–210.

Hayes, M.O., 1975. Morphology of sand accumulations in estauries. In Cronin, L.E. (ed.), *Estuarine Research*, Vol. 2. New York: Academic Press, pp. 3–22.

Hayes, M.O., 1979. Barrier island morphology as a function of tidal and wave regime. In Leatherman, S.P. (ed.), *Barrier Islands: From the Gulf of St. Lawrence to the Gulf of Mexico*. New York: Academic Press, pp. 1–28.

Hayes, M.O., FitzGerald, D.M., Humes, L.J., and Wilson, S.J., 1976. *Geomorphology of Kiawah Island, South Carolina*, Columbia: Coastal Research Division, University of South Carolina, pp. 80–100.

Jarrett, J.T., 1976. Tidal prism–inlet area relationships. Vicksburg, MS: Us Army Corps of Engineers, Waterways Experiment Station, GITI Report No. 3.

Moslow, T.F., and Heron, S.D., 1978. Relict inlets: preservation and occurrence in the Holocene stratigraphy of southern Core Banks, North Carolina. *Journal of Sedimentary Petrology*, **48**: 1275–1286.

Moslow, T.F., and Tye, R.S., 1985. Recognition and characteristic of Holocene tidal inlet sequences. *Marine Geology*, **63**: 129–151.

O'Brien, M.P., 1931. Estuary tidal prisms related to entrance areas. *Civil Engineering*, **1**: 738–739.

O'Brien, M.P., 1969. Equilibrium flow areas of inlets on sandy coasts. *Journal of Waterways*, *Harbors, and Coastal Engineering ASCE*, **95**: 43–55.

Stauble, D.K., and Cialone, M.A., 1996. Ebb shoal evolution and sediment management techniques Ocean City Inlet, Maryland. *Procedings 9th National Conference on Beach Nourishment*, St. Petersburg, FL, pp. 209–224.

Walton, T.L., and Adams, W.D., 1976. Capacity of inlet outer bars to store sand. *Proceedings of 15th Coastal Engineering Conference*, ASCE, Honolulu, Hawaii, pp. 1919–1937.

Cross-references

Bars
Barrier Islands
Bypassing at Littoral Drift Barriers
Coasts, Coastlines, Shores, and Shorelines
Longshore Sediment Transport
Shore Protection Structures
Spits
Tidal Prism
Tide-Dominated Coasts
Wave-and-Tide Dominated Coasts
Wave-Dominated Coasts

TIDAL FLATS

Introduction and definition

Tidal flats are low-gradient tidally inundated coastal surfaces. Jackson (1997) defines them as extensive, nearly horizontal, marshy or barren tracts of land alternately covered and uncovered by the tide, and consisting of unconsolidated sediment. Tidal flats may be muddy, sandy, gravelly, or covered in shell pavements, and compositionally they may be underlain by siliciclastic or carbonate sediments. Depending on climate, tidal level, substrate and salinity, tidal flats may be covered biologically in parts by salt marsh, mangroves, sea grass, algal mats, microbial mats, biofilms, as well as mussel beds, oyster beds and reefs, and worm-tube beds and reefs, and inhabited by a burrowing benthos of molluscs, polychaetes, and crustacea.

Tidal flats have been of great interest to sedimentologists and stratigraphers as coastal systems that are readily accessible to sampling and study, and rich in processes and products resulting from oceanographic, sedimentologic, geohydrologic, hydrochemical, and biotic interactions (Ginsburg, 1975; Klein, 1976; Alexander *et al*., 1998; Black *et al*., 1998). They contrast with other steeper gradient wave-dominated sedimentary coasts, such as sandy beaches, composed dominantly of sand, and with a relatively limited biota, because with their generally lower energy conditions, and less scope for physical reworking, tidal flats develop a profusion of natural history coastal features. For instance, there are the sedimentologic products of interactions between waves and tides (e.g., cross-laminated sand, ripple-laminated sand, lenticular bedding, flazer bedding, laminated mud, ripple-laminated silt in clay), the products of interactions between sediments and biota (e.g., various burrow forms zoned tidally across the shore, various types of root-structuring, skeletal remains related to tidal levels), the geomorphic products of tides (e.g., tidal runoff on low gradient slopes to form meandering tidal creeks), and the products of hydrochemical interactions with sediments (e.g., dissolution of carbonate by acidic pore water; cemented crusts and their breccia and intraclast derivatives; carbonate nodules; gypsum precipitates; and products of redox reactions such as biologically mediated precipitation of iron sulfide). For stratigraphers and students of sedimentary rocks, identifying tidal flats in the geologic record is often an important step in the reconstruction of paleoenvironments, the location of facies associated with coastlines, and the recognition of such markers in stratigraphic sequences in basin analyses. Tidal flat signatures derived from studies of modern environments provide important analogs in such analyses.

Coastal settings of tidal flats

Tidal flats around the globe occur in a variety of regional geomorphic settings (Table T4 and Figure T21). Since they are surfaces exposed and inundated by tides, they may simply be part of larger coastal systems, that is, the shores of deltas, estuaries, lagoons, gulfs, bays, straits, rias, sounds, and cuspate forelands. Alternatively, they may be the sole coastal form developed along an open coast or broad embayment, or may comprise wholly tidal lagoons leeward of barriers. The best-developed tidal flats occur along estuarine coasts, protected embayments, or barred lagoons, where the shore slopes are gentle due to sediment accretion, and tides are large. Along many coasts, tidal flats are part of prograded shores (Kendall and Skipwith, 1968; Thompson, 1968; Hagan and Logan, 1975; Reineck and Singh, 1980); but in some instances, they may comprise modern sediment veneers on wave or tidally cut unconformities on rock or Pleistocene sediment, or earlier Holocene sediments (Semeniuk, 1981).

Tides and tidal levels

The tidal ranges that expose tidal flats vary globally from less than 1 m to ca. 15 m amplitude, and are diurnal (one tide daily), semidiurnal (two tides daily), or mixed (two tides daily, but with inequality between tide maxima and tide minima across the day). Over a lunar cycle, tides vary from a lower amplitude neap range (during quarter and three-quarter moon phases) to a higher amplitude spring range (during new and full moon phases). Higher than normal tides occur during equinoctial periods, and in response to the Lunar Nodal Periodicity. As a result, and depending on shore slope, tidal flat width may vary from being a narrow coastal strip, to being broad and expansive coastal forms.

Part of the coast emergent during low tide and submerged during high tide is the *intertidal* zone. That part of the coast permanently submerged below the low-water line is the *subtidal* zone. That occurring above the zone of high-tide inundation is the *supratidal* zone. Some authors consider the "supratidal zone" as the zone above the mean high-water line but sometimes under the water during extremely high tides, or even spring tides, but it is preferable to refer to all gently inclined surfaces and terrain *above* the highest tides as supratidal, and to treat all surfaces flooded by both neap, spring, and equinoctial spring tides as intertidal, and to separate these various tidal zones and levels.

Tidal ranges have been classed by Davies (1980) into three groups: *microtidal* <2 m, *mesotidal* 2–4 m, and *macrotidal* >4 m. While this classification has been generally accepted, large tidal ranges >8 m, might be further classed as *extreme macrotidal*. Generally, tides are microtidal along open oceanic coasts, and tend towards macrotidal where tides are semidiurnal. Tidal range amplification also may occur due to bay geometry and coastal constriction. For example, the Bay of Fundy, in Nova Scotia, because of its basin geometry, amplifies the tide from ca. 5.4 m at entrance to the bay to 15 m at its head.

Zones across the tidal flats are best exhibited in macrotidal settings, where there are marked distinctions in slope, sediments, and biology between the interval of spring tidal and neap tidal range. On microtidal flats, these various differences related to tidal levels are less pronounced.

Various levels within a tidal flat, often delineated by biological and/or sediment zones, can be distinguished as follows:

- low tidal flats—exposed by the mean and extreme low spring tides, generally underlain by sand, and vegetation free,
- middle tidal flats—the flats and low gradient slopes centered around mean sea level, exposed and inundated by neap tides; the upper parts of these flats may be vegetated by samphire in temperate latitude areas, and by mangrove in tropical latitudes,
- high tidal flats—inundated by the mean and extreme high spring tides, generally underlain by mud, and vegetated by salt marsh or mangrove, or in more arid settings, vegetation free and salt encrusted (salt flat).

Typical cross sections through some microtidal to extreme macrotidal flats are shown in Figure T22.

Tidal flats and their particle sizes and sediment composition

Tidal flats may be underlain by mud, sand, rock gravel, and shell pavements, or mixtures of these. Often, where all particle sizes are present, there is a zonation of sediment types across the flats, or an interlayering at a specific tidal level, but in many instances, one sediment type may dominate across the entire tidal flat. This partitioning of sediments across the tidal flat lends itself to a classification of tidal flats, or zones within tidal flats, according to particle size. For example, those composed wholly of mud may be termed muddy tidal flats, and those composed wholly of sand are sandy tidal flats. Tidal level zones within the tidal flat may be classed according to substrate, for example, sandy low tidal flats, muddy high tidal flats. A range of possible tidal flat types based on substrate, with field examples, is presented in Table T5.

In regard to sediment composition, two major groups are recognized: *siliciclastic tidal flats*, composed of terrigenous sediments such as quartz sand, quartz silt, and phyllosilicate clay, and *carbonate tidal flats*, composed of carbonate silt and clay, various sand-sized carbonate grains, and products of cementation (e.g., crusts, breccias, intraclasts). These major groups reflect two extremes in settings: an abundant supply of terrigenous sediment to the tidal coast, such as in deltas or estuaries versus a low supply relative to the rate of carbonate sediment production (as along terrigenous sediment starved coasts). From a historical perspective, the majority of earlier investigations of tidal flats were centered on siliciclastic systems, and much information emerged from studies in the North Sea (Reineck, 1972; Evans, 1975). Later,

Table T4 Some well-known tidal flats, and some extreme macrotidal flats, ordered in tidal range

Tidal flat location	Tidal range (m)	Composition	Tidal flat setting
Bay of Fundy (Nova Scotia)	15.0 m Extreme Macrotidal	Siliciclastic	Broad tidal flats of gravel, sand and mud, with local salt marsh, peripheral to an estuarine gulf in a humid temperate climate (Knight and Dalrymple, 1975)
Bay of Mont St Michel (NW France)	15.0 m Extreme Macrotidal	Siliciclastic	Broad tidal flats of sand and mud, with salt marsh, within complex of funnel-shaped estuary in humid temperate climate (Larsonneur, 1975)
King Sound (NW Australia)	11.0 m Extreme Macrotidal	Siliciclastic	Broad tidal flats of sand and mud, with some cheniers, and erosional tidal channels, with mangrove; peripheral to a seasonal estuarine gulf in a semi-arid tropical climate (Semeniuk, 1981)
Roebuck Bay (NW Australia)	10.5 m Extreme Macrotidal	Carbonate	Broad tidal flats along semi-sheltered embayment, dominated by mud; erosional tidal channels, with mangrove; in a semi-arid subtropical climate (Semeniuk, 1993)
Gulf of California (USA)	6–8 to 10 m Macrotidal to extreme macrotidal	Siliciclastic	Broad tidal flats, dominated by mud, with intermittent beach ridges, with salt marsh; part of the Colorado River Delta within a gulf in a semiarid subtropical climate (Thompson, 1968)
The Wash (England)	7.0 m Macrotidal	Siliciclastic	Broad tidal flats of sand and mud, with salt marsh; along the shore of a large embayment in humid temperate climate (Evans, 1975)
Delta of the Klang and Langat Rivers (Malaysia)	4.5 m Macrotidal	Siliciclastic	Compound delta, with insular/peninsular development of tidal flats, traversed by tidal creeks with mangrove; in a humid tropical climate (Coleman *et al*., 1970)
The Jade and the Dutch Wadden Sea (North Sea)	2.6–4.1 m Mesotidal	Siliciclastic	Broad tidal flats of sand and mud, with salt marsh, leeward of barriers in humid temperate climate (Reineck, 1975)
Niger Delta (Western Africa)	1.0–2.8 m Microtidal	Siliciclastic	Extensive mangrove vegetated tidal flats of mud and sand, developed behind a beach barrier in a delta system in a humid tropical climate (Allen, 1970)
Gascoyne Delta (Western Australia)	2 m Microtidal	Siliciclastic	Local narrow tidal flats of sand and mud, with mangrove, fringing lagoons within a delta in an arid subtropical climate (Johnson, 1982)
Trucial Coast (western Persian Gulf)	2 m Microtidal	Carbonate	Broad tidal flats of carbonate muds and gypsum, with algal mats, salt marsh and mangroves, shoreward of prograding carbonate complex fringing a large gulf in an arid tropical climate (Purser, 1973)
Chesapeake Bay (eastern USA)	1.5–2.1 m Microtidal	Siliciclastic	Narrow to broad tidal flats, with salt marsh, within inlets and along the shore of an estuary in a humid temperate climate
Delmarva Peninsula to Sapelo Island (eastern USA)	<1 m Microtidal	Siliciclastic	Broad protected tidal flats, with salt marsh, leeward of barriers in a humid subtropical climate (Howard *et al*., 1972; Harrison, 1975)
Shark Bay (Western Australia)	0.5 m Microtidal	Carbonate	Local tidal flats of sand or pelleted mud, with salt marsh and algal mat, shoreward of prograding sea grass banks and hypersaline platforms in large elongate embayments in an arid subtropical climate (Hagan and Logan, 1975)
Andros Island (Bahamas)	0.5 m Microtidal	Carbonate	Broad tidal flats of pelleted mud, with mangrove, salt marsh and algal mat, developed capping the Bahama Bank Carbonate Complex in a humid subtropical climate (Shinn *et al*., 1969)

as interest in carbonate rocks grew during the 1960s, linked to their petroleum reservoir potential, a range of studies were undertaken in carbonate tidal flats (Shinn *et al*., 1969; Purser, 1973; Hagan and Logan, 1975; Shinn, 1983).

Generally, regardless of whether the tidal flats are dominantly siliciclastic or carbonate, their sediments commonly contain both siliciclastic *and* carbonate particles. In dominantly siliciclastic settings, there may be minor to moderate carbonate components of shell gravel, shell grit, skeletal sand (e.g., shell fragments, foraminifera), skeletal silt-sized material, and carbonate clay transported to or generated on the flats. Similarly, in dominantly carbonate environments there may be siliciclastic sand, mud, or gravel from oceanic, aeolian, or local erosional sources. The range and origin of mud, sand, and gravel-sized particles comprising tidal flat sediments are noted in Table T6.

Some of the best known siliciclastic tidal flats are along the North Sea coast, for example, the Jade and the Dutch Wadden Sea, The Wash in southeastern England, the Gulf of California, the Bay of Fundy, the compound high-tidal delta of the Klang and Langat Rivers, King Sound in northwestern Australia, Bay of Mont St. Michel in France (Klein, 1963; Thompson, 1968; Allen, 1970; Coleman *et al*., 1970; Reineck, 1972; Evans, 1975; Larsonneur, 1975; Semeniuk, 1981). With most of these examples, there is a grain size variation across the flats from sand in low tidal zones to mud in high tidal zones, with specific biogenic contributions in particular tidal zones, depending on climate setting and biogeography, and sediment types and sedimentary structures are dominantly the result of physical and biologic processes. With increase upslope in pore water salinity, particularly in semiarid and arid climates, the upper parts of siliciclastic tidal flats may develop carbonate nodules or gypsum crystals, or be salt encrusted.

Carbonate tidal flats generally occur in mid- to low latitude warm climates. The best known are Andros Island of the Bahama Banks (Shinn *et al*., 1969), the Trucial Coast along the Persian Gulf Coast (Kendall and Skipwith, 1968; Purser, 1973), and Shark Bay in northwestern Australia (Hagan and Logan, 1975). In these examples, there is little or no terrigenous influx from terrestrial sources to dilute the carbonate accumulation contributed by local biogenic and abiotic sources, and hence the sediments are carbonate-rich. There are a range of diagnostic sediments and structures formed on carbonate tidal flats as result of tidal deposition, biogenic contribution and alteration, and primary and secondary effects of cementation. Cementation of sediments, and formation of their (secondary) structural and sedimentary derivatives is an important and common feature on upper parts of carbonate tidal flats. Under conditions of hypersalinity on the higher zones of such tidal flats, precipitation of carbonate-minerals often is prevalent, and in contrast to siliciclastic tidal flats, since there is an abundance of carbonate grains to act as nuclei for interstitial cements, there is a plethora of diagenetic and sedimentary products such as cemented layers and crust development, progressing to surface mounding, formation of compressional polygons and teepees, and then leading to fragmentation, brecciation, and formation of intraclasts. Carbonate tidal flats set in the

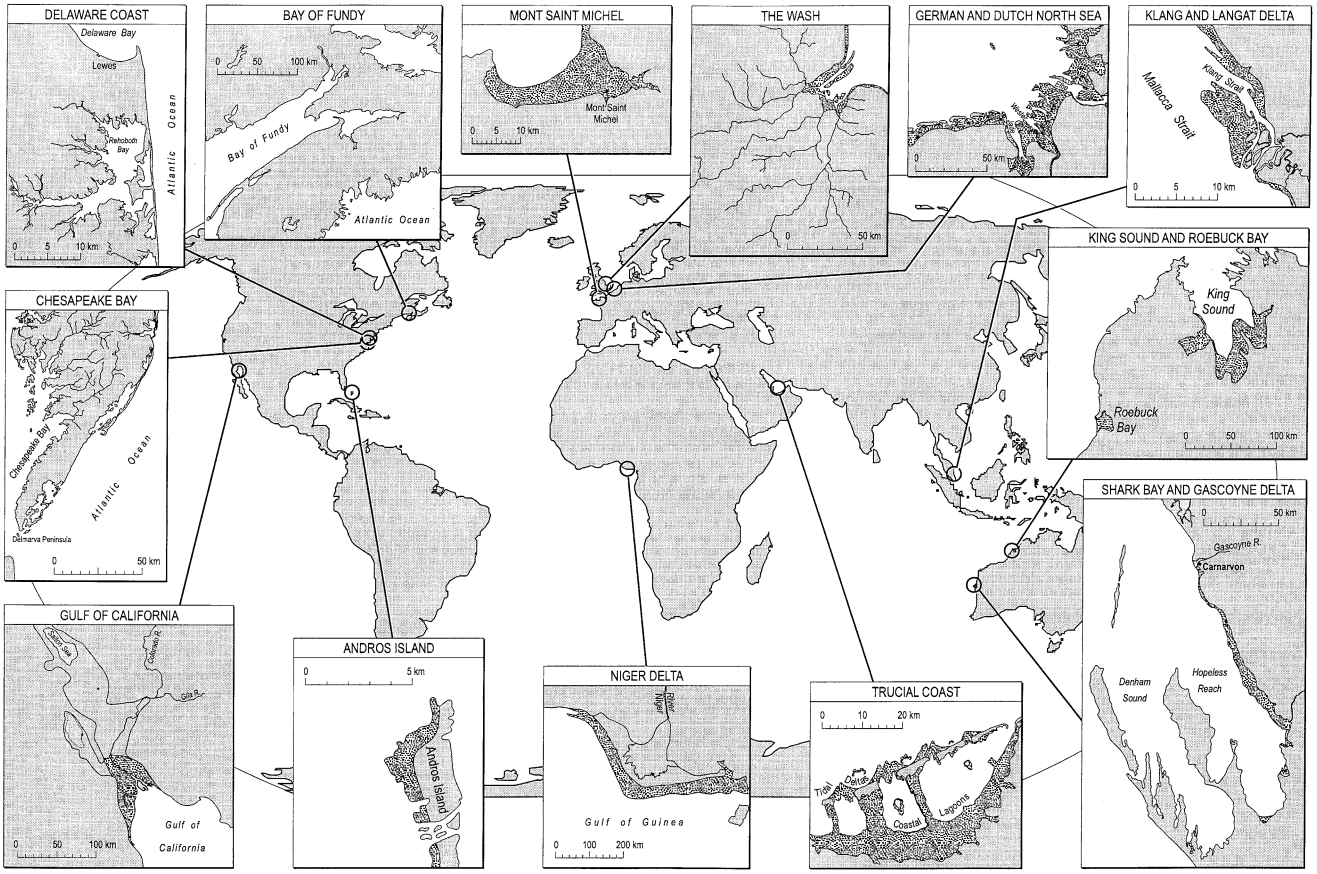

Figure T21 Location, settings, and sizes of various tidal flats around the globe. Table T4 provides more detailed information and references.

more arid climates also develop evaporitic mineral suites such as beds of gypsum nodules, gypsum platey crystals, gypsum mud, halite crusts.

Geomorphic features of tidal flats

While the surface of a tidal flat at the macroscale generally is flat to gently inclined, there may be a range of mesoscale to microscale features therein (Table T7, Figure T23). At the macroscale, the tidal flat may exhibit varying degrees of slope (Figure T22), reflecting the effects of position within either the low and high spring tidal zones, or the neap tidal zone. For example, the low tidal zone may be nearly flat or very gently inclined, the middle tidal flat may be more moderately inclined, and the high tidal flat again may be nearly flat or very gently inclined.

At mesoscale, the geomorphic features of tidal flats may include local cliffs, cheniers, sand waves, shell mounds, skeletal reefs, and gullies, channels and creeks (also called tidal creeks). Cliffs, commonly cut into mud, often separate vegetated and vegetation-free tidal flat zones, but some cliffs are formed due to either the effect of wave energy concentrated at a specific tidal level, or the undercutting of mud through erosion of the underlying sand. Tidal creeks may be ramifying or meandering, with point bars and steep banks. At smaller scales, the surface of tidal flats may be planar and smooth, or hummocky to slightly irregular, or may exhibit linear scours, surface mounding and teepees, desiccation polygons, or mud cracks, produced physically, chemically, or biogenically.

Hydrology

The groundwater hydrology of tidal flats is important for several reasons. Interstitial pore water salinity gradients and moisture gradients, for instance, influence macrophytes (such as mangroves and samphires), microbial mats, and invertebrate biota in relation to their occurrence and zonation. Interstitial pore water salinity and moisture gradients also influence precipitation of evaporitic minerals. Microscale shallow groundwater hydrologic recharges and discharges influence development of sedimentary structures (e.g., seepage zones out of sand mounds to initiate sand erosion, or to initiate hydrochemical exchanges and cementation; formation of bubble sand). The hydrologic functioning of tidal flats additionally can drive geochemical processes that diagenetically modify sediments (e.g., formation of iron sulfide precipitation to form gray sediments, or the oxidation of buried iron sulfide impregnated vegetation to form goethite pseudomorphs).

Tidal flat groundwater levels fluctuate on a diurnal to semidiurnal basis, following the tides, with a dampened effect from mid-tidal levels to upslope. All tidal flat groundwater rises during flood tide, and of course is inundated on high tide. Recharge and discharge, and lateral groundwater flow through tidal flat sediments may be facilitated by specific lithologic layers, or stratigraphic intervals, and at the small scale by burrow and root structures.

Groundwater salinity across tidal flats is commonly zoned, generally with near marine water salinities at about mean sea level, unless the marine waters fronting the tidal flats are hypersaline (e.g., Shark Bay, Australia), grading to hypersaline and extremely hypersaline upslope, and in wet climates becoming fresh where tidal flats interact with terrestrial freshwater. The main source waters for groundwater of tidal flats are marine water, rain, and (through seepage and land overflow) land-derived freshwater. Evaporation, macrophyte transpiration, and increasing infrequency of tidal inundation upslope combine to develop a gradient of increasing salinity across tidal flats. This gradient results in zonation of biota, exemplified by zonation of mangroves, and in zonation of evaporitic minerals and pore water precipitates. Where marine waters are oceanic (ca. 35,000 ppm salinity) and evaporation is extreme, high tidal groundwater may reach 100,000–200,000 ppm salinity, that is, carbonate mineral and gypsum precipitating, but where source waters are already hypersaline, tidal flat groundwater reaches up to ca. 300,000 ppm salinity, resulting in precipitation of halite.

Key processes on tidal flats

Tidal flats are located at the triple junction between land, sea, and atmosphere. In this context, as low-gradient shores, they exhibit a myriad of

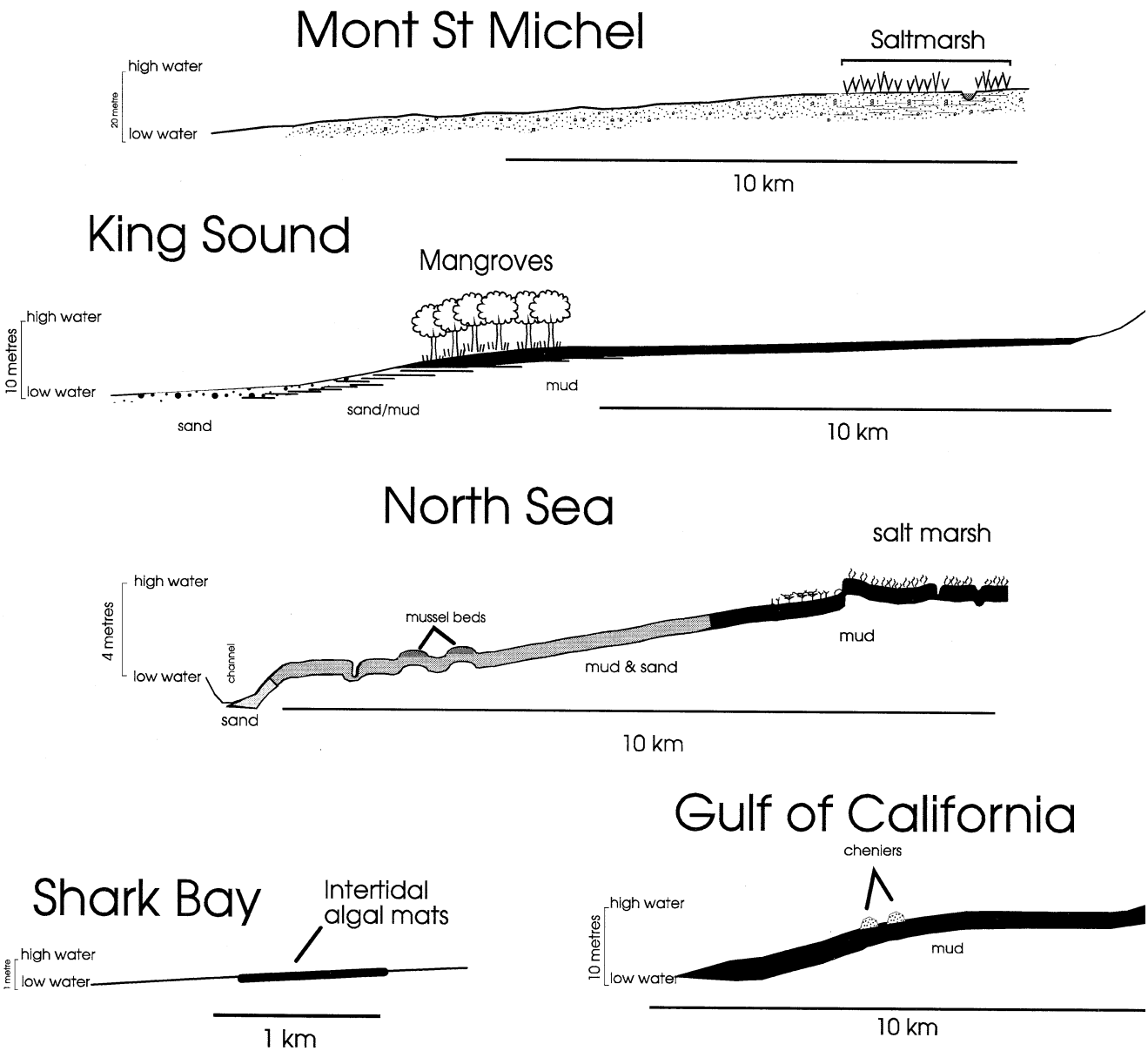

Figure T22 Profiles across various macrotidal to microtidal siliciclastic and carbonate tidal flats (see Table T4) showing nature of the slopes, sediments, vegetation, or morphology.

Table T5 Tidal flat types, according to substrate

Substrate type underlying tidal flat	Terminology	Examples
Whole tidal flats		
Mix of particle sizes across the whole tidal flat, or differentiation not intended	Tidal flat	North Sea, The Wash, Bay of Mont St. Michel, King Sound
Tidal flats wholly underlain mainly by		
mud	Muddy tidal flat	Gulf of California
sand	Sandy tidal flat	
gravel	Gravelly tidal flat	Parts of the Bay of Fundy
shelly pavement across tidal flat	Tidal shell pavement	
Specific zones on tidal flats		
High tidal flats wholly underlain mainly by mud	Muddy high-tidal flat	King Sound
Mid-tidal flats wholly underlain mainly by mud	Muddy mid-tidal flat	King Sound
Mid-tidal flats underlain mainly by mud and sand	Mixed mid-tidal flat	North Sea
Low tidal flats wholly underlain mainly by sand	Sandy low-tidal flat	North Sea; Bay of Mont St. Michel
Shelly pavement on specific zone of tidal flat, e.g., low tidal	Low-tidal shell pavement	Parts of Shark Bay
Crust pavement on specific zone of tidal flat, e.g., high tidal	High-tidal crust pavement	Dampier Archipelago
Breccia pavement on specific zone of tidal flat, e.g., high tidal	High-tidal breccia pavement	Parts of Shark Bay

Table T6 Types of sedimentary particles on tidal flats, and their origin

Sediment particle	Origin (information from various tidal flats)
Clay (<4 μm particle size)	
Phyllosilicate clay (kaolinite, illite, montmorillonite)	Fluvially delivered to the coastal system Reworked Pleistocene coastal deposits Reworking of glacial deposits Aeolian
Calcitic and aragonitic clay	Reworked, comminuted skeletons Precipitated from seawater Disintegrated calcareous algae
Goethite	Fluvially delivered to the coastal system Aeolian
Quartz clay	Aeolian
Amorphous silica	Diatom (*in situ* or transported)
Silt (4–63 μm particle size)	
Quartz, felspar, various silicate minerals	Fluvially delivered to the coastal system Reworked Pleistocene coastal deposits Reworking of glacial deposits Aeolian
Skeletal silt	Reworked and *in situ* comminuted shelly exoskeletons
Amorphous silica	Diatom (in situ or transported)
Sand (63–2,000 μm particle size)	
Quartz, felspar, various silicate minerals, rock fragments	Fluvially delivered to the coastal system Reworked Pleistocene coastal deposits Reworking of glacial deposits Aeolian
Skeletal sand	Comminuted to whole reworked and *in situ* exoskeletons, e.g., shell fragments, foraminifera
Carbonate sand (ooids, pellets)	Generated nearshore and reworked onto tidal flat, and for pellets, carbonate grain destruction by boring algae
Carbonate intraclast sand	Reworking of cemented carbonate crusts
Gravel (>2,000 μm particle size)	
Quartz pebbles, rock fragments	Fluvially delivered to the coastal system Reworked Pleistocene coastal deposits Reworking of glacial deposits
Mud pebbles and cobbles	Eroded tidal mud
Armored mud balls	Mud pebbles and cobbles with adhering gravel and shell
Skeletal gravel	Comminuted to whole, reworked and in situ shell
Carbonate intraclast gravel	Reworking of cemented carbonate crusts

Table T7 Geomorphic features of the tidal flats

Geomorphic, or surface feature	Origin
Microscale surface features (<meter sized)	
Smooth planar surface	Deposition on and erosion of the surface
Linear scours (mm to cm deep)	Tidal erosion
Slightly irregular	Tidal erosion of the surface, and/or bioexcavations by small biota and fish
Hummocky surface	Tidal erosion of the surface, and/or bioexcavations by stingrays, fish, and large burrowing benthos
Mud cracks	Desiccation
Surface moundings grading to teepees and brecciation	Mineral precipitation in surface sediments and
Mounded surface	resultant surface crust expansion Mineral precipitation in surface sediments
Mesoscale surface features (>meter-sized, up to tens of meters long)	
Meandering gullies, channels, creeks, meandering or ramifying	Tidal erosion, with local deposition on point bars
Crust lined, and locally brecciated meandering channels	Tidal erosion, with local deposition on point bars, with mineral precipitation in surface sediments and resultant surface crust expansion
Sand waves	Large bodies of sand developed in low tidal zones
Spits	Shoestring sand and sandy gravel body across tidal flat from local headland, formed by tidal currents and wave action
Cheniers	Isolated shoestring sand and sandy gravel body on tidal flat, variably formed by tidal currents, wave action, and storms/cyclones
Salting cliff	Small cliff, 30–100 cm high, cut in to salt marsh, marking junction between high-tidal salt marsh and vegetation-free mid-tidal to low-tidal flat
Mid-tidal cliff	Small cliff, up to 100 cm high, marking junction between mangrove front at ca. MSL and vegetation-free mid-tidal to low-tidal flat

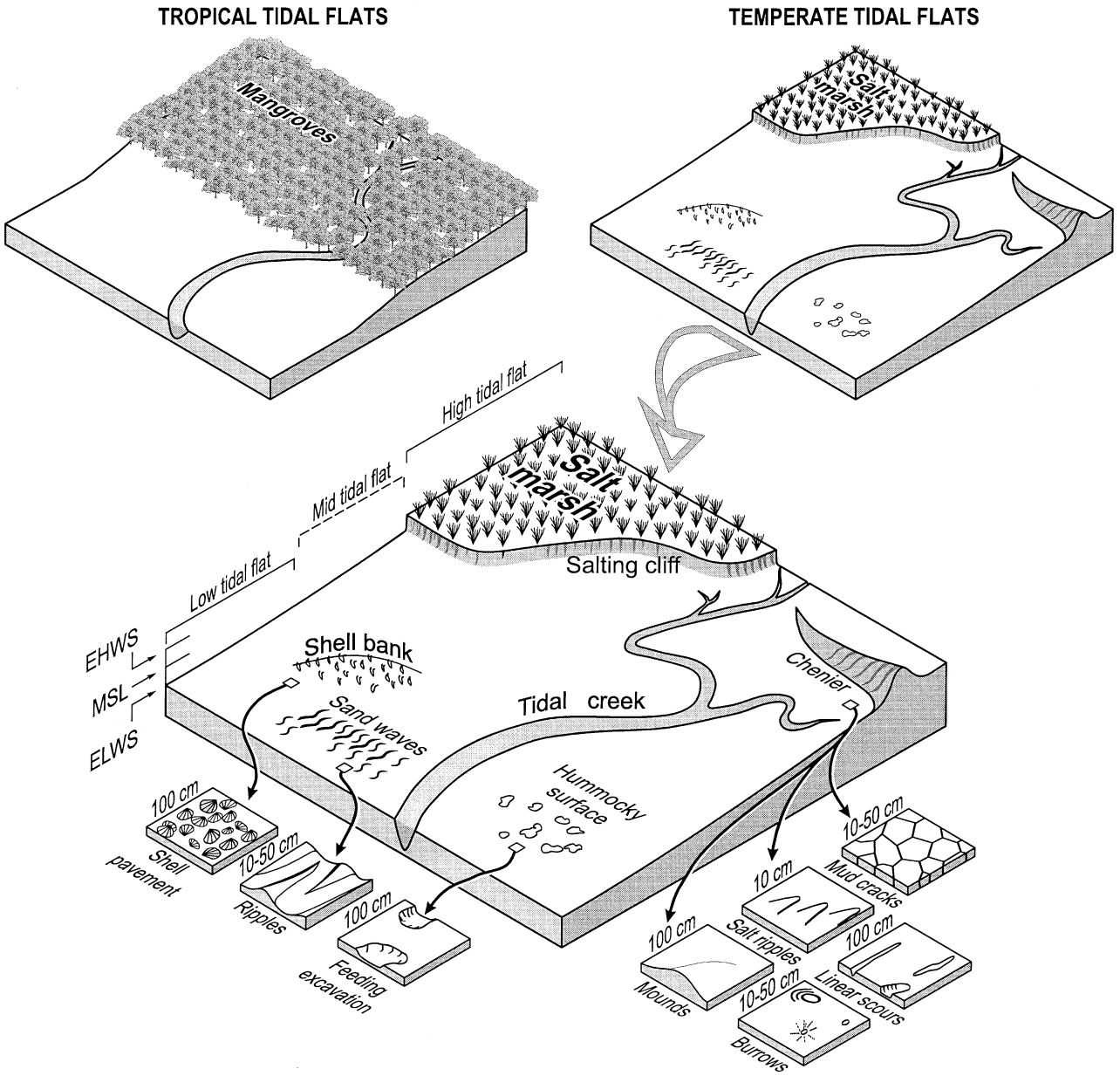

Figure T23 Generalized geomorphology of tidal flats. Macroscale geomorphology of tropical climate tidal flats with mangroves, and temperate climate tidal flats with salt marsh. More detail shown of mesoscale and microscale features of a temperate climate tidal flat.

products resulting from interactive, interrelated and overlapping exogenous and endogenous agents and processes, which include oceanographic, meteorologic, atmospheric, fluvial, hydrologic and hydrochemical, and biological processes (Table T8). These processes commonly are distributed along physicochemical gradients (e.g., tidal, wave, chemical) and operate on a range of basic sediment types such as mud, sand, and shell gravel to develop a complex of geomorphic, sedimentologic, and diagenetic products which are commonly zoned across the tidal flats and are often specific to a coastal setting, sediment setting, climate, and biogeography.

Oceanographic processes involve erosion, transport, and deposition associated with tidal currents, wave action, storms, and cyclones. Meteorologic/atmospheric processes involve evaporation, wind erosion, transport and deposition, rain, ice crystallization, and water temperature fluctuations. Fluvial processes include the delivery of sediment and freshwater to the shore, especially in estuaries and deltas. Hydrologic and hydrochemical processes involve the rising and falling of the water table under the tidal flat, the solution and precipitation of carbonate minerals, evaporite minerals and iron minerals, and redox reactions. Biological processes include: at the largest scale, the accumulation of beds of biogenic material (shell beds, biostromal reefs, and plant material), the modification of tidal current by macrophytes (e.g., mangroves) to induce sedimentation, and the trapping and binding of sediment by vegetation and algal mats; at intermediate scales, the burrow structuring and root-structuring of sediment; and at the smallest scales, the boring of shells, the pelletization of grains by endolithic algae, and the biomediation of the precipitation of minerals such as iron sulfides.

The dynamics of tidal currents is a major factor in the transport and deposition of sediment on tidal flats. Tidal currents transport mud in suspension, and sand by traction. The rise and fall of the tide, with periods of slack water, result in a systematic increasing, decreasing, zero flow, and then reversal of tidal currents. Transport of sand is effected during the main part of the flooding and ebbing tidal cycle when tidal currents are progressing to and regressing from their maximum velocities, with various bedforms developed as the currents systematically increase and then decrease across the tidal cycle resulting in the development of ripples, then megaripples, and then ripples. Deposition of mud is effected during periods of low current velocity and slack water (the times of near-zero to zero current velocities). Mud deposition is accentuated further by fluctuations in water temperature, since cold water and warm water have different viscosity which results in varying mud particle settling velocities (Krogel and Flemming, 1998).

Table T8 Key processes

Some selected processes	Examples of products on the tidal flat
Oceanographic	
Flood and ebb-tidal currents, and slack water	Deposition of mud from suspension, and sand transport by traction; silt ripples, sand ripples, sand waves and megaripples; laminated mud, lenticular bedding, and flazer bedding; scour, and cut-and -fill; tidal creek formation; erosion of mud beds along creek banks and clifflines to form mud ball conglomerate; rolling of mud balls on sandy/gravelly floors to form armored mud balls
Waves	Winnowed sand sheets and shell gravel; rippling; erosion of clifflines cut into mud
Meteorologic/atmospheric	
Wind (erosion, transport, deposition)	Sand transport and fall-out deposition onto tidal flats; formation of adhesion ripples
Evaporation minerals	Mud desiccation and cracking; increasing pore water salinity of groundwater; precipitation of minerals
Rain, ice crystallization	Rain imprints; ice crystal imprints; cryogenic disruption
Water temperature variation	Mud deposition from suspension; mortality of benthos
Groundwater hydrologic/hydrochemical	
Rising and falling of tide	Wetting and drying to form desiccated sediment; development of bubble sand
Solution/precipitation of carbonate minerals	Shell voids, other vughs; cemented crusts, teepees
Evaporite mineral precipitation	Beds of nodular to platey crystalline gypsum; precipitation of gypsum disrupting primary structures
Iron mineral precipitation	Staining of sediment to dark gray with iron sulfide; staining of sediments to orange-brown with iron oxides
Biological	
Accumulation of shell beds and biostromal reefs	Shelly sediments and coquinas, and skeletal biostromes
Plant detritus accumulation	Organic rich sediments, peat
Sediment trapping and binding by vegetation and algal mats	Root-structured sediment; algal-laminated sediment
Feeding/foraging by nekton	Pocked, excavated and hummocky surfaces
Burrowing by benthos	Burrow-structured to fully bioturbated sediment

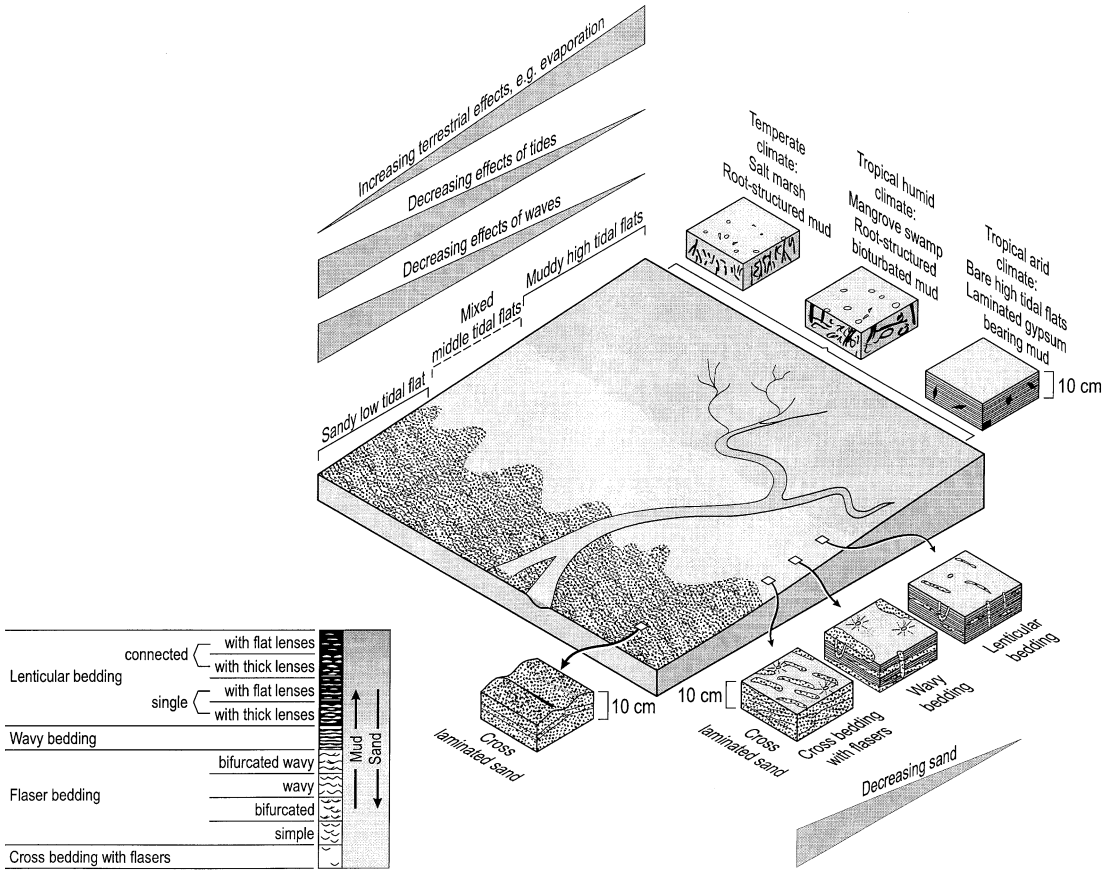

Figure T24 Generalized sedimentology of a typical tidal flat, relating sediment types to oceanographic and terrestrial processes, and inset detail of some sediment types in relation to facies setting and position on tidal flat. Also shown is the systematic variation in bedding types as the sand to mud ratio changes (modified after Reineck and Singh, 1980).

The basic tidal flat sediment types are strongly related to their position on the tidal flat slope as a result of the interplay of tidal action and waves (Figure T24). If there is sand and mud on the tidal flat, tidal and wave processes result in a partitioning of particle sizes: generally, sand dominates the low tidal flats, mixed sand and mud occur on mid-tidal flats, and mud on the high tidal flats. If biogenic activity is not intense enough to bioturbate sediments, the sand and mud on mid-tidal flats are separated in layers and laminae to develop flazer bedding, lenticular bedding, wavy bedding, or interlaminated sand and mud. With more intense burrowing, mid-tidal flats are thoroughly mixed muddy sand with bioturbation structures.

Accumulation of mud in the upper parts of tidal slopes is a general product of tidal processes. There are three main reasons for this. First, with scour lag and settling lag, mud is progressively transported up the tidal slope to accumulate ultimately at the level of the highest tide (Postma, 1961). Scour lag and settling lag processes are particularly accentuated if the tidal flood and ebb are asymmetric. Second, mid- to lower tidal slope environments, more constantly under water, are subject to more continuous and intense wave and tidal current reworking, and hence any mud settled there is prone to remobilization. In contrast, high tidal areas generally are inundated by tides on slackening water, with low to nil current, and any wave trains arriving here are dampened by translation across the tidal flat floor. Hence, there is less scope for reworking. Third, high tidal zones in many regions are vegetated by mangrove or salt marsh, which function in current baffling, and sediment trapping and binding.

The interplay of tidal currents with mud and sand results in an interesting and geologically important range of bedforms and sedimentary structures. Sand transported during flood and ebb tide develops ripple bedforms with internal cross-lamination. Mud deposited during slack water blankets these ripples, or preferentially settles in inter-ripple troughs. Tidal currents, during the ensuing flood or ebb tide, rework the mud layers to diminish their thickness, leave inter-ripple lenses of mud, and remobilize sand forming ripples to bury the mud layers and to form more ripple cross-lamination. Ongoing deposition and burial of these bedforms results in mud-dominated bedding with scattered sand lenses (lenticular bedding), to subequal mud and sand (wavy bedding), to sand-dominated bedding with thin inter-ripple mud lenses (flazer bedding). Thus depending on the proportion of mud to sand, which is a function of the location of the sediment type on the tidal flat, or the inherent proportion of mud to sand regionally, the sedimentary structures produced by the processes described above range from mud-dominated lenticular bedding to flazer bedding (Figure T24).

Sedimentology, sedimentary structures, and stratigraphic sequences

Sediment bedforms, surface features, and near-surface features on tidal flats are produced by oceanographic, other physical, biotic, and hydrochemical processes. Wave action and tides and winnowing result in ripples, megaripples, sand waves, plane sand beds, linear scours, plane mud beds, and gravel pavements. A range of other physical processes result in mud cracks, air escape holes, bubble structures. Biological activity results in burrow-pocked surfaces, animal tracks, crab burrow workings, vesicular structures, crab balls, accumulation of shell banks and shell gravel. Chemical and physical processes combine to develop sheets of gypsum mush and nodules, platey gypsum pavements, carbonate crusts, and breccia pavements.

Sedimentary structures deriving from burial of the sediment bedforms, and the surface and near-surface features include cross-bedding and cross-lamination, herring bone cross-lamination, sand ripple cross-lamination, silt ripple cross-lamination, lenticular bedding, flazer bedding, laminated mud, sand dykes, mud dykes, bubble sand, vesicular mud, root-structuring, vertical burrows to labyrinthoid burrow networks, shell laminae and beds, shell reefs, silt and sand balls, bioturbation and swirl structures, breccias, nodular gypsum beds, platey gypsum beds, and teepee structures.

Key sediments, diagnostic of their formative processes, occur in different parts of the tidal flat. For example, mangrove-vegetated muddy tidal flats develop root-structured and bioturbated (shelly) mud, and crustacean-dominated mixed tidal flats develop burrow structured interbedded sand and mud varying to bioturbated muddy sand. Some examples of sediments and the processes involved in their development from siliciclastic tidal flats are noted in Table T9.

Table T9 Examples of sediments in their setting, and processes in their development

Environment	Main processes	Resulting sediment(s)
Siliciclastic sediment settings		
Mangrove or salt marsh vegetated high-tidal mudflat	Mud accumulation; root-structuring, bioburbation; shell contribution; groundwater alteration	Gray bioturbated root-structured (shelly) mud
Algal mat covered high-tidal mudflat	Mud accumulation; binding; trapping; redox reactions; cracking	Laminated mud; desiccated laminated mud
Bare high-tidal mudflat	Mud accumulation; surface shear; cracking of mud; reworking of desiccation polygons; gypsum precipitation	Laminated mud; desiccated mud; mud chip breccia; gypseous mud
Burrow-pocked midtidal mudflat	Mud accumulation; surface shear; benthic fauna burrowing	Burrow-structured laminated mud; bioturbated mud
Mollusc inhabited mid-tidal mudflat	Mud accumulation; surface shear; accumulation of shell winnowing to concentrate shells	Laminated shelly mud; shell gravel bed
Mid-tidal mudflat with sand ripples	Mud accumulation; surface shear; traction transport of sand	Flaser bedding
Megarippled low- to mid-tidal sand flat	Traction transport of sand; air trapped by rise and fall of tide	Cross-laminated sand; bubble sand
Mid-tidal burrow-pocked sand flat	Traction transport of sand; benthic fauna burrowing	Burrow-structured cross-laminated sand; bioturbated sand
Carbonate sediment settings		
High-tidal breccia pavement	Mud accumulation; carbonate cementation; root-structuring; groundwater alteration	Limestone breccia sheet
High-tidal algal mat covered mudflat	Mud accumulation; binding; trapping; redox reactions; cracking	Laminated mud; desiccated laminated lime mud
High-tidal bare mudflat	Mud accumulation; surface shear; cracking of mud; reworking of cracks; gypsum precipitation	Laminated lime mud; desiccated lime mud; mud chip breccia; gypseous lime mud laminated gypsum; gypsum nodule bed
Mid-tidal burrow-pocked mudflat	Mud accumulation; surface shear; benthic fauna burrowing	Burrow-structured laminated mud; bioturbated mud

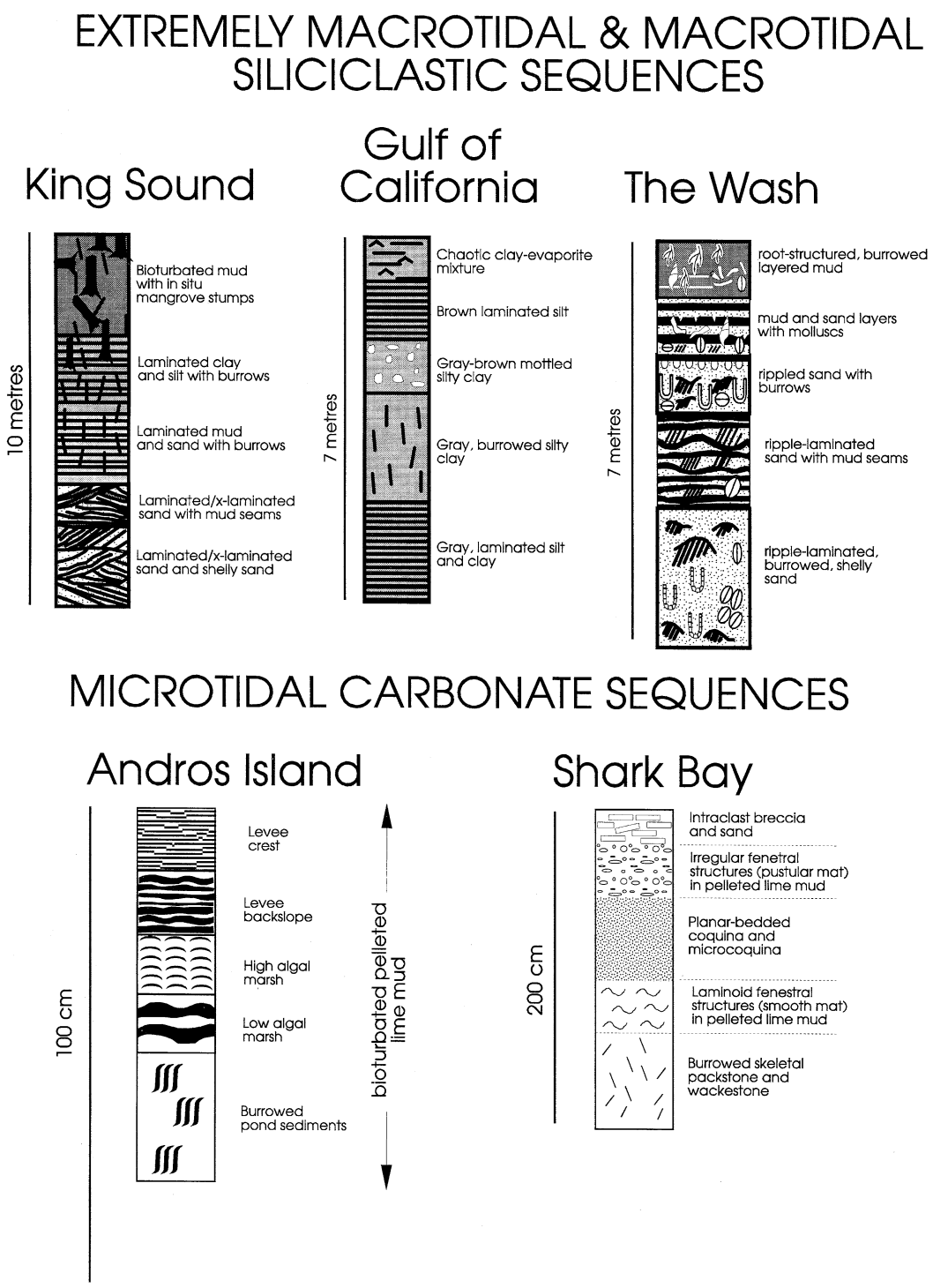

Figure T25 Stratigraphic sequences from various tidal flats (see Table T4). For the macrotidal siliciclastic settings there is comparison for three sequences: a tropical semiarid mangrove-vegetated tidal flat, shoaling from sand to mud, with burrows, root-structures, and *in situ* mangrove stumps; a subtropical semiarid vegetation-free tidal flat dominated by mud, with local burrows, and evaporitic mineral structures; and a temperate humid salt marsh vegetated tidal flat, shoaling from sand to mud, with burrows, root-structures, and shell. The microtidal carbonate sequences compare the structures of a subtropical humid tidal flat with that of a subtropical arid tidal flat.

With progradation, siliciclastic tidal flats develop characteristic stratigraphic sequences. A range of stratigraphic sequences are shown in Figure T25, from various macrotidal to microtidal settings, from flats that are mud dominated, to sand to mud sequences, from temperate to tropical climates. Some examples of sediments from carbonate tidal flats, and the processes involved in their development, are noted in Table T9. With progradation, carbonate sediment tidal flats also develop characteristic stratigraphic sequences, some of which are shown in Figure T25.

Table T10 Key biota of the tidal flats

Biota	Occurrence and function
Mangroves	Tropical tidal flats; massive primary production in the mid-upper tidal zone; detritus sustains biota in adjoining tidal zones (Tomlinson, 1986)
Samphires (salt marsh)	Temperate to tropical tidal flats; primary production in the mid-upper tidal zone; detritus sustains biota in adjoining tidal zones (Chapman, 1977; Beeftink *et al.*, 1985)
Spartina (salt marsh)	Temperate tidal flats; primary production in the mid-upper tidal zone; detritus sustains biota in adjoining tidal zones (Chapman, 1977)
Algal mats and stromatolites	Tropical tidal flats; primary production in the mid-upper tidal zone (Kendall and Skipwith, 1968; Ginsburg and Hardie, 1975)
Molluscs, polychaetes, crustacea	These invertebrates present generally on all tidal flats, although species diversity may decrease towards the temperate regions; molluscs, polychaetes, and crustacea are primary and secondary consumers, and sustain higher level trophic feeders (Dankers *et al.*, 1983; Knox, 1986)
Fish and avifauna	On tidal flats; fish and avifauna generally are primary and secondary consumers, and sustain higher level trophic feeders, and in many instances are the highest trophic level in the region (Knox, 1986; Sylva, 1975; Owen and Black, 1990)

Some key biota of tidal flats

The well-known biota of tidal flats include mangroves, salt marsh, algal mats and stromatolites, polychaetes, molluscs, crustacea, resident fishes and invading nektonic fishes, and avifauna (Table T10). Biogeography and climate, substrate and hydrochemistry are major factors that determine what biota inhabit tidal flats. Species abundance and zonation at site-specific level is determined by physicochemical and biological conditions. For example, with macrophytes, at a global scale, mangroves dominate mid- to upper tidal flats in tropical climates and are replaced by salt marsh in temperate climates. With increased salinity, the upper tidal interval may be inhabited by algal mats and stromatolites. Diversity of flora and fauna is linked to climate setting, with high species richness and abundance in tropical areas, and relatively lower species richness in temperate areas.

Primary production within specific parts of the tidal flat, for example, from mangroves and salt marsh, often drives the ecosystems of tidal flats. With mangroves and salt marshes, these macrophytes fix nutrients and carbon on the mid- to upper tidal flats, supporting the local resident fauna, and the export of detritus sustains benthic biota of polychaetes, molluscs, and crustacea elsewhere on the mid- to low-tidal flats. The biologically rich tidal flat environments also support nekton and avifauna. Fish and other nekton invade the tidal zone for feeding on the high tide, and the avifauna invade the tidal flats at low tide.

Tidal flats typically are biologically zoned. For any benthic group, such as polychaetes, molluscs, or crustacea, there is species zonation across the flats related to frequency of inundation, substrate, pore water salinity, inter-species competition and predation pressure, among other factors. Macrophytes (mangrove and salt marsh) also exhibit zonation, as related to groundwater salinity, substrates, and elevation of habitat above mean sea level. Many of the benthos are burrowing forms, and the macrophytes have diagnostic root structures, and hence sedimentologically, zonation of the biota results in facies and tidal level specific signatures across tidal flats: sand-constructed *Arenicola* burrows, for instance, are diagnostic of low-tidal sand flats, vertical to u-shaped to labyrinthoid crustacean burrows in a root-structure-free mud are diagnostic of mid- to low tidal flats, coarse root-structured substrates and associated faunal burrows are diagnostic of mangrove vegetated high tidal flats, while fine root-structured substrates are diagnostic of salt marsh vegetated high tidal flats. Some diagnostic biogenic structures, and biofacies related to tidal assemblages, are often signatures for specific tidal levels and lithofacies within a given region.

V. Semeniuk

Bibliography

Alexander, C.R., Davis, R.A., and Henry, V.J. (eds.), 1998. *Tidalites: Processes and Products*. SEPM (Society for Sedimentary Geology), Special Publications, 61.

Allen, J.R.L., 1970. Sediments of the modern Niger Delta: a summary and review. In Morgan, J.P. (ed.), *Deltaic Sedimentation: Modern and Ancient*. Society of Economic Paleontologists and Mineralogists, Special Publication No. 15, pp. 138–151.

Beeftink, W.G., Rozema, J., and Huiskes, A.H.L. (eds.), 1985. *Ecology of Coastal Vegetation*. Dordrecht: Dr W. Junk Publishers.

Black, K.S., Paterson, D.M., and Cramp, A. (eds.), 1998. *Sedimentary Processes in the Intertidal Zone*. Geological Society, London, Special Publications, 139.

Chapman, V.J. (ed.), 1977. *Ecosystems of the World, Vol 1, Wet Coastal Ecosystems*. Amsterdam: Elsevier Scientific Publishing Co.

Coleman, J.M., Gagliano, S.M., and Smith, W.G., 1970. Sedimentation in a Malaysian high tide tropical delta. In Morgan, J.P. (ed.), *Deltaic Sedimentation: Modern and Ancient*. Society of Economic Paleontologists and Mineralogists, Special Publication No. 15, pp. 185–197.

Dankers, N., Wolff, W.J., and Zijlstra, J.J. (eds.), 1983. Fishes and fisheries of the Wadden Sea, Report 5. In Wolff, W.J. (ed.), *Ecology of the Wadden Sea*, *Vol 2*. Rotterdam: A. A. Balkema.

Davies, J.L., 1980. *Geographical Variation in Coastal Development*, 2nd edn. London: Longman.

Evans, G., 1975. Intertidal flat deposits of the wash, western margin of the North Sea. In Ginsburg, R.N. (ed.), *Tidal Deposits: A Casebook of Recent Examples and Fossil Counterparts*. Berlin: Springer-Verlag, pp. 13–20.

Ginsburg, R.N. (ed.), 1975. *Tidal Deposits: A Casebook of Recent Examples and Fossil Counterparts*. Berlin: Springer-Verlag.

Ginsberg, R.N., and Hardie, L.A., 1975. Tidal and storm deposits, northwestern Andros Island, Bahamas. In Ginsburg, R.N. (ed.), *Tidal Deposits: A Casebook of Recent Examples and Fossil Counterparts*. Berlin: Springer-Verlag, pp. 201–208.

Hagan, G.M., and Logan, B.W., 1975. Prograding tidal-flat sequences: Hutchinson Embayment, Shark Bay, Western Australia. In Ginsburg, R.N. (ed.), *Tidal Deposits: A Casebook of Recent Examples and Fossil Counterparts*. Berlin: Springer-Verlag, pp. 215–221.

Harrison, S.C., 1975. Tidal flat complex, Delmarva Peninsula, Virginia. In Ginsburg, R.N. (ed.), *Tidal Deposits: A Casebook of Recent Examples and Fossil Counterparts*. Berlin: Springer-Verlag, pp. 31–38.

Howard, J.D., Frey, R.W., and Reineck, H.-E., 1972. Georgina Coastal Region, Sapelo Island, U.S.A.: Sedimentology and biology. VIII Conclusions. *Senckenbergiana marit*. **4**: 217–222.

Jackson, J.A., 1997. *Glossary of Geology*, 4th edn. Alexandria: American Geological Institute.

Johnson, D.P., 1982. Sedimentary facies in an arid zone delta: Gascoyne delta, western Australia. *Journal of Sedimentary Petrology*, **52**: 547–563.

Kendall, C.G.St.C., and Skipwith, Sir Patrick A. d'E., 1968. Recent algal mats of a Persian Gulf Lagoon. *Journal of Sedimentary Petrology*, **38**: 1040–1058.

Klein, G. deV., 1963. Bay of Fundy intertidal zone sediments. *Journal of Sedimentary Petrology*, **33**(4): 844–854.

Klein, G. deV. (ed.), 1976. *Holocene Tidal Sedimentation*. Stroudsburg: Dowden, Hutchinson and Ross, Inc.

Knight, K.J., and Dalrymple, R.W., 1975. Intertidal sediments from the South Shore of Cobequid Bay, Bay of Fundy, Nova Scotia, Canada. In Ginsburg, R.N. (ed.), *Tidal Deposits: A Casebook of Recent Examples and Fossil Counterparts*. Berlin: Springer-Verlag, pp. 47–55.

Knox, G.A., 1986. *Estuarine Ecosystems: A Systems Approach*, Vol. II. Boca Raton: CRC Press, Inc.
Krogel, F., and Flemming, B., 1998. Evidence for temperature-adjusted sediment distributions in the back-barrier tidal flats of the East Frisian Wadden Sea (Southern North Sea). In Alexander, C.R., Davis, R.A., and Henry, Vernon, J. (eds.), *Tidalites: Processes and Products*. Tulsa: Society for Sedimentary Geology.
Larsonneur, C., 1975. Tidal deposits, Mont Saint-Michele Bay, France. In Ginsburg, Robert N. (ed.), *Tidal Deposits: A Casebook of Recent Examples and Fossil Counterparts*. Berlin: Springer-Verlag, pp. 21–30.
Owen, M., and Black, J.M., 1990. *Waterfowl Ecology*. New York: Chapman and Hall.
Postma, H., 1961. Transport and accumulation of suspended matter in the Dutch Wadden Sea. *Netherlands Journal of Sea Research*, **1**(1,2): 148–190.
Purser, B.H. (ed.), 1973. *The Persian Gulf: Holocene Carbonate Sedimentation and Diagenesis in a Shallow Epicontinental Sea*. Berlin: Springer-Verlag.
Reineck, H.-E., 1972. Tidal flats. In Rigby, J.K., and Hamblin, W.K. (eds.), *Recognition of Ancient Sedimentary Environments*. Society of Economic Paleontologists and Mineralogists, Special Publication No. 16, pp. 146–159.
Reineck, H.-E., 1975. German North Sea Tidal Flats. In Ginsburg, Robert, N. (ed.), *Tidal Deposits: A Casebook of Recent Examples and Fossil Counterparts*. Berlin: Springer-Verlag.
Reineck, H.-E., and Singh, I.B., 1980. *Depositional Sedimentary Environments*, 2nd edn. Berlin: Springer-Verlag.
Semeniuk, V., 1981. Sedimentology and the stratigraphic sequence of a tropical tidal flat, north-western Australia. *Sedimentary Geology*, **29**: 195–221.
Semeniuk, V., 1993. The mangrove systems of Western Australia—1993 Presidential Address. *Journal Royal Society W.A.*, **76**: 99–122.
Shinn, E.A., 1983. Tidal flats. In Scholle, Peter, A., Bedout, Don, G., and Moore, Clyde, H. (eds.), *Carbonate Depositional Environments. Tulsa*. The American Association of Petroleum Geologists, pp. 171–210.
Shinn, E.A., Lloyd, R.M., and Ginsburg, R.N., 1969. Anatomy of a modern carbonate tidal-flat, Andros Island, Bahamas. *Journal of Sedimentary Petrology*, **39**(3): 1202–1228.
Sylva, de, D.P., 1975. Nektonic food webs in estuaries. In Cronin, L.E. (ed.), *Estuarine Research, Vol. 1, Chemistry, Biology, and the Estuarine System*. New York: Academic Press, Inc.
Thompson, R.W., 1968. *Tidal Flat Sedimentation on the Colorada River Delta, Northwestern Gulf of California*. Boulder: Geological Society of America Memoir 107.
Tomlinson, P.B., 1986. *The Botany of Mangroves*. Cambridge: Cambridge University Press.

Cross-references

Bay Beaches
Coastal Sedimentary Facies
Endogenic and Exogenic Factors
Hydrology of Coastal Zone
Mangroves, Ecology
Mangroves, Geomorphology
Muddy Coasts
Ripple Marks
Salt Marsh
Tidal Creeks
Tidal Flats, Open Ocean Coasts
Tides
Vegetated Coasts

TIDAL FLATS, OPEN OCEAN COASTS

Definitions and distribution

Although tidal-flat deposits have been studied extensively over several decades, most studies were focused on embayment and estuary tidal flats, where wave energy is typically low. In contrast, studies of open-coast tidal flats, which differ significantly from the embayment and estuary tidal flats, are scarce. This entry describes the characteristics of open-coast tidal flat in comparison with the well-documented embayment and estuary tidal flats.

A tidal flat is generally defined as an extensive, nearly horizontal, marshy or barren tract of land that is alternately covered and uncovered by the tide, and consisting of unconsolidated sediment, mostly mud and sand (Bates and Jackson, 1980). The tidal flat is also often referred to as an intertidal zone, although in some general discussions, it may include subtidal and supratidal zones. In the following discussion, the term tidal flat strictly refers to the intertidal zone, lying between low-spring tide and high-spring tide levels, as defined in the Glossary of Geology (Bates and Jackson, 1980). A tidal flat generally shows a zonation related to the duration of submergence, which is reflected in apparent differences in sedimentary characteristics. Therefore, based on characteristics of the sedimentary structures and the general trend of lamina thickness, a tidal flat is often divided into upper, middle, and lower intertidal zones (Reineck and Singh, 1980). Although the transitions between the zones are gradual and somewhat subjective, the division provides convenience in describing sedimentary characteristics.

Tidal currents are generally considered to be the dominant driving force for sediment movement on tidal flats, whereas wave-driven sediment motion is often regarded to be minimal and is often neglected. Over 70% of locations classified as tidal flat occur in wave-sheltered areas, such as bays, estuaries, lagoons, and behind spits or barriers, while the remainder occur along open coasts, the majority of which are characterized by low wave conditions (Eisma, 1998). Although high wave energy is often considered to be unfavorable for the development of gentle tidal flats (Boggs, 1995), they can nonetheless develop rather extensively along open coasts given a large tidal range and tremendous sediment supply. Examples of this type of open-coast tidal flats are found in the vicinity of the large river mouths along the Chinese coast (Figure T26; Chen, 1998; Shi and Chen, 1996).

In comparison with extensively studied wave-sheltered tidal flats, open-coast tidal flats are characterized by: (1) facing an open ocean or sea; and (2) flooding and ebbing tidal currents are not confined and/or regulated by tidal channels. In other words, large tidal channels are generally absent along open-coast tidal flats, especially those along the Chinese coasts.

Hydrodynamics and sediment dynamics

Most of the published studies on modern tidal flat deposition have concentrated on wave-sheltered areas in Europe and North America (e.g., Klein, 1976; Boersma and Terwindt, 1981; Dalrymple *et al.*, 1991; Allen and Duffy, 1998; Eisma, 1998). Not surprisingly, therefore, sedimentary characteristics associated with tidal currents, especially those flowing through tidal channels, have been studied extensively, with little attention being paid to sediment motions driven by waves. Generally speaking,

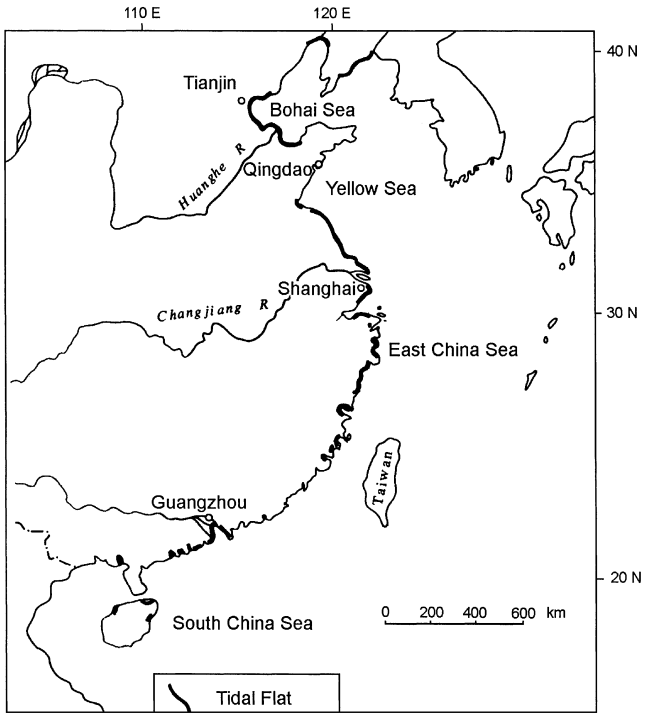

Figure T26 Distribution of open-coast tidal flats in China.

open-coast tidal flats are rather poorly studied and documented, and as a result, the characteristics of hydrodynamics and sediment dynamics presented subsequently are largely based on the studies along the Chinese coasts.

Along open-coast tidal flats, tidal channels are generally absent and, therefore, do not significantly regulate flood and ebb currents. Sedimentary features, such as mega-ripples and dunes, associated with bedform migration in the tidal channels are rare to non-existent. Wave energy is significantly dissipated over the extensive and gentle muddy flats during normal weather. However, during storms, due to the lack of wave shelter, open-coast tidal flats are vulnerable to the impact of storm waves, which may induce substantial reworking and redeposition of normal weather tidal deposits. The tidal flats, especially the middle and upper intertidal zones, are much sandier during the storm seasons than during the calm-weather seasons.

Sediment dynamics along open-coast tidal flats carry strong regional characteristics. The sediment dynamics along the Chinese open-coast tidal flats are significantly influenced by the tremendous sediment supplies from the adjacent large rivers, for example, the Changjiang river (Figure T26). Most open tidal flats along the Chinese coast are accretional owing to the abundant fine (silt and clay) riverine sediment supply. Coastal erosion is typically caused by starvation of sediment supply due to switching of river mouths, artificial flood controls, or drainage withdrawal. Mean sediment grain size along the Chinese open-coast tidal flat ranges from 4 to 8 ϕ (0.063–0.004 mm). The fine nature of the sediment also contributes to the absence of the mega-ripples in addition to the general lack of tidal channels. The width of the tidal flats ranges from 3 to 4 km with a maximum of approximately 8 km. The average slope of the tidal flat is typically 1 : 1,000 with a maximum of 1 : 200 and a minimum of 1 : 5,000.

Characteristics of sedimentary structures

The sequence of sedimentary structure variation from upper to lower intertidal zones as described by Reineck and Singh (1980) was also observed on open-coast tidal flats. The upper intertidal zone is characterized by relatively finer sediment with thicker muddy laminae. Lenticular bedding is common in the upper intertidal zone. The lower intertidal zone is characteristic of coarser sediment and thicker sandy laminae. Flaser bedding is common in the lower intertidal zone. Wavy bedding is common in the middle intertidal zone.

It is generally accepted that four laminae may theoretically be deposited during one tidal cycle (Allen, 1985). Two sandy laminae may be formed during flood and ebb phases, and two muddy laminae deposited during high and low tide slack water. It was also found that thicker sand laminae correspond to relatively higher-energy events during spring tides, while thinner sand laminae correspond to relatively low-energy events during neap tides (Boersma and Terwindt, 1981; Allen, 1985). Time-series analysis of laminae thickness has been applied to quantify the paleo-tide periodicities and paleo-sedimentation rates in both modern and ancient tidal deposits (Yang and Nio, 1985; Kvale *et al*., 1989; Tessier and Gigot, 1989; Kuecher *et al*., 1990; Kvale and Archer, 1990; Tessier, 1993; Miller and Eriksson, 1997), and an approximate 14-day periodicity related to neap–spring cycles has been identified in most of these studies. In the above studies, deposition and erosion induced by waves have largely been neglected. Along open-coast tidal flats, four laminae were rarely observed to have been deposited during one tidal cycle due to their poor preservation potential. Over a continuous daily observation of eight months, the preservation of all four laminae after one tidal cycle was only recorded twice (Li *et al*., 1965).

Two different grouping patterns of sandy and muddy laminae were distinguished on open-coast tidal flat deposits (Figure T27). Groups with generally thicker sandy laminae than adjacent groups, are termed sand-dominated layers (1), while groups with generally thinner sandy laminae than adjacent groups, are referred to as mud-dominated layers (2). Although determination of the exact boundaries between sand- and mud-dominated layers was somewhat subjective, the overall differences between adjacent sand- and mud-dominated layers were apparent (Figure T27). The thickness and number of sandy and muddy laminae in each sand- or mud-dominated layer were not necessarily identical. Detailed description of sand- and mud-dominated layers can be found in Li *et al*. (2000).

Daily, monthly, and yearly sedimentation monitoring along a Chinese open-coast tidal flat near the Changjiang river mouth indicated that the mud-dominated layers described above correspond to calm-weather deposition, while the sand-dominated layers are related to high-energy storm events. These findings are contrary to the neap–spring-cycle interpretation of lamina-thickness variations. The above interpretation of event-related lamina-thickness variation incorporated the much more significant influence of waves, especially storm waves, to the open-coast tidal flat deposits. High-energy storm events along the east-central Chinese coasts are mainly driven by the typhoon passages typically during the months of August to November, and to a lesser extend the passages of winter cold fronts.

Sedimentation rate and preservation potential

The correspondence of thick–thin variations of tidal laminae with the neap–spring tidal cycles has provided a promising tool to study the paleo-tide periodicities and the paleo-sedimentation rate (Tessier and Gigot, 1989; Miller and Eriksson, 1997). Time-series analysis of the tidal bundle thickness variation has been applied successfully in tidal channel deposits (Yang and Nio, 1985). However, direct application of this neap–spring analysis is not valid along open-coast tidal flats due to the non-negligible and largely random impact of wave-induced erosion and sedimentation. Sedimentation rate and preservation potential vary from region to region, and are strongly influenced by sediment supplies and regional hydrodynamics. In the following, a case study from east-central China is discussed as an example.

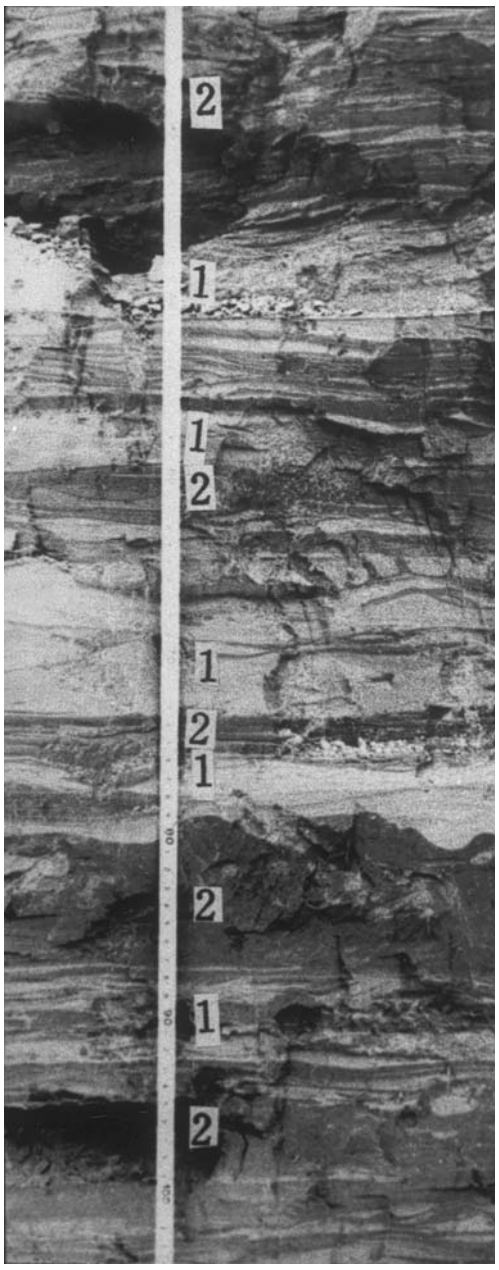

Figure T27 Different grouping patterns of tidal bedding. 1 Denotes a sand-dominated layer, and 2 denotes a mud-dominated layer.

Realizing that 100% preservation potential may be far from realistic on an open-coast tidal flat, Li *et al*. (2000) conducted an intensive, time-series *in situ* monitoring of the sedimentation rate and preservation potential. Their methodology included two aspects to understand and quantify the deposition and preservation of tidal bedding. The first aspect emphasized *in situ* observations on the modern tidal flat. Selected points were visited daily during low tide to examine deposition and erosion of the previous two tidal cycles. This daily observation had been conducted for 17 days over a neap–spring tidal cycle. Seasonal sedimentation and erosion observations across an intertidal profile were conducted over a four-month period extending from calm-weather season to storm season. The second aspect of the study focused on examination of the vertical characteristics of tidal laminae and bedding, in terms of the lamina numbers and lamina-thickness variations. Knowledge gained from the *in situ* observations was applied to interpret the vertical distribution of tidal bedding and the preservation potential of individual sandy and muddy laminae in cores and trenches.

Short-term observation was conducted using two thin plastic plates (40 cm long, 40 cm wide, and 2 mm thick). The plates were placed in the transition area between middle and upper intertidal zones. The thin plates were placed flush with the average sediment surface, and their surfaces were sanded to increase the roughness. Plate 1 was left in place for a period of 17 days and one observation was made at the end of the experiment. The objective for monitoring plate 1 was to obtain short-term information without daily disturbance. Deposits on plate 2 were measured daily, or every two days in cases of poor weather conditions. The objective of the plate 2 experiment was to quantify daily sedimentation rate and the number of laminae formed.

The daily monitoring spanned one neap–spring tidal cycle. No apparent trend of lamina-thickness variation was observed from the daily plate experiments. The daily sedimentation rates were rather uniform ranging 17–22 mm/day, except two abnormal values of 12 and 45 mm/day, both measured during spring tides. The calculated 17-day deposition was 378 mm with 50 sandy and muddy laminae, while 12 laminae with a total thickness of 75 mm were measured on the 17-day plate. Thus, the uninterrupted 17-day sedimentation was 20% of the cumulative daily deposition in terms of thickness (75 mm versus 378 mm), or 24% in terms of total number of laminae (12 versus 50). Furthermore, comparison between the results from the 17-day monitoring (12 laminae) and the theoretical estimate (4 laminae per tidal cycle for 33 tidal cycles over 17 days) of 132 laminae indicates that only approximately 9% of the laminae were preserved, even during a short period of one neap–spring tidal cycle. Continuous daily observation of tidal lamina number and thickness, conducted over three neap–spring cycles in 1999, yielded similar preservation potential.

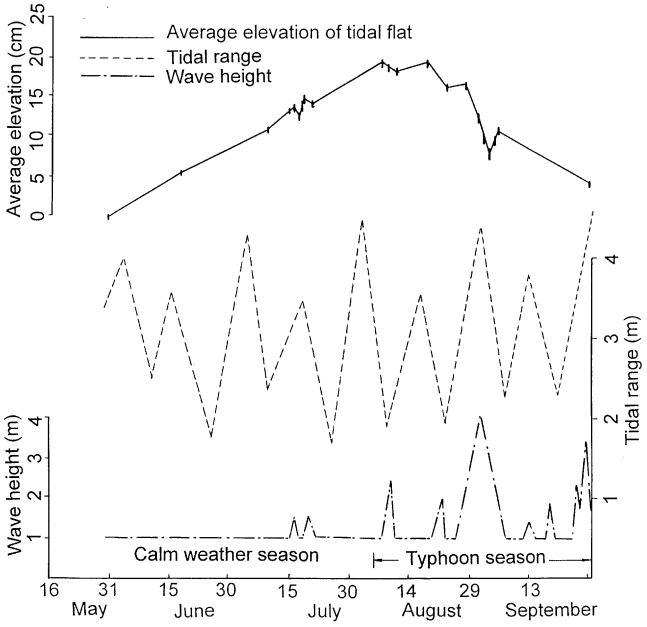

Figure T28 Average elevation change at Donghai Farm on the southern flank of the Yangtze delta, neap–spring tidal cycles and wave heights during a 4-month study, 1992. Wave heights lower than 1 m were neglected.

Seasonal monitoring spanned four months with two months at the end of a calm-weather season and two months at the beginning of the following storm season. Sedimentation and/or erosion were measured at 35 locations relative to a series of graduated rods. A total of 22 measurements were conducted during the four-month period. Overall, the intertidal zone was accreting during the studied calm-weather season (Figure T28), as indicated by the increasing of the average elevation at all the rods. During the studied storm season, net erosion (elevation decrease) was measured and the flat was covered by a sandy lamina that was much thicker than those deposited during the calm-weather season. Sharp elevation decrease was usually measured directly after the storms, apparently indicating the erosion caused by storm waves. For the convenience of discussion, the calm- and storm-weather season was divided somewhat subjectively by the first significant typhoon impact in the study area. The frequent observations throughout the four-month period indicated that the tidal flat was generally muddier in the calm-weather season than during the stormy season. The changes of average elevation were related not to the neap–spring tidal cycles, but closely to high wave events (Figure T28). Deposition of a relatively thicker sandy lamina was directly related to the high-energy wave events induced by the passage of a typhoon, instead of during spring-tide conditions.

Long-term sedimentation rate and preservation potential were determined through counting the number of laminae and mud- and sand-dominated layers in core sections that were deposited over 100 years. Details are described in Li *et al*. (2000). The centennial sedimentation rate was found to be on the order of 4 cm per year. It is worth emphasizing that the high sedimentation rate is closely related to the tremendous sediment supply from the adjacent river. Such a high sedimentation rate should not be expected at locations without overwhelming sediment supply. Over the 100-year period, the preservation potential of individual lamina, including both calm-weather and storm deposits, was found to be on the order of 0.2%, which was 45 times smaller than the 9% estimated for a short-term of a neap–spring cycle. It is expected that the preservation potential decreases as temporal interval increases. The 100-year preservation potential of storm-induced sand-dominated layers was estimated to be of the order of 10%, 50 times higher than the overall potential of 0.2%.

Summary

Waves, especially high storm waves, have a significant influence on sedimentation and preservation of intertidal deposits along the open-coast tidal flats. The thickness variation of sandy laminae on an open-coast tidal flat is related not to neap–spring tidal cycles, but directly to storm activities. The mud-dominated layers containing thinner sandy laminae were deposited during calm-weather conditions, while the sand-dominated layers containing relatively thicker sandy laminae were deposited during storm seasons. In other words, the thick–thin variation of sandy laminae may reflect a much longer cycle of calm-weather and storm seasons, instead of the fortnightly neap–spring tidal cycles as suggested from studies on wave-sheltered tidal flats.

One hundred percent preservation of both the number and thickness of individual laminae in tidal flat deposits, which has often been assumed in the interpretation of time-series analysis of laminae-thickness variation, was found to be unrealistic along the studied open-coast tidal flat. Preservation potential decreases as timescale increases. During one neap–spring tidal cycle under calm-weather conditions, the preservation potential of individual lamina was approximately 9%. However, over a period of 100 years, the preservation rate of individual lamina decreased to about 0.2%. The preservation rate of storm-induced, sand-dominated layers during the 100-year period was found to be on the order of 10%, much higher than the 0.2% of the individual sandy and muddy lamina. Storm deposits have a much higher potential for being preserved due to the higher energy level at which they were deposited.

Congxian Li, Ping Wang and Daidu Fan

Bibliography

Allen, J.R.L. 1985. *Principles of Physical Sedimentology*. London-Boston-Sydney: George Allen & Unwin.

Allen, J.R.L., and Duffy, M.J., 1998. Temporal and spatial depositional patterns in the Severn Estuary, southwestern Britain: intertidal studies at spring–neap and seasonal scales, 1991–1993. *Marine Geology*, **146**: 147–171.

Bates, R.L., and Jackson, J.A. (eds.), 1980. *Glossary of Geology*. Alexandria, VA: American Geological Institute.

Boersma, J.R., and Terwindt, J.H.J., 1981. Neap–spring tide sequences of intertidal shoal deposits in a mesotidal estuary. *Sedimentology*, **28**: 151–170.

Boggs, S., 1995. *Principles of Sedimentology and Stratigraphy*. Upper Saddle River, NJ: Prentice Hall.
Chen, X., 1998. Changjian (Yangtze) river delta, China. *Journal of Coastal Research*, **14**: 838–858.
Dalrymple, R.W., Makino, Y., and Zaitlin, B.A., 1991. Temporal and spatial patterns of rhythmite deposition on mud flat sedimentation in the macrotidal Cobequid Bay–Salmon River estuary, Bay of Fundy, Canada. In Smith, D.G., Reinson, G.E., Zaitlin, A., and Rahmani, R.A. (eds.), *Clastic Tidal Sedimentation*. Canadian Society of Petroleum. *Geology, Memoir* 16, 137–160.
Eisma, D., 1998. *Intertidal Deposits—River Mouths, Tidal Flats, and Coastal Lagoons*. Boca Raton, FL: CRC Press.
Klein, G. deV., 1976. *Holocene Tidal Sedimentation*. Stroudesburg: Dowden, Hutchinson & Ross.
Kuecher, G.J., Woodland, B.G., and Broadhurst, F.M., 1990. Evidence of deposition from individual tides and of tidal cycles from the Francies Creek Shale. *Sedimentary Geology*, **68**: 211–221.
Kvale, E.P., Archer, A.W., and Johnson, H.R., 1989. Daily, monthly, and yearly tidal cycles within laminated siltstones of the Masfield Formation of Indiana. *Geology*, **17**: 365–368.
Kvale, E.P., and Archer, A.W., 1990. Tidal deposits associated with low sulfur coals, Brazil FM (Lower Pennsylvanian), Indiana. *Journal of Sedimentary Petrology*, **60**: 563–574.
Li, C., Yang, X., Zhuang, Z., Zian, Q., and Wu, S., 1965. Formation and evolution of the intertidal mudflat. *Journal of Shangdong College of Oceanography*, **2**: 21–31 (in Chinese with Russian abstract).
Li, C., Wang, P., Fan, D., Dang, B., and Li, T., 2000. Open-coast intertidal deposits and the preservation potential of individual lamina: a case study from east-central China. *Sedimentology*, **47**: 1039–1051.
Miller, D.J., and Eriksson, K.A., 1997. Late Mississippian prodeltaic rhythmites in the Appalachian Basin: A hierarchical record of tidal and climatic periodicities. *Journal of Sedimentary Research*, **67**: 653–660.
Reineck, H.E., and Singh, I.B., 1980. *Depositional Sedimentary Environments*. New York: Springer-Verlag.
Shi, Z., and Chen, J., 1996. Morphodynamics and sediment dynamics on intertidal mudflats in China (1961–94). *Continental Shelf Research*, **16**: 1909–1926.
Tessier, B., 1993. Upper intertidal rhythmites in the Mont-Saint-Michel Bay (NW France): perspectives for paleo-reconstruction. *Marine Geology*, **110**: 355–367.
Tessier, B., and Gigot, P., 1989. A vertical record of different tidal cyclicities: an example from the Miocene Marine Molasse of Digne. *Sedimentology*, **36**: 767–776.
Yang, C., and Nio, S., 1985. The estimation of palaeohydrodynamic processes from subtidal deposits using time-series analysis methods. *Sedimentology*, **32**: 41–57.

Cross-references

Asia, Eastern, Coastal Geomorphology
Coastal Lakes and Lagoons
Deltas
Tidal Environments
Tidal Flats
Tides
Waves

TIDAL POWER

Tidal energy

Tidal energy is derived from the earth's inherent force, the earth's rotation within the disturbing field of moon and sun. In relatively shallow seas friction dissipates almost all the energy. Though tides can be predicted very accurately, they are not in phase with moon and sun movements, the tide waves being distorted as landmasses, narrow passages and shallow depth areas impede and/or influence their progression. (Charlier, 1982). The tidal current is the rotary current accompanying the turning tide crest in an open ocean. It becomes a reversing current, nearshore, moving in and out as flood and ebb currents. Both of these can be harnessed to produce mechanical and/or electrical power (Charlier and Justus, 1993).

Major disadvantages of tidal power electricity generation is that tides are linked to the lunar rather than to the solar cycle, and vary in range throughout the year due to their periodic components. These negative aspects can be partially overcome by ingenious engineering and retiming of use of potential energy accumulated at low-demand periods. Such retiming had even been suggested several decades ago using retaining basins, compressed-air, or hydrogen—even electrolytically produced—usable as fuel when tide and peak-power demand are not synchronic (Gilbert, 1982). Storing has been proposed in exhausted deposits, abandoned mines, and artificial cavities.

Of the 3,000 million kilowatts equivalent dissipated by tidal energy, one billion (10^9) develop in shallow seas. But only a fraction of this "power" can be captured. The geographical site must be suitable from engineering and economics viewpoints and the "usable head" has to be high (5 m or more). The latter requirement has drastically changed with the development of low, and ultra-low, head turbines, greatly increasing the number of potential sites; thus the 200 million kW theoretically harnessable 20 years ago has sizably increased. The economic geographical factor has also been altered as a result of improvement in transmission possibilities; indeed, national grid systems and high voltage transmission lines have minimized the problem of distance between generating plant and consumer (e.g., in Canada) and the problem of protection (insulation) against extreme temperature amplitudes was resolved more than a decade ago by the Soviets. Finally, where the emphasis has been placed on huge, even gigantic (e.g., Chausey Islands, France) projects, small plants are often favored currently, an advantage for developing countries or isolated areas (Suriname, Half Moon Cove [Maine, USA], China).

The plant

The tide mill (gm) and the tidal power plant are similar. The latter has an electric generator. The plant's major components are a dam which houses the powerhouse, a retaining basin, and a link to the electricity grid. Construction of a barrage or dam is necessary; earthen dams have been used in construction of Chinese plants. The dam consists additionally of dikes connecting with the natural embayment and a sluiceway. A passage way for fishes is now provided. A reasonable tidal range is required, although quite small ones will suffice today. Estuaries and gulfs in shallow areas are privileged sites. A closed basin is thus created which fills and empties daily, sometimes more than once, depending on the local tidal regime. Equipped with sluices and turbines placed in the barrage, the system retains the water entering at flood tide and releases it at ebb tide.

Generally turbines produce electricity as the water flows out of the retention basin (or "pool") but reversible blade (the so-called *bulb*) turbines, originally invented by Harza and later developed by French engineers (Hollenstein and Soland, 1982), can produce electricity both as the water enters and when it exits the basin. Practice—based upon 30 years of operation of the Rance River, France, plant—has, however, shown that entering water generation is perhaps not always economically profitable. By judiciously selecting tide gates opening and closing times, power generation can be synchronized with peak-demand periods, even if these do not coincide with tide peaks. The hydraulic head can be increased by reversing power units, temporarily turning the turbine-generator into a pump-motor; the bulb turbine precisely regulates flow in both directions and acts as turbine and pump. Pumping, however, consumes electricity.

A so-called "site value coefficient" for plants (k) was calculated by Robert Gibrat based on dam length and natural energy (k = L/NE), however, these are not the only "factors" involved in site selection; considered should be tidal range, potential pool size, ratio of basin aperture section to basin surface, length of dam, basin characteristics (such as geometric shape and surface, opening, widening shape), geological structure, lithology and petrology, foundation soil quality, gradient of resistance layer, probability of silting, rate of sedimentation, climate, market distance, competitiveness of conventional and/or alternative (e.g., nuclear, aeolean) power sources. Some economists maintain that today tidal power is competitive and may even be less expensive than fossil fuel and nuclear generation. Calculations made by Voyer and Penel (1957) have been revised (Charlier, 1998). All the factors are seldom, if ever, simultaneously favorable, which, with the high capital investment for large plants, probably accounts for the small number of plants constructed (Charlier and Justus, 1993).

Types of plants

Plants are single- or multiple-basins systems, a tide-powered air storage scheme, tide-powered hydrostatic pump scheme or Gorlov setup. Single-basin plants function either as a one-way operation (ebb generation only), two-way operation (generation at both ebb and flood

flow), two-way operation with pump-turbines generation (excess used to pump water in storage reservoir[s]), or high-tide pumped storage (non-tide-connected power production). Multiple-basin schemes are either double-pool (station placed in-between basin, filling one basin at flood, emptying the other at ebb), both basins pumping (pumping high pool up and low pool down, pumping at off-peak), pool-to-pool dam pumping, pool-to-pool dam pumping combined with pump-turbines, tide-boosted pumped storage (basins may be of different sizes and in different places), or variations of the latter.

The tide-powered air storage scheme differs in that it uses the tidal energy to drive air turbo-compressors and stores the compressed air. In the tide-powered hydrostatic pump a propeller turbine is linked to a pump and the tidal energy is converted in a flow of high-pressure oil which turns a Pelton wheel coupled to an alternator. The Gorlov proposal involves a thin plastic barrier hermetically anchored to bottom and bay sides supported by a bay-spanning cable. The tidal energy would be converted into power by an air motor piston at ebb with direct generation or compressed air storage (Gorlov, 1982). Finally, one technology would anchor in line a series of floating turbine and generator units along the flow of the tidal current (Charlier and Justus, 1993). This approach, less onerous probably than a "traditional" tidal power plant, would perhaps be attractive for small local or regional schemes.

Reversible blade (bulb) turbines have been placed in the Rance River (France) and the Kislogubskaia (Russian Federation) single-basin plants. The Russian plant was built in modules, which considerably reduced construction costs and avoided construction of expensive cofferdams. The turbines can be used as low-head pumps.

Operating plants

If the literature on tidal power plants is extensive (cf. Charlier, 1982, 1998, 2003; Charlier and Justus, 1993), it is not easy to always determine where plants were built (Figure T29). Little is known of a plant built in the mid-1920s in Suriname (then Dutch Guyana) or in Boston Bay (end of 19th century, and dismantled because of harbor extension). Information on China's post-World War II "more than one hundred" plants is scant and even in the country itself is poor, though a few papers have been recently published (Ch'iu Hou-Ts'ung, 1958). Occasionally construction of plants is announced, as in Korea or India (cf. Sharma, 1982; Song, 1987), but proves premature. Three major plants have been built and are operating: the Rance River (France), the Kislogubskaia (Russia), and the Annapolis-Royal (Nova Scotia, Canada) plants. The first one is large and dates from 1956, the second, a pilot plant, is much smaller and was heralded as a forerunner of more ambitious ones to come, and the third one is an experimental and pilot installation.

The Rance River Plant

Twenty-four bulb groups of 10,000 kW were placed in horizontal hydraulic ducts entirely surrounded by water at the Rance plant. The cost of the cofferdams represented a third of the building cost, an expense which can now be dispensed with as was in the Russian plant and to some extent in the Canadian plant. The cost of the project ran about US$100 million (in 1966-$).

Started in 1993 and completed in 1966, the 53 m wide and about 390 m long plant protrudes 15 m above water, with foundations 10 m below sea level, accommodates a four-lane roadway (eliminating a ferry) and has substantially contributed to the economic development of the former lethargic region besides furnishing 544 MW h of usable power. The mean net annual energy production exceeds slightly 500 GW h and the mean capacity throughout the year is 65 MW. It has six modes of operation. The operation policy has aimed at optimizing the value of the energy generated, reaching maximum profit, instead of eyeing to generate the maximum amount of energy. Generation by overemptying the basin (by pumping) has been done only rarely during the last decade.

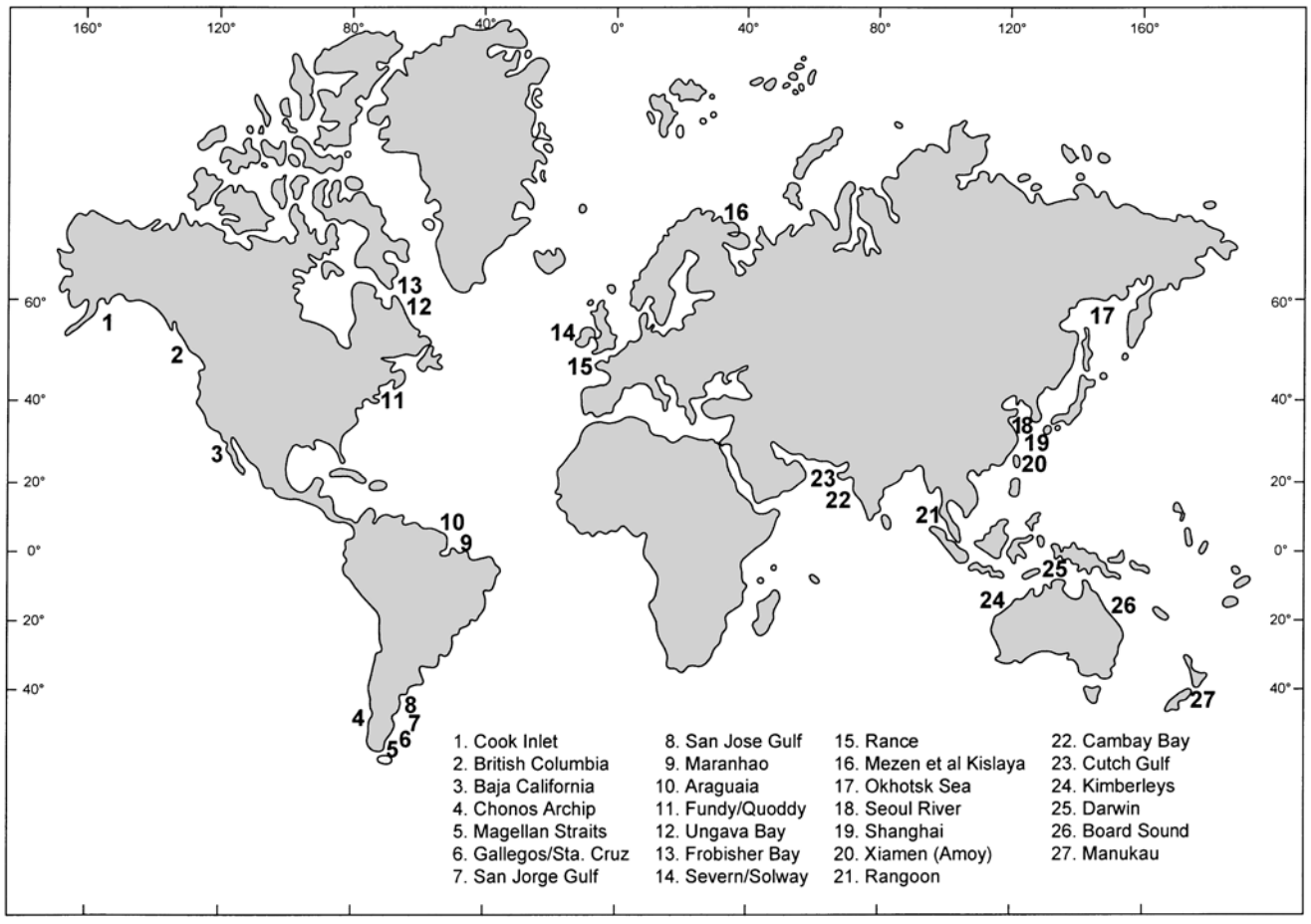

Figure T29 Location of major tidal power plants (after Charlier, 1993, with permission from Elsevier Science).

Environmental aspects at the Rance Plant. Environmental impact, at the French Rance River Plant, has been extremely mild causing only the disappearance of one species of fish. No major biological modifications have occurred. New species have appeared. Sandbanks have disappeared, high speed currents have appeared near sluices and also near the powerhouse where sudden surges have been observed. Tidal ranges have been reduced from 13.5 m to 12.8 m and minima increased. The fishing industry has not been affected contrarily to fears, and tourism has increased.

The Russian plant

The Kislaya Bay plant is located near Mezen on the Arctic. The small Russian Arctic coastal bays hold a 3.2 billion kW potential. Completed in 1968, the 18 m long, 36 m wide, 15 m high, with a 15.2 m head, plant was built by towing preconstructed concrete caissons to the site and then sinking them into place. A narrow passage connects bay and sea; no long dikes were necessary as the powerhouse itself closes the basin. Transmission lines existed close to the site. The power set capacity is 400 kW. The reversible hydraulic turbine is coupled with a synchronous generator, with the help of a multiplicator.

Russians are still considering a variety of schemes and stress that by harnessing tides in the Sea of Okhotsk bays, some 174 billion kW h could be produced.

The Canadian plant

An experimental plant was constructed in the early 1980s at Annapolis-Royal (Nova Scotia) in the Bay of Fundy whose "electricity potential" is huge; studies on Fundy tidal power go back to at least 1944. It is here that the first tide mill was built in North America (1607) using tidal and river water. A low-head STRAFLO turbine has been installed in the new plant whose generator and turbine form a coupled unit without driving shaft, particularly compact, and thus cutting powerhouse costs (Douma and Stewart, 1982). The costs amounted to CA$46 million (approximately US$44 at the time). Situated on Hog's Island in the middle of an intake canal on the lower reaches of the Annapolis River where tidal ranges reach 7 m, it took advantage of an existing dam protecting farm land. The Chinese, similarly, have commonly used existing (often earthen) dams to install tidal plants.

The turbine is a single effect one and generates electricity only during discharge of water from the retaining pool. In the event that the pool level would be below sea level, the turbine's water passage would sluice seawater into the basin during each tidal cycle. A cofferdam of local material was used to construct, in the dry, the powerhouse. Turbine and generator are located in the center of the turbine pit. The dam is 225 m long, 60 m wide at low water level, and 18 m wide at the crest. A fish pathway is provided. Fifty million kilowatts are generated.

Environmental impact. The Canadian project was designed to assess both the operational characteristics and the reliability of the Straflo turbine, and, of course, the possibility of implementing major tidal power utilization in eastern Canada. The impact study showed that interactions can be mitigated and that physical, biological, and human impact would be minimal and residual impacts small, while economic outfall would be considerable both for the short- and long-terms.

The Chinese plants

Information is difficult to secure, even in China. Claims of a large number of plants—as many as 105—and their successful operations have been repeatedly made, and so have plans to undertake new construction (Ch'iu, 1958). There are also records of the "temporary" abandon of some plants due to siltation.

Chinese engineers acknowledged a problem with siltation whose extent proves difficult to assess, but it has been said that some tidal power plants were put out of commission because of sediments accumulation. A comparative study on devising siltproof systems was carried out using data from the Baishakou tidal power plant and envisioned environmental protection to control sedimentation in the tallwater channel and reservoir (Xhikui Zu, 1992); at about the same time other studies explored the optimum patterns for double-effect single-basin plants (Shuyu Want *et al*., 1991) and calculated (modelization) of the optimum tidal energy at any location (Lee Kwang Soo *et al*., 1994). Zhikui Zhu presented in 1992 an analysis of data pertaining to the Baishakou tidal power station. It describes measures apparently taken to control sedimentation in the tallway channel and the reservoir area. Comprehensive management is outlined, including mechanical sandproofing methods and environmental protection.

The interest of Chinese researchers in tidal power plants has not waned, nor has it been somnolent as in Europe and the United States, due undoubtedly to the abundance and generally low cost of fossil fuel. An exploratory study and modelization were recently conducted (Zhuang Ji, 1991).

A review article on Chinese activity in tidal power utilization covering the 1950–90 period was published in the somewhat unfamiliar [to westerners] *Collection of Oceanographic Works*. The information rather contradicts other releases which talk about a hundred small tidal power plants. Guixiang Li (1991) mentions eight small power stations and discusses their tangible economic and social benefits. He further discloses that "many more" small and medium size, even one or two large, plants "will be built by the year 2000" along the coasts of China's mainland and the coastal islands. The publication is rather difficult to obtain, except perhaps through the good offices of the University of Karlsruhe (Germany).

Other geographical locations

No accurate information is available about the two-basin plant that functioned in Boston harbor at the turn of the preceding century until it was dismantled to make room for the port's extension, nor of the Van Bemmelen plant in Suriname. The tidal current plant in Iceland seems to have left no traces either. Plans were afoot in the 1990s to build a tidal power plant in [South] Korea (e.g., Garolim Bay) but came to a halt for political reasons (recognition of North Korea by France whose Sogreah was to build the facility) (Song, 1987). Other sites which have been considered, and for which periodically plans re-surface are the Kimberleys in Australia, San Jorge Gulf in Argentina (Aisiks and Zyngierman, 1984), and the Severn River in Great Britain (Severn Barrage Committee, 1986). There are of course numerous other suitable sites worldwide (Charlier and Justus, 1993), and studies were conducted for some of them, for instance for India (Sharma, 1982).

Tidal stream's rapid currents have been recently examined as sources of power, for example, in the Orkney and Shetland islands (Bryden *et al*., 1993–1995), perhaps using Darrieus turbines (Khio *et al*., 1996), and conversion of kinetic to electrical energy with a barrage in New York's East River (Birman, 1994). In Maine and South Carolina experiments proved that using tidal stream power with speeds up to 1.5 knots cuts the cost of seeding rafts with a wooden scoop on the bow that directs the following water to an enclosed compartment containing upwelling units and is less expensive that using other sources of power (Hadley, 1994; Rhode *et al*., 1994).

Roger H. Charlier

Bibliography

Aisiks, E.G., and Zyngierman, I., 1984. The San Jose Gulf tidal power plant, Argentina. *Proceedings of ECOR '84 & 1st Altern. Ener. Argent. Conf.* **II**, pp. 1–9.

Birman, G., 1994. Prospects of tidal energy generation. *Bulletin of N.Y. Academy of Science*, pp. 147–149.

Bryden, I.G. *et al*., 1993–1994. Tidal stream power for the Orkneys and Shetlands? *Underwater Technology*, **19**(4): 7–11.

Bryden, I.G. *et al*., 1995. An assessment of tidal streams as energy source in the Orkneys and Shetlands. *Underwater Technology*, **21**(2): 21–29.

Ch'iu Hou-Ts'ung, 1958. The building of the Shamen TPP. *Tien Chi-Ju Tung-Hsin*, **9**: 52–56.

Charlier, R.H., 1982. *Tidal energy*. New York: Van Nostrand-Rheinhold.

Charlier, R.H., 1998. *Re-invention or aggorniamento? Tidal power at 30 years. Renewable and Sustainable Energy Review*, **I**(4): 271–289.

Charlier, R.H., 2003. Justainable cogeneration from the tides: bibliography. *Renewable & Sustainable Energy Reviews*, **7**(3): 215–247.

Charlier, R.H., and Justus, J.R., 1993. *Ocean Energies. Environmental, Economic and Technological Aspects of Alternative Power Sources*. Amsterdam, London, New York, Tokyo: Elsevier Science.

Douma, A., and Stewart, G.D., 1982. Annapolis Straflo turbine will demonstrate Bay of Fundy tidal power concept. *Hydro Power Modern Power Systems*, **I**: 53–65.

Gilbert, R., 1982. Retiming with hydrogen. *Proceedings of International Conference on New Approaches to Tidal Power*, New Bedford N.S. **3**: 1–4.

Gorlov, A.M., 1982. Hydropneumatic approach to harnessing tidal power. *Proceedings of International Conference New Approaches to Tidal Power (Bedford Institute of Oceanography Dartmouth, NS)* **5**: 5–11.
Guixiang Li, 1991. Prospects for the resources on the tidal energy development in China. *Collection of Oceanographic Works—Haiyang Wenji*, **14**(1): 128–134.
Hadley, N.H. *et al*., 1994. Performance of a tidal powered upwelling nursery system for juvenile clams in South Carolina. *Journal of Shellfish Research*, **13**(1): 285.
Hollenstein, M., and Soland, W., 1982. The bulb turbine for the Rance power station. *Escher-Wyss News*, 54/55.
Khio, S., Shiono, M., and Suzuki, K., 1996. the power generation from tidal current by Darrierus turnines. *Renewable Energy*, **9**(1/4): 1242–1245.
Lee Kwang Soo *et al*., 1994. A simple analytical model for the design of the tidal power scheme. *Ocean Research*, **16**(2): 111–124.
Rhode, R.J. *et al*., 1994. Coast analysis of a tidal powered upwelling nursery for juvenile clams in South Carolina. *Journal of Shellfish Research*, **13**(1): 286.
Severn Barrage Committee, 1986. *Tidal Power from the Severn*. London: Telford.
Sharma, H.R., 1982. India embarks on tidal power. *Water Power & Dam Construction*, **34**(6): 32.
Shuyu Wang, Xigi Su, and Zhiyu Jin, 1991. Exploratory study on the optimum pattern of the tidal power plant. *The Ocean Engineer/Haiyand Gongcheny*, **9**(2): 82–90.
Song, W.O., 1987. Reassessment of Garolim tidal power project. *Ocean Research [Korea]*, **9**(1/2): 29–33.
Voyer, M., and Penel, M., 1957. Les calculs de la production d'une usine marémotrice. *La Houille Blanche (Conférence Quatrièmes Journées de l'Hydraulique)* **II**: 472–485.
Zhikui Zhu, 1992. Comparison of siltation protection measures in a Chinese tidal power station. In Larsen, P., and Eisenhauer, N. (ed.), *Proceedings of 5th International Symposium On River Sedimentation, Karlsruhe 6/10 April 1992. Sediment Management*, Vol. 2, pp. 847–852.
Zhuang Ji, 1991. Exploring study of optimum patterns of the tidal power plant. *The Ocean Engineer—Haiyang Gongcheng*, **9**(2): 82–90.

Cross-references

Engineering Applications of Coastal Geomorphology
Microtidal Coasts
Tidal Environments
Tidal Prism
Tide-Dominated Coasts
Tide Mill
Tides
Wave Power

TIDAL PRISM

The tidal prism is the amount of water that flows into and out of an estuary or bay with the flood and ebb of the tide, excluding any contribution from freshwater inflows. For this reason, it is often reported as the volume of the incoming tide, and the contribution of river inflow calculated from the difference of the ebb and flood volumes. The tidal prism can be determined from hydrographic charts, where the volume in the estuary between low water and high water is calculated from sounding data. The tidal prism can also be determined by measuring the amount of water flowing into an estuary using a technique known as a tidal gauging. This is normally undertaken at a narrow section in an estuary of regular shape, and at a time when river inputs are low. Measurements of current velocity and water depth are made continuously at various points throughout the section using current meters suspended from a boat or bridge, along with measurements of water (tide) level in the section over the tide. The tidal prism is computed as the product change in cross-section area and mean velocity in section, integrated over half the tidal cycle. Today a vessel mounted ADCP (acoustic doppler current profiler) which returns depth, tidal change, and current at many points in the water column as the vessel travels back-and-forth across the section greatly simplifies and improves the accuracy of a tidal gaugings.

The tidal prism is an important metric for an estuary. It is an indicator of the hydrodynamic processes operating in an estuary. In shallow estuaries where the tidal prism forms a large proportion of the water in the estuary at high tide, tidal processes dominate and flushing is good. In deep estuaries with relatively small tidal prisms density-driven flows and river inputs play a greater role in the hydrodynamics. In estuaries where there are semidiurnal tides and a large difference in spring and neap tidal ranges, the amount of water flowing into the estuary (the tidal prism) on a spring tide may be double that on a neap tide and tidal currents and sand transport increase along with this. Empirical relationships developed between tidal prism and various estuary parameters help with the conceptual understanding of processes and provide a simple tool for easy calculations of stable channel design (e.g., Bruun, 1990).

The tidal prism is related to inlet dimensions, the amount of sand stored in tidal deltas, and has been used to describe inlet stability. The empirical relationship between the gorge cross-sectional area and tidal prism of a tidal inlet has been described in numerous studies (O'Brien, 1931; Jarrett, 1976; Hume and Herdendorf, 1992) by:

$$A = c\Omega^n,$$

where A is the gorge cross-sectional area (m^2), Ω is the tidal prism (m^3) and c and n are constants. Inlet gorges that are stable conform to the relationship and there is considered to be a balance between the inlet geometry and tidal flow through the gorge. Those lying off the line are out of equilibrium and characterized by either scour or deposition. A similar relationship has been found to exist between the ebb tidal delta sand volume, which increases with increasing tidal prism. In this situation, the volume of the sand body also increases with decreasing wave energy and as the angle that the ebb jet makes with the beach on the adjacent barrier shore increases (Walton and Adams, 1976; Hicks and Hume, 1996). On coasts where there is little wave energy and estuaries have large tidal prisms the delta will be elongated offshore under the influence of the ebb tidal jet. Where estuaries with small tidal prisms occur on coasts with high wave energy the ebb tidal sand body will be more flattened against the shore. A–Ω relationships have been used to quantify the morphological stability of tidal inlets. Bruun and Gerritsen (1960) showed that the size of the tidal gorge is one of the main factors determining the ability of flow to transport sediment through the entrance. Inlet gorges that are morphologically stable (i.e., have the ability to return to their original configuration after a disturbance) conform to the relationship because there is a balance between tidal flow and littoral drift to the gorge, so the inlet stays open. They demonstrated that when the ratio of the tidal prism to total (gross) annual littoral drift delivered to the inlet from the ocean is in excess of 300 the inlet has a high degree of stability. In cases where the ratio is less than 100 there will be a low degree of stability and entrance bars will shallow and navigation difficult. A–Ω relationships like those for tidal inlets on sandy shores also hold for many different estuary types ranging from lagoon to river mouth and even to large coastal embayments, and have been used to characterize and classify inlets (Hume and Herdendorf, 1993).

Terry M. Hume

Bibliography

Bruun, P., 1990. *Port Engineering*. Houston, TX: Gulf Publishing Co.
Bruun, P., and Gerritsen, F., 1960. *Stability of Coastal Inlets*. Amsterdam: North Holland.
Hicks, D.M., and Hume T.M., 1996. Morphology and size of ebb tidal deltas at natural inlets on open-sea and pocket bay coasts, North Island, New Zealand. *Journal of Coastal Research*, **12**: 47–63.
Hume, T.M., and Herdendorf, C.E., 1992. Factors controlling tidal inlet characteristics on low drift coasts. *Journal of Coastal Research*, **8**: 355–375.
Hume, T.M., and Herdendorf, C.E., 1993. On the use of empirical stability relationships for characterising inlets. *Journal of Coastal Research*, **9**: 413–422.
Jarrett, J.T., 1976. Tidal prism-inlet area relationships. Vicksburg, MS: US Army Corps of Engineers, Coastal Engineering Research Center and Waterways Experimental Station, *GITI Report No. 3*.
O'Brien, M.P., 1931. Estuary tidal prisms related to entrance areas. *Civil Engineer*, **1**: 738–739.
Walton, T.L., Jr., and Adams, W.D., 1976. Capacity of inlet outer bars to store sand. In *Proceedings, 15th International Conference on Coastal Engineering*. American Society of Civil Engineers, New York, pp. 1919–1937.

Cross-references

Estuaries
Instrumentation (see Beach and Nearshore Instrumentation)

Tidal Environments
Tidal Flats
Tidal Power
Tide-Dominated Coasts
Tide Gauges
Tides

TIDE-DOMINATED COASTS

As first enunciated by Price (1955), and later elaborated upon by others (e.g., Hayes, 1975), tides play an important role in defining the geomorphology of depositional shores, namely coastal and deltaic plains. On such shores, it is the ratio of tidal energy, usually dictated by tidal range, to wave energy, a function of average wave height, that determine the morphology of the coast, with sediment supply being an important modifier near major river mouths. As a generalization, coasts with small tidal ranges (microtidal ≤2 m (Davies, 1964)) are dominated by wave energy. Such coasts were termed *wave-dominated coasts* by Price (1955). On the other hand, coasts with large tidal ranges (macrotidal ≥4 m) are typically dominated by tidal energy, and were hence termed *tide-dominated coasts* by Price. The effectiveness of wave energy diminishes (i.e., waves cannot break in a concentrated area for a long period of time), and tidal current energy increases as the vertical tidal range increases. Exceptions to this generalization occur where waves are so small that even small tides generate adequate energy to shape the coast. An example of a *tide-dominated coast* with a relatively small tidal range occurs at the head of the embayed coastline of northwest Florida (Hayes, 1979). Coasts with intermediate wave energy and tidal ranges (typically mesotidal = 2–4 m) were termed *mixed-energy coasts* by Hayes (1979).

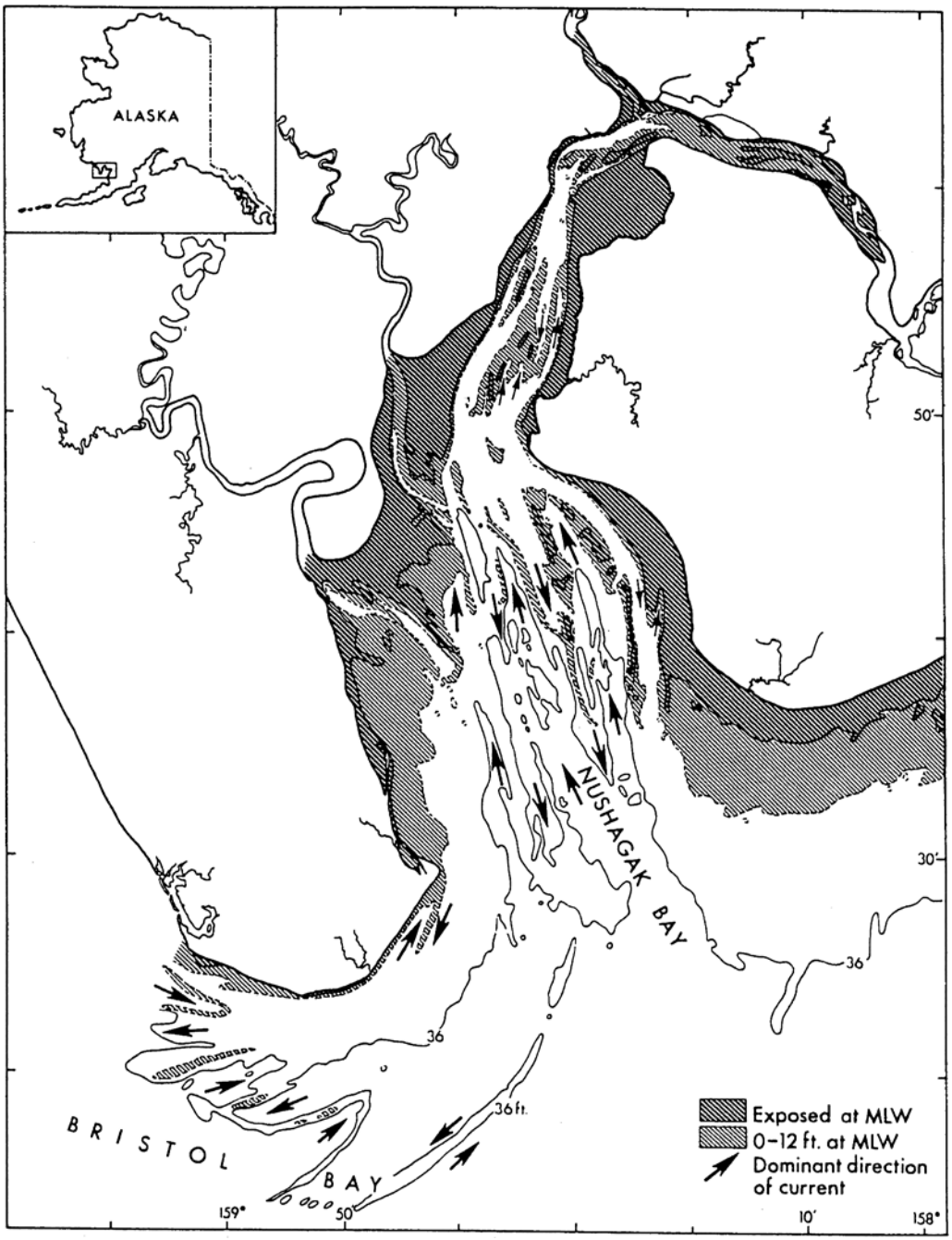

Figure T30 Nushagak Bay, Alaska, a tide-dominated embayment (tidal range = 5.5 m). Note lineation of shoals parallel with tidal currents.

Tide-dominated, non-deltaic coasts

The bathymetry of a typical tide-dominated, non-deltaic shore, Nushagak Bay, Alaska, is illustrated in Figure T30. The coastal morphology of major river mouths on tide-dominated coasts are most commonly open-mouthed estuaries, as shown in Figure T30. Between major rivers on these types of coasts, the shore is occupied by extensive salt marshes and tidal flats. Barrier islands are completely missing, because wave action is not focused enough at a single topographic level to build a barrier island and tidal currents are strong enough to disperse the sand to offshore regions. Examples of this type of coast occur in northwest Australia (Coleman and Wright, 1975), western Korea (Kim *et al*., 1999), the Bay of Bengal, northern end of the Gulf of California (Thompson, 1968), the Wash, England (Evans, 1979), and many other depositional coasts with tidal ranges greater than 4 m. Generally speaking, the sediment distribution patterns on coasts of this type are exactly opposite to those on wave-dominated coasts, inasmuch as finest sediments occur on mudflats and in wetlands of the upper intertidal zone and coarsest sediments occur lower in the intertidal zone and offshore where tidal currents are strongest.

Studies by Evans (1975) documented the characteristics of the sediments of the tidal flats of the Wash, an indention in the coastline of the east coast of England, which has a tidal range of 7.0 m. The seaward portions of the flats are made up of complex sand bodies covered by sand waves, whereas the upper part is fringed by a salt marsh composed of fine-grained sediments. Studies of the tidal flats of the Bay of Fundy, by Knight and Dalrymple (1975), Dalrymple *et al*. (1990), Yeo and Risk (1981), and numerous others, describe the sedimentology, sediment transport dynamics, and potential stratigraphy of this intertidal zone, which has the largest tidal range in the world.

Figure T31 gives a hypothetical prograding stratigraphic sequence for the intertidal zone of a tide-dominated coast based on the references cited above and other sources.

Tide-dominated deltas

On tide-dominated coasts where the rivers have enough sediment load to have filled the antecedent lowstand valley and build a bulge in the shore (within the time frame of the present highstand), the resulting river deltas are typically referred to as *tide-dominated deltas* (Fisher *et al*., 1969; Galloway, 1975). However, the distinction between such deltas and estuaries is somewhat obscure. Tide-dominated deltas usually are composed of a series of funnel-shaped water bodies (estuaries?) at multiple river mouths with a series of shore perpendicular sand ridges that extend offshore of the river mouths. Broad tidal flats and marsh or mangrove wetlands occur along the shore of the embayments. A generalized model of a tide-dominated delta is given in Figure T32.

The tide-dominated Ord River Delta, described by Coleman and Wright (1979), is located on the coast of northwest Australia were the tidal range varies between 3.8 and 6.6 m. Tidal currents are oriented primarily in an onshore and offshore direction within an embayment which composes the major mouth of the Ord River. Linear sand ridges, which range in relief from 10 to 22 m and average 2 km in length, occur in the most seaward portion of the embayment. These sand ridges are formed and shaped primarily by tidal currents, which dominate over wave energy effects. A composite prograding stratigraphic column for this delta shows a fining upward sequence resulting from the progradation of muddy upper intertidal flats and marsh sediments over the sand bodies of the lower intertidal and shallow subtidal regions.

Tide-dominated estuaries

The concept of tide and wave dominance has also been applied to estuaries by Dalrymple *et al*. (1992). However, they state that estuaries are unlike many other coastal systems, because they are "geologically ephemeral." If the rate of sediment supply is sufficient to eventually fill the lowstand valley within which the estuary is located, the filled valley then becomes a delta. The estuaries they term wave-dominated are composed of a sand body complex (barrier/tidal inlet) at the entrance, a muddy central basin, and a bayhead delta system. *Tide-dominated estuaries*, on the other hand, contains elongate sand bars and sandy tidal flats at the entrance and complex tidal channel/ wetland habitats further inland.

Miles O. Hayes

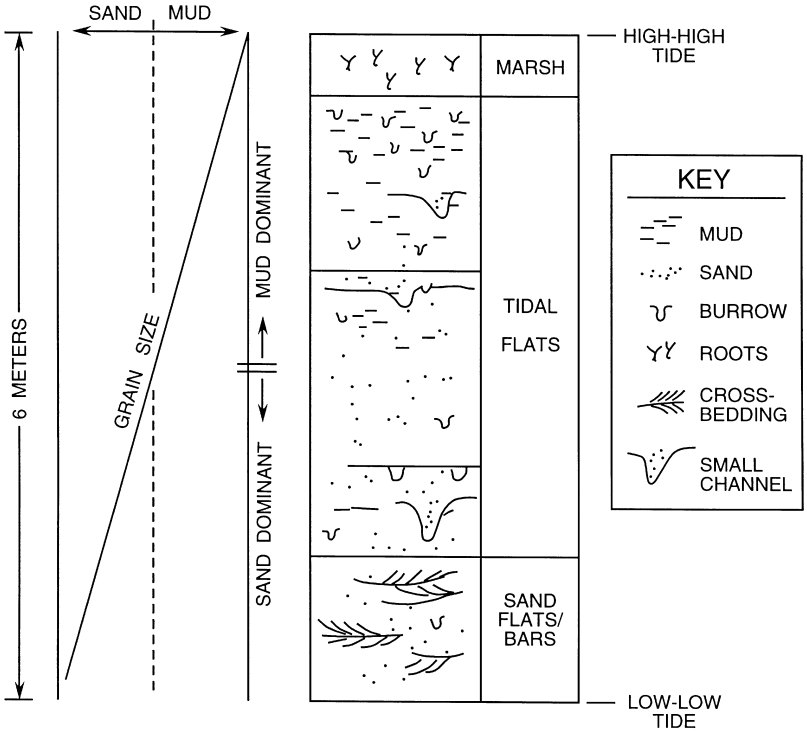

Figure T31 Hypothetical regressive sequence for the intertidal zone of a prograding macrotidal (tide-dominated) shoreline in a non-deltaic setting.

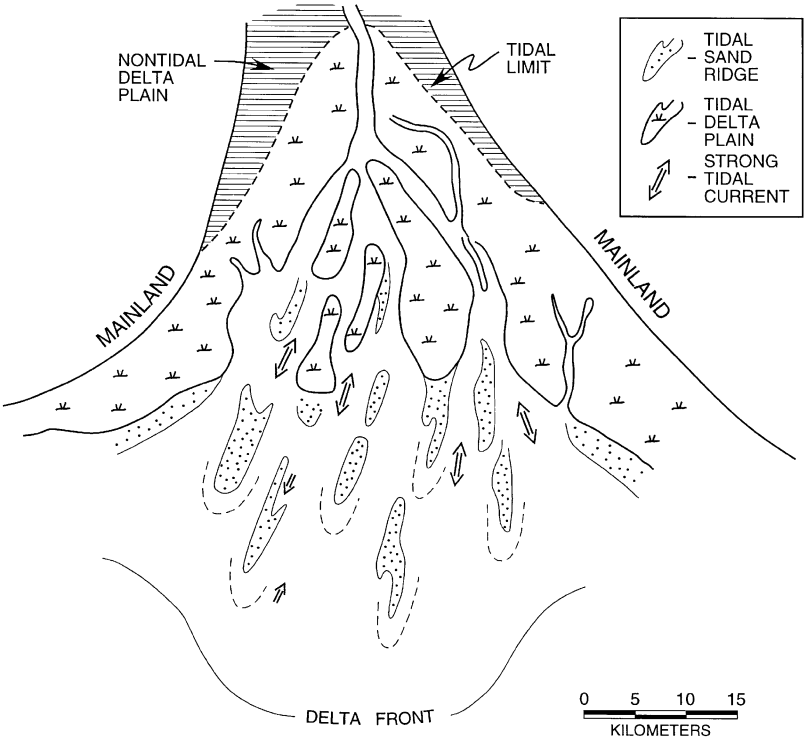

Figure T32 Schematic sketch in plan view of a tide-dominated delta. Note the presence of tidal sand ridges at the offshore entrances to the delta complex.

Bibliography

Coleman, J.M., and Wright, L.D., 1979. Sedimentation in an arid macro-tidal alluvial river system: Ord River, Western Australia. *Journal of Geology*, **85**: 621–642.

Dalrymple, R.W. *et al*., 1990. Dynamics and facies model of a macrotidal sand-bar complex, Cobequid Bay-Salmon River Estuary (Bay of Fundy). *Sedimentology*, **37**: 577–612.

Dalrymple, R.W., Zaitlin, B.R., and Boyd, R., 1992. Estuarine facies models: conceptual basis and stratigraphic implications. *Journal of Sedimentary Petrology*, **63**: 1130–1146.

Davies, J.L., 1964. A morphogenic approach to world shorelines. *Zeitschrift fur Geomorphologie*, **8**: 27–42.

Evans, G., 1975. Intertidal flat deposits of the Wash, western margin of the North Sea. In Ginsburg, R.N. (ed.), *Tidal Deposits*. Springer-Verlag: New York, pp. 13–20.

Fisher, W.L. *et al*., 1969. *Delta Systems in the Exploration for Oil and Gas, a Research Colloquium*. Texas University Bureau of Economic Geology.

Galloway, W.E., 1975. Process framework for describing the morphological and stratigraphic evolution of deltaic depositional systems. In Broussard, M.L. (ed.), *Deltas*. 2nd edn. Houston, TX: Houston Geological Society, pp. 87–98.

Hayes, M.O., 1975. Morphology of sand accumulation in estuaries. In Cronin, L.E. (ed.), *Estuarine Research*, Vol. 2. New York: Academic Press, pp. 3–22.

Hayes, M.O., 1979. Barrier island morphology as a function of tidal and wave regime. In Leatherman, S. P. (ed.), *Barrier Islands from the Gulf of St. Lawrence to the Gulf of Mexico*. New York: Academic Press, pp. 1–27.

Kim, Y.H. *et al*., 1999. Holocene transgressive stratigraphy of a macrotidal flat in the southeastern Yellow Sea: Gomso Bay, Korea. *Journal of Sedimentary Research*, **69**: 328–337.

Knight, R.J., and Dalrymple, R.W., 1975. Intertidal sediments from the south shore of Cobequid Bay, Bay of Fundy, Nova Scotia, Canada. In Ginsburg, R.N. (ed.), *Tidal Deposits*. New York: Springer-Verlag, pp. 47–56.

Price, W.A., 1955. *Development of Shorelines and Coasts*: Department of Ocean. Project 63, Texas A&M University.

Thompson, R.W., 1968. *Tidal Flat Sedimentation on the Colorado River Delta, Northwestern Gulf of California*. Geological Society of America Memoir 107.

Yeo, R.K., and Risk, M.J., 1981. The sedimentology, stratigraphy, and preservation of intertidal deposits in the Minas Basin system, Bay of Fundy. *Journal of Sedimentary Petrology*, **51**: 245–260.

Cross-references

Barrier Islands
Deltas
Estuaries
Tidal Environments
Tides
Wave-and-Tide Dominated Coasts
Wave-Dominated Coasts

TIDE GAUGES

Historical origin

Tide gauges have a relative long history. At some places, systematic sea level observations have been performed and recorded since the late 17th or early 18th century. This is the case in Amsterdam, for instance, since 1682, in Liverpool since 1768, or in Stockholm since 1774.

The first devices were simply graduated rods, usually called tide poles, placed at locations where the instantaneous water level height of the sea could be read off at any time by an observer. Most of such measurements were undertaken in or at the entrance of harbors. They were restricted to observations of high and low water levels, as well as the time of their occurrences (Cartwright, 1999).

Automatic recording devices appeared only in the 1830s, although basic instructions were already detailed and published in an Italian journal in 1675. An extract was transcribed in the "Journal des Sçavans" of April 22, 1675 (Observatoire de Paris, 1675). These were

mechanical gauges, equipped with float, wires, counterweights, clock, pen, paper chart recorder, and stilling well. They provided the first complete tidal curves which could be examined in detail and digitized for further analysis.

Tide or sea-level gauges?

Whatever technique is employed, the basic quantity provided by tide gauges is an instantaneous height difference between the level of the sea surface and the level of a fixed point on the adjacent land. The vertical reference point is a nearby benchmark which can be observed by traditional surveying techniques. Thence, tide gauges not only record ocean tides but also a large variety of sea-level signals that can be caused by variations in atmospheric pressure, density, currents, continental ice melt ... as well as vertical motions of the land upon which the measurement instrument is located, due to tectonic changes, isostatic adjustments, volcanism inflation, sediment consolidation, pier subsidence, etc. Records of such devices are indicative of what are called relative sea-level changes (Pugh, 1987). The recorded processes have characteristic timescales from several minutes to centuries.

Therefore, tide gauge data is valuable information to a wide range of activities over a variety of timescales, for scientific research as well as for many practical applications. For instance, data have uses: for navigation and ship traffic (guidance, tidal timetables...), for coastal engineering design (dike building, dredging works...), for statistics of extreme levels over long periods, for studies of upwelling and fisheries, for hydrographic surveys (sound charts, chart datum ...), for storm-surge predictions and alert, for analysis of the risk of flooding and coastal protection, for input or validation of ocean circulation models, for long-term trend of sea-level variations, for global change research and monitoring and, of course, for tidal analysis, prediction and validation of tidal models. In spite of the numerous applications, the historical and conventional term of tide gauge still prevails for such devices, although sea-level gauge would be more adequate.

Technical evolution

The most common type of gauge in use around the world still consists of the float and stilling well system which was devised more than a century ago. In this system, the height measurement of a floating gauge is taken by measuring, on a reduced scale, the length of the wire holding a counter-balanced float. The float sits on the surface of the water inside a well. The vertical movement of the float is transmitted and reduced in scale through a more or less sophisticated system of wires, pulleys, and counterweights to a pen. A continuous record of water height against time is obtained in this way as a drawn curve on paper, the paper being in motion at a fixed speed in a normal direction to the pen displacement. The stilling well is a vertical tube long enough to cover any possible range of tide. It prevents the float from drifting in the presence of currents or winds. The well is designed to provide a mechanical filtering of short-period oscillations due to waves by restricting the flow of water into and out of the well.

Traditional mechanical float devices are progressively replaced by new technologies. Modern type gauges are mainly based either on the measurement of the subsurface pressure or on the measurement of the time of flight of a pulse, acoustic or radar.

The principle of a pressure system is the measurement of the hydrostatic pressure of the water column above a fixed point below the lowest expected tide level. The conversion of that hydrostatic pressure into a sea-level equivalent height is performed according to the law: $\boldsymbol{h} = (\boldsymbol{p} - \boldsymbol{p}_a)/(\rho g)$ by measuring or assuming values of water density ρ, air pressure $\boldsymbol{p}_a$, and local acceleration due to gravity g. Pressure sensors usually exploit strain gauge or ceramic technology. Water pressure translates then into changes in resistance or capacitance in the pressure element. The resulting signal is normally a specific frequency which is converted into physical units of pressure.

The acoustic or radar systems determine the vertical distance from a transducer, located above the sea surface, to the water by measuring the elapsed time of a pulse that is emitted, reflected, and returned back to the sensor. The distance to the water is then derived from the velocity of the type of wave considered (sound or radar).

Whereas technical description may be provided by manufacturers, IOC manuals (1985, 1993, 1997) are a helpful source of information. Valuable detailed information can be found there on each type of gauge, their respective advantages, drawbacks, performances, and limitations, as well as advice on operational methods and environmental conditions of use.

A critical part of the tide gauge system is probably the benchmark on land as it provides the fundamental zero point or datum to which the values of sea level are referred. This benchmark is extremely important as it serves to build useful long-term sea-level time series, even if parts of the time series were obtained from different gauges and different benchmarks (as long as they were geodetically connected). Tide gauge benchmarks are ultimately the source of the long-term coherence and stability of the measurements. It is therefore common sense to preserve the datum by installing and connecting a set of 5–10 benchmarks within a few hundred meters of the tide gauge. Usually, one of them is arbitrarily called the tide gauge benchmark, the "most" stable, the "most" secure or the closest, although all of them are representive of the datum. Even though the station is equipped with the most modern equipment, long-term instrumental drift and local stability surveying should be performed at least annually.

In the era of modern communication technologies, data in electronic form is essential as it can be retrieved immediately from a gauge to a data center by automated modem dial-up or satellite transmissions. Data can then easily be made accessible worldwide via the Internet. Paper chart recorders are no longer acceptable. They require slow labor-intensive digitization and are cost-effective. Moreover, they contain many sources of inaccuracy and are inadequate for certain applications.

Scientific applications

Many scientific applications other than the natural tidal research and modeling benefit from tide gauge records. For instance, tide gauge data are used to establish vertical reference systems on land and on sea in order to define the height and depth datums. The belief, about a century ago, that the average level of the sea was constant over long periods of time led to define the concept of geoid and, subsequently, to establish the origin of the leveling networks on "mean sea level." Typically, countries chose one tide gauge station to compute this quantity over an arbitrary time period: in France, for example, the datum was determined at Marseilles from continuous tide gauge records performed during the period 1885–97; in Britain, the Ordnance Datum was determined at Newlyn from records extending from May 1915 to April 1921. However, mean sea level varies from place to place and at one specific place over time. Today, mean sea level at Marseilles is about 11 cm above the local 1885–97 datum, whereas it is about 0.2 m above the Ordnance Datum at Newlyn. Thus, the datums no longer represent the "real" average of the sea level at these sites.

Tide gauge data are also used to establish the datums to which the depths are referred on nautical charts and above which tide predictions are provided for practical purposes. Since 1996, the International Hydrographic Organization has recommended that Lowest Astronomical Tide be adopted as the International Chart Datum. This datum is defined as the lowest tide level which can be predicted in average meteorological conditions and in any combination of astronomical conditions.

Owing to the rhythmic nature of the tide, the components of its oscillations can be represented by a series of sinusoidal curves, mainly depending on the relative positions of the moon and the sun. In each place, the major tide components are determined empirically from hourly records during at least 29 days (a moon cycle), by the use of harmonic analysis. Because astronomical orbits are known, tides can be predicted at any time. Random deviations from the predicted tide can be due to changes in air pressure or wind (sea surges), currents, changes in water density, discharge (especially at a river mouth) and can be analyzed after filtering the astronomical tide. The occurrence of short-lived oscillations in random deviations, following a sea surge, may correspond to seiches. Finally, if periodic, short-lived and random components are removed by filtering processes, and if the series investigated are long enough, long-term trends will appear.

Tide gauges have been carefully studied for indications of recent global sea-level rise. They include land movement and sea-level movement and depend, therefore, on local or regional tectonics as well as global climate change effects (eustasy). By analyzing the difference in trend between the records in two stations, local and regional components can be easily revealed, though their interpretation may be not univocal. In order to keep the statistical accuracy of a trend estimation below ± 0.5 mm/yr, almost continuous records of at least 40 to 60 years long are usually necessary. At the present time, less than 300 stations in the world can provide such long records. Their geographical distribution is unfortunately very uneven, most of the stations being located in the Northern Hemisphere, with a great majority on both sides of the North Atlantic and few or no data in very wide coastal areas. Since the late 1980s, international projects like GLOSS have made deserving efforts to improve the existing tide-gauge network, but the duration of the new records is still too short to assess long-term trends. In spite of such globally unrepresentative distribution, of the difficulty in separating the

various components of relative sea-level change, and of the fact that long-term trends show a great spatial variability, several authors have attempted an estimation of the recent global (average) sea-level rise from tide-gauge records, with various approaches (Emery and Aubrey, 1991; Pirazzoli, 1996). The results obtained are quite variable: a "global" sea-level rise between 0.5 and 3.0 mm/yr is inferred by various authors, with several estimates around 1 mm/yr; higher rates are obtained when tide-gauge trends are "corrected" using isostatic models; however, other authors infer that an accurate global sea-level trend is indeterminable of the basis of tide-gauge data alone. This precludes for the moment a more precise quantification of the recent global rise in sea level only with tide gauges.

Perspectives: synergy with space techniques

Recent advances in space geodesy and gravity measurements allow consideration of monitoring of land movements in a global geocentric reference frame rather than in a local one. Repeated or continuous precise positioning of tide gauge benchmarks by geodetic techniques like GPS or DORIS, over periods of a decade or so, will enable vertical crustal movement to be determined and, subsequently, provide a possible discrimination between eustatic sea-level rise and land subsidence within tide gauge records (IOC, 1997; Neilan *et al*., 1998). Moreover, tide gauge data will then be expressed in the same global geodetic reference frame as satellite altimeter observations and can therefore be directly compared and combined with the altimetric sea levels, providing at last a more reliable and accurate estimate of sea-level variations.

Probably the most significant improvement in sea-level research comes from satellite radar altimetry. However, altimetry cannot provide detailed local high-frequency sea-level information due to the specific sampling pattern. Tide gauges continue to possess important attributes for certain applications, like continuity with historic measurements, high accuracy, continuous sampling, and ability to record at the coast at a relatively low cost.

Guy Woppelmann and Paolo Antonio Pirazzoli

Bibliography

Cartwright, D.E., 1999. *Tides—a scientific history*. Cambridge: Cambridge University Press.

Emery, K.O., and Aubrey, D.G., 1991. *Sea Levels. Land Levels, and Tide Gauges*. New York: Springer Verlag.

IOC, 1985 and 1994. *Manual on Sea-Level Measurement and Interpretation*. Intergovernmental Oceanographic Commission Manuals and Guides No. 14, Vol. 1 (1985) and Vol. 2 (1994).

IOC, 1993. *Joint LAPSO-IOC workshop on sea level measurements and quality control*. Intergovernmental Oceanographic Commission, Workshop Report No. 81.

IOC, 1997. *Global Sea Level Observing System (GLOSS) Implementation Plan 199*. Intergovernmental Oceanographic Commission, Technical Series No. 50.

Observatoire de Paris (ed.), 1675. *Extrait du Journal d'Italie contenant quelques avertissements pour observer les différens périodes de la marée; avec la description and la figure de la machine dont il est parlé. Journal des Sçavans, du 22 avril 1675*. Tome 2176, pp. 65–67.

Neilan, R.E., Van Scoy, P.A., and Woodworth, P.L. (eds.), 1998. Workshop on methods, for monitoring sea level: GPS and tide gauge benchmark monitoring. GPS altimeter calibration. In *Proceedings of the Workshop Organized by the IGS and PSMSL*, Pasadena, March 17–18, 1997.

Pirazzoli, P.A., 1996 . *Sea-Level Changes. The Last 20000 Years*. Chichester: John Wiley & Sons.

Pugh, D.T., 1987. *Tides, Surges and Mean Sea Level: A Handbook for Engineers and Scientists*. Chichester: John Wiley & Sons.

Cross-references

Altimeter Surveys, Coastal Tides and Shelf Circulation
Changing Sea Levels
Coastal Climate
Coastal Currents
Geodesy
Global Positioning Systems
Greenhouse Effect and Global Warming
Storm Surge
Submerging Coasts
Tectonics and Neotectonics
Tidal Datums
Tides
Uplift Coasts

TIDE MILL

Tide Mills (*moulins à marée, molinos de mar, Gezeitenmoehlen, getijdenmolens*) dotted the coasts and estuaries for several centuries until more efficient, but not less costly, alternatives all but wiped them off the map. A few are making a comeback. Some were still functioning during World War II in England and Wales, but most were derelict or their buildings transformed and used for other purposes (Wailes, 1941). History records show that tide mills once functioned on the rivers Thames (London Bridge), Tiber (in besieged Rome), and Danube (Charlier and Menanteau, 1998). A mill stood at the entrance of Dover Harbor in (1000) according to the *Domesday Book*.

Tide Mills consisted of a dam with sluices, a retaining basin, and a float or a water wheel and transformed the energy of running water into mechanical power to run flour-mills, saw-mills, even breweries, and as late as 1880 to pump sewage. They apparently were also put to work in the *polder-works*.

Tide Mills require sites with tidal amplitude—and thus a tidal current—though even a tidal creek may do. They are the forerunners of today's tidal power plant in the same manner as the windmill is the precursor of the contemporary air turbines. The tide mill is in fact a conventional water mill using the tidal current as its source of power, occasionally both ebb and flood tide, but most used only the ebb current as the retaining basin filled at flood time, emptied at ebb time. A few mills used a proportion of freshwater from the stream in addition to seawater.

The most common idea was the "float method" by which the incoming water raised a floating mass which, as it fell down to original position, provided "work;" another approach included a shaft-mounted rotating paddle wheel activated by ebb and flood, with power transmitted by the shaft; finally somewhat more sophisticated types would let air contained in a metal or concrete conduit be compressed by the incoming tide, thus furnishing compressed air power, an idea which has resurfaced today in proposed schemes (Gorlov, 1982). The fourth system, even more elaborate, dams part of the sea (bay, gulf) and this pool fills up at incoming tide; the water when released at low tide passes through turbines to flow back to sea or to another basin. The latter scheme appeared in the 19th century and with its wheel rotating at as much as 150 rpm, had a much higher yield.

Tidal mills were quite numerous in England, Wales, The Netherlands, Brittany, and Spain. The Europeans brought them to the United States, seemingly on both coasts (Creek, 1952) and Canada. There are some claims that they were not uncommon along the South China Sea coast. Besides the touristic value of restored mills, as near Southampton (Ewing Mill), Plougastel (Brittany), and in Massachusetts (Chatham Spice Mill), tide mills are making a timid come back, in an improved version, to provide power in remote areas.

Roger H. Charlier

Bibliography

Charlier, R.H. and Menanteau, L., 1998. The saga of tide mills. *Renewable and Sustainable Energy Review,* **1**(3): 1–39.

Creek, H., 1952. Tidal mill near Boston. *Civil Engineering* **22**: 840–841.

Gorlov, A.M., 1982. Hydropneumatic approach to harnessing tidal power. New approach. *Proceedings of Tidal Power Conference [New Bedford, NS, Canada],* **4**: 1–5.

Wailes, R., 1941. Tide mills in England and Wales. *Junior Institute of Engineering, Journal and Record of Transactions*, **51**: 91–114.

Cross-references

Polders
Tidal Creeks
Tidal Power
Tidal Prism
Tides

TIDES

Introduction

Tides are the periodic motion of the waters of the sea caused by the changing gravitational effects of the moon and the sun as they change position relative to the rotating earth. The tides in the oceans are actually very long waves hundred or thousands of miles long. Although produced by astronomical forces, their behavior in the oceans and connected bays (and the size of resulting water level oscillations) is determined by hydrodynamics (i.e., the physics of the water movement).

The vertical rise and fall of the water surface is usually referred to as the *tide*, while the accompanying horizontal movement is referred to as the *tidal current*, with the tidal flow into a bay called the *flood* and the flow out of a bay called the *ebb*. For most areas of the earth the rise and fall, and flood and ebb, occur twice a day (referred to as a *semidiurnal* tide), but in some areas there may only be one *high water* and one *low water* per day (referred to as a *diurnal* tide). In many areas, there are two high waters and two low waters per day, but one high water and/or one low water is a different height than the other (referred to as a *mixed* tide).

The tide is only one phenomenon that produces variations in water level and currents. Such variations can also be caused by changes in the wind, atmospheric pressure, river discharge, and water density (due to changes in salinity and temperature), but they are not periodic like the astronomical tide and are not nearly as predictable, being associated with weather. Nontidal water level changes caused by changes in the wind and barometric pressure are usually referred to as *storm surges* (*q.v.*). The term *sea level* is generally used for longer-period, slower changes in water level. *Mean sea level* is the average of water level measurements over some time period (such as a day, a month, or a year), which averages out shorter-term oscillations like the tide.

Water level is the height of the water surface above some reference level, called a *datum*. A datum for a particular waterway is generally defined as an average height of a particular stage of the tide. For example, *chart datum* on a nautical chart in the United States is defined as the mean lower low water (MLLW) at each location. (*Lower low water* is the lower of the two low waters that occur each day, and MLLW is the average of all the lower low waters over some time period, usually at least a year). Depth soundings on a nautical chart are the depths below the chart datum, and the predicted tidal heights found in Tide Tables are the heights above the chart datum. Adding the two together gives the total water depth at that moment in time. These tidal datums also provide the legal definition of *marine boundaries*. MLLW, for example, is the dividing line between federal territorial seas and state submerged lands, and mean high water (MHW) is the dividing line between state tidelands and private uplands. Tidal datums at a particular tide gauge are referenced to the land through geodetic leveling to a number of *benchmarks*, which are brass markers driven into solid rock or other permanent structures. Tidal datums can change over decades if the land subsides (or rises due to glacial rebound) or if relative sea-level rises due to other effects.

The tide dominates our thinking about changes in water level, not only because it usually causes the largest changes (except during storms), but also because it is very predictable (especially in comparison to how well we can predict the weather). After analyzing only a month's worth of water level measurements from a tide gauge, we can predict the tide quite accurately (for that location) for years into the future. This high predictability is due to the tide's periodic nature and our very precise knowledge of its astronomical forcing. The earth–moon orbit, the revolution of the earth around the sun, and the rotation of the earth on its axis involve periodic motions with fixed and precisely known time periods. Tidal energy is found at the same frequencies that describe these astronomical motions.

To fully understand and predict the tides one must understand both its astronomical forcing and the hydrodynamics of the oceans and bays. While it is the astronomical forcing of the tide that is the basis for the tide's predictability, it is the hydrodynamics of the tide that is responsible for the size of the *tidal range* (i.e., the height difference from low water to high water), the timing of high and low waters, and the *type of tide* (i.e., semidiurnal, mixed, or diurnal). It is the length, width, and depth of the bay or river (and of any adjoining waterways) that control the hydrodynamics. In shallow waterways, the hydrodynamics also transfers tidal energy to new frequencies, and distorts the shape of the tide curve away from perfect sine curves. These same shallow-water processes also lead to interactions between the tide and nontidal phenomena such as storm surge and river discharge.

The largest tidal ranges occur in shallow coastal waters, in particular, at the ends of certain bays and along coasts with very wide continental shelves. The increase in tidal range and tidal current speeds that one sees in the shallow waters of bays, rivers, and straits can go to dramatic extremes if the circumstances are right. Tidal ranges reach 15 m (50 ft) in Minas Basin in the Bay of Fundy. Tidal ranges greater than 12 m occur at the northern end of Cook Inlet near Anchorage in Alaska, in the Magellan Strait in Chile, in the Gulf of Cambay in India, along the Gulf of St. Malo portion of the French coast bordering the English Channel, in the Severn River in England, and along the open coast of southern Argentina. In a few rivers, a portion of the tide wave propagates up the river as a tumultuous wall of water, called a *tidal bore*. The largest tidal bores are found in the Tsientang River near Hanchow, China, and in the Amazon River, Brazil, where at certain times they can reach 7.5 m in height and travel up the river at a speed of 7 m/s. Smaller bores occur in the Meghna River in India, in the Peticodiac River at the end of the Bay of Fundy, in Turnagain Arm near Anchorage, and in the Severn River in England. Tidal current speeds greater than 7.5 m/s occur in Seymour Narrows, between Vancouver Island and the mainland of British Columbia, Canada. Tidal currents of 5 m/s are found in South Inian Pass in southeast Alaska and in Kanmon Strait, Japan. In some narrow or shallow straits, the tidal currents create dangerous whirlpools or *maelstroms*. Most famous is the whirlpool in the Strait of Messina (between Sicily and the southern tip of the Italian mainland), which Homer depicted in his *Odyssey* as the second of two monsters, Scylla and Charybdis, faced by Ulysses.

The generation of tides

The tides are caused by both the moon and the sun, but the moon though smaller has roughly twice the effect because it is much closer to the earth than the sun. Although the moon appears to orbit around the earth, the earth and moon both actually revolve around a common point, which, because the earth is much more massive than the moon, is inside the earth, but not at the earth's center (see Figure T33). At the

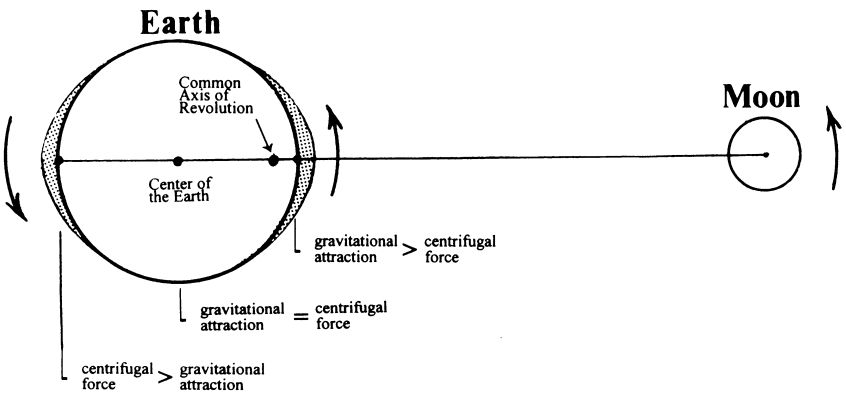

Figure T33 The earth–moon system (viewed from above the North Pole) revolving around a common axis (inside the earth). The earth is shown with a hypothetical ocean covering the whole earth (with no continents) and *two* bulges, resulting from the imbalances of gravitational and centrifugal forces.

center of the earth there is a balance between the gravitational attraction (trying to pull the earth and moon together) and the centrifugal force (trying to push the earth and moon apart). At a location on the earth's surface closest to the moon, the gravitational attraction of the moon is greater than the centrifugal force. On the opposite side of the earth, facing away from the moon, the centrifugal force is greater than the moon's gravitational attraction. Figure T33 shows a hypothetical ocean (covering the whole earth with no continents) with *two* bulges, one facing the moon and one facing away from the moon, that result from the two imbalances of gravitational and centrifugal forces. However, if we look at the side of the earth facing the moon, the force vertically upward from the earth toward the moon is so small compared with the earth's gravitational force that it could not cause the bulges. If we move away from the equator to another point on the earth that is not directly under the moon, we see that the attractive force is still pointing toward the moon, but is no longer perfectly vertical relative to the earth (see Figure T34). At this point, the force toward the moon can be separated in a vertical component of the force and a horizontal component, the latter one being parallel to the earth's surface. This horizontal force, though small, has nothing opposing it, and so it can move the water in the ocean. One can see from Figure T34 that all the horizontal components shown tend to move the water into a bulge centered around the point that is directly under the moon. Similarly, on the other side of the earth another bulge results.

One can easily envision the earth rotating under these bulges in this hypothetical ocean that covers the entire earth. In one complete rotation in one day there will be two high tides (when under a bulge) and two low tides (when halfway between bulges), and thus one entire tidal cycle would be completed in approximately half a day (actually 12.42 h, for reasons to be explained below). However, this is an extreme simplification (called the *equilibrium tide*) used merely to show how the tide generating forces change as the earth rotates. Not only are the continents left out, but this assumes that the oceans respond instantly to the tide-generating force, which they do not.

Now consider the addition of continents and look at one of the oceans, with a bay connected to it. The tide-generating forces are too small to cause a tide directly in a small body of water like a bay. Only in a large ocean are the cumulative effects of the tide-generating forces throughout the ocean large enough to produce a tide. What is actually generated is a very long wave with a small amplitude, on the order of a half a meter or less (see Figure T35). However, when this wave reaches the reduced depths of the continental shelf, there is a partial reflection of the wave, and the part of the wave that continues toward the coast is increased in amplitude. At the coast another reflection further increases the height of this long wave, now reaching at least a meter along most coasts. When the wave moves up into a bay there can be even more amplification depending on the depth, length, and width of the bay, with tidal ranges reaching 5, 10, or even 15 m for bays with the right dimensions.

How large the tide range is depends on how close the natural period of free oscillation of the basin is to the period of the tide-generating force. If the natural period of the basin is same as the period of the tide-generating force, then the energy from the tidal forcing will be input in the same direction as the water is already moving and the resulting tide range will be larger. This is called *resonance*. The natural period of a basin, T_n, is approximately equal to $2L/(gD)^{1/2}$, where L is the length of the basin, D is the depth, and g is the acceleration due to gravity. The Atlantic Ocean is too wide for there to be resonance (its 19-h natural period being much longer than the 12.42-h tidal period). The largest tide ranges in the world are in shallower basins with just the right length and depth combination to have natural periods close to the tidal period.

Astronomical considerations

Because it is a forced oscillating system, the tide will oscillate with the periods determined by the relative motions of the earth, moon, and sun. There are many different periods involved due to the complex nature of the orbit of the moon around the earth and of the orbit of the earth around the sun. However, astronomers have very precisely determined all of these periods. To predict the tide at a specific location for any time in the future one must simply analyze water level data from that location to determine the amplitude and phase associated with each of the important tidal periods.

If the earth–moon orbit and the earth–sun orbit were circular and in the plane of the earth's equator, there would only be two tidal frequencies, and only thus two semidiurnal constituents, M_2 and S_2 (defined below), would be needed to make tidal predictions. However, the orbital motions are more complicated. Distances between the moon and earth and between the earth and sun vary with time (the latter changes over a 20,942-year period and so is of no concern, except perhaps in paleoclimatology). Orbital planes are at angles relative to the earth's equatorial plane and these angles also vary with time. All these motions modulate the tidal forces, so that tidal energy shows up at many more frequencies than at just M_2 and S_2. The changing angles of the orbital planes also means that the moon and sun will not always be directly over the earth's equator, thus making the two tidal bulges (on the opposite sides of the earth) asymmetric with respect to the axis of rotation, which introduces diurnal tidal frequencies. The fundamental periods in the motions of the earth, moon, and sun are shown in Table T11. Table T12 shows how key tidal constituents are derived from these fundamental frequencies. (The *Doodson numbers* used in many tidal papers are a shorthand that indicates which of the six frequencies, ω_L, ω_1 through ω_5 from Table T11, are used to produce a particular constituent.) To make this a little clearer, we will describe the origins of a few of the more important tidal frequencies.

The moon orbits around the earth in the same approximate direction as the rotation of the earth, so that one lunar day (i.e., one complete rotation of the earth *with respect to the moon*) is 24.8412 h long ($1/\omega_L$, see Table T12). There are two tidal high water bulges on the earth, so the period of the largest semidiurnal lunar harmonic constituent, M_2, is half a lunar day, or 12.4206 h.

The earth turns under the sun exactly once every solar day, which leads to the main solar semidiurnal tidal constituent, S_2, with a period of 12.0000 h. Because the sun is so much farther from earth than the moon (and the tidal force is inversely proportional to the cube of the distance), S_2 is much smaller in size than M_2. When the moon and sun are in alignment (at new and full moons) their tidal forces work together to create *spring tides* with larger tidal ranges, while they work against

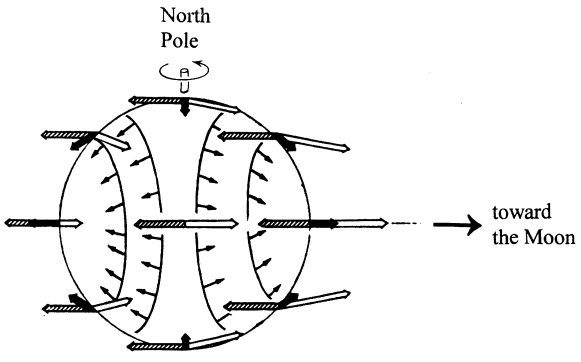

Figure T34 The tide generating forces (the thick black arrows) on the earth resulting from the difference between gravitational attraction (the open arrows) and centrifugal force (the hatched arrows). The small blacks arrows are the *horizontal* components of the tide generating forces, which tend to move the water into the two bulges shown in Figure T33.

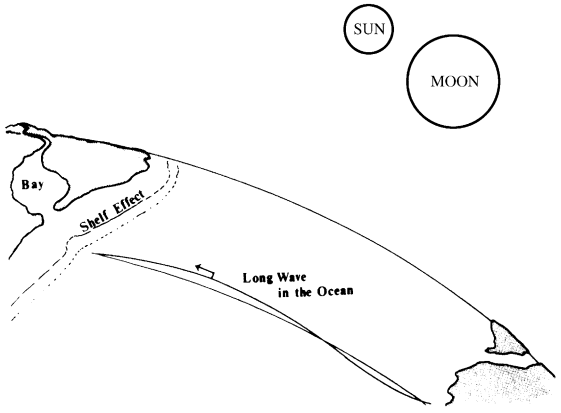

Figure T35 The tide-generating forces caused by the moon and sun produce a very long wave of relatively small amplitude in the ocean. When this long wave reaches the continental shelf, then the coast, and finally propagates up a bay, it is amplified by an amount that depends on the length and depth of each of the basins.

Table T11 Fundamental periods in the motions of the earth, moon, and sun (after Parker *et al.*, 1999)

Description	Period (mean solar units)	Frequency (1/period)
Sidereal day (one rotation wrt vernal equinox)	23.9344 h	Ω
Mean solar day (one rotation wrt to the sun)	24.0000 h	ω_S
Mean lunar day (one rotation wrt to the moon)	24.8412 h	ω_L
Period of lunar declination (tropical month)	27.3216 days	ω_1
Period of solar declination (tropical year)	365.2422 days	ω_2
Period of lunar perigee	8.847 years	ω_3
Period of lunar node	18.613 years	ω_4
Period of perihelion	20,940 years	ω_5

Table T12 Tidal constituents and their origins (after Parker *et al.*, 1999)

Symbol	Description	Period	Speed (°/h)	Derived from	Coefficient C
Semidiurnal tides					
K_2^L	declinational to M_2	11.967 h	30.0821373	$2\omega_L + 2\omega_1$ (=2Ω)	0.0768
K_2^S	declinational to S_2	11.967 h	30.0821373	$2\omega_S + 2\omega_2$ (=2Ω)	0.0365
S_2	principal solar	12.000 h	30.0000000	$2\omega_S$	0.4299
M_2	principal lunar	12.421 h	28.9841042	$2\omega_L$	0.9081
N_2	elliptical to M_2	12.658 h	28.4397295	$2\omega_L - (\omega_1 - \omega_3)$	0.1739
L_2	elliptical to M_2	12.192 h	29.5284789	$2\omega_L + (\omega_1 - \omega_3)$	0.0257
Diurnal tides					
K_1^L	declinational to O_1	23.934 h	15.0410686	$(\omega_L - \omega_1) + 2\omega_1$ (=Ω)	0.3623
K_1^S	declinational to P_1	23.934 h	15.0410686	$(\omega_S - \omega_2) + 2\omega_2$ (=Ω)	0.1682
P_1	principal solar	24.066 h	14.9589314	$(\omega_S - \omega_2)$	0.1755
O_1	principal lunar	25.819 h	13.9430356	$(\omega_L - \omega_1)$	0.3769
Q_1	elliptical to O_1	26.868 h	13.3986609	$(\omega_L - \omega_1) - (\omega_1 - \omega_3)$	0.0722
Long-period tides					
Mf	declinational to M_0	13.661 days	1.0980331	$2\omega_1$	0.1564
Mm	elliptical to M_0	27.555 days	0.5443747	$(\omega_1 - \omega_3)$	0.0825
Ssa	declinational to S_0	182.621 days	0.0821373	$2\omega_2$	0.0729

The speed is another form of frequency. M_0 and S_0 represent constant lunar and constant solar forces. The coefficient, C, gives a global measure of each constituent's relative portion of the tidal potential (i.e., it ignores a latitudinal variation that is different for each species).

each other at first and third quarters to create *neap tides* with smaller ranges (see Figure T36).

The earth–moon orbit is elliptical, so that the distance between them varies over a 27.5546-day period ($1/[\omega_1 - \omega_3]$, see Table T12), from perigee (the moon closest to the earth, and so a stronger tidal force) to apogee (the moon farthest from the earth, and so a weaker tidal force) and back to perigee. This modulates the lunar tidal force. This modulation of M_2 shows up in a spectra (of water level or current data) as a line to the left of the line for M_2, this lower frequency line representing a second lunar harmonic constituent, N_2, whose period is 12.6583 h. The stronger *perigean* tidal force will occur when M_2 and N_2 come into phase (leading to larger tidal ranges), while the weaker *apogean* tidal force will occur when M_2 and N_2 are exactly out of phase (leading to smaller tidal ranges). We can use Figure T36 to illustrate this, if, in that figure, we replace S_2 with N_2, spring tide with perigean tide, and neap tide with apogean tide. The difference is that with the M_2 plus S_2 case there really are two distinct effects being added, but in the case of the changing distance between the moon and earth, this directly varies the amplitude of the tide; and N_2 is merely a convenient way (in combination with M_2) to represent this variation of amplitude. There are several times a year when lunar perigee is reasonably close in time to new or full moon to produce the largest tidal ranges of the year, called *perigean spring tides*.

The plane of the moon's orbit around the earth is at an angle to the plane through the earth's equator. Thus, as the earth rotates under the moon, there will be times of the month when the moon is north of the equator (Northern Declination), over the equator (Equatorial Declination), and south of the equator (Southern Declination). When the moon is north or south of the equator, one of the tidal bulges is more north of the equator and one is more south, so that at a particular location on the earth there will either be only one high water per day (a diurnal tide), or, if there are two, they will be of different heights (the difference being the *diurnal inequality*) (see Figure T37). The diurnal lunar tidal forces resulting from lunar declination are represented by two tidal constituents, O_1 and K_1, with periods of 25.8193 and 23.9345 h, since they must cancel each other out every 13.66 days ($1/2\omega_1$, see Table T12), at the times when the moon is over the equator. (The maximum angle between the plane of the moon's orbit and the earth's equator varies from 18.3° to 28.5° over a 18.6-year period; see below for further discussion of this *nodal* cycle.) The sum of the O_1 and K_1 frequencies is equal to the M_2 frequency, so that the time of the diurnal high water does not change with respect to the times of the two semidiurnal high waters.

The plane of the earth's orbit around the sun (called the *ecliptic*) is also at an angle to the plane through the earth's equator. Around December 21st the sun is furthest south of the equator (December solstice) and around June 21st it is furthest north of the equator (June solstice), the angle between the ecliptic and the equator reaching 23.5° in each case. December solstice marks the beginning of winter in the Northern Hemisphere and the beginning of summer in the Southern Hemisphere, and *vice versa* for June solstice. Around March 21st the sun is over the equator (vernal equinox) and again around September 21st (autumnal equinox). This movement of the sun north and south of the equator also leads to diurnal tidal constituents, in this case P_1 with a period of 24.0658 h ($1/(\omega_S - \omega_2)$, see Table T12), and another K_1. Thus, the K_1 used for tidal prediction has both lunar and solar parts. P_1 and the solar part of K_1 cancel each other out every 182 days, at vernal and autumnal equinoxes.

As mentioned above, the angle between the plane through the moon's orbit and the plane through the equator varies over a 18.6-year period ($1/\omega_4$, see Table T12). This is referred to a *lunar nodal regression* because the intersection of the moon's orbital plane with the ecliptic, called the ascending lunar node, regresses backwards along the ecliptic over this 18.6-year period. Lunar distance also varies with time because the longitude of the lunar perigee rotates with an 8.85-year period ($1/\omega_3$, see Table T12). The spectral splitting due to these long-period effects can also be represented by harmonic constituents, called "satellite" constituents, but harmonic analyses using them must use data series that

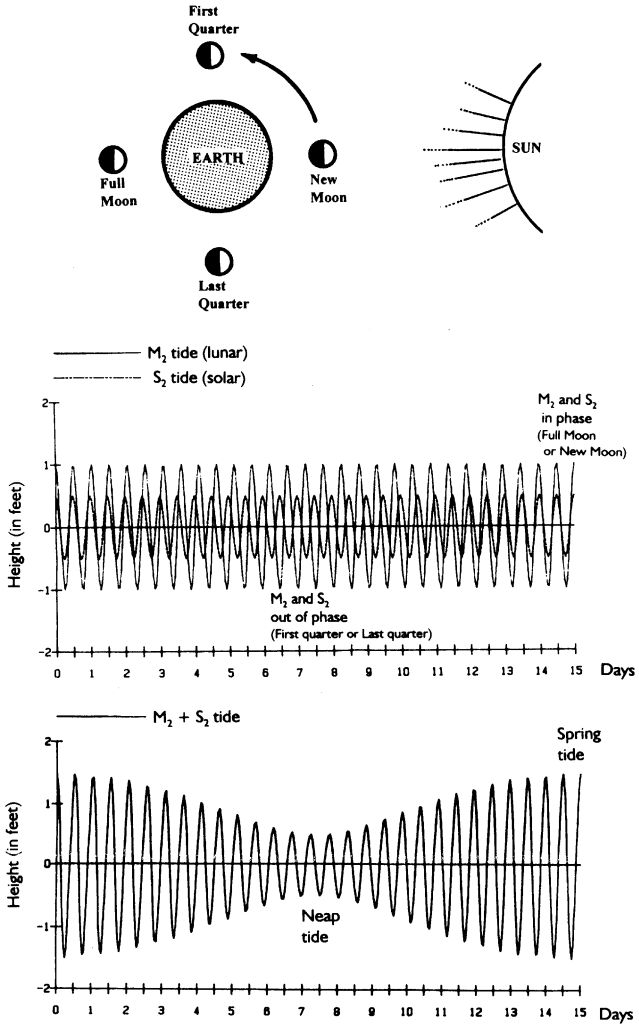

Figure T36 The combined effect of the moon and sun varies throughout the month. When the moon and sun are working with each other (at full moon and new moon) one sees the largest tidal ranges (*spring tides*). At First Quarter and Last Quarter the moon and sun work against each other resulting in smaller tidal ranges (*neap tides*).

are 18.6 years long. Traditionally the nodal effects have been handled in a form that directly represents the modulation of each lunar tidal constituent. The amplitude of each modulation is called the *node factor, f*, and the phase is called the *equilibrium argument, u. f* and *u* are regarded as constants for the period of analysis (or prediction) and are obtained from astronomically calculated tables (e.g. Tables 14 and 15 in Schureman, 1958). The largest variation in *f* over a 18.6-year period is found in O_1, which varies ±18%, and in K_1, which varies ±11%. The variation of *f* for M_2 is ±4%, but since M_2 is much larger than O_1 and K_1 in many locations, it may only be the 4% variation with which one is usually concerned. There is no direct nodal effect on solar constituents such as S_2 or P_1.

Tidal analysis and prediction

Knowing only the periods of these and other smaller tidal constituents, one can analyze a data series of water level observations from a particular location. The result of such a *harmonic analysis* is an *amplitude* and *phase* for each of these tidal constituents, which represent how large each effect is *at that particular location*, and when in time the peak of each effect will take place (such as relative to when the moon passes over (transits) that location). The hydrodynamics affect both the amplitude and phase (timing) of each tidal constituent, but we really do not need to know the details of how it happened, only that it did happen. Hydrodynamics in shallow-water areas will also produce additional tidal constituents not seen in deeper water (discussed in the next section) that

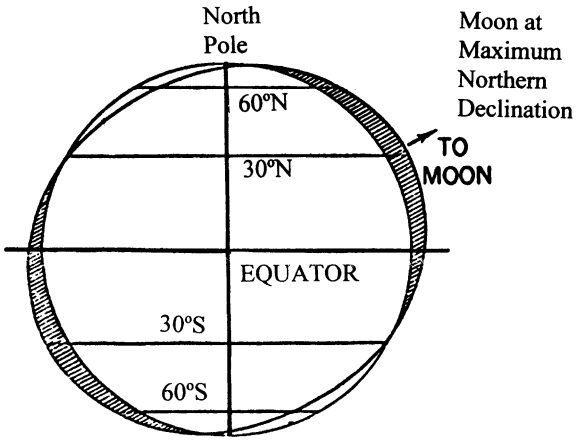

Figure T37 When the moon is at maximum declination north or south of the equator the tidal bulge also shifts north or south. When this happens certain locations on the earth would rotate under only one high water "bulge," that is, there will be a diurnal component of the tidal forces. Hydrodynamics will determine which oceans and bays have significant diurnal tides.

can also be easily handled by the harmonic method. As long as the hydrodynamics stay the same (i.e., the depth of the basin stays the same), the tide predictions from these calculated harmonic constants will be accurate. For small bays, shoaling or dredging can change the hydrodynamics and thus change the tide range and times of high and low waters.

Harmonic analysis is still the most common method used for the analysis and prediction of tides and tidal currents. It has not changed much from the theory first developed by Lord Kelvin in 1867 and later refined by George Darwin, except that the Fourier analysis solution technique (e.g., Schureman, 1958) has generally been replaced by a least-squares solution technique (e.g., Foreman and Henry, 1989) that minimizes the squared differences between measurements and computed tidal predictions. Doodson (1921) carried out a complete harmonic development of the tide-generating potential, determining over 400 tidal constituents (most very small), which has been the standard reference work for tidal analysis and prediction. This was recalculated and updated 50 years later by Cartwright and Tayler (1971).

Harmonic analysis is used to produce the predictions at the reference stations in all nationally published Tide and Tidal Current Tables. Nonharmonic analysis, which is simply one of several methods of comparing the tide or tidal current at two locations, is used to calculate the time differences, height differences, velocity ratios, etc. for the thousands of secondary stations in these tables that are referred to the reference stations. Several refinements to the harmonic methods have been developed in recent decades, as well as the nonharmonic/cross-spectral approach of the response method developed by Munk and Cartwright (1966). Whatever the method used, some principles will always apply. For example, the analysis of longer data time series will lead to more accurate predictions because more tidal frequencies can be resolved in a longer series.

Using the harmonic method the tide is represented by the sum of various tidal constituents, each representing one of these frequencies. The height of the tide at any time is typically represented by a formula such as (Schureman, 1958):

$$h = H_0 + \sum f\, H \cos[at + (V_0 + u) - \kappa],$$

where

h	=	height of tide at any time t
H_0	=	mean height of water level above the datum used for prediction
H	=	mean amplitude of any constituent A
f	=	node factor
a	=	speed of constituent A (i.e., its frequency)
t	=	time, reckoned from some initial epoch (such as the beginning of the year of predictions)

$(V_0 + u)$ = value of equilibrium argument of constituent A at $t = 0$.
κ = epoch (phase) of constituent A.

The *"speed" of a constituent* is merely its frequency, but it has been traditionally given in terms of degrees per solar hour, where 360° is one complete cycle. Thus, M_2, which has a period of 12.42 h and a frequency of 1.932 cycles per day, has a speed of 28.984104°/h.

For tidal current predictions the same equation is used twice, once for each of two orthogonal components (e.g., major and minor axes of flow), which when combined will give the speed and direction of the flow. The major and minor component for each tidal constituent can be combined to produce a *tidal constituent ellipse*, which shows what the constituent flow would be for each instant in a constituent cycle.

The more tidal constituents that can be calculated the more accurate the tidal prediction will be. The number of constituents that can be calculated depends on the length of the data series. The length of a data series needed to resolve two tidal constituents is inversely proportional to the difference in the frequencies. Table T13 lists the 37 typically most important tidal constituents, listed in order of length of time needed to resolve that constituent from a nearby larger constituent. One sees natural groupings near 15 days, 29 days, 6 months, and one year.

If one has only 15 days of data, for example, then a harmonic analysis will provide values for the major constituents M_2, S_2, K_1, and O_1, plus a few higher harmonics and a couple of less important constituents. However, these calculated values will also include energy from the constituents that could not be separated out in only 15 days. For example, the M_2 will include energy from N_2 (which could have been resolved from M_2 if there had been 29 days of data). This N_2 contribution could make the M_2 value calculated from 15 days of data larger than it should be, or smaller than it should be, depending on when the data were measured. Likewise, K_1 will include the effects of P_1 (which could have been resolved from K_1 if there were 6 months of data). If we harmonically analyzed successive 15-day periods, we would see the amplitude of K_1 slowly vary over a 6-month period because of the influence of P_1. The key to an accurate tidal prediction is determining amplitudes and phases for the most tidal constituents that can be calculated with a given length data time series.

To carry out a tide prediction in the era before the above equation could be programmed on a computer (as it is done routinely today), large machines were built with gears and pulleys connected by a wire to a pen. Each tidal constituent had a different size rotating gear and a pin and yoke system connected to a pulley (see Figure T38). The pin and yoke system turned the rotating motion of the gear into a vertical up and down motion of the pulley, which moved the wire over it and thus moved the pen up and down on a roll of moving paper. The wire ran over a number of pulleys so all the constituent effects could be added together. The first tide predicting machine was a wooden model built for Kelvin in 1872, but later models were huge brass machines with dozens of finely made gears and pulleys. The first one built in the United States was by William Ferrel in 1885. Prior to the use of harmonic analysis there were other less sophisticated methods based on recognized relationships between the tides and the movements of the moon and sun. For example, for a particular place, high tide might occur a certain number of hours after the moon was directly overhead, and the highest (spring) tide might occur a certain number of days after full moon or after new moon. In many of the early maritime nations, tide prediction schemes were treasured family secrets passed on to the next generation. The two earliest tide tables discovered were for the tidal bore in the Tsientang River in China in 1056 and for London Bridge in England in the early 1200s.

Table T13 Thirty-seven tidal constituents that can be calculated from a one-year series, listed in order of length of data time series needed to resolve each constituent from a nearby larger constituent, and size

Constant	Speed (°/h)	Origin	Days needed to separate	From	Amplitude at Trenton, NJ (feet)
M_2	28.984104	Lunar	–	–	3.547
M_4	57.968208	Shallow-water	0.5	M_2	0.517
M_6	86.952313	Shallow-water	0.5	M_4	0.266
M_8	115.936417	Shallow-water	0.5	M_6	0.120
K_1	15.041069	Lunisolar	1.1	M_2	0.349
S_6	90.000000	Shallow-water	4.9	M_6	0.005
S_4	60.000000	Shallow-water	7.4	M_4	0.005
O_1	13.943036	Lunar	13.7	K_1	0.288
MK_3	44.025173	Shallow-water	13.7	$2MK_3$	0.120
$2MK_3$	42.927140	Shallow-water	13.7	$M\mathrm{K}_3$	0.116
OO_1	16.139102	Lunar	13.7	K_1	0.030
$2Q_1$	12.854286	Lunar	13.8	O_1	0.028
S_2	30.000000	Solar	14.8	M_2	0.461
MS_4	58.984104	Shallow-water	14.8	M_4	0.148
$2SM_2$	31.015896	Shallow-water	14.8	S_2	0.025
M_3	43.476156	Lunar	27.3	MK_3	0.034
M_1	14.492052	Lunar	27.3	K_1	0.027
N_2	28.439730	Lunar	27.6	M_2	0.553
MN_4	57.423834	Shallow-water	27.6	M_4	0.176
Mm	0.544375	Lunar[a]	27.6	Mm	0.124
Q_1	13.398661	Lunar	27.6	O_1	0.022
J_1	15.585443	Lunar	27.6	K_1	0.016
$2MN_2/L_2$	29.528479	Shallow-water/lunar	31.8	S_2	0.409
$2MS_2/\mu_2$	27.968208	Shallow-water/lunar	31.8	N_2	0.219
MSf	1.015896	Lunar[a]	182.6	$M\mathrm{f}$	0.186
Mf	1.098033	Lunar[a]	182.6	MSf	0.132
P_1	14.958931	Solar	182.6	K_1	0.110
K_2	30.082137	Lunisolar	182.6	S_2	0.094
ν_2	28.512583	Lunar	205.9	N_2	0.210
λ_2	29.455625	Lunar	205.9	$2MN_2$	0.102
$2NM_2/2N_2$	27.895355	Shallow-water/lunar	205.9	$2MS_2$	0.042
ρ_1	13.471514	Lunar	205.9	Q_1	0.013
Sa	0.041069	Solar[a]	365.2	Ssa	0.430
Ssa	0.082137	Solar[a]	365.2	Sa	0.169
S_1	15.000000	Solar	365.2	K_1	0.062
T_2	29.958933	Solar	365.3	S_2	0.056
R_2	30.041067	Solar	365.3	S_2	0.028

Amplitudes from a 1981 analysis of water level data (from Trenton, NJ, on the Delaware River) are provided as an example (after Parker *et al*., 1999).
[a] Values are determined predominantly by long-term meteorological effects and thus vary from year to year.

Hydrodynamic considerations in coastal waters

When the very long tide wave generated in the ocean reaches the shallower water of the continental shelf and the even shallower water of the bays and rivers, it is slowed up, amplified, modulated, and distorted by a number of hydrodynamic mechanisms. The long wave enters and propagates up a river as a *progressive wave*, that is, the crest of the wave (high water) moves progressively up the river, as does the trough of the wave (low water) (see Figure T39). In such a progressive tide wave the flood current (the tidal current flowing up the river) is fastest at approximately the same time as high water, and the ebb current (the tidal current flowing down the river) is fastest at approximately the same time as low water. Slack water (the time of no current) occurs approximately halfway between the times of high water and low water.

If there is nothing in a river to impede or stop the tide wave (like a dam or rapids or a sudden decrease in width), it will continue to travel up the river until bottom friction wears it down. However, if the width of the river decreases as the tide wave moves upriver, then the tidal range will be increased, because the same energy is being forced through a smaller opening. If the depth of the river decreases there is a similar but less dramatic amplifying effect generally outweighed by the increased frictional energy loss.

The greatest amplification of a tide wave usually occurs in a bay (or in a river with a dam). In this case, the tide wave is reflected at the head of the bay and travels back down the waterway toward the ocean. This *reflected* wave is not observable by someone on the shore because it is superimposed on the next incoming tide wave that is propagating up the bay, and it is the combination of the two waves that one observes. The resulting combined wave is called a *standing wave*, because the high and low waters do *not* progress up the bay or river. The water simply moves up and down everywhere at the same time (see Figure T40), with the greatest tidal range at the head of the bay. With a standing wave, the tidal range decreases as one moves from the head of the bay toward the ocean entrance, and, if the bay is long enough, reaches a minimum at one location (called a *node*) and then starts increasing again. This node occurs at one-fourth of a tidal wavelength from the head of the bay (see Figure T40). (In a progressive wave high water comes half a wavelength before low water, so if a high water travels a distance equal to one-fourth of a tidal wavelength up the bay to the head, where it is reflected, and then travels one-fourth of a wavelength back down the bay, it will have gone half a wavelength and so coincide with low water of the next incoming wave, and the two will cancel each other out at that location, producing a very small tidal range.) For a standing wave high waters occur at the same time everywhere on one side of the node, which is the same time as low waters occur on the other side of the node. The strongest tidal currents occur when water level is near mean tide level, approximately halfway between the times of high water and low water. At the times of high water and low water there is no flow (slack water). The water flows into the bay, stopping the inward flow at high water, reverses direction, flows out of the bay until low water, at which time it reverses again and starts flowing into the bay again.

When length of a bay is exactly one-fourth of a tidal wavelength, then resonance occurs, which creates the largest tides possible. When the water in the bay is forced to move up and down by the tide at the entrance, it will freely oscillate (slosh up and down) with a natural period that depends directly on its length and inversely on the square root of its depth. If the basin has the right combination of length and depth so that the natural period is the same as the tidal period, then the oscillation inside the bay will be synchronized with the oscillation at the entrance due to the ocean tide. In other words, the next ocean tide will be raising the water level in the bay at the same time that it would already be rising due to its natural oscillation (stimulated by the previous ocean tide wave), so that both are working together, thus making the tidal range inside higher.

Most bays actually fall in between the extremes of pure progressive wave and pure standing wave described above, because bottom friction reduces the amplitude of the tide wave as it travels. Thus, the reflected wave will always be smaller than the incoming wave, especially near the bay entrance, and the combination of the two frictionally damped progressive waves will not be a pure standing wave. There will be no point of zero tidal range, but only an area of minimum tidal range. There will be some progression of high waters and low waters up the bay, and maximum flood or ebb currents will not occur exactly half way between high water and low water. A basin one-fourth of a wavelength long will still produce the largest possible tidal range at the head of the bay, but friction keeps that tidal range much smaller than it would be without friction.

In some bays, the very high tidal range at the head of the bay is due to a combination of both a narrowing width and a near resonant situation (due to the right length and depth). The highest tidal ranges may involve several amplifications, the bay being perhaps connected to a gulf with perhaps a wide continental shelf beyond that, with amplifications of the tide wave occurring in each basin. This is the case with the Bay of Fundy tides, the tide wave being already amplified by the Gulf of Maine and the continental shelf prior to entering the Bay of Fundy.

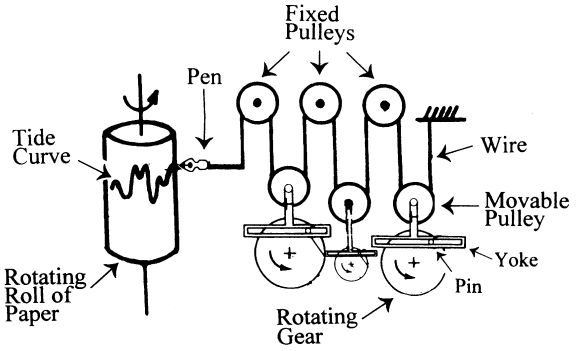

Figure T38 A schematic of an early tide prediction machine. Each gear and pulley combination represented one tidal constituent. The wire running over every pulley summed the motions and moved a pen on a moving roll of paper to draw a tide curve.

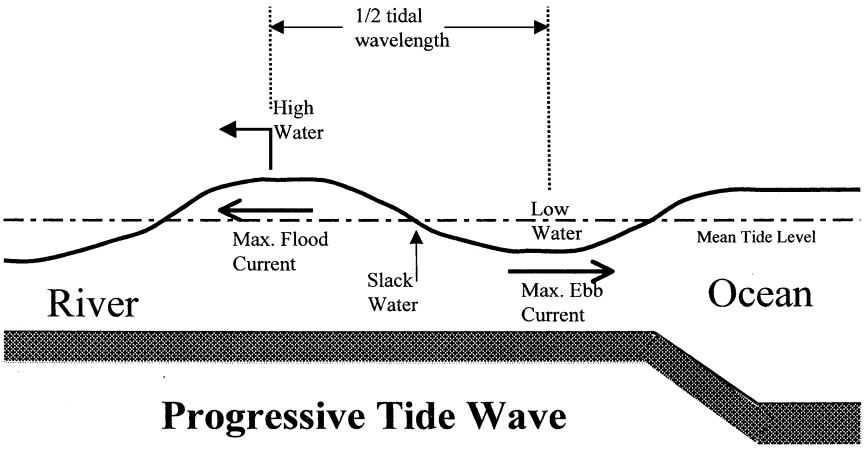

Figure T39 The tide propagating up a river as a *progressive wave*. High water occurs later as one moves upstream. The tidal wavelength is typically on the order of hundreds of miles.

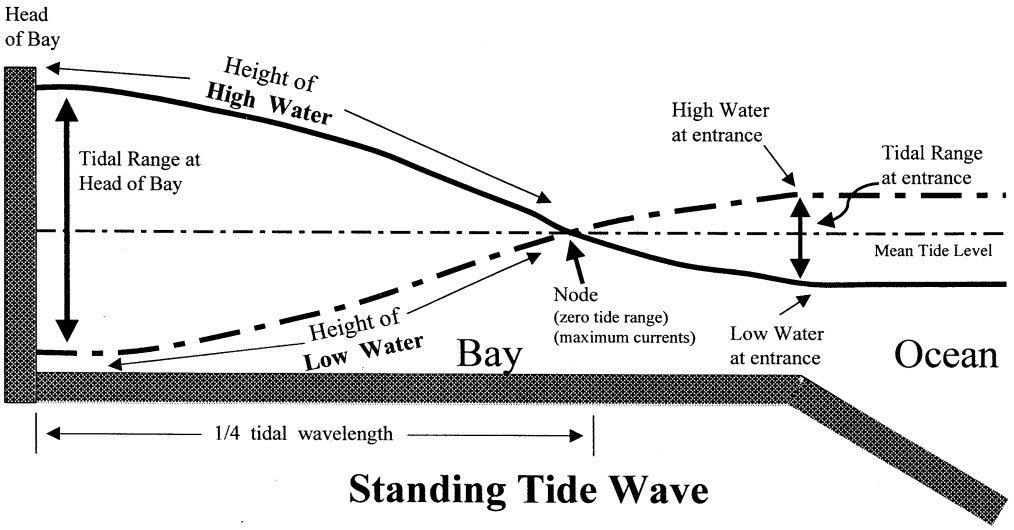

Figure T40 The tide in a bay as a *standing wave* (the water level is shown for two extremes, high water and low water). High water occurs at approximately the same time everywhere on one side of the node (the point of zero tidal range). This is an idealized case assuming there is no bottom friction effect. With friction the tidal range at the node is not zero and the times of high water do progress slightly up the bay.

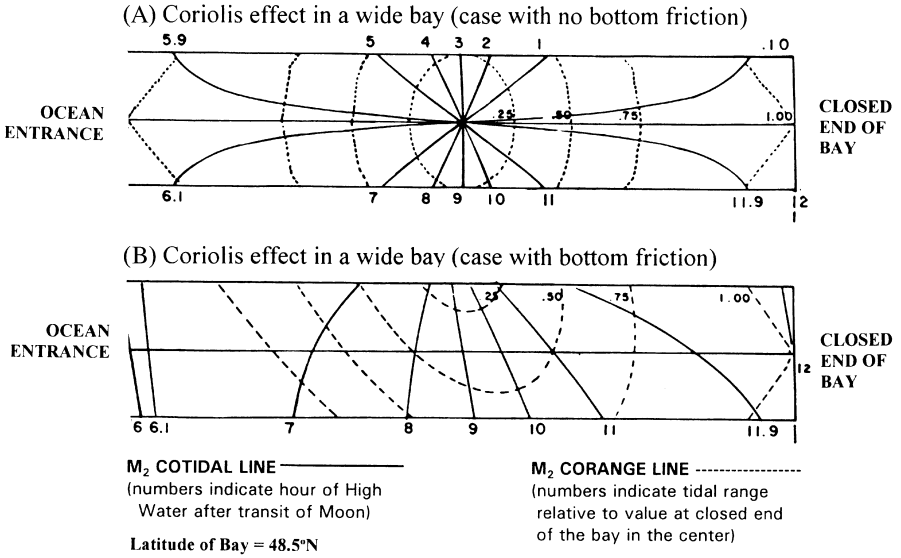

Figure T41 The effect of Coriolis force on M_2 tidal range (corange lines) and the times of high water (cotidal lines) for an idealized rectangular bay. The top figure assumes no bottom friction effects, and a single point of zero tidal range in the middle of the bay results. The bottom figure, which includes friction, is more realistic, and there is no point with zero tidal range.

If a bay is wide enough one also sees larger tidal ranges on the right side of the bay (looking up the bay) due to the Coriolis effect. Figure T41(A) shows lines of locations with the same time of high water (cotidal lines) and lines of constant tidal range in an idealized rectangular basin for the case where the effect of bottom friction is ignored. A single point of zero tidal range occurs in the center of the bay. A more realistic case, including the damping effect of bottom friction, is shown in Figure T41(B), with the point of no tidal range disappearing onto land. (The effect of Coriolis can also be seen in Figure T42, where the shape of the M_2/K_1 lines near Victoria are caused by the point of zero M_2 tidal range having moved to the left on land.)

Huge tidal ranges are not restricted to bays. If the continental shelf is the right combination of depth and width, a near resonant situation can also result. This is the reason for the 12 m tidal ranges along the coast of southern Argentina. The continental shelf there is over 1,000 km (600 miles) wide, and includes the Falkland Islands near the edge of the shelf (where the tidal range only reaches 2 m. The distance from the Argentinean coast to the edge of the shelf is fairly close to one-fourth of a tidal wavelength for that depth of water. Essentially, that wide shelf has a natural period of oscillation that is fairly close to the tidal period.

The largest tidal currents in bays tend to be near the entrances. Maximum tidal current speeds are zero at the head of the bay (since there is no place for the water to flow). As one moves down the bay toward the ocean the maximum flood and ebb tidal current speeds increase, with the greatest speeds occurring at the entrance, or, if the bay is long enough, at the area of smallest tidal range (the nodal area). However, if the width of the bay decreases at any point, the current speeds will be increased in that narrow region (since the same volume of water is being forced to flow through a smaller cross section, it must flow faster). This can be especially dramatic if there is a sudden decrease in width and depth. The largest tidal currents are found in narrow straits in which the tides at either end have different ranges or times of

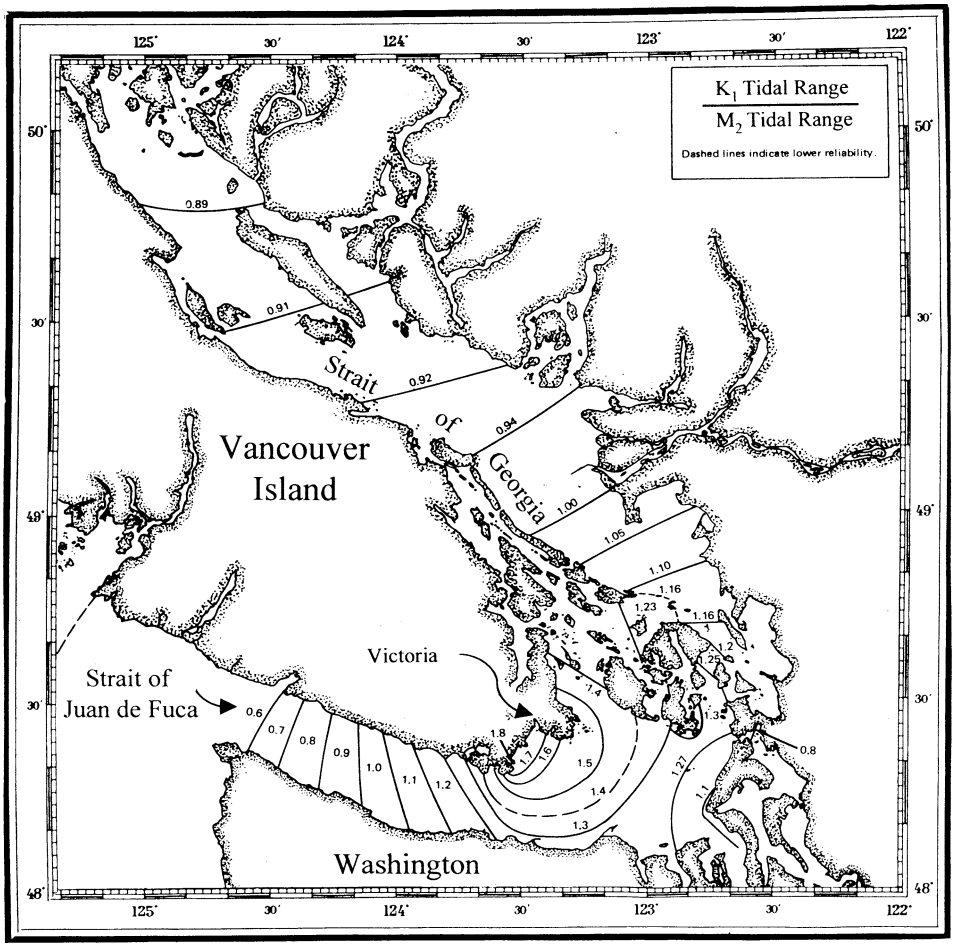

Figure T42 The ratio of the largest diurnal component of the tide (K_1) to the largest semidiurnal component of the tide (M_2) along the length of the Strait of Georgia-Strait of Juan de Fuca. The highest ratio of diurnal range to semidiurnal range occurs near Victoria, British Columbia, because that is the area of the semidiurnal node (minimum M_2 tidal range), which is one-fourth of a semidiurnal tidal wavelength from the northern end of the Strait of Georgia (see text).

high water. Where a strait suddenly becomes very narrow or where it bends, eddies and whirlpools can be formed as the result of the sheltering effect of the land and the inertia of the coastal flow.

The dimensions of a basin can also determine the size of the diurnal tidal signal compared with the usually dominant semidiurnal tidal signal. A particular bay could have a natural period of oscillation that is closer to the diurnal tidal period (approximately 24.84 h) than to the semidiurnal period, thus amplifying the diurnal forcing at the entrance to the bay more than the semidiurnal signal. Depending on the size of the diurnal signal at the entrance the result could be a mixed tide or a diurnal tide. At such locations (such as parts of the Gulf of Mexico) the tide will be diurnal near times of maximum lunar declination, but will be semidiurnal near times when the moon is over the equator.

The wavelength, L, of a tide wave in a bay depends on the depth of the water, D, and on the tidal period, T, according to $L = T(gD)^{1/2}$ (if we ignore frictional effects). The shallower the bay the shorter the wavelength. The longer the tidal period the longer the wavelength. A diurnal tidal component has a wavelength twice as long as a semidiurnal tidal component since its period is twice as long. When a waterway is shallow enough and long enough so that more than one-fourth of a semidiurnal wavelength fits in the waterway, there will be a nodal area with a very small semidiurnal tidal range. This will be an area where the diurnal tide could dominate, since the diurnal tide would still be large at the semidiurnal nodal area (its the diurnal node being twice as far from the head of the bay). Thus near the head of the waterway the tide could be semidiurnal, but near the semidiurnal nodal area the tide could be mixed or even diurnal. This is the case near Victoria, British Columbia, at the southeastern end of Vancouver Island (see Figure T42). At that location along the Strait of Georgia-Strait of Juan de Fuca waterway, the semidiurnal tidal component decreases to a minimum, but the diurnal component does not, and so the tide becomes diurnal (while at the northern end of the Strait of Georgia the tide is semidiurnal).

Whether due to a basin size conducive to amplifying the diurnal signal or due to the existence of a semidiurnal nodal area (leaving the diurnal signal as the dominant one), there are numerous areas around the world with strong diurnal tides—places like Norton Sound in Alaska near the Bering Strait, and various (but not all) locations in the Philippines, New Guinea, and the islands of Indonesia. In southern China, at Beihai, and at Do Son, Vietnam, the diurnal signal is very dominant, with tidal ranges that reach 5 m and 3 m, respectively (near times of maximum southern declination of the moon); the tide remains diurnal even near times when the moon is over the equator.

The primary effect of shallow water on the tide that we have discussed so far is that it shortens the tidal wavelength down to the same order of magnitude as the lengths of bays and river basins, thus bringing the dynamic situation closer to resonance and increasing the tidal ranges. (Or, one can also look at it from the point of view of the shallower depths increasing the natural periods of these bays and rivers (which are very small basins compared to the ocean) to be closer to the tidal period.) However, very shallow water can have other effects on the tide, for example, distorting the shape of the tide wave, that is, making it very asymmetric, so that its rise and fall (and its flood and ebb) are no longer equal (see the second curve in Figure T43). The tide can then no longer be described by a simple sine wave (the first curve in Figure T43). In some cases such distortion leads to double high waters or double low waters (see third curve in Figure T43). The extreme case of distortion is a tidal bore (the fourth curve in Figure T43).

Shallow water distorts the tide through several mechanisms. The speed, C, at which a long tide wave travels depends on the depth of the water, D, according to the formula $C = (gD)^{1/2}$. When depth of the

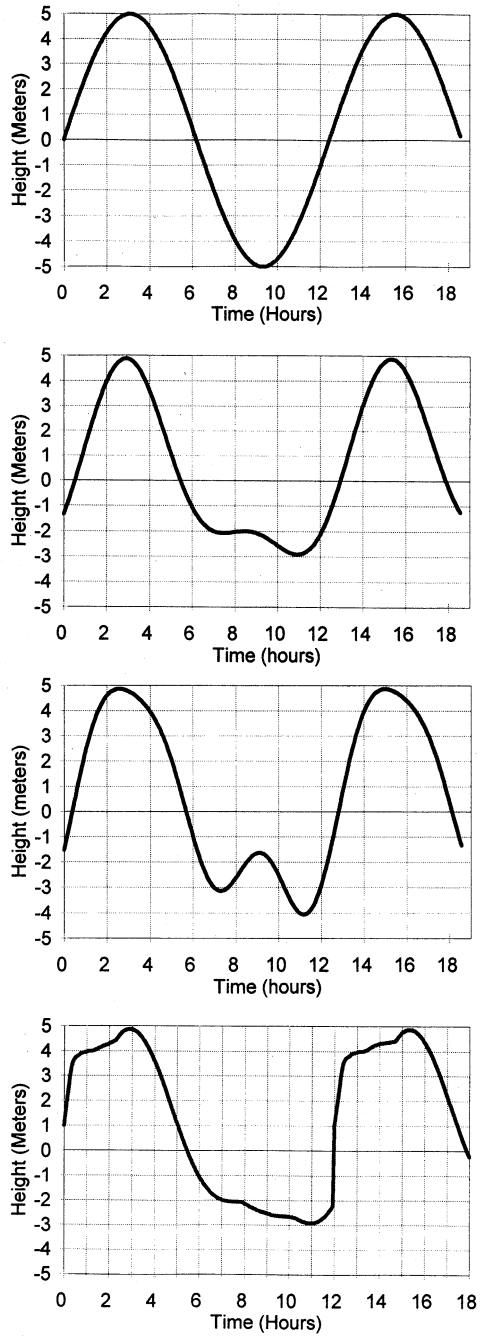

Figure T43 Typical tide curves (i.e., tidal height plotted with respect to time), over one-and-half tidal cycles for an area with no shallow-water effects (top panel) and for three areas with different degrees of distortion caused by the shallow water. In the third panel a double low water occurs. The fourth panel shows the almost instantaneous rise in water level due to the passage of a tidal bore.

water is much greater than the tidal range, the speed of the crest of a tide wave and the speed of the trough are virtually the same, since the tide wave itself has only a very small effect on the total water depth. But in the shallow water where the depth is not much greater than the tidal range, the total water depth under the crest is significantly larger than the total water depth under the trough. In this case, the crest of the wave (high water) travels faster than the trough of the wave (low water). If the tide wave travels far enough the crest begins to catch up with the trough ahead of it (which is falling behind the crest ahead of it). The shape of the tide wave then begins to look like the second curve in Figure T43, with a more rapid rise to high water and a slower fall to low water. In terms of harmonic constituents, this distortion transfers energy from M_2 into a constituent called M_4, with half the period.

Another shallow-water distorting mechanism is caused by bottom friction, which can have both asymmetric and symmetric effects. The asymmetric effect (similar to that just discussed and represented in Figure T43) results because friction has a greater effect in shallow water than in deepwater (there being less water to have to slow down), and so it slows down the trough more than the crest, contributing to the distortion of the tide wave and the generation of M_4. A symmetric effect results because energy loss due to friction is proportional to the square of the current speed. This means that there will be much more energy loss during times of maximum flood and maximum ebb than near slacks. This results in the generation of another higher harmonic, M_6, with a period of one-third that of M_2. This effect, combined with the asymmetric effect, can lead to double high or low waters (see third curve in Figure T43). Higher harmonic tidal constituents like M_4 and M_6 are referred to as *overtides*.

The above symmetric frictional effect also causes the interaction of two tidal constituents, for example, M_2 and N_2. M_2 and N_2 go in and out of phase over a 27.6-day cycle (perigee to apogee to perigee). In this case, the greatest energy loss occurs when M_2 and N_2 are in phase and producing the strongest tidal currents, and the lowest energy loss occurs 13.8 days later with M_2 and N_2 are out of phase and producing the weakest tidal currents. The increased energy loss when M_2 and N_2 are in phase is greater than the decreased energy loss when they are out of phase, and the result is that each constituent will be smaller than if it existed without the other present. There is a 27.6-day modulation of this energy loss from M_2 and N_2, which produces two new *compound* tidal constituents called $2MN_2$ and $2NM_2$. (Similarly, the above asymmetric mechanisms also cause interactions between constituents, producing higher frequency constituents such as MN_4 from M_2 and N_2.)

Friction, of course, dissipates energy from the entire wave and slowly wears the entire wave down. However, if, as the wave propagates up the river, the river's width is decreasing significantly, this can keep the amplitude of the wave high in spite of the friction. Thus, the tide wave can continue to travel up a narrowing river, getting more and more distorted in shape. A further distortion can be caused by the river flow interacting with the tide (see below). In the extreme case, the distortion from all these effects can lead to the creation of a tidal bore (see fourth curve in Figure T43).

In a river there will also be the river current itself (resulting from fresh water flowing downhill) added onto the tidal current, the result being a faster and longer lasting ebb current and a slower shorter flood current phase. Far up a river where the river flow is faster than the strongest tidal current, the flow of water will always be downstream, but the speed of flow will oscillate, flowing the fastest downstream at the time of maximum ebb for the tidal current and flowing the slowest downstream at the time of maximum flood for the tidal current. This is a simple addition to the tide, but the river flow also interacts with the tide and distorts it through interaction caused by bottom friction. As just mentioned, energy loss due to friction is proportional to the square of the total current speed. When the river current, flowing in the same direction as the ebb current, creates a larger combined ebb current, there is a greatly increased energy loss. Likewise, when the river current flowing opposite to the flood current reduces the total speed, the energy loss is greatly reduced. This not only has an asymmetric effect that distorts the tide (causing a faster rise to high water, delaying the time of low water, and contributing to M_4), but it also further wears down the entire wave because the increased energy loss during ebb is larger than the decreased energy loss during flood.

Another type of shallow-water effect causes interactions between tide and storm surge (generated by the wind) that have periods longer than tidal periods. In this case, when the water level is raised by an onshore wind, that increases the water depth and changes the tidal dynamics, usually increasing the tidal range. When an offshore wind lowers the water level, decreasing the water depth, the result is usually a decreased tidal range. Knowing that river discharge and storm surge can modify the tide, it is important when harmonically analyzing water level data to make sure that these data were not taken only during such meteorological events. These shallow-water effects that distort and modulate the tide and cause interactions with storm surge and river discharge are called *nonlinear* effects because the mechanisms that produce these effects are represented by several *nonlinear* terms in the equations of motions used to model the tidal hydrodynamics.

We have shown how tidal prediction can be accomplished quite accurately by harmonic analysis of a water level data time series knowing only the astronomical frequencies involved, and ignoring hydrodynamics. Accurate inclusion of the additional tidal constituents produced by nonlinear shallow-water effects into the harmonic prediction method

does involve some knowledge of hydrodynamics (especially when deciding the formula for each constituent's node factor). However, recently tidal prediction has begun to involve the use of sophisticated hydrodynamic numerical models, which have two important advantages over statistical techniques. First, such models can provide tide and tidal current predictions at locations where there are no water level data, thus providing predictions at hundreds or thousands of locations in an area, as opposed to the few locations where statistical methods can provide them (limited by needing data to analyze). Second, such models handle very nicely the nonlinear interaction between the tide and nontidal phenomena like storm surge and river discharge.

Bruce Parker

Bibliography

Cartwright, D.E., 1999. *Tides: A Scientific History*. Cambridge: Cambridge University Press. UK, 292 pages.

Cartwright, D.E., and Tayler, R.J., 1971. New computations of the tide-generating potential. *Geophysical Journal of the Royal Astronomical Society*, **23**: 45–74.

Doodson, A.T., 1921. The harmonic development of the tide-generating potential. *Proceedings of the Royal Society A*, **100**: 305–329.

Foreman, M.G.G., and Henry, R.F., 1989. The harmonic analysis of tidal model time series. *Advances in Water Resources*, **12**(3): 109–120.

Munk, W.H., and Cartwright, D.E., 1966. Tidal spectroscopy and prediction. *Philosophical Transactions of the Royal Society A*, **259**: 533–581.

Parker, B.B. (ed.), 1991. *Tidal Hydrodynamics*. New York: John Wiley & Sons.

Parker, B.B., Davies, A.M., and Xing, J., 1999. Tidal height and current prediction. In Mooers, C.N.K. (ed.), *Coastal Ocean Prediction*. Coastal and Estuarine Studies, American Geophysical Union. **56**, 277–327,

Platzman, George, 1971. Ocean tides and related waves. *Lectures in Applied Math*, **14**: 239–291.

Pugh, D.T., 1987. *Tides, Surges, and Mean Sea Level*. New York: John Wiley & Sons.

Schureman, P., 1958. *Manual of Harmonic Analysis and Prediction of Tides*. S.P. 98 (Revised 1940 edn with corrections. Washington, DC: Coast and Geodetic Survey, US Department of Commerce.

Cross-references

Altimeter Surveys, Coastal Tides and Shelf Circulation
Coastal Currents
Meteorologic Effects on Coasts
Sea-Level Changes During the Last Millennium
Sea-Level Datum
Storm Surges
Tidal Environments
Tidal Inlets
Tidal Prism
Tide Gauges

TIME SERIES MODELING

Fundamental concepts of coastal time series

There has been a considerable expansion in the coastal database in the past two decades. Discrete and continuous data are collected from the coast and its interacting hydrodynamic, biological, morphological, sedimentological, and other associated subsystems in order to make better decisions on coastal management and sustainable development. While the quality and length of the collected coastal data vary greatly, many datasets fall within the domain of time series analysis. Any time series can be considered as a time (or space) ordered sequence of realizations (or observations) of a variable of interest. The set of observations generated sequentially in time could be either continuous or discrete. In statistical terms, a time series is a realization or sample function from a certain stochastic or random process. The time series to be analyzed can be considered as a particular realization, produced by the underlying probability mechanism of the system (i.e., coastal) under consideration. The observed values of a stochastic process are generally considered as a realization of the stochastic process. Time series analysis can consider a class of stochastic processes, called stationary processes, which assume that the process is in a particular state of statistical equilibrium (Box *et al*., 1994). In the analysis of stationary stochastic processes it is worthwhile to note that "stationary processes generally arise from any 'stable' system which has achieved a 'steady-state' mode of operation" (Priestley, 1981, p. 14), whereas a nonstationary series is regarded as having properties which change with time.

Since in time series analysis, inferences can be made from a realization to the generating process, it is necessary to consider the statistical properties of the time series. Essentially, the properties of a time series can be obtained from a single realization over a time interval or based on several realizations at a particular time. The properties based on a time interval of a single realization are referred to as time-averaged properties. The properties from several realizations at a given time are considered as the ensemble properties. "Since different sections of a time series resemble each other only in their average properties, it is necessary to describe these series by probability laws or models" (Jenkins and Watts, 1969, p. 2).

Coastal time series modeling

Since stochastic processes deal with systems which develop in accordance with probabilistic laws, stochastic models can be used to gain insights on the spatial and temporal behavior of the coastal system (Lakhan, 1982; Lakhan and Trenhaile, 1989). Time series modeling of the many natural phenomena occurring in the coastal environment, which appear to behave in random or probabilistic ways, is essential for understanding not only the operating processes, but also for many coastal applications. Many examples of the use and applications of probabilistic and time series models in coastal studies have been provided by Guedes Soares (2000). Even the modeling of one sea-state parameter has many applications in coastal and offshore engineering. For example, modeling a time series of significant wave height at a location is a useful complement to long-term probabilistic models that describe the wave climate in different areas (Cunha and Guedes Soares, 1999).

The complex nature of the coastal system makes it necessary to develop models which can explain both the deterministic and random features of the time series for any coastal process (Lakhan, 1989). For example, sea-states can be visualized as random and unpredictable. However, there is some constancy of a sea-state for a short duration of several minutes to fractions of minutes, and therefore it is possible to assume stationarity for such short wave records. Conversely, a wave record of long duration will not exhibit stationarity because the significant wave height and other statistics are known to vary with respect to time (Goda, 2000). To characterize and predict the probabilistic nature of the sea surface a time series model can be developed to represent the sea surface elevation as a nonstationary stochastic process, with the sea-state considered to be a Gaussian, statistically stationary stochastic process in short time periods. In modeling stationary or nonstationary time series, coastal and allied researchers have utilized either the frequency domain or the time domain approach.

Approaches to time series analysis

Given the fact that there are various terminology, theoretical and practical aspects of time series analysis, this short review will introduce only the fundamental concepts for coastal and allied researchers. Hannan *et al*. (1985) pointed out that since its inception the theory and practice of the analysis of time series has followed two lines. One of these proceeds from the Fourier transformation of the data and the other from a parametric representation of the temporal relationships. The two approaches to time series analysis, commonly referred to as the frequency domain approach (or spectral analysis approach) and the time domain approach, have been discussed in several books (e.g., Anderson, 1975; Otnes and Enochson, 1976; Gottman, 1981; Kendall and Ord, 1990; Wei, 1990; Bendat and Piersol, 1993; Harvey, 1993; Hamilton, 1994; Brockwell and Davis, 1996; Pollock, 1999; Shumway and Stoffer, 2000). In brief, the frequency domain approach uses spectral functions to study the nonparametric decomposition of a time series into its different frequency components. The time domain approach concentrates on the use of parametric models to model some future value of a time series as a parametric function of the current and past values.

While the frequency and time domain approaches can be used to provide different insights into the nature of the actual time series it should, however, be pointed out that both approaches are mathematically equivalent. According to Gottman (1981), the two approaches are

linked by the famous theorem called the Wiener-Khintchine Theorem which provides a shuttle between the frequency and time domains. The Wiener-Khintchine Theorem shows that there is a one-to-one relationship between the autocovariance function of a stationary process and its spectral density function (Pollock, 1999). Knowing the correlation structure in the time domain corresponds to knowing the form of the spectrum in the frequency domain. Essentially, the autocorrelation function and the spectrum function form a Fourier transform pair (Kendall and Ord, 1990).

Although the two approaches are complementary rather than competitive (Harvey, 1993), there are situations when one approach is more appropriate to use than the other. According to Shumway and Stoffer (2000) the two approaches may produce similar answers for long series, but the comparative performance over short samples is better done in the time domain. Given this observation, brief remarks and selected coastal applications for both approaches will, therefore, be provided. Emphasis will then be placed on modeling in the time domain because there are well-established techniques for model selection, identification, and estimation.

The frequency domain approach

Extensive discussions on the frequency domain, or spectral approach, to time series analysis can be found in several books (e.g., Jenkins and Watts, 1969; Rayner, 1971; Kanasewich, 1973; Koopmans, 1974; Brillinger, 1975; Bloomfield, 1976; Priestley, 1981; Brillinger and Krishnaiah, 1983; Brigham, 1988; Brockwell and Davis, 1996; Fuller, 1996; Ramanathan, 1998; Pollock, 1999). According to Jenkins and Watts (1969, p.16), "spectral analysis brings together two very important theoretical approaches, the statistical analysis of time series and the methods of Fourier analysis." Since, in the frequency domain approach, Fourier transforms play a very important role (Brillinger and Krishnaiah, 1983), some brief remarks will be made on Fourier's methods which form the basis of all spectral analysis (Rayner, 1971).

Time series spectral analysis can be traced to Jean Baptiste Joseph de Fourier (1768–1830) who made the claim in 1807 that an arbitrary function defined on a finite interval could be represented as a infinite summation of cosine and sine functions (see Lasser, 1996). Many mathematicians have worked on the development of the techniques of Fourier analysis, and contemporary books (e.g., Körner, 1988; Lasser, 1996; Ramanathan, 1998; Howell, 2001) have presented various aspects of the mathematics of Fourier analysis. Without discussing the details of Fourier techniques it is worthwhile to note that one notable early investigation which focused on analyzing time series in the frequency domain was Schuster (1898) who employed the technique of periodogram analysis. The early underlying model expressed the series as a weighted sum of perfectly regular periodic components upon which a random component was superimposed. While much of the theory of spectral analysis of random processes focused on stationary processes, in recent years, "a new form of spectral analysis has been developed which, while not accommodating all nonstationary processes, does however enable us to treat a fairly large class of such processes in a unified theory which includes stationary processes as a special case" (Priestley, 1981, p. 17).

The Fourier analysis of stochastic processes can provide a representation of an infinite sequence in terms of an infinity of trigonometric functions whose frequencies range continuously. The underlying stochastic process can be represented by the Fourier integral. This can be attained by describing the stochastic processes which generate the weighting functions. There are two weighting processes, associated respectively with the sine and cosine functions; and the function that defines their common variance is the so-called spectral distribution function whose derivative is the spectral density function or the "spectrum" (Pollock, 1999). For practical purposes, the spectral density function can be referred to as the power spectrum. "Since the power spectrum is the Fourier cosine transform of the autocovariance function, knowledge of the autocovariance function is mathematically equivalent to knowledge of the spectrum, and vice-versa" (Box *et al*., 1994, p. 39). The power spectrum provides significantly more information about the time series than simply the total power. The estimated spectrum can be used to obtain insights about the mechanism that generated the data (Koopmans, 1974).

The power spectrum plays a very important role in the analysis of coastal time series. By considering the probability distribution of the sea surface as nearly Gaussian, a good approximate description is provided by the covariance function, the Fourier transform of which is referred to as the wave spectrum. In coastal studies, the wave spectrum has physical meaning because it can be demonstrated to be the density function specifying the distribution of energy over wave components with different wave number vectors and frequencies. Its integral over all wave components is proportional to the total wave energy per unit area (see Komen *et al*., 1994). It should be noted that the components of the spectrum are the squares of the wave amplitude at each frequency, which are related to wave energy. Since the covariance function can be related directly to the energy spectrum or the wave spectrum, the covariance function is computed, and then its Fourier transform is calculated to obtain the power spectrum (Dean and Dalrymple, 1984).

With the implementation of the Fast Fourier Transform (FFT) algorithm of Cooley and Tukey (1965), many researchers have followed the contributions of some significant early studies (e.g., Pierson and Marks, 1952; Munk *et al*., 1959; Hassleman *et al*., 1963) and utilized spectral concepts for either the analysis or the modeling and prediction of ocean waves. Simplified discussions on the use of spectral techniques for the analysis and modeling of the spectrum of ocean waves have been provided by Dean and Dalrymple (1984), Tucker (1991), and Goda (2000). Timely reviews on the importance and applications of spectral concepts to the description and modeling of water waves have been presented by several authors, among them Cardone (1974), Cardone and Ross (1979), Komen *et al*. (1994), and Cardone and Resio (1998). Recent advances in the development of spectral wave modeling for various application purposes have been presented by several researchers (e.g., Holthuijsen *et al*., 1993; Rivero *et al*., 1998; Booij *et al*., 1999; Ris *et al*., 1999; Monbaliu *et al*., 2000; Schneggenburger *et al*., 2000).

In the frequency domain perspective, some researchers (e.g., Guedes Soares and Ferreira, 1995; Lakhan, 1998) have modeled parameters such as significant wave height. A Fourier representation described the periodic components of time series of significant wave height values from different coastal locations. In addition, Hegge and Masselink (1996) also demonstrated the usefulness of spectral techniques to model data from topographic profiles. The results of the spectral analysis represented the amount of variance of the time series as a function of frequency. With spectral modeling, coastal researchers are obtaining greater insights on the physical characteristics of the generating mechanisms of coastal time series.

The time domain approach

The time domain approach, which focuses on the contribution of parametric models for single series or models for two or more causally related series, can be traced to the classical theory of correlation. Details on modeling and forecasting in the time domain can be found in several books (e.g., Box and Jenkins, 1970, 1976; Kendall, 1973; Anderson, 1975; Gottman, 1981; Abraham and Ledolter, 1983; Hoff, 1983; Pandit and Wu, 1983; Pankratz, 1983; Vandaele, 1983; Chatfield, 1984; Montgomery *et al*., 1990; Bowermand and O'Connell, 1993; Harvey, 1993; Box *et al*., 1994; Hamilton, 1994; Hipel and McLeod, 1994; Armstrong, 2001; Pourahmadi, 2001). The time domain models that originated with Yule (1927) and Slutsky (1937) provided a strong foundation for time series analysis in the time domain. Yule (1927) pioneered the concept of autoregression and his autoregressive model was generalized by Walker (1931) to allow for dependence on more than two previous values. Wold (1938) followed the practice of Yule and Walker and plotted correlation coefficients against their lags. According to Pourahmadi (2001, p. 35), "the term correlogram was coined by Wold (1938, p. 7) as a substitute to the Schuster's periodogram and has been used effectively ever since as a means of identifying model or appropriate probabilistic description of time series data." The early autoregressive (AR) model of Yule (1927) and moving average (MA) models of Walker (1931) and Slutsky (1937) were not widely used because of the lack of appropriate methods for identifying, fitting, and checking these models (Jenkins, 1979). AR and MA types of models were combined into the mixed autoregressive moving average (ARMA) model.

ARMA models have their foundation in the work of Box and Jenkins (1970, 1976) who utilized concepts from mathematical statistics and classical probability theory. Box and Jenkins also extended ARMA models to include certain types of nonstationary series, and proposed an entire family of models, called autoregressive integrated moving average (ARIMA) models, which can be applied to practical problems in several disciplines. Besides ARMA and ARIMA models, Box and Jenkins (1976) presented other models, including transfer function noise (TFN) models and seasonal autoregressive integrated moving average (SARIMA) models. "The ARMA and ARIMA classes can provide very useful descriptions for a wide range of time series data and the Box-Jenkins approach (as it has become known) has been used extensively by time series practitioners in a wide variety of fields" (Priestley, 1997, p. 16). In the field of coastal research, several autoregressive models have been utilized for data on sea-state parameters. For example, Lakhan (1981) and Lakhan and LaValle (1986) modeled the correlation

structure of wave heights and wave periods, and then parameterized stochastic models with autocorrelated distributed variates. Spanos (1983) used ARMA processes to simulate individual waves in short-term periods. Scheffner and Borgman (1992) also simulated individual waves but accounted for long-term variability. Several other studies (e.g., Guedes Soares and Ferreira, 1996; Cunha and Guedes Soares, 1999; Guedes Soares and Cunha, 2000) have modeled time series of sea-state parameters with autoregressive models. Besides sea-state parameters, researchers (e.g., Walton, 1999; LaValle *et al.*, 2001) have also modeled shoreline changes with time series techniques. The study by LaValle *et al.* (2001) utilized Box–Jenkins modeling procedures to identify models which best described a time series (1978–94) of beach and shoreline data. By following the Box–Jenkins model construction approach described below, it was found that a spatial model described the variation for beach net sediment flux, and a space–time autoregressive model provided the best fit for data on spatial–temporal variations of shoreline retreat. Here, it must be mentioned that ARMA models can be generalized to include spatial location (Cressie, 1993).

Time domain modeling—the Box–Jenkins approach

The success of the Box–Jenkins modeling approach in coastal and other studies can be attributed to the fact that Box–Jenkins models have several advantages over traditional models because there is a large class of models, there is a systematic approach to model identification, and the validity of models can be verified (Hoff, 1983). While a publication of this kind cannot provide technical details on the construction of Box–Jenkins models, it is, nevertheless, worthwhile to note that no matter what type of stochastic model is to be fitted to a given dataset it is recommended that the identification, estimation, and diagnostic check stages of model construction be followed (Box and Jenkins, 1976). By following Box and Jenkins, univariate models for any coastal time series can be constructed by using the iterative approach presented in Figure T44.

Consideration stage

In the consideration stage, it is necessary to be cognizant of all standard time series models. Consideration must be given to the various families of stochastic models, which can be fitted to the coastal time series. It is of paramount importance to consider those models, which on the basis of theory, practical experience, understanding of the problem, and the published literature, have the potential to fit the observed data.

Identification stage

At the beginning of the identification stage it is best to ascertain the subclasses of models that hold greater promise for adequately modeling the coastal time series. The first step is to obtain a graphical plot of the data because a plot of the time series can demonstrate some of the essential mathematical characteristics of the data. From the plot, it can be determined whether the series contains a trend, outliers, seasonality, nonconstant variances, and other non-normal and nonstationary phenomena. This knowledge allows for possible data transformations. Differencing and variance stabilizing transformations can be used. The normal procedure is to apply variance stabilizing transformations before taking differences because differencing may create some negative values. To stabilize the variance the Box–Cox power transformation can be used. For a series with nonconstant variance a logarithmic transformation can be employed (Wei, 1990). In modeling time series of significant wave height data, Guedes Soares and Ferreira (1996) tried both the Box–Cox transformation and the logarithmic transformation. Following transformation to stationarity it is necessary to compute and examine the sample autocorrelation function (ACF) and the sample partial autocorrelation coefficient (PACF) of the original series to determine the need for further differencing.

After performing the necessary differencing, the ACF and PACF are computed for the properly transformed and differenced series. The autocorrelations and partial autocorrelations of a series are considered principal tools for identifying the correct parameters to include in a Box–Jenkins ARIMA model. Autocorrelations are statistical measures computed from the time series data. An autocorrelation measures how strongly time series values at a specified number of periods apart are correlated to each other over time. The number of periods apart is called the lag. The rule of thumb is that the maximum number of lags should not exceed one-fifth of the number of observations. The partial autocorrelation is similar to autocorrelation, except that when calculating it, the (auto)correlations with all the elements within the lag are partialled out (Box and Jenkins, 1976). In univariate Box–Jenkins modeling, it is

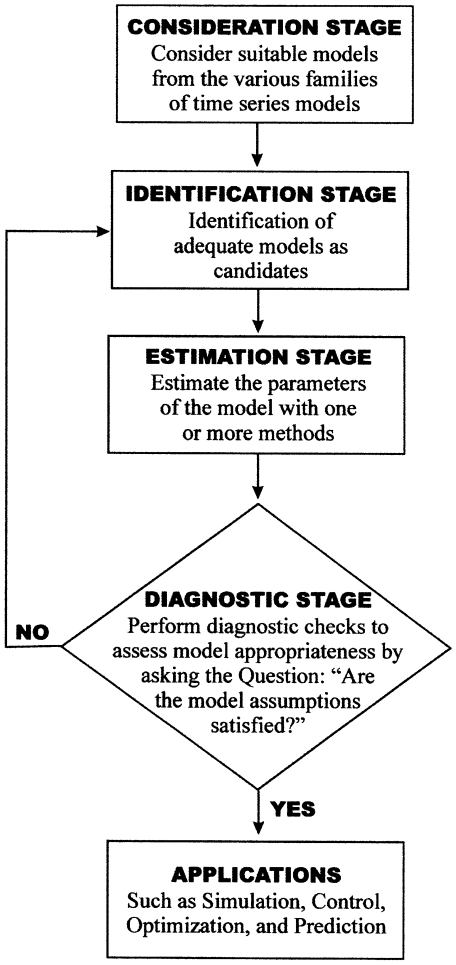

Figure T44 Stages in the iterative approach to model construction (modified from Box *et al.* (1994, p. 17)).

normal practice to produce correlograms depicting the autocorrelation coefficients plotted against the lag intervals. According to Harvey (1993), the correlogram is the basic tool of analysis in the time domain. An inspection of the correlogram provides important information as to whether the series exhibits a pattern of serial autocorrelation which can be modeled by a particular stochastic process or whether the series is random. Figure T45 is a correlogram of significant wave height data which shows that the data values are not independent of each other. The series is not random because the autocorrelations should be near zero for randomness. By understanding the association between the ACF and PACF and their corresponding processes, a tentative model can be identified. In the case of Figure T45, with the autocorrelation function decaying exponentially, and knowing that the PACF has a distinct spike at lag 1, it is possible to specify an AR(1) model. It should, however, be stressed that several other models could fit the data. The primary goal is to identify a model with the smallest number of estimated parameters.

Parameter estimation

Subsequent to identifying an adequate model for fitting to a particular series, the next step is to estimate the parameters in the model. Hoff (1983) outlined several objectives in estimating a model, among them obtaining fitted values that are nearly identical to the original series values, obtaining residuals that are not correlated to each other, and using a minimum number of parameters as necessary. A good model incorporates the smallest number of estimated parameters which are needed to fit the patterns in the data. To estimate parameters such as the mean of the series, AR parameters, MA, and other parameters for an identified ARMA model, several estimation procedures can be utilized. Details in estimation theory and estimation procedures can be found in several publications (e.g., Kruskal and Tanur, 1978; Sachs, 1984; Mendel, 1987;

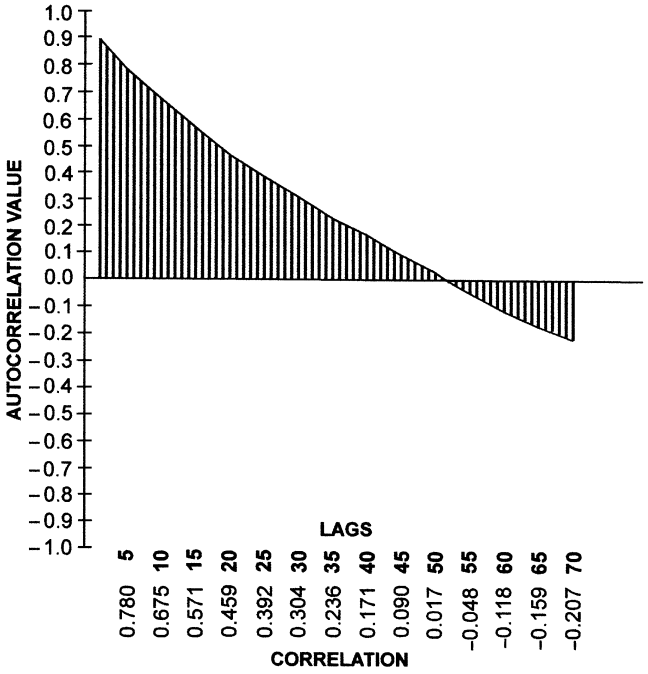

Figure T45 Correlogram of significant wave height (from Lakhan, 1998).

Kotz and Johnson, 1988; Box *et al*., 1994). For the time series modeling of coastal data, the method of moments, and the maximum likelihood method are widely used approaches to parameter estimation.

Diagnostic checking

Once the parameters of the identified model have been estimated, the next phase is to perform diagnostic checks to determine whether certain assumptions about the model can be verified. Two assumptions to be checked are usually the normality of residuals of the model, and independence. To ascertain whether the residuals are white noise, the residuals from the estimated model are used to calculate the autocorrelation coefficients. Ideally, the residual autocorrelation function for a properly constructed ARIMA model will have autocorrelation coefficients that are all statistically zero. If the residuals are autocorrelated they are not white noise, and this requires formulating another model with residuals that are consistent with the independence assumption (Pankratz, 1983).

The portmanteau lack of fit test is usually applied for testing the independence of a time series. The portmanteau lack of fit test, originally proposed by Box and Pierce (1970), was improved by Ljung and Box (1978). Applications of the portmanteau test for physical time series can be found in several studies (e.g., Hipel and McLeod, 1977; Salas *et al*., 1980; Hipel and McLeod, 1994). The test statistic is the modified Q statistic which uses all the residual autocorrelations as a set to check the joint null hypothesis. The Q statistic approximately follows a chi-square distribution, with degrees of freedom equal to the total number of lags used minus the number of model parameters and their associated probability values. Recent studies (e.g., LaValle *et al*., 2000, 2001) have demonstrated that the Q statistic is appropriate for determining the goodness-of-fit of autoregressive models fitted to data on water levels and beach and shoreline changes.

Applications

When a model is accepted it could be used for various applications, among them filtering and control, simulation and optimization, and prediction. A model that fails one or more diagnostic checks is rejected. To construct a good model it becomes necessary to return to the identification stage, and repeat the iterative process of identification, estimation, and diagnostic checking.

Selection of the best model

In coastal time series analysis, it is possible to have several appropriate models that can be used to represent a given dataset. To solve the problem of choosing the best model from the various adequate models, several model determination procedures and model selection criteria have been proposed (e.g., Stone, 1979; Hannan, 1980). Selection criteria are different from the model identification methods discussed above because when there are several adequate models for a given dataset the selection criterion is normally based on summary statistics from residuals computed from a fitted model or on forecast errors calculated from the out-sample forecasts (Wei, 1990).

Some well-known model selection criteria based on residuals are the Akaike Information Criterion (AIC) of Akaike (1974), Parzen Criterion for Autoregressive Transfer (CAT) Functions of Parzen (1977), and the Schwartz's Bayesian Criterion (SBC) of Schwartz (1978). Of the various selection criteria, the AIC is widely used in time series model fitting because it increases the speed, flexibility, accuracy, and simplicity involved in choosing the "best" model. In addition, the AIC is useful for application to many different kinds of time series (Hipel, 1981; Hipel and McLeod, 1994), and facilitates the selection of a parsimonious model that, at the same time, provides a good statistical fit to the data being modeled.

V. Chris Lakhan

Bibliography

Abraham, B., and Ledolter, J., 1983. *Statistical Methods for Forecasting*. New York: John Wiley and Sons, Inc.

Akaike, H., 1974. A new look at the statistical model identification. *IEEE Transactions on Automatic Control*, **19**: 716–723.

Anderson, O.D., 1975. *Time-Series Analysis and Forecasting: The Box–Jenkins Approach*. London: Butterworths.

Armstrong, J.S., 2001. *Principles of Forecasting: A Handbook for Researchers and Practitioners*. Boston, MA: Kluwer Academic Press.

Bendat, J.S., and Piersol, A.G., 1993. *Engineering Applications of Correlation and Spectral Analysis*, 2nd edn. New York: John Wiley and Sons, Inc.

Bloomfield, P., 1976. *Fourier Analysis of Time Series: An Introduction*. New York: John Wiley and Sons, Inc.

Booij, B., Ris, R.C., and Holthuijsen, L.H., 1999. A third-generation wave model for coastal regions: 1. Model description and validation. *Journal of Geophysical Research*, **104**(C4): 7649–7666.

Bowermand, B.L., and O'Connell, R.T., 1993. *Time Series and Forecasting: An Applied Approach*, 3rd edn. N. Scituate, MA: Duxbury Press.

Box, G.E.P., and Jenkins, G.M., 1970. *Time Series Analysis: Forecasting and Control*. San Francisco, CA: Holden-Day.

Box, G.E.P., and Jenkins, G.M., 1976. *Time Series Analysis Forecasting and Control*, 2nd edn. San Francisco, CA: Holden-Day.

Box, G.E.P., and Pierce, D.A., 1970. Distribution of the residual autocorrelations in autoregressive integrated moving average models. *Journal of the American Statistical Association*, **65**: 1509–1526.

Box, G.E.P., Jenkins, G.M., and Reinsel, G.C., 1994. *Time Series Analysis. Forecasting and Control*, 3rd edn. Englewood Cliffs, NJ: Prentice-Hall, Inc.

Brigham, E.O., 1988. *The Fast Fourier Transform and its Applications*. Englewood Cliffs, NJ: Prentice Hall.

Brillinger, D.R., 1975. *Time Series: Data Analysis and Theory*. New York: Holt, Rinehart, and Winston.

Brillinger, D.R., and Krishnaiah, P.R. (eds.), 1983. *Time Series in the Frequency Domain. Handbook of Statistics*, Vol. 3. Amsterdam, The Netherlands: Elsevier Science Publishers.

Brockwell, P.J., and Davis, R.A., 1996. *Introduction to Time Series and Forecasting*. New York: Springer.

Cardone, V.J., 1974. Ocean wave predictions: two decades of progress and future prospects. In Society of Naval Architects and Marine Engineers. *Seakeeping 1953–1973/Sponsored by Panel H-7 (Seakeeping Characteristics) at Webb Institute of Naval Architecture, Glen Cove, New York, October 28–29, 1973*. pp. 5–18.

Cardone, V.J., and Resio, D.T., 1998. An assessment of wave modelling technology. *Proceedings of the 5th International Workshop on Wave Hindcasting and Forecasting*. Melbourne, FL, pp. 468–495.

Cardone, V.J., and Ross, D.B., 1979. State-of-the-Art wave prediction methods and data requirements. In Earle, M.D., and Malahoff, A. (eds.), *Ocean Wave Climate*. New York: Plenum Press, pp. 61–91.

Chatfield, C., 1984. *The Analysis of Time Series: An Introduction*. London and New York: Chapman and Hall.

Cooley, J.W., and Tukey, J.W., 1965. An algorithm for the machine calculation of complex Fourier Series. *Mathematics of Computation*, **19**: 297–301.
Cressie, N.A.C., 1993. *Statistics for Spatial Data*. New York: John Wiley and Sons, Ltd.
Cunha, C., and Guedes Soares, C., 1999. On the choice of data transformation for modelling time series of significant wave height. *Ocean Engineering*, **26**: 489–506.
Dean, R.G., and Dalrymple, R.A., 1984. *Water Wave Mechanics for Engineers and Scientists*. Englewood Cliffs, NJ: Prentice-Hall, Inc.
Fuller, W.A., 1996. *Introduction to Statistical Time Series*, 2nd edn. New York: John Wiley and Sons, Inc.
Goda, Y., 2000. *Random Seas and Design of Maritime Structures*. Singapore: World Scientific Publishing Co.
Gottman, J.M., 1981. *Time-Series Analysis*. Cambridge, England: Cambridge University Press.
Guedes Soares, C., 2000. Probabilistic based models for coastal studies. *Coastal Engineering*, **40**: 279–283.
Guedes Soares, C., and Cunha, C., 2000. Bivariate autoregressive models for the time series of significant wave height and mean period. *Coastal Engineering*, **40**: 297–311.
Guedes Soares, C., and Ferreira, A.M., 1995. Analysis of the seasonality in nonstationary time of significant wave height. In Spanos, P.D. (ed.), *Computational Stochastic Mechanics*. New York: Balkema, pp. 501–521.
Guedes Soares, C., and Ferreira, A.M., 1996. Representation of nonstationary time series of significant wave height with autoregressive models. *Probabilistic Engineering Mechanics*, **11**: 139–148.
Hamilton, J.D., 1994. *Time Series Analysis*. Princeton, NJ: Princeton University Press.
Hannan, E.J., 1980. The estimation of the order of an ARMA process. *The Annals of Statistics*, **8**: 1071–1081.
Hannan, E.J., Krishnaiah, P.R., and Rao, M.M. (eds.), 1985. *Time Series in the Time Domain. Handbook of Statistics*, Vol. 5. Amsterdam, The Netherlands: Elsevier Science Publishers.
Harvey, A.C., 1993. *Time Series Models*, 2nd edn. Cambridge, MA: The MIT Press.
Hassleman, K., Munk, W., and MacDonald, G., 1963. Bispectrum of ocean waves. In Rosenblatt, M. (ed.), *Time Series Analysis*. New York: John Wiley and Sons, Inc., pp. 125–139.
Hegge, B.J., and Masselink, G., 1996. Spectral analysis of geomorphic time series: auto-spectrum. *Earth Surface Processes and Landforms*, **21**: 1021–1040.
Hipel, K.W., 1981. Geophysical model discrimination using the Akaike information criterion. *IEEE Transactions on Automatic Control*, **AC-26**(2): 358–378.
Hipel, K.W., and McLeod, A.I., 1977. Advances in Box–Jenkins modeling. 1. Model construction. *Journal of Water Resources Research*, **13**(3): 567–575.
Hipel, K.W., and McLeod, A.I., 1994. *Time Series Modelling of Water Resources and Environmental Systems*. Amsterdam, The Netherlands: Elsevier Science Publishers.
Hoff, J.C., 1983. *A Practical Guide to Box–Jenkins Forecasting*. Belmont, CA: Wadsworth, Inc.
Holthuijsen, L.H., Booij, N., and Ris, R.C., 1993. A spectral model for the coastal zone. *Proceedings of the 2nd International Symposium on Ocean Wave Measurement and Analysis*. New Orleans, LA, pp. 630– 641.
Howell, K.B., 2001. *Principles of Fourier Analysis*. Boca Raton, FL: Chapman & Hall/CRC.
Jenkins, G.M., 1979. Practical experiences with modelling and forecasting time series. In Anderson, O.D. (ed.), *Forecasting*. Amsterdam, The Netherlands: North-Holland Publishing Company, pp. 43–166.
Jenkins, G.M., and Watts, D.G., 1969. *Spectral Analysis and its Applications*. San Francisco, CA: Holden-Day, Inc.
Kanasewich, E.R., 1973. *Time Series Analysis in Geophysics*. Edmonton, AB: University of Alberta Press.
Kendall, M., 1973. *Time-Series*. New York: Hafner Press.
Kendall, M., and Ord, J.K., 1990. *Time Series*, 3rd edn. New York: Oxford University Press.
Komen, G.J., Cavaleri, L., Donelan, M., Hasselmann, K., Hasselmann, S., and Janssen, P.A.E.M., 1994. *Dynamics and Modelling of Ocean Waves*. Cambridge: Cambridge University Press.
Koopmans, L.H., 1974. *The Spectral Analysis of Time Series*. New York: Academic Press, Inc.
Körner, T.W., 1988. *Fourier Analysis*. Cambridge, England: Cambridge University Press.
Kotz, S., and Johnson, N.L. (eds.), 1988. *Encyclopedia of Statistical Sciences*, Vols 1 to 9. New York: John Wiley and Sons, Inc.
Kruskal, W.H., and Tanur, J.M., 1978. *International Encyclopedia of Statistics*, Vols 1 and 2. New York: The Free Press.
Lakhan, V.C., 1981. Parameterizing wave heights in simulation models with autocorrelated Rayleigh distributed variates. *Journal of the International Association of Mathematical Geology*, **13**(4): 345–350.
Lakhan, V.C., 1982. *Stochastic simulation of wave action on concave-shaped nearshore profiles*. Ph.D. thesis. Toronto, ON: University of Toronto.
Lakhan, V.C., 1989. Modeling and simulation of the coastal system. In Lakhan, V.C, and Trenhaile, A.S. (eds.), *Applications in Coastal Modeling*. Amsterdam, The Netherlands: Elsevier Science Publishers, pp. 17–41.
Lakhan, V.C., 1998. Modeling waves and sediments associated with mudbank formation along the Guyana coast. Berbice, Guyana: Canada Caribbean Research Group, *Technical Report No. 38*.
Lakhan, V.C., and LaValle, P.D., 1986. Development and testing of a stochastic model to simulate nearshore profile changes. *Studies in Marine and Coastal Geography*, Halifax, NS: Saint Mary's University, pp. 61–81.
Lakhan, V.C., and Trenhaile, A.S., 1989. Models and the coastal system. In Lakhan, V.C, and Trenhaile, A.S. (eds.), *Applications in Coastal Modeling*. Amsterdam, The Netherlands: Elsevier Science Publishers, pp. 1–16.
Lasser, R., 1996. *Introduction to Fourier Series*. New York: Marcel Dekker, Inc.
LaValle, P.D., Lakhan, V.C., and Trenhaile, A.S., 2000. Short term fluctuations of Lake Erie water levels and the El Niño/Southern Oscillation. *The Great Lakes Geographer*, **7**(1): 1–8.
LaValle, P.D., Lakhan, V.C., and Trenhaile, A.S., 2001. Space-time series modelling of beach and shoreline data. *Environmental Modelling and Software*, **16**: 299–307.
Ljung, G.M., and Box, G.E.P., 1978. On a measure of lack of fit in time series models. *Biometrika*, **65**: 297–303.
Mendel, J.M., 1987. *Lessons in Digital Estimation Theory*. Englewood Cliffs, NJ: Prentice-Hall.
Monbaliu, J., Padilla-Hernández, R., Hargreaves, J.C., Carretero Labiach, J.C., Luo, W., Sclavo, M., and Günther, H., 2000. The spectral wave model, WAM, adapted for applications with high spatial resolution. *Coastal Engineering*, **41**: 41–62.
Montgomery, D.C., Johnson, L.A., and Gardiner, J.S., 1990. *Forecasting and Time Series Analysis*. 2nd edn. New York: McGraw-Hill, Inc.
Munk, W.H., Snodgrass, F.E., and Tucker, M.J., 1959. Spectra of low frequency ocean waves. *Bulletin Scripps Institution of Oceanography*, **7** (4): 283–362.
Otnes, R.K., and Enochson, L.D., 1976. *Applied Time Series Analysis*. New York: John Wiley and Sons, Inc.
Pandit, S.M., and Wu, S-M., 1983. *Time Series and System Analysis with Applications*. New York: John Wiley and Sons, Inc.
Pankratz, A., 1983. *Forecasting with Univariate Box–Jenkins Models*. New York: John Wiley and Sons, Inc.
Parzen, E., 1977. Multiple time series modeling: determining the order of approximating autoregressive schemes. In Krishnaiah, P. (ed.), *Multivariate Analysis IV*. Amsterdam, The Netherlands: North-Holland, pp. 283–295.
Pierson, W.J., and Marks, W., 1952. The power spectrum analysis of ocean wave records. *Transactions of American Geophysical Union*, **33**: 834–844.
Pollock, D.S.G., 1999. *A Handbook of Time-Series Analysis, Signal Processing and Dynamics*. London: Academic Press.
Pourahmadi, M., 2001. *Foundations of Time Series Analysis and Prediction Theory*. New York: John Wiley and Sons, Inc.
Priestley, M.B., 1981. *Spectral Analysis and Time Series*, Vols 1 and 2. New York: Academic Press.
Priestley, M.B., 1997. A short history of time series. In Subba Rao, T., Priestley, M.B., and Lessi, O. (eds.), *Applications of Time Series Analysis in Astronomy and Meteorology*. London: Chapman & Hall, pp. 3–23.
Ramanathan, J., 1998. *Methods of Applied Fourier Analysis*. Boston, MA: Birkhäuser.
Rayner, J.N., 1971. *An Introduction to Spectral Analysis*. London: Pion Limited.
Ris, R.C., Holthuijsen, L.H., and Booij, B., 1999. A third-generation wave model for coastal regions: 2. Verification. *Journal of Geophysical Research*, **104**(C4): 7667–7681.
Rivero, F.J., Arcilla, A.S., and Carci, E., 1998. An analysis of diffraction in spectral wave models. In Edge, B.L., and Hemsley, J.M. (eds.), *Ocean Wave Measurement and Analysis*, Vol. 2. Reston, VA: American Society of Civil Engineers, pp. 431–445.
Sachs, L., 1984. *Applied Statistics. A Handbook of Techniques*, 2nd edn. New York: Springer-Verlag.

Salas, J.D., Delleur, J.W., Yevjevich V., and Lane, W.L., 1980. *Applied Modeling of Hydrologic Time Series*. Littleton, CO: Water Resources Publications Ltd.
Scheffner, N.W., and Borgman, L.E., 1992. Stochastic time series representation of wave data. *Journal of Waterway, Port, Coastal and Ocean Engineering*, ASCE, **118**(4): 1955–2012.
Schneggenburger, C., Günther, H., and Rosenthal, W., 2000. Spectral wave modelling with non-linear dissipation: validation and applications in a coastal tidal environment. *Coastal Engineering*, **41**: 201–235.
Schuster, A., 1898. On the investigation of hidden periodicities with application to a supposed twenty-six day period of meteorological phenomena. *Terrestrial Magnetism*, **3**: 13–41.
Schwartz, G., 1978. Estimating the dimension of a model. *The Annals of Statistics*, **6**: 461–464.
Shumway, R.H., and Stoffer, D.S., 2000. *Time Series Analysis and Its Application*. New York: Springer-Verlag New York, Inc.
Slutsky, E., 1937. The summation of random causes as the source of cyclical processes. *Econometrica*, **5**: 105–146.
Spanos, P.D., 1983. ARMA algorithms for ocean wave modelling. *Journal of Energy Resources Technology* ASME, **105**: 300–309.
Stone, M., 1979. Comments on model selection criteria of Akaike and Schwartz. *Journal of Royal Statistical Society*, Series B, **41**: 276–278.
Tucker, M.J., 1991. *Waves in Ocean Engineering*. New York: Ellis Horwood Limited.
Vandaele, W., 1983. *Applied Time Series and Box–Jenkins Models*. New York: Academic Press.
Walker, G., 1931. On periodicity in series of related terms. *Proceedings of the Royal Society*, A **131**: 195–215.
Walton, T.L., Jr., 1999. Shoreline rhythmic pattern analysis. *Journal of Coastal Research*, **15**(2): 379–387.
Wei, W.W.S., 1990. *Time Series Analysis. Univariate and Multivariate Methods*. Redwood City, CA: Addison-Wesley Publishing Company, Inc.
Wold, H., 1938. *A Study in the Analysis of Stationary Time-Series*. Uppsala, Sweden: Almquist & Wiksell.
Yule, G.U., 1927. On a method of investigating periodicities in distributed series, with special reference to Wölfer's sunspot numbers. *Philosophical Transactions of the Royal Society*, A, **226**: 267–298.

Cross-references

Coastal Modeling and Simulation
Numerical Modeling
Simple Beach and Surf Zone Models
Surf Modeling
Wave Climate

TOPIC CATEGORIES—See APPENDIX 6

TORS

The word "tor," Celtic in origin, is used generally in the British Isles to denote a rather tall rock column (Cunningham, 1968; Jackson, 1997). Linton (1955) was the first to propose it as a scientific term in describing the tors at Dartmoor, Devonshire, England, now considered the type area for the feature (Palmer and Neilson, 1962). Early hypotheses for the origin of tors invoked deep weathering along joint planes in granite, with subsequent removal of the loose material leaving exposed columns. Alternate possibilities outlined by Cunningham (1968) include differential erosion during scarp recession and relict subaerial prominences formed in the Tertiary. Since tors have been found worldwide, often in granite but also in other igneous, sedimentary, and metamorphic rocks, it is appropriate to consider Palmer and Neilson's (1962) pronouncement that "It is not possible to offer a definition that will encompass the many landforms to which the name "tor" has been given." With such wide distribution and varied lithology it is arguable that the most scenic among all of these are coastal tors, as can be seen in the Seychelles and Virgin Islands.

Seychelles

The Seychelles, along with Madagascar, were displaced in a northeasterly direction away from the African landmass during the early formation, in the Jurassic, of the Indian Ocean (Brathwaite, 1984). As such, 42 of the 116 islands comprising the Seychelles Archipelago are the world's only mid-ocean islands composed of granitic rocks (Cílek, 1978). Grey and pink amphibolitic granite, of late Precambrian age, is spectacularly displayed on the northern island of La Digue and at Mahe as discussed by Wagle and Hashimi (1990).

La Digue Island has long been known for its world-class resorts featuring tropical flora, white-sand beaches, swimming in crystal clear waters, snorkeling among coral reefs and magnificent scenic views. Anse source d'argent beach, located on the island, is the site of several tors, chief among them that is pictured in Figure T46. The size of the pink tor can be judged when compared with the heads of the three swimmers seen in the mid-foreground. Graphic too is the weathered "fluting" described as typical of tors by Linton (1955) in his pioneering work, and by Brathwaite (1984) for a tor on Mahe.

Figure T46 The tor at Anse Source D'argent, La Digue Island, Seychelles, Indian Ocean; often considered to be the most beautiful beach in the world (Photo courtesy of New Adventures).

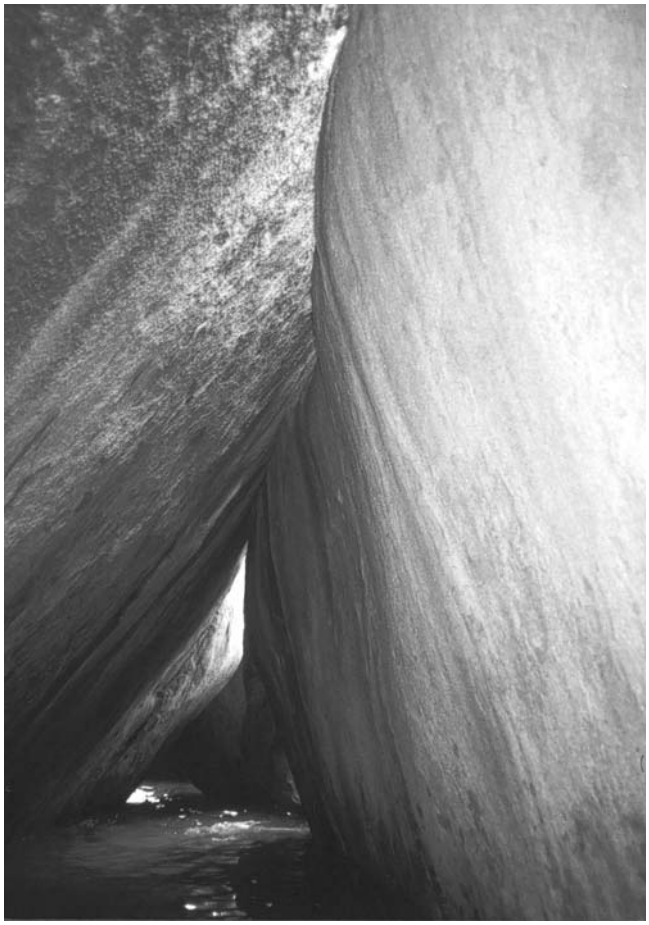

Figure T47 Grotto at the base of the tors at The Baths, Virgin Gorda, British Virgin Islands (Photo, M. Schwartz).

Virgin Islands

The Virgin Islands, located in the northeastern Caribbean along the leading edge of the Caribbean plate, are composed of Mesozoic and lower Tertiary deformed island-arc terrane. Much of the northeastern British Virgin Islands region is underlain by the Virgin Gorda granitic pluton or batholith, which was intruded into the surrounding country rock in mid- to later Eocene time (Mattson *et al*., 1990). Weathered exposures in tonalitic rocks at the southern end of the island of Virgin Gorda reveal huge boulders now located upon the beaches (Weaver, 1962) in a park system managed by the B.V.I. National Parks Trust.

The origin of these boulders has been described by Ratté (1986) in the classic Linton (1955) style for tors of deep weathering along joints followed by removal of the rotted material. A favorite with tourists, the site is called "The Baths," not because of the underlying batholith as a geologist would imagine, but for the salt water pools in the grotto at the base of the tors (Figure T47). Here one may walk, and crawl, along a trail between boulders that range up to 4 m in height.

Maurice Schwartz

Bibliography

Brathwaite, C.J.R., 1984. Geology of the Seychelles, In Stoddart, D.R. (ed.), Biogeography and ecology of the Seychelle Islands. The Hague: W. Junk, pp. 17–38.

Cílek, V., 1978. Geological investigations on the beaches of Mahe in the Seychelles Archipelago. *Casopsis pro Mineralogii a Geologii*, **23**(2): 149–157.

Cunningham, F.F., 1968. The significance of Caribbean evidence in the elucidation of tors. *Caribbean Journal of Science*, **8**: 187–197.

Jackson, J.A. (ed.), 1997. Glossary of Geology, 4th edn. Alexandria, VA: American Geological Institute.

Linton, D.L., 1955. The problem of tors. *Geographical Journal*, **121**(4): 470–486.

Mattson, P., Draper, G., and Lewis, J.F., 1990. Puerto Rico and the Virgin Islands. In Dengo, G., and Case, J.E. (eds.), *The Caribbean Region, The Geology of North America*, H, Boulder: Geological Society of America, pp. 112–120.

Palmer, J., and Neilson, R.A., 1962. The origin of granite tors on Dartmoor, Devonshire. *Proceedings of the Yorkshire Geological Society*, **33**(3): 315–339.

Ratté, C.A., 1986. *The Story of the Boulders*. Burlington, Vermont: Queen City Printers.

Wagle, B.G., and Hashimi, N.H., 1990. Coastal geomorphology of Mahe Island, Seychelles. *International Journal of Remote Sensing*, **11**(2): 281–287.

Weaver, J.D., 1962. Notes on some erosional features in Virgin Gorda, B. Virgin Islands. *Caribbean Journal of Science*, **2**(4): 159–167.

Cross-references

Boulder Beaches
Caribbean Islands, Coastal Ecology and Geomorphology
Coastal Hoodoos
Indian Ocean Islands, Coastal Ecology and Geomorphology
Tourism, Criteria for Coastal Sites
Weathering in the Coastal Zone

TOURISM AND COASTAL DEVELOPMENT

Coastal tourism is a process involving tourists and the people and places they visit. It is more specifically defined as tourism brought to bear on the coastal environment and its natural and cultural resources. Most coastal zone tourism takes place along the shore and in the water immediately adjacent to the shoreline. Coastal tourism activities occur outdoors and indoors as recreation, sport and play, and as leisure and business (Miller and Ditton, 1986). As with other human endeavors in the coastal zone associated with development, tourism is viewed positively by some for the opportunities it creates. Others condemn coastal tourism for its unacceptable consequences.

Coastal tourism destinations fall all along an urban–rural continuum (see *Demography of Coastal Populations, q.v.*). At one end of the scale are major cities and ports (Hong Kong, Venice, New York, Rio de Janeiro, and Sydney come to mind) known for their cultural, historical, and economic significance. At the other end of the continuum are the relatively isolated and pristine coastlines found around the world that are valued for their natural beauty, flora, and fauna. Of course, many coastal tourism destinations offer rich mixtures of cultural, historical, social, environmental, and other values to visitors.

Coastal tourism technologies of travel include both those which carry tourists from their homeland (e.g., airplanes, ships, cars, buses, and trains) and which are regarded by travelers as mere means to the end of arriving at destinations, and those which transport tourists at coastal destinations but which become part of the touristic experience (e.g., cruise ships, personal watercraft, sailboats, dive boats, motorcycles, bicycles, and forms of animal transportation). Again, some transportation technologies can, depending on the circumstance, be important for being both convenient and for being interesting or pleasing.

In a manner of speaking, all tourism is a matter of supply and demand. With this perspective, coastal tourism is a business for those who make a living by developing accommodations and attractions, and by providing touristic and recreational products and services. Competing marketing programs of a multifaceted industry alert tourists and would-be travelers to coastal tourism amenities. Today, tourists travel to the coastal zone for parts of a day, for weekends, for short vacations, and for prolonged stays. Depending on the circumstances, they may travel alone, with family, or in groups. Some coastal tourism is organized for a special purpose such as ecotourism, adventure tourism, scientific tourism, and dive tourism. Coastal tourism accommodations range from small residences and camping sites rented out as opportunities arise, to single bed-and-breakfast and hotel rooms, to luxury suites in resort enclaves.

Many coastal tourism activities count as a business for those in the tourism industry and as an experience for tourists. Scuba diving, for example, provides an excellent example of how advances in technology have provided foundations for business and have facilitated touristic access to the marine environment. Other coastal activities that have a business aspect (involving, for example, guides and instructors, or

special equipment) include recreational and sport fishing, boating, sailing and parasailing, and whale and bird watching. Then too, there are many forms of coastal tourism—swimming and body surfing, snorkeling, beachcombing, hiking and rock climbing, sketching and painting, photographing, sightseeing—that are "free," or for which costs to providers are recovered indirectly through taxes, or are incorporated in standard hotel or accommodation billing practices. In recent years, windsurfing, body-boarding, wake-boarding, kite-surfing in addition to surfing (*q.v.*), have reached new levels of popularity in the coastal zone.

At the same time that coastal tourism fosters economic relationships between industry producers and tourist consumers, the process has shown itself to be an enormously potent force in transforming the natural environment and the lives of people who are neither part of the business of tourism nor a member of the community of tourists.

Coastal tourism is inherently controversial. The coastal zone is a scarce resource prized not only by those who engage in and profit by tourism, but also by those with personal residences near the sea, and those who find employment in fishing, aquaculture (*q.v.*), maritime shipping, nuclear energy, and national defense, among other industries. Congestion and competition in the coastal zone frames the characterization and the resolution of tourism issues. Coastal tourism problems and opportunities are therefore properly debated as "multiple-use" or "multiple-value" conflicts.

Origins of tourism

Although the early Greeks and Romans were known to enjoy the seashore for leisure purposes, coastal tourism has its roots in the Grand Tour traditions beginning with the Renaissance. As an educational institution, the Grand Tour offered young men first-hand exposure to European courts, customs, and prominent cities and ports. Not surprisingly, the Grand Tourists and their "bear-leader" tutors mixed education with pleasure. By the start of the 18th century, these tourists had begun to develop an aesthetic vocabulary that allowed them to more fully appreciate not only the "beautiful" in nature, but the "picturesque" and the "sublime" as well. Especially popular with the Grand Tourists were seascape paintings by Claude Lorrain (1600–82), Salvator Rosa (1615–73), and Gaspard Poussin (1615–75), depicting storms, shipwrecks, harbors, rocky coastlines, and ruins.

The mid-18th century European "discovery" of the seashore for spa and medicinal purposes in England gave rise to early forms of coastal tourism. In the first half of the 19th century, coastal resorts saw a faster rate of population increase than manufacturing towns and by the mid-19th century the medicinal beach was replaced by the pleasure beach. In 1841, the London to Brighton railway was opened, and in the same year Thomas Cook began a legendary career by promoting his first group excursion (Manning-Sanders, 1951; Hern, 1967; Corbin, 1994). Since that time, beaches, atolls, islands, and harbors around the world have supported coastal tourism (see *Beach use and Behaviors, g.v.*).

Magnitude of coastal tourism

Although there are no standardized practices for reporting tourism statistics within the coastal zone, it is not difficult to see how tourism has a major coastal aspect. More than 70% of the earth is covered by water, and only several dozen out of well over 200 nations in the world lack coastlines (Miller and Auyong, 1991a).

International trends

World Tourism Organization statistics confirm that tourism is the world's largest industry as measured by the number of people involved and by economic impacts. From 1945 to 2000, international arrivals increased from 25 million to a record 699 million (WTO, 1996 and 2001). Between 1970 and 1990, tourism grew by nearly 300% (United Nations Environment Programme, 1992).

By the year 2020, it is estimated that international tourist arrivals will reach over 1.56 billion. Statistical estimations for total tourist arrivals by region show that in 2020 the top three receiving regions will be Europe (717 million tourists), east Asia and the Pacific (397 million tourists), and the Americas (282 million tourists), followed by Africa, the Middle East, and south Asia (WTO, 2001).

The World Travel and Tourism Council (WTTC, 1995) reports that between 1980 and 1989, economic expenditures on international travel (excluding transportation) doubled to $209 billion, rising one-third faster than the world gross national product. Additionally, travel and tourism generated an estimated $3.4 trillion in gross output in 1995—creating employment for 211 million people, and producing nearly 11% of the world gross domestic product. This growth reflects investments of $694 billion in new facilities and equipment, and contributions of more than $637 billion to global tax revenues (WTTC, 1995).

In 2000, tourism generated total international receipts of US$ 476 billion (WTO, 2001). Of the world's top 15 tourism destination countries in 2000, 12 were countries having coastlines (WTO, 2001). In 2000, the cruise ship industry expected to host over 6.5 million passengers which would represent a 1,200% increase in number of passengers since 1966 (Godsman, 2000).

Sun, beautiful beaches, and warm ocean waters have become standard vacation requirements for many tourists. Of those visiting the Caribbean 49% do so for the beaches, while 28% are primarily interested in sightseeing, and 17% in water sports (Waters, 2001). The Pacific region (which includes Australia) has enjoyed a healthy annual growth rate of nearly 4% since the mid-1990s, though arrivals represent only 1.4% of the world's inbound travelers. Of the Pacific territories, French Polynesia is the most dependent on travel with 78% of the nation's GDP coming from tourism. Tourism in the African region has been growing at a faster rate than for many other parts of the world (Waters, 2001).

US trends

The Travel Industry Association of America (TIA, 2001) reports that tourism is the nation's largest services export industry, the third largest retail industry, and one of America's largest employers. TIA (2001; see also WTTC, 1995) has tabulated that travel and tourism in the United States alone has an impact exceeding $541 billion a year in expenditures which includes spending by US resident and international travelers within the United States on travel-related expenses (i.e., transportation, lodging, meals, entertainment, and recreation, as well as international, fares on US flag air carriers). This generates more than 17.5 million jobs, and fuels the largest trade surplus of any industry, totaling nearly $25 billion in 1999. Between 1986 and 1996, international visitation to the United States grew by 78% and expenditures by foreign visitors grew by 223%. It is estimated that more than 90% of foreign-tourist spending occurs in coastal states (US Travel and Tourism Administration, 1994).

US coastlines are popular sites for tourism and recreational activities. Coastal beaches, wetlands, fisheries, aesthetic landscapes, and the human-designed facilities and attractions in the touristic hinterland combine in an endless list of inviting opportunities for visitors, local residents, and entrepreneurs. The major recreational elements of coastal tourism are visiting beaches, swimming, snorkeling and scuba diving, boating, fishing, surfing, and wildlife watching.

It is important to note that coastal tourism and recreation activities often overlap and are not always confined to the marine and coastal environment. For example, diving, fishing, and whale watching are often done while boating, surfing, swimming, and bird watching are usually done while visiting beaches and coastlines; and not all recreational boats are used exclusively in marine and coastal waters.

In the United States, beaches are the leading foreign and domestic tourist destinations (Houston, 1996). In 1995, coastal states made up 11 of the top 15 destinations for overseas travelers visiting the United States (Waters, 1997). A 1999 survey that measured travelers' satisfaction with their visits revealed that Hawaii, Alaska, California, and Florida—all coastal states—were the top four "most liked" destinations in the United States (Volgenau, 2000).

Tourism and recreation are highly significant economic activities in the US coastal zone. By one estimate, approximately 180 million people visit the coast for recreational purposes, and 85% of tourist-related revenues are generated by coastal states (Houston, 1996). Overall, beach tourism and recreation have been estimated to contribute $170 billion annually to the US economy (Houston, 1995). Coastal states receive 85% of all tourist-related revenues in the United States (Houston, 1995). Coastal districts (defined in terms of state congressional districts) received more than $185 billion in tourism expenditures in 1997 (TIA, 1998). In addition, it has been estimated that US beaches and marine waters support 28.3 million jobs (Environmental Protection Agency, 1995).

Comprehensive and time-series statistics measuring employment, and the economic and social value of coastal tourism and recreation in the United States are not available. Quantitative and reliable data measuring involvement in specific coastal recreation and tourism activities in the United States are limited (and often proprietary). Nonetheless, many small and unconnected studies have been conducted on specific tourism topics and destinations in the coastal zone.

Several boating and fishing statistics provide some idea of the economic and social importance of coastal tourism. In 1998, according to the US Coast Guard, registered boats numbered 12.3 million, with 10 coastal and Great Lakes states (Michigan, California, Florida, Minnesota,

Texas, Wisconsin, New York, Ohio, South Carolina, and Illinois) accounting for nearly half of them (National Marine Manufactures Association, 2000). In 1999, 77.8 million people participated in recreational boating and recreational boaters spent nearly $23 million on related products and services (National Marine Manufacturers Association, 2000). Between 1991 and 1996 the number of Americans (age 16 and older) who participated in recreational saltwater fishing increased 5.6% from 8.9 million to 9.4 million (Cordell *et al*., 1997).

Coastal tourism systems

Coastal tourism systems involve interactions between people and place in destinations that include small communities and villages, self-contained resorts, and cosmopolitan cities. From a sociological perspective, coastal tourism systems have three kinds of actors: (1) *tourism brokers*, (2) *tourism locals*, and (3) *tourists* (Miller and Auyong, 1998a).

A "broker-local-tourist" (BLT) model of a coastal tourism system is displayed in Figure T48 (see, Miller and Auyong, 1991a, 1998b). Tourism brokers consist of persons who in one way or another pay professional attention to tourism. Main subcategories include (1) private sector brokers who are part of the tourism industry, (2) public sector brokers at various levels of government who study, regulate, and plan tourism, and (3) social movement brokers in nongovernmental, nonprofit, and environmental organizations who address tourism issues. Tourism brokers of these and other types do not necessarily agree on the kind of tourism that is "best" for coastal tourism systems. Indeed, broker–broker conflict is as common as cooperation. Tourism locals consist of persons who reside in the general region a coastal tourism destination, but do not derive an income from tourism or engage in its management and regulation. Finally, tourists consist of persons of domestic and international origin who travel for relatively short periods of time for business, recreation, and educational purposes before returning home.

Motivation

From the times polite society planned their Grand Tour itineraries through Europe to Rome and other Italian destinations in the 18th and 19th centuries, all who have participated in or witnessed the growth of tourism have pondered the motivations of those fortunate enough to travel. While there are many psychological, social psychological, and social concepts and frameworks for accounting for tourism, only several are mentioned here.

First and looking to the motives of tourists, Miller and Ditton (1986, p. 11) suggest that the fundamental promise of travel "lies in its promise of *contrast*." In elaboration, these authors show that individual trips and vacations allow opportunities for contrast or personal change along three dimensions. *Recreational tourism* as engaged in by the athlete or escapist has a restorative purpose, and provides for change in the physiological or emotional state of the tourist. *Educational tourism* as pursued by the student has a philosophical purpose and provides a basis for change in the intellectual and artistic understanding of the tourist. *Instrumental tourism* as involving entrepreneurs, reformers, and pilgrims exhibits an economic, political, or religious purpose and leads to change in business, network, or moral opportunities available to the tourist. With this framework, a trip by one tourist to, say, a South Pacific island might be experienced as highly recreational, mildly educational, and not at all instrumental. Those accompanying such a tourist could, of course, experience the trip with different weightings along the three dimensions of touristic contrast.

A second way of considering the motivation of tourists emphasizes their intention to experience a psychological state of *challenge* that Csikszentmihalyi (1975, 1990) terms *flow* or *optimal experience*. When in a state of flow—as one might be when surfing, sailing, scuba diving, or even engaging in stimulating conversation—the tourist has found a fine match between his or her abilities and the physical, intellectual, or social challenge at hand. Flow, then, is a state of mind between boredom and anxiety. More fully:

> [f]low denotes the wholistic sensation present when we act with total involvement. It is the kind of feeling after which one nostalgically says: 'That was fun,' or 'That was enjoyable' (Csikszentmihalyi, 1975, p. 43).

According to Csikszentmihalyi (1975) the flow experience is engaged in for its own sake and is marked by (1) a merging of action and awareness, (2) a centering of attention on a limited stimulus field, (3) a feeling variously described as "loss of ego," "self-forgetfulness," "loss of self-consciousness," and even "transcendence of individuality," and "fusion with the world," (4) a feeling of control over one's actions and the environment, (5) coherent, noncontradictory demands for action, and clear unambiguous feedback, and (6) its autotelic [from Greek *auto* = self and *telos* = goal, purpose] nature.

It is often remarked that people who travel together gradually develop a kind of touristic solidarity. By seeing and doing the same things, by sharing emotions and reactions, by facing a common set of logistic obstacles, and even by jointly creating a set of "story lines" with which they might talk about a trip with others, tourists are brought together through the small and multiple secular rituals of travel. In acknowledging this ritual potential, a third perspective on touristic motivation stresses the passionate *commitment* that some tourists exude in performing their favorite coastal touristic activity.

In a series of sociological studies of amateurs, volunteers, and hobbyists in sports, science, and the arts, Stebbins (1992, p. 3) noted intense levels of personal involvement and high levels of technical competence, and coined the term *serious leisure* to describe commitment that was tantamount to professionalism:

> [S]erious leisure can be defined as the systematic pursuit of an amateur, hobbyist, or volunteer activity that is sufficiently substantial and interesting for the participant to find a career there in the acquisition and expression of its special skills and knowledge.

In the realm of coastal tourism, tourists who pursue serious leisure are omnipresent as evidenced by scuba divers, sailors, whale watchers, amateur naturalists and marine conservationists, and the like.

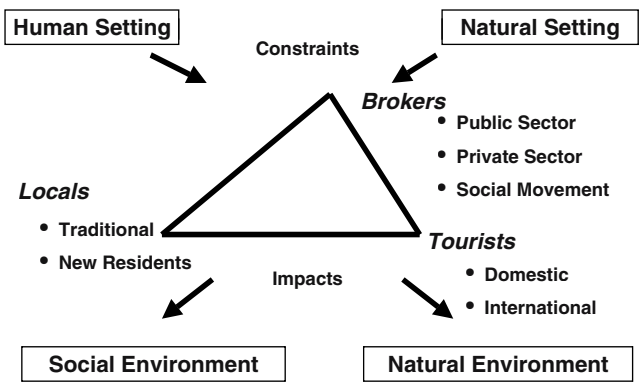

Figure T48 Broker-local-tourist (BLT) model of coastal Tourism (adapted from Miller and Auyong, 1991a, p. 75).

System dynamics

Coastal tourism systems change in size and character over time. To understand and ultimately to predict these changes, and also to plan for desired societal and environmental outcomes, analysis must focus on the behavior of components of the system. In this regard, two processes merit attention.

First, population dynamics of the BLT model should be monitored. It is not unusual for individuals in the system to change statuses. This can occur as, for example, tourists who visit a coastal destination decide to stay and take on a residence, either as a broker of some kind (e.g., as a scuba dive shop entrepreneur or restaurant owner), or as a local (e.g., as a lawyer or teacher). Other transformations in status take place as locals change occupations and become private sector brokers by engaging in a tourism business, or become public sector tourism brokers by finding government employment that concerns tourism. Of course, locals and brokers take on the role of a tourist when they vacation on travel of their own.

Second, power dynamics of the BLT model should be taken into account. Tourism is often examined as a product of the aggregate decisions of individual tourists. The relationship forged between the tourist and the local is accordingly depicted as socioeconomic in nature; tourists and locals interact as "guests" and "hosts" or as consumers and producers. Where power relationships are perceived to exist (e.g., as between First World tourists and Third and Fourth World locals), it is argued that these reveal the colonial and imperialistic leverage tourists have over those whom they visit. From this perspective, tourism

systems are controlled and determined—often in unfortunate ways—by the behavior of tourists.

While there certainly are many instances in which tourists have exercised their influence to selfish and inappropriate advantage in coastal tourism settings, a narrow concentration on the power of tourists can result in analysts missing the power of tourism brokers. As Cheong and Miller (2000) have pointed out, tourists are frequently vulnerable to the power and control of brokers and locals. This is the case when, for example, tourists abide by laws and regulations of public sector brokers, and when they follow the advice and instructions of private sector brokers such as tour guides and travel agents.

Tourism development

Coastal tourism development in the coastal zone has become a constant since the end of World War II. Well-known examples are found on the coastlines and islands of Europe, North and South America, Africa, and Asia (Miller and Auyong, 1991b, 1998a; Conlin and Baum, 1995; Lockhart and Drakakis-Smith, 1997). Tourism development necessarily leads to changes in society and the environment of some kind. While conclusions about the "appropriateness," "success," "inappropriateness," or "failure" of coastal tourism development projects vary to a degree with the political and economic orientations, aesthetic standards, and environmental philosophies of analysts and observers, there is no question about the power of tourism development to quickly effect dramatic change.

From a societal point of view, tourism development promises better quality of life. In theory, poverty is alleviated through the creation of new jobs. Personal income and taxes derived from tourism then fosters better health, education, and other social services. In practice, these goals are only sometimes met. In many cases, failures of political institutions have led to unfair distributions of tourism-generated revenues and to problems of environmental justice.

As noted above, the tourism process provides incentives for locals to become tourism brokers. The lives, then, of both locals and new brokers are changed by coastal development. In some instances changes in the community that are derivative of tourism are undeniably positive. In other cases, the effect is negative. In a study of tourism in a Mexican coastal community, McGoodwin (1986) has identified a *tourist impact syndrome* which identifies the possible cultural costs to tourism system locals as including: (1) loss of political and economic autonomy (including loss of real property), (2) loss of folklore and related cultural institutions, (3) social disorganization (including radical changes in value orientations and in norms regarding social relations; heightened desire for material objects; changes in norms regarding work, sexual behavior, and drug use; promotion of illusory life aspirations; and loss of parental control and of respect for elders), and (4) hostility towards tourists (e.g., thievery, hustling, verbal aggression).

From an environmental perspective, tourism development is often seen to promise degradation of ecosystems (see *Human Impacts on Coasts, q.v.*). This, of course, is unavoidable with the building of airports, ports, road systems, hotels, resorts, and other facilities. This said, tourism development can also provide financial support for the protection of the marine environment and endangered species, as for example, in the creation of underwater and marine parks (*q.v.*) and protected areas.

Over the last decades, there has been growing recognition of the social and environmental trade-offs of tourism and also of the unintended consequences and economic externalities of tourism development (e.g., see Mathieson and Wall, 1982; Edwards, 1988; Pearce, 1989; Clark, 1996; Orams, 1999). With this, coastal tourism development is increasingly designed, debated, and evaluated against the ideal of *sustainable development*. Two prominent statements on this important concept follow:

> Economic growth always brings risk of environmental damage, as it puts increased pressure on environmental resources. But policy makers guided by the concept of *sustainable development* will necessarily work to assure that growing economies remain firmly attached to their ecological roots and that these roots are protected and nurtured so that they may support growth over the long term. (World Commission on Environment and Development, 1987, p. 40)

> (*Sustainable development* means) improving the capacity to convert a constant level of physical resource use to the increased satisfaction of human needs. (World Conservation Union, the United Nations Environment Programme, and the World Wide Fund for Nature, 1990, p. 10)

Toward the resolution of coastal tourism issues

Coastal tourism has been seen to be responsible for both positive and negative impacts to the natural and social environment (see Figure T48). The impacts of coastal tourism on the social environment involve social, cultural, political, and economic issues. On the positive side, coastal tourism can foster community pride, improved quality of life and new job opportunities; on the negative side, coastal tourism can lead to problems of overcrowding, social displacement, and crime. Impacts on the natural environment are often biological, physical, and ecological in nature. Increased protection and conservation of many areas and species has been a positive result of coastal tourism; nevertheless problems of erosion, pollution, and loss of species diversity occur far too frequently. It should not surprise that many coastal tourism issues simultaneously affect the social and natural environment.

The viability of coastal tourism systems and the natural environment in which they occur is very much dependent on human behavior. The resolution of coastal tourism issues can arise from the work of tourism system brokers and also from the individual decisions of locals and tourists.

Of the multiple ways available to society to control human conduct, three broker-driven mechanisms are prominent in the coastal tourism context. These mechanisms are *tourism management*, *tourism planning*, and *tourism education*.

Tourism management, planning, and education are crucial to the sustainable evolution of a touristic destination. It is therefore imperative that each are administered in such a way as to provide for the social and economic needs of the community, while at the same time ensuring that environmentally sensitive areas and ecologically important habitats are identified and excluded from tourism pressure. It is also recognized that tourism management, planning, and education are necessarily not only for scientific purposes and to conserve the environment for the benefit of residents, but also for the protection of long-term investments in tourism infrastructure, attractions, facilities, services, and marketing programs. It deserves to be noted that coastal tourism management, planning, and education programs are often designed and implemented by the same agencies and organizations. This overlap is often desirable and is found in some instances of larger efforts of government to promote integrated coastal zone management (see *Coastal Zone Management, q.v.*; see, also, Clark, 1996; Cicin-Sain and Knecht, 1998).

The manner in which a country, region, or community chooses to conduct touristic management, planning, and education activities is framed by societal (political, economic, etc.) and environmental (geography, natural resource, etc.) constraints. In the long run, the wisest course of action is to balance environmental, business, management, and social concerns so that tourism development is recognized as a potentially dangerous, but also potentially valuable and responsible course of action.

Coastal tourism management

Very generally, management concerns the actions of an executive decision-making entity in accordance with overarching goals of the larger enterprise in which it is housed. Although resorts, hotels, restaurants, transportation businesses, and many other firms in the coastal tourism sector do make decisions in strategic and professional ways, management, as the term is employed here, points to work engaged in or sponsored by public sector brokers to address problems and opportunities of coastal tourism.

Throughout the world, coastal tourism is managed by regulatory entities in accordance with the structure and procedures of the prevailing political system. In the United States, coastal tourism management is undertaken by federal agencies, and by regional, state, and local authorities at other levels of government. These executive entities rely on the two other branches of government for guidance. Thus, legislatures provide the mandate for tourism management in the design of laws, and the judicial branch of government interprets law as it applies to regulatory actions and the behavior of constituencies and tourists.

In the United States the growing importance of coastal tourism to the Nation was communicated to the general public with publication of *Year of the Ocean: Discussion Papers* in 1998. In a major chapter in this document, "Coastal Recreation and Tourism" is defined as embracing:

> the full range of tourism, leisure, and recreationally oriented activities that take place in the coastal zone and the offshore waters. These include coastal tourism development (hotels, resorts, restaurants, food industry, vacation homes, second homes, *etc.*), and the infrastructure supporting coastal development (retail businesses, marinas, fishing tackle stores, dive shops, fishing piers, recreational

> boating harbors, beaches, recreational fishing facilities, and the like). Also included is ecotourism and recreational activities such as recreational boating, cruises, swimming, recreational fishing, snorkeling, and diving. Coastal tourism and recreation … likewise includes the public and private programs affecting all the aforementioned activities (US Federal Agencies, 1998, p. F-2).

In stressing the need to coordinate federal coastal tourism policies and programs, the chapter discusses governmental management and planning, management of clean water, and healthy coastal ecosystems, management of coastal hazards, and beach restoration programs.

At the federal level, the United States does not have a "Department of Tourism" with regulatory authority. Instead, touristic, recreational, and leisure activities are regulated by a host of executive agencies in accordance with a suite of legal mandates. Prominent in the control of coastal tourism and recreation are the National Park Service, the National Marine Fisheries Service, the Fish and Wildlife Service, and the US Army Corps of Engineers (Table T14). These agencies oversee many programs that conserve and protect natural resources and the environment while also fostering public access to the shore and to the marine environment.

At the state-level and at the local-level of government, coastal tourism is managed through the regulatory efforts of a variety of departments (e.g., departments of fish and wildlife, and park departments) with mandates that resemble those of federal counterparts. It is also common for city governments to cooperate with chambers of commerce in the development of infrastructural and business practice standards.

In practice, then, coastal tourism management is conducted by public sector brokers at all levels of government, by private sector brokers in businesses, and by some NGOs and environmental and social movement brokers. An array of tourism management tools (e.g., licensing regulations, zoning rules, tourist quotas, time and areas restrictions, and carrying capacity and limits of acceptable change regulations) have been used successfully throughout the Pacific, in the Caribbean, in the Atlantic and elsewhere (see Pearce, 1989; Miller and Auyong, 1991b, 1998; Conlin and Baum, 1995; Lockhart and Drakakis-Smith, 1997; Orams, 1999). The concepts of *zoning* and *carrying capacity* deserve further attention due to their particular applicability to the management of tourism in coastal areas.

Two very significant parks utilize zoning as a means of tourism management. The Great Barrier Reef Marine Park in Australia is a multiple-use protected area. With zoning, conflicting uses are physically separated. The range of protection in the park varies from virtually no protection to zones where human activity is conditionally permitted. The adoption of this zoning scheme allows the park authority, in association with interested members of the public and with other agencies, to develop and apply a tourism strategy for the entire Great Barrier Reef Marine Park. Zoning ensures that the Reef will not become overpopulated with tourist and other structures, but also allows for careful development in areas which are suitable for that purpose. The Galapagos Islands National Park in Ecuador also employs zoning strategies. The park is effectively managed with intensive use, extensive use, and scientific use (off limits to all but a few visitors) zones.

Table T14 US federal statutes and actions influencing coastal tourism (selected)

- Antiquities Act (1906)
- National Park Service Organic Act (1916)
- Fish and Wildlife Coordination Act (1934)
- The Wilderness Act (1964)
- National Sea Grant College Program Act (1966)
- National Historic Preservation Act (1966)
- Executive Reorganization Plan Number 4 and Executive Order 11564 establishing the National Oceanic and Atmospheric Administration (1970)
- Coastal Zone Management Act (1972)
- National Marine Sanctuaries Act (1972)
- Fishery Conservation and Management Act (1976; renamed Magnuson-Stevens Fishery Conservation and Management Act)
- Archaeological Resources Protection Act (1979)
- Fish and Wildlife Conservation Act (1980)
- Presidential Proclamation 5030 establishing a 200-mile Exclusive Economic Zone (1983)
- The Recreational Boating Safety Act (1986)
- Abandoned Shipwreck Act (1987)
- Executive Order 13158 establishing a national system of Marine Protected Areas (2000)

Carrying capacity (*q.v.*) regulations illustrate the "precautionary principal" method of natural resource management and are highly regarded by practitioners of tourism management. Coastal tourism managers who seek to determine the appropriate level of use that can be sustained by the natural resources of an area are well aware that carrying capacities and use-intensity limits of tourism destinations are dynamic, and depend greatly on the biological and ecological processes of natural resources.

Coastal area carrying capacity can be evaluated in four ways (Sowman, 1987). Physical carrying capacity is concerned with the maximum number of "use units" (e.g., people, vehicles, boats) which can be physically accommodated in an area. Economic carrying capacity relates to situations where a resource is simultaneously utilized for outdoor recreation and economic activity. Ecological carrying capacity (sometimes referred to also as physical, bio-physical, or environmental carrying capacity) is concerned with the maximum level of recreational use that can be accommodated by an area or an ecosystem before an unacceptable or irreversible decline in ecological values occur. Social carrying capacity (also referred to as perceptual, psychological, or behavioral capacity) is concerned with the visitor's perception of the presence (or absence) of others simultaneously utilizing the resource of an area. This concept is concerned with the effect of crowding on the enjoyment and appreciation of the recreation site or experience.

The *limits of acceptable change* (LAC) framework developed by Stankey *et al*. (1985) enables managers to move beyond calculation of carrying capacity figures to address actions needed for management goals. This approach concentrates on establishing measurable limits to human-induced changes in the natural and social setting of parks and protected areas, and on identifying appropriate management strategies to maintain and/or restore desired conditions (Stankey *et al*., 1985). Knowledge of the natural (physical, biological) setting is combined with knowledge of the human (social, political) setting in order to define appropriate future conditions.

The LAC method employs nine steps as follows: (1) identification of area concerns and issues, (2) definition and description of opportunity classes, (3) selection of indicators of resource and social conditions, (4) inventory of resource and social conditions, (5) specification of standards for resource and social indicators, (6) identification of alternative opportunity class allocations, (7) identification of management actions for each alternative, (8) evaluation and selection of an alternative, and (9) implementation of actions and monitoring of conditions. To date, the LAC system has proved to be a valuable tourism management tool in several wilderness areas in the United States and has direct applications to coastal areas as well.

Coastal tourism planning

Planning, broadly conceived, entails the consideration of a range of actions likely to contribute to the attainment of organizational goals. In some instances, overarching goals are well known in advance and planning professionals concentrate on the means that will ensure these ends. In other situations, the determination of goals requires prolonged deliberation.

Coastal tourism planning is often integrated with other resource analyses in the development of coastal area or region. Planners take into account not only visitation rates and statistics, but also the fact that tourists increasingly insist that destinations be high-quality and pollution-free, as well as inherently interesting. Therefore, it is in both the public and private sector brokers' interest to implement a planning strategy for tourism. The goals and policies of government agencies and businesses are, however, frequently different from one other and may even be in direct conflict. To minimize and even prevent disruptions and loss of time, communication between tourism brokers is crucial. Planning also leads to equitable distributions of coastal tourism benefits.

The success or failure of a tourism project frequently hinges on the conditions of natural amenities in the surrounding environment. This is especially true for tropical environments found, for example, on Pacific and Caribbean islands. Parks and natural resource areas, scenic vistas, archaeological and historic sites, and coral reefs are all touted tourism attractions. Marketing strategies for coastal, marine, and island tourism especially promote destinations for being close to white sand beaches. However, development of permanent structures for tourism near beaches often exacerbates beach erosion, property damage, and requires construction of shore protection structures. If touristic facilities are to be sited near beaches, proper planning is essential for the protection of the coastal zone and private property.

In many numerous coastal and island states located in the Mediterranean, Caribbean, and the Pacific where tourism is a major economic force, major national-level departments of government shape coastal tourism through the design of investment incentives and international joint venture opportunities. In nations such as Mexico and Costa Rica, these activities are linked to the preparation of strategic tourism plans.

In the United States—and with notable exceptions such as those provided by the National Park Service—very little coastal tourism planning takes place in the federal government. At the state-level, it is commonplace for departments of tourism to promote tourism. While many states have experienced great success in attracting tourists with advertising strategies, most state departments of tourism have yet to augment the marketing of tourism with the monitoring and assessment of coastal tourism's effects on the environment and quality of life. At the local-level, many city governments have utilized their planning departments to recommend approaches to issues having to do with public use of the coastline and natural resources, the revitalization of waterfronts, and zoning appropriate to resort and marina development.

Within the private sector, coastal tourism planning is an established professional specialty. Firms of all sizes develop coastal tourism plans tailored by expert consultants to the needs of developer clients. Increasingly, social movement brokers are being seen to engage in professional coastal tourism planning.

Coastal tourism planning falls into two main categories, depending on whether the project in question is driven by a preservation or a development ethic. Preservation goals predominate in the planning of recreational areas, in national park and marine protected area planning, and in planning that is part of natural resource management. The development framework has found application in seaside resort and theme park planning, in condominium time-share planning, and in varieties of coastal city planning. There are many examples worldwide of coastal tourism zones, replete with both preservation and development projects, that extend from major cities. The Costa Brava in Spain, the French Riviera, the Yucatan Peninsula, the East Coast of Australia, and the coastlines of the United States and many Polynesian islands illustrate mixed planning.

Landscape architecture and urban planning are important in shaping coastal tourism. Both fields have public and private applications, and design and planning aspects. Both tailor products and services to preservation and development goals and, accordingly, address biophysical and social and economic objectives.

Landscape architects design parks and gardens, resort and hotel facilities, marinas and waterfronts, plazas and squares, and transportation corridors providing access to coastal touristic destinations. Urban planners design circulation facilities, city districts and spaces, and produce master planning and site design products.

Planning activities and products of landscape architects include resource management plans, environmental analyses, and multidisciplinary feasibility studies, and needs assessment and community structure plans. In overlapping ways, urban planners produce tourism policy plans, functional plans, and environmental assessments.

Because coastal tourism planning efforts are attuned to local conditions, constituencies, and financial constraints, there is no single planning process for guaranteeing success. This said, most professional planning endeavors share a general structure. Grenier *et al*. (1993) suggest a three-phase tourism planning process. With this, a first "Front-end Planning" phase encompasses scoping (entailing a statement of project philosophy, pre-assessments of key issues and themes, and formulation of objectives) and research (involving data collection and analyses supporting cultural, institutional, and environmental profiles; site reconnaissance; eco-determinant mapping; and analyses of constraints and opportunities). A second "Project Planning" phase is focused on refinement of project objectives, design and evaluation of alternative development plan concepts, and selection and approval of the preferred development plan concept. A third and final "Project Management" phase concerns activities of implementation, monitoring and evaluation, and refinement.

In summary, coastal tourism planning has been fostered by public sector brokers at all governmental levels, by consultants among other private sector brokers, and by an impressive range of nongovernmental and environmental organizations in roles these have taken on as social movement tourism brokers. Coastal tourism planning practitioners have developed an array of planning methodologies (e.g., comprehensive land-use planning, integrated coastal zone planning, and strategic and special use planning) and have utilized these throughout the world, in many instances by cooperating with tourism brokers with management expertise (see, Gunn, 1988; Pearce, 1989; Miller and Auyong, 1991a, 1998a; Conlin and Baum, 1995; Lockhart and Drakakis-Smith, 1997; Orams, 1999; Hadley, 2001).

Coastal tourism education

The two mechanisms for the control of human behavior in coastal tourism systems discussed above—management and planning—are similar to one another in that the tourism experts who analyze coastal tourism situations channel their recommendations upward to regulatory and planning authorities. These tourism brokers then implement policies and plans downward, influencing tourism businesses, tourists, and locals.

A third mechanism concerns coastal tourism education and communication. Although education about coastal science and environmental issues is effectively transmitted in classrooms, discussion here focuses on education and outreach in nontraditional settings and how people learn through the experience of being tourists or learn in the course of daily life. Guided tours, museums, brochures, public lectures, newspapers, and signage are but a few of the devices that figure importantly in the educational processes linked to coastal tourism.

In a manner of speaking, tourism education contrasts with management and planning in that the first clients of analysts are not managers and planners in positions of authority, but tourists and locals. Whereas managers achieve goals through policies and regulations and planners depend on plans, coastal tourism educators succeed when people take personal initiative to change their own behavior because they have been taught something. Tourism education, then, is a process in which analyst brokers direct their ideas outward to people involved in tourism. Tourism educators and communicators do not evaluate success or failure at attaining their goals with studies of "enforcement" or "compliance." This is so because successful education motivates individuals by persuasion, not coercion.

By definition and referring to Figure T48, coastal tourism educators are public sector, private sector, and social movement brokers. These brokers design products and strategies to educate people and through this to change human behavior in coastal tourism systems. While educator brokers seek to impart their message to tourists and to locals, they also educate one another as, for example, when a nongovernmental organization (NGO) educates public sector and private sector brokers.

Efforts to resolve problems and opportunities of coastal tourism through education are steadily growing throughout the world. Tourism brokers who are advancing this promising agenda are benefiting from the work of educators who have focused on environmental and sustainability issues. Monroe (1999) has characterized successful environmental education and communication projects as having features that allow for: (1) empowerment of local communities and use of their expertise, (2) attention to scientific, social, economic, political, and cultural topics, (3) identification of a variety of stakeholders and integration of them into the process, (4) advancement of an environmental ethic as well as assistance to residents in developing decision-making skills, (5) development of a gender component, (6) flexibility in project design (including realistic timetables), and (7) project evaluation.

Coastal tourism brokers (e.g., those in government or in NGOs) that provide international aid in developing and poverty-plagued states have also benefited from the cross-cultural advice of Brazilian educator and philosopher, Paulo Freire. Freire has contended that the education process has for too long been regarded as a "delivery service" from the scientific and technological elite of the Western World to those suffering in the Third World. Freire's (1999, p. 61, emphasis added) solution lies in education projects that emphasize collaborations between experts and clients at all stages of the process:

> Through dialogue, the teacher-of-the-students and students-of-the-teacher cease to exist and a new term emerges: teacher-student with student-teachers. The teacher is no longer merely the-one-who-teaches, but one who is himself taught in dialogue with the students, who in turn while being taught also teach. *They become jointly responsible for a process in which all learn*.

Few would disagree with the proposition that coastal tourism education has great potential to enhance the quality of tourism for tourists and locals, and to also protect the environment through responsible human conduct. The importance of education (and of overlapping fields such as communication, journalism, and environmental and science reporting by the media) is recognized by virtually all marine scientists and researchers (see Pearce, 1989; Miller and Auyong, 1991b, 1998; Conlin and Baum, 1995; Lockhart and Drakakis-Smith, 1997; Orams, 1999). Still, many opportunities to integrate coastal tourism education with the mechanisms of management and planning have been missed.

Challenges ahead

Over the last several centuries, the world's coastlines have been substantially transformed to support recreational and touristic pursuits. In some

cases, coastal tourism dominates the skyline. In others, tourism is one of many industries. As coastlines become more populated and accessible, it is ever more clear that, however, beneficial coastal tourism is to the tourist, it is neither a panacea that will invigorate any local economy, nor a pollution that will necessarily ruin environments and corrupt cultural traditions and values. Coastal tourism is a process amenable to management, planning, and education. Sustainable coastal tourism obliges humanity to have respect for other life forms and the environment, while it affords opportunities for people to learn, recreate, and reach their potential as individuals through travel.

Because the stakes are high and because mistakes can be virtually irreversible, societal resolution of pressing tourism and coastal development issues requires imagination as well as sustained scientific and policy attention. Work to be done falls in the areas of research, and tourism broker and individual responsibility.

Tourism research

Researchers in government, academe, and in the private and social movement sectors constitute a first group of practitioners whose work induces positive change in coastal tourism systems. Fundamental questions about physical, biological, ecological, social, cultural, economic, demographic, and political processes of coastal tourism are posed and answered in assessments, impact statements, profiles, and other products of natural, biological, and social scientists. With reference to the condition of the environment and society, the possibilities of coastal tourism development raise not only the question "What is?" but also questions about "What is ethical?," "What is fair?," and "What is beautiful?" As a result, analyses by professionals with backgrounds in the humanities and arts have proven to be useful in complementing those of scientists.

The need to formally study tourism is recognized more than ever in academe. Tourism research methods are under continual development in such fields as public affairs, business and marketing, architecture, urban planning and design, political science, sociology, geography, cultural anthropology, marine affairs, and environmental studies (e.g., see Gunn, 1979; Murphy, 1985; Ritchie and Goeldner, 1987; McIntosh and Goeldner, 1990).

Tourism broker responsibilities

A second professional group made up of the different types of coastal tourism brokers will be counted upon heavily in the future to cooperate with one another. This can occur, for example, when investors and developers in the private sector coordinate goals and activities with those of government agencies and NGOs to make sustainable tourism a reality. Another kind of cooperation calls for tourism brokers to work effectively with government, business, and nongovernmental organizations in other economic sectors. Better understandings of tourism-fishery interactions, tourism-aquaculture interactions, and tourism-ocean shipping interactions can lead to an improvement on single-sector governance with partially (or, under ideal conditions, fully) integrated coastal management.

In the aftermath of the terrorism attack on the World Trade Center in 2001, the responsibilities of tourism brokers have been enlarged. Brokers now must function not only as stewards of the coastal environment, businessmen, and representatives of constituencies, but also as protectors of residential and traveling publics.

Uncertainties generated by the terrorism of 2001 will change the ways in which coastal tourism is conducted in the United States and elsewhere. It has long been known that too much tourism can be bad by when it leads to degraded ecosystems and undesirable changes in quality of life. Now it is apparent that too little tourism can put entire coastal economies at risk. Declines in coastal tourism can create serious social problems in the same way declines in fishery resources can threaten livelihoods. Ultimately, coastal tourism and recreation destinations negatively affected by security-related changes in itineraries will become sustainable only to the extent brokers make tourism safe.

Individual responsibilities

The discussion above has concerned the proactive roles researchers and brokers can play in promoting sustainable tourism and coastal development. To this must be added a comment about the personal responsibilities of tourists and locals to contribute toward sustainability in the coastal tourism systems which they visit or in which they live.

To a certain extent, the social role of the ethical tourist can be formulated to resemble that of the good citizen. Good citizens learn from their families and schools to reach their potential in society while knowing how to behave in socially appropriate ways. Using this template, tourists would be expected to behave in ecologically and culturally appropriate ways in the course of their domestic and international travel. Ecotourism and ethnic tourism are two forms of tourism that have emerged to stress this self-conscious orientation. Many tourism brokers in business, in government, and in non-governmental organizations are now promoting the development of "best practices" and "tourism guidelines" to this end.

It is obvious that there are many benefits of coastal travel that accrue to the tourist. These are found in recreational, aesthetic, and educational activities. In exchange, the ethical tourist will strive to behave in a culturally and environmentally responsible manner. As this occurs, locals are given an added incentive to orient their conduct to the same ends. Improvements in the behavior of tourists and locals toward one another and toward the coastal environment will assist tourism providers and managers as they do their part to monitor and control tourism, and improve the tourism experience for all involved.

Concluding remarks

Coastal tourism has demonstrated its considerable power to influence the fundamental configurations of coastlines and the social structures these support. Coastal tourism is sometimes found to be unfortunate in every respect. Coastal tourism can, however, be designed to improve the lives of tourists and those who are part of the tourism industry, conserve natural resources and protect the environment, and not offend locals. For this to occur, coastal tourism brokers—in government, business, and non-governmental organizations—will need to cooperate to insure that tourism is sustainable and safe.

It will also be necessary for tourists and locals to adopt "best practices" that underwrite cross-cultural communication and respect for the environment. In the eyes of many, it is time for all to abide by a coastal system *tourism ethic*. Such an ethic might reasonably incorporate Aldo Leopold's (1949, p. 224–225) famous caution about natural resource use based solely on economic self-interest:

> [a] thing is right when it tends to preserve the integrity, stability, and beauty of the biotic community. It is wrong when it tends otherwise.

Through the implementation of responsible management, planning, and education policies—together with the diffusion of a tourism ethic—tourism and coastal development can be shaped to reflect the best tendencies of humanity.

Marc L. Miller and Nina P. Hadley

Bibliography

Cheong, S.-M., and Miller, M.L., 2000. Power and tourism: a Foucauldian observation. *Annals of Tourism Research*, **27**(2): 371–390.

Cicin-Sain, B., and Knecht, R.W., 1998. *Integrated Coastal and Ocean Management: Concepts and Principles*. Washington, DC: Island Press. (with the assistance of D. Jang and G.W. Fisk).

Clark, J., 1996. *Coastal Zone Management Handbook*. Boca Raton, FL: CRC Press.

Conlin, M.V., and Baum, T. (eds.), 1995. *Island Tourism: Management Principles and Practice*. New York: John Wiley & Sons.

Corbin, A., 1994 [1988]. *The Lure of the Sea: The Discovery of the Seaside 1750–1840*. (translated by J. Phelps) New York: Penguin Books.

Cordell, H.K., Teasley, J., Super, G., Bergstrom, J.C., and McDonald, B., 1997. *Outdoor Recreation in the United States: Results from the National Survey on Recreation and the Environment*. Athens, GA: US Forest Service and the Department of Agriculture and Applied Economics, University of Georgia.

Csikszentmihalyi, M., 1975. Play and intrinsic rewards. *Journal of Humanistic Psychology*, **15**(3): 41–63.

Csikszentmihalyi, M., 1990. *Flow: The Psychology of Optimal Experience*. New York: Harper Perennial.

Edwards, F., (ed.), 1988. *Environmentally Sound Tourism in the Caribbean*. Calgary: The University of Calgary Press.

Environmental Protection Agency (EPA), 1995. *National Demand for Water Based Recreation*. Washington, DC: EPA.

Freire, P., 1999 [1970]. *Pedagogy of the Oppressed*, Revised edn. New York: Continuum.

Godsman, J., 2000. *2001 Outlook for the Cruise Industry*. White paper presented at the 2000 TIA [Travel Industry Association] Marketing Outlook Forum. (October 25–28, 2000) New York: *National Geographic Traveler*.
Grenier, D., Kaae, B.C., Miller, M.L., and Mobley, R.W., 1993. Ecotourism, landscape architecture and urban planning. *Landscape and Urban Planning*, **25**: 1–16.
Gunn, C.A., 1979. *Tourism Planning* (2nd edition). New York: Crane, Russak.
Gunn, C.A., 1988. *Vacationscape: Designing Tourist Regions*. New York: Van Nostrand Reinhold.
Hadley, N., 2001. Cooperative tourism management of midway atoll national wildlife refuge: planning, assessment, and strategy. *Tourism*, **49**(3): 189–202.
Hern, A., 1967. *The Seaside Holiday: The History of the English Seaside Resort*. London: The Cresset Press.
Houston, J.R., 1995. Beach nourishment. *Coastal Forum, Shore and Beach*, **64**(1): 21–24.
Houston, J.R., 1996. International tourism and US beaches. *Coastal Forum, Shore and Beach*, **64**(2): 3–4.
Leopold, A., 1949. *A Sand County Almanac and Sketches Here and There*. New York: Oxford University Press.
Lockhart, D.G., and Drakakis-Smith, D. (eds.), 1997. *Island Tourism: Trends and Prospects*. New York: Pinter.
Manning-Sanders, R., 1951. *Seaside England*. London: B.T. Batsford.
Mathieson, A., and Wall, G., 1982. *Tourism: Economic, Physical, and Social Impacts*. New York: John Wiley & Sons.
McGoodwin, J.R., 1986. The tourism-impact syndrome in developing coastal communities: a Mexican case. *Coastal Zone Management Journal*, **14**(1/2): 131–146.
McIntosh, R.W., and Goeldner, C.R., 1990. *Tourism: Principles, Practices, Philosophies*, 6th edn. New York: John Wiley & Sons.
Miller, M.L., and Auyong, J. 1991a. Coastal zone tourism: a potent force affecting environment and society. *Marine Policy*, **15**: 75–99.
Miller, M.L., and Auyong, J. (eds.) 1991b. *Proceedings of the 1990 Congress on Coastal and Marine Tourism: A Symposium and Workshop on Balancing Conservation and Economic Development (Volumes I and II)*. Newport, OR: National Coastal Resources Research and Development Institute.
Miller, M.L., and Auyong, J. (eds.), 1998a. *Proceedings of the 1996 World Congress on Coastal and Marine Tourism: Experiences in Management and Development*. Seattle: Washington Sea Grant Program and the School of Marine Affairs, University of Washington and Oregon Sea Grant College Program, Oregon State University.
Miller, M.L., and Auyong, J., 1998b. Remarks on tourism terminologies: Anti-tourism, mass tourism, and alternative tourism. In Miller, M.L., and Auyong, J. (eds.), *Proceedings of the 1996 World Congress on Coastal and Marine Tourism: Experiences in Management and Development*. Washington Sea Grant Program and the School of Marine Affairs, University of Washington and Oregon Sea Grant College Program, Oregon State University, pp. 1–24.
Miller, M.L., and Ditton, R., 1986. Travel, tourism, and marine affairs. *Coastal Zone Management Journal*, **14**(1/2): 1–19.
Monroe, M.C. (ed.), 1999. *What Works: A Guide to Environment Education and Communication Projects for Practitioners and Donors*. Gabriola Island, British Columbia: New Society Publishers.
Murphy, P.E., 1985. *Tourism: A Community Approach*. New York: Methuen.
National Marine Manufacturers Association, 2000. *Boating 2000: Facts and Figures at a Glance*. Chicago, IL: NMMA.
Orams, M. 1999. *Marine Tourism: Development, Impacts and Management*. New York: Routledge.
Pearce, D. 1989. *Tourist Development*, 2nd edn. New York: John Wiley & Sons.
Ritchie, J.R., and Goeldner, C.R., (eds.), 1987. *Travel, Tourism, and Hospitality Research: A Handbook for Managers and Researchers*. New York: John Wiley & Sons.
Sowman, M., 1987. A procedure for assessing recreational carrying capacity for coastal resort areas. *Landscape and Urban Planning*, **14**(4): 331–344.
Stankey, G., Cole, D., Lucas, R., Peterson, M., and Fissell, S., 1985. The Limits of Acceptable Change (LAC) system for wilderness planning. Seattle: US Department of Agriculture, *Technical Report INT-176*.
Stebbins, R.A., 1992. *Amateurs, Professionals, and Serious Leisure*. Montreal: McGill-Queen's University Press.
Travel Industry Association of America (TIA), 1998. *Travel and Tourism Congressional District Economic Impact Study*. Washington, DC: TIA and US Department of Commerce.
Travel Industry Association of America (TIA), 2001. *Impact of Travel on State Economies 1999*. Washington, DC: TIA.
United Nations Environment Programme (UNEP), 1992. Sustainable tourism development. *UNEP Industry and Environment*, **15**(3–4): 1–96.
US Federal Agencies (with ocean-related programs), 1998. *Year of the Ocean Discussion* Papers. Washington, DC: US Department of Commerce (NOAA).
US Travel and Tourism Administration, 1994. *Impact of International Visitor Spending On State Economies*. Washington, DC: US Department of Commerce.
Volgenau, G., 2000. The Plog survey: Our favorite places. *The Seattle Times*. Travel Section K, pg. 6 (Sunday, 16 January).
Waters, S. (ed.), 1997. *Travel Industry World Yearbook—The Big Picture 1996–97*, Vol. 40. Spencertown, NY: Travel Industry Publishing Inc.
Waters, S. (ed.), 2001. *Travel Industry World Yearbook—The Big Picture 2001,* Vol. 44. Spencertown, NY: Travel Industry Publishing Inc.
World Commission on Environment and Development, 1987. *Our Common Future ("The Brundtland Report")*. New York: Oxford University Press.
World Conservation Union (IUCN), the United Nations Environment Programme (UNEP), and the World Wide Fund for Nature (WWF), 1990. *Caring for the World: A Strategy for Sustainability*. (Second Draft). Gland: IUCN.
World Tourism Organization (WTO), 1996. *Compendium of Travel 1989–1996*. Madrid: WTO.
World Tourism Organization (WTO), 2001. *Tourism Highlights 2001*. Madrid: WTO.
World Travel and Tourism Council (WTTC), 1995. Agenda 21 for the Travel and Tourism Industry: Towards Environmentally Sustainable Development. London: WTTC, *Progress Report No. 1.*

Cross-references

Aquaculture
Beach Use and Behaviors
Carrying Capacity in Coastal Areas
Coastal Zone Management
Demography of Coastal Populations
Economic Value of Beaches
Environmental Quality
Human Impacts on Coasts
Marine Parks
Surfing
Tourism, Criteria for Coastal Sites

TOURISM, CRITERIA FOR COASTAL SITES

Historically, seaside resorts date back to Roman times with a string of resorts along the Campanian littoral on the northern shore of the Bay of Naples (Turner and Ash, 1976, p. 24). The modern seaside resorts had their origin in England and their early growth was attributed to the therapeutic value of seawater drinking and bathing. From the mid-19th century, the era of railway saw the rapid growth of more seaside resorts, spreading to western Europe (Romeril, 1984; Walton, 1997). Partly as the result of the railway ending at about right angles to the coast, the European coastal resort has a basic T-shaped morphology, although factors varied. Usually, coastal resort morphology is dependent on site characteristics, tourist elements, and other urban functions (Pearce, 1995, pp. 136–140; Nordstrom, 2000, pp. 10–13).

This entry is concerned with such physical site factors as the "emphasis … on aspects of the physical implications of site selection such as coastal erosion rather than resort form … underlies the potential which this approach has to complement the more traditional resort morphologies" (Pearce, 1995, p. 137). This approach is increasingly significant, as developing countries seek out appropriate beaches and islands for tourism development. On a worldwide scale, coastal tourism (see *Tourism and Coastal Development*) in the traditional Mediterranean area is complemented by the Caribbean area, South Pacific area, and Southeast Asia. Islands, especially *small islands (q.v.)*, are actively sought for tourism development. To the usual three "Ss" (sun, sea, and sand) for coastal tourism, one could add two more "Ss" (sunrise and sunset) if one were on a small island.

Coastal site criteria

Coastal tourism development involves the identification of a suitable site, developing the site by clearing, and providing access, accommodation, recreation facilities, and services for the tourists (Ahmad, 1982). Site criteria for coastal tourism are more than just association with white sand beaches and coral reefs. An analysis of the site criteria includes a wide variety of physical and other factors such as land-use, ownership, etc. The objective is to assess the site opportunities and constraints which have a significant implication for the resort entrance, backdrop, views, beaches and swimming areas, buildable area, vegetation, boating tours, fishing and diving opportunities, etc. In addition, various site planning considerations and development standards, including architectural, landscaping, and engineering design, have to be considered (Inskeep, 1991, pp. 303–335).

Planners and architects usually acknowledge that two powerful forces make coastal tourism distinctive and have a bearing on site criteria. The first is the special amalgam where land meets the sea and the coastal site is a junction of landscape and seascape. The second is the linear character of the coast in which the natural resources for tourism are arranged in a linear fashion (Gunn, 1988, p. 87).

The linearity of the coast presents special challenges for planning and tourism design. Generally, four zones with different characteristics can be identified with the more important criteria and implications for tourism development given in Table T15 (Gunn, 1988, p. 88; Mieczkowski, 1990, pp. 243–246). On the seaward side is the marine zone or neretic zone which is the ecological zone from the continental shelf to the beach. This area contains the marine life, reefs, and sandbars and is suitable for a number of marine-based activities. The beach consisting of the foreshore and backshore is the most important of the four zones. It is used for many activities, especially if it is sufficiently wide and sandy. More specific requirements identified for beach resort development in this zone include beach protection and beach capacities (Baud-Bovy and Lawson, 1998, pp. 71–72). The third zone is the shoreland which includes the dunes and is the area for camping, hiking, and other accommodation, food, shopping, and other service businesses. Its serves as the visual linkage between land and sea. The most landward zone is the vicinage or hinterland which provides the setting for tourist business and vacation homes. It is often the zone of population and supporting services and is enhanced by variations in topography and vegetation. Its nearness and access to the sea is more important than the visual linkage.

An example of the application of the linear zones is the planning of development for southern Thai beaches facing the Andaman Sea (Tourism Authority of Thailand, 1989). Three zones for development with 12 categories of landuse have been identified. The first two zones have specific widths. The beachfront area extends 300 m away from the beach; the interior area is 700 m wide and the hinterland is landward of the interior area.

As the coast is a basic component in coastal tourism, any potential resort site can be assessed by an initial understanding of its coastal geomorphology. As coasts differ widely, each type of site has implications for coastal tourism. For example, the potential of a specific coastal type or landform, such as, coral reef, coastal dune, sand spit, river-mouth barrier, rocky headland, can be known. Also, specific advantages and disadvantages of each landform, coastal type, or ecosystem have their influence on the choice of resort sites and also influence the pattern and development of resorts. Coastal geomorphology also helps to reduce negative impacts, protect valuable habitats and provide valuable information for subsequent alteration to the coastal environment, for example, changes to the drainage and water bodies (Wong, 1999, 2000).

More important and often underestimated, geomorphology also takes note of the seasonal factor which can have a marked impact on the coast. For example, in Southeast Asia and Indian Ocean islands, a strong seasonality prevails in the coastal environment. Beaches undergo accretion/erosion cycles and during the onshore wind season, wave action can reach a higher level or further inland. With reversals in wind, wave action and currents, sand movement varies in the offshore–onshore

Table T15 Major criteria in coastal zones for tourism development

Zone[a]	Factor	Comments
Sub-tidal to offshore (Marine or neretic zone)	• Climate • Waves • Tides • Currents • Water temperature; clarity of water • Biodiversity, e.g., marine life, corals, seaweeds	• Physical conditions determine type, extent and seasonality of many recreational activities, e.g., swimming, water skiing, surfing, sailing, boating, travel to nearby island • Biodiversity presents additional attractions for recreational use, e.g., snorkeling, scuba diving, fishing • Free of pollution
Intertidal-nearshore (Beach)	• Beaches: width, gradient, material size, color • Risks from tidal movements • Potential erosion • Public access • Shore platforms: width, access • Wetlands: extent, access	• Physical properties of beach and coast influence type and extent of recreational activities • Beach capacity as useful management tool • Soft protection measures are preferred if need arises • Environmental guidelines, especially for wetlands
Backshore (Shoreland)	• Area • Views • Geomorphology (cliffs, dunes, wetlands) • Coastal vegetation • Microclimate • Scope for improvement • Access, e.g., roads	• Location of various tourist accommodation and service businesses • Proper setback, conditions for use • Preserve view (visual linkage is important) • Maximize specific advantages of geomorphological features • Dunes normally preserved as defense line and for selective uses • Good views from cliffs, headlands • Phased development; minimize degradation • Improvement, e.g., drainage
Onshore (Hinterland or vicinage)	• Topography • Vegetation • Existing development, e.g., population, supporting services	• Provides setting or backdrop • Separate planning zone • Access to sea is important

[a] Terms in parentheses are used by Gunn, 1988 and Mieczkowski, 1990.
Sources: Compiled from Baud-Bovy and Lawson, 1998; Gunn, 1988; Mieczkowski, 1990; Viles and Spencer, 1995; Wong, 1991.

direction and alongshore direction. The seasonal site features include beach morphological changes, a backshore with two berms, nearshore topographic changes, changing stream mouths, flooding, shifts in beach vegetation belts, etc. In particular, the analysis of the seasonal factor provides some idea of the potential hazards in various coastal zones. The seasonality arising from waves, wind, and tides, and the potential erosion and pollution are among the coastal hazards considered in environmental planning for site development (Beer, 1990, pp. 63–64).

Besides geomorphological criteria associated with tourist sites, other criteria in planning and development of resorts also have a strong physical base. These include adequate access, *setbacks* (*q.v.*), and EIA (environment impact assessment) before construction and carrying capacity. Pearce and Kirk (1986) have suggested specific types of carrying capacity that are closely associated with the linear zones of the coast. One recent development has been the application of a single criterion in the form of an ecolabel to assess the suitability of resort beaches. An example is the Blue Flag award for European beach resorts that focuses on *water quality* (*q.v.*), beach management, and safety (see *life saving and beach safety*) (UNEP/WTO/FEEE 1996).

Coastal site classification

Of various types of *classification of coasts* (*q.v.*) (Bird, 2000) none is suitable for determining site criteria for coastal tourism. Classifications with an emphasis on coastal processes can be useful for resort sites focusing on recreation, such as *surfing* (*q.v.*). For example, Bird (1993) identified various types of surf reflecting geomorphological and oceanic factors. Since the mid-1980s, the beach morphodynamics model with its identification and explanation of beach hazards, such as steep beaches and rip currents, is particularly useful for resort beaches in Australia (Short, 1999).

Generally, physical or morphological types of coastal classification are more useful for recreation/tourism planning, development, and management. For recreational purposes in the temperate countries, coastal landforms are classified as sand and shingle beaches, tidal forms (mudflats, salt marshes), estuaries, cliffs, and shore platforms (Pickering, 1996). Defert (1966 in Mieczkowski, 1990, pp. 247–248) provided one of the earliest classifications for coastal resort development, in which four types of coasts were identified:

1. *Oceanic: continuous and linear*: Straight oceanic beaches with tourism facilities following straight sandy coasts.
2. *Oceanic: discontinuous and concentrated*: Bays alternate with promontories and peninsulas with tourism located in the bays.
3. *Mediterranean: continuous and linear*: Wide and gentle beaches prevail as a result of the absence of tides or very small tides.
4. *Mediterranean: discontinuous and concentrated*: This consists of two types (1) wide bays bordered by promontories or capes, and (2) coves with small beaches.

In a situation where the site is clearly restricted or limited to one coastal type, it is possible to have further categorization in terms of criteria other than physical. For example, in the Ko Samui/Surat Thani region located in the Gulf of Thailand, the beaches are further identified for tourism development as follows: (1) conservation beaches, where tourism activities are not allowed; (2) nature-oriented development beaches where activities and services are permitted to a certain extent; and (3) progressive development beaches where activities and services can be developed to meet international standard (Tourism Authority of Thailand, 1985).

For the east coast of Peninsular Malaysia which is exposed to the northeast monsoon, resort sites are identified for tourism development with a strong consideration given to the seasonal factor. Four major types of sites are identified on the mainland coasts (Tourist Development Corporation, 1979).

1. Beach front site. This is backed by relatively flat land, sandy soils, and coconut groves and exposed to the sea.
2. Site oriented to both ocean and river or brackish lagoon. The topography is generally flat or rolling gently with coconuts and other vegetation.
3. Site situated adjacent to a substantial headland promontory with sufficient flat land for development. The beach may be interrupted by large boulders. Hill and weather patterns influence architectural design and site plan.
4. Site on hillside or hilltop with panoramic views located on headlands adjacent to good beaches. Weather and wind can be either greater or sheltered depending on the position of the development area. More constraints are placed on resort design.

Table T16 Types of resort sites on tropical coasts

Coastal type	Form/feature	Resort sites
A. Rock coast	1. Cliff	1. Good view; generally exposed; adequate setback necessary
	2. High headland	2. Good view; stability is crucial; can be sheltered or exposed. Requires compact design solutions
B. Mainland beach Coast	1. Linear	1. Large area available; can be exposed
	2. Crescentic bay	2. Can be at head of bay but has higher wave energy; decreasing wave energy towards the limbs of bay
	3. J-shaped bay (zetaform)	3. Sheltered in upcoast curve; increasing exposure to downcoast straight sector
	4. U-shaped bay	4. Can be at head of bay; often decreasing sand toward the limbs of bay
	5. Cuspate foreland	5. Only on large foreland; need to determine stability of convexity
	6. Spit	6. Only on large stable spits; river can be integrated into design; adequate setback from channel to avoid flooding
	7. River mouth associated with above	7. To be avoided because of rapid changes and seasonal closure of mouths, especially of small streams
C. Barrier coast	With/without dunes	Can be on barrier; but behind active dunes. Maintain seaward line of dunes as buffer zone. Lagoon can be integrated into design
D. Small island	As in A and B, where applicable.	Wider choice on many types of beaches on sheltered side. Limited beaches on exposed side. Access is important, especially during seasonal weather
E. Coral island	1. With/without lagoon	1. Adequate setback required avoid destruction of reefs
	2. Cay	2. Adequate setback required. Strong seasonal changes; no dredging or structures interfering with sand movement
F. Mangrove coast		On piles to minimize impact on ecosystem. Tidal range can be critical factor in accessibility and jetty length
G. Developed coast	1. Original sandy coast	1. Sufficient setback from protection measures. Beach nourishment required
	2. Original low rock coast	2. Selective removal or rock to create bays, artificial beaches. Beach nourishment required. Also raised sandy platform with coastal protection

Sources: Revised from Wong, 1990, 1991, 1999, 2000.

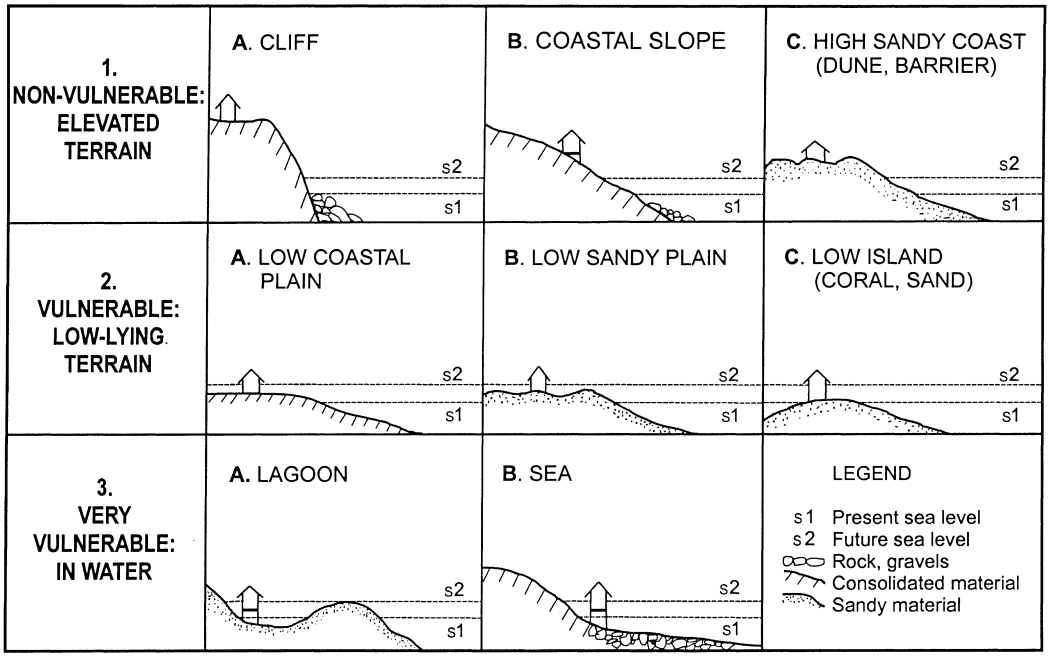

Figure T49 Types of resort sites affected by a sea level rise (redrawn from Teh, 2000).

These four types of sites can also be found on the islands which may provide a change of wind and sun orientation not possible with the mainland coastal site. However, access to islands is an important factor in construction and operation.

Based mainly on field examples from Southeast Asia and Indian Ocean islands a classification of resort sites is proposed for tropical coasts (Table T16). Where possible, the type of coast or coastal form is followed by an identification of specific suitable sites. Mainland *sandy coasts* (*q.v*) are the most important for resort development, with various suitable sites depending on the planform and degree of protection offered by rock headlands. Small islands, especially *coral reef islands* (*q.v*), are also favored for resort sites but they have fragile environments. Mangrove coasts hold a potential although the vegetation is being cleared cut down for other uses. Dunes are limited on tropical coasts and lagoons are actively used for local fishing. Stream mouths can be integrated into the resort site but requires adequate setback from possible flooding. Except for selective headlands, rock coasts (see *rocky coasts*) are underutilized for resorts. High rock coasts offer good views but require careful design and engineering. Low limestone coasts can be altered variously for resort sites, as evident on Mactan Island, where the modification can be limited or minimal (e.g., short seawalls, stone bunds), localized (e.g., groins, breakwaters, artificial islands) or effective (e.g., artificial beaches, selective excavation of rock to form small bays) (Wong, 1999).

With a *sea-level rise* (*q.v.*) in the future, many resorts on low-lying sandy plains or beach-ridge plains will be threatened as the coastline is cut back by the rising sea. For small islands dependent on tourism, the situation can be serious. Perhaps the most badly hit would be the island resorts of the Maldives, where the height of cays are within a couple of meters of the sea level and the entire island resort industry can be wiped out (Domroes, 2001). Mauritius has projected its loss of tourist beaches and in the major tourist area of Flic-en-Flac, an estimated 26,000 m^2 of beaches could be flooded by a meter sea-level rise (Mauritius National Climate Committee, 1998, p. 45). The response to the threat of rising sea level can be adaptive strategies classified as (managed) retreat, accommodation, and protection. Although various hard structural and soft structural options are considered for protection, new methodologies are being sought to estimate coastal vulnerability and resilience to the sea-level rise. For some low islands in the Pacific, coastal types can be used to assess vulnerability if further information is available. For example, while the upper shore can be of sand or shingle or a mixture of both, the lower shore can be a conglomerate platform, ramp outcrop, beachrock, mangroves, or seawall. Such details would be useful for assessing the vulnerability of a resort coast (Mimura and Harasawa, 2000).

Except for some island resorts, the vulnerability of resort sites to a sea-level rise has not been fully appreciated. In Malaysia, Teh (2000) has classified coastal resort sites according to their vulnerability to inundation arising from a sea-level rise. The sites can be (1) non-vulnerable (on a coastal slope or a high beach-ridge plain), (2) vulnerable (on a low coastal plain, low beach-ridge plain, or low island of coral, sand, or mud), and (3) highly vulnerable (in a lagoon or built over the sea). An additional coastal type (cliff) is added to this classification to cover other coastal types in Southeast Asia and the Indian Ocean islands (Figure T49). Compared with the classification of coasts for resort sites, this classification emphasizes the sea level relative to the two-dimensional coastal profile and much of the variety of coastal types and landforms is consequently made redundant. Nevertheless, it is an initial step in providing some idea of the vulnerability of resort sites to a sea-level rise.

Conclusion

Although many factors have to be considered in coastal sites for tourism, geomorphology remains basic as long as the coast is a necessary resource for tourism. Site analysis has to assess various types of coasts and its various zones. As coastal tourism caters to a widening demand, coastal sites for resorts are also being assessed for their suitability for other demands such as golf courses, marinas, oyster culture, and other related types of development. In the future, resort sites are likely to extend beyond the usual sandy coast and rock headland and include more adaptive use of the mangrove coast which has a potential for coastal ecotourism. Coastal sites are also likely to incorporate better technology not only for resort construction and infrastructure but also for coastal protection against erosion and beach management.

P.P. Wong

Bibliography

Ahmad, Y.F., 1982. *Environmental Guidelines for Coastal Tourism*. Nairobi: UNEP Environmental Management Guidelines, No. 6.

Baud-Bovy, M., and Lawson, F., 1998. *Tourism and Recreation: Handbook of Planning and Design*. Oxford: Architectural Press.

Beer, A.R., 1990. *Environmental Planning for Site Development*. London: E & FN Spon.

Bird, E., 1993. Geomorphological aspects of surfing in Victoria, Australia. In Wong, P.P. (ed.), *Tourism vs Environment: the Case for Coastal Areas*. Dordrecht: Kluwer Academic Press, pp. 11–18.

Bird, E., 2000. *Coastal Geomorphology: An Introduction*. Chichester: John Wiley, Chichester.

Domores, M., 2001. Conceptualizing state-controlled resort islands for an environment-friendly development of tourism: the Maldivian experience. *Singapore Journal of Tropical Geography*, **22**: 122–137.

Gunn, C.A., 1988. *Vacationscape: Designing Tourist Regions*, 2nd edn. New York: Van Nostrand Reinhold.
Inskeep, E., 1991. *Tourism Planning : An Integrated and Sustainable Development Approach*. New York: Van Nostrand Reinhold.
Mauritius National Climate Committee, 1998. *A Climate Change Action Plan*. Mauritius.
Mieczkowski, Z., 1990. *World Trends in Tourism and Recreation*. New York: Peter Lang.
Mimura, N., and Harasawa, H. (eds.), 2000. *Data Book of Sea-Level Rise*. Ibaraki: Centre for Global Environmental Research.
Nordstrom, K.F., 2000. *Beaches and Dunes of Developed Coasts*. Cambridge: Cambridge University Press.
Pearce, D., 1995. *Tourism Today: A Geographical Analysis*. 2nd edn. Harlow: Longman Scientific & Technical.
Pearce, D.G., and Kirk, R.M., 1986. Carrying capacities for coastal tourism. *UNEP Industry and Environment*, **9**(1): 3–7.
Pickering, H., 1996. Limitations for coastal recreation. In Goodhead, T., and Johnson, D. (eds.), *Coastal Recreation Management*. London: E & FN Spon, pp. 69–91.
Romeril, M., 1984. Coastal tourism—the experience of Great Britain. *UNEP Industry and Environment*, **7**(1): 4–7.
Short, A.D., 1999. Beach hazards and safety. In Short, A.D. (ed.), *Handbook of Beach and Shoreface Morphodynamics*. Chichester: John Wiley, pp. 293–304.
Teh, T.S., 2000. Sea level rise implications for coastal and island resorts. In Teh, T.S. (ed.), *Islands of Malaysia: Issues and Challenges*. Kuala Lumpur: University of Malaya, pp. 297–317.
Tourism Authority of Thailand, 1985. *Master Plan for Tourism Development of Ko Samui/Surat Thani*. Bangkok: Thailand Institute of Scientific and Technological Research. Unpublished Agency Report.
Tourism Authority of Thailand, 1989. *The Study on Potential Tourism Development for the Southern Region of Thailand. Tourism Data : Phuket, Surat Thani/Ko Samui, Songkhla/Hat Yai. Final Report, Vol. 3*. Tokyo: Japan International Cooperation Agency. Unpublished Agency Report.
Tourist Development Corporation, Malaysia, 1979. *Malaysia's East Coast: Master Plan Study for the Development of Tourism in the areas of Merang-Besut-Dalam Phu, Rompin-Endau-Mersing*. Los Angeles: Pannell Kerr Foster. Unpublished Agency Report.
Turner, L., and Ash, J., 1976. *The Golden Hordes: International Tourism and the Pleasure Periphery*. New York: St. Martin's Press.
UNEP/WTO/FEEE (United Nations Environment Programme/World Tourism Organization/Foundation for Environmental Education in Europe), 1996. *Awards for Improving the Coastal Environment: the Example of the Blue Flag*. Paris: UNEP.
Viles, H., and Spencer, T., 1995. *Coastal Problems: Geomorphology, Ecology and Society at the Coast*. London: Edward Arnold.
Walton, J.K., 1997. The seaside resorts of Western Europe, 1950–1939. In Fisher, S. (ed.), *Recreation and the Sea*. Exeter: University of Exeter Press, pp. 36–56.
Wong, P.P., 1990. The geomorphological basis of beach resort sites—some Malaysian examples. *Ocean and Shoreline Management*, **13**: 127–147.
Wong, P.P., 1991. *Coastal Tourism in Southeast Asia*. Manila: International Center for Living Aquatic Resources Management.
Wong, P.P., 1999. Adaptive use of a rock coast for tourism—Mactan Island, Philippines. *Tourism Geographies*, **1**: 226–243.
Wong, P.P., 2000. Coastal tourism in Southeast Asia: research from the environmental perspective. In Chon, K.S. (ed.), *Tourism in Southeast Asia: A New Direction*. New York: Haworth Hospitality Press, pp. 107–121.

Cross-references

Bay Beaches
Coral Reef Islands
Classification of Coasts (see Holocene Coastal Geomorphology)
Cliffed Coasts
Headland-Bay Beach
Human Impact on Coasts
Indian Ocean Islands, Coastal Ecology and Geomorphology
Lifesaving and Beach Safety
Natural Hazards
Pacific Ocean Islands, Coastal Geomorphology
Rating Beaches
Rock Coasts Processes
Sandy Coasts
Sea-Level Rise, Effect
Setbacks
Shore Protection Structures
Small Islands
Surfing
Tourism and Coastal Development
Water Quality

TRACERS

Introduction

Tracers are essentially sediment particles that can be easily identified within a large mass of grains having different characteristics. The concept is widely used in sedimentary petrography, where particular mineral assemblages are inherited from the characteristics of the provenance basin. Another approach is to use sediment from the environment to be studied and tag it using an artificial agent (e.g., paint or radioactivity).

Since the early stages of research on sediment transport, it became evident that natural and artificial tracers had a high potential, both for qualitative and quantitative assessments. The first examples of tracing experiments using artificial materials date back to the beginning of the 20th century, with the experiments of Richardson at Chesil Beach (UK) in 1902 and the reports of the Royal Commission on Coast Erosion published in 1907 (in Kidson and Carr, 1971). Although the last 20 years have seen the development of alternative methodologies for measuring sediment transport (see entry on *Instrumentation*), it can be noted that tracers are the only technique that can be applied at a broad range of temporal and spatial scales. Although both the sandy and the coarser fractions have been the object of tracer studies in sedimentary research, sand size material is generally used. A comprehensive review of tracer studies using pebbles can be found in Kidson and Carr (1971), while recent field studies and applications are described in Cooper *et al*. (1996).

Historical and technical development of the tracer technique

Fluorescent tracers

From the 1950s onwards, a group of investigators in the former Soviet Union started to use sands marked with fluorescent paints on a large scale (Zenkovitch, 1960; Zenkovitch and Boldyrev, 1965). The methodology consisted in marking sand grains with a fine film of a colloid (agar-agar) containing fluorescent material. The film was resistant to water, chemical reactions, and mechanical abrasion. The marked sand was then dried and injected on the beach. Thereafter, at regular time intervals (e.g., from minutes to days), samples were collected at fixed distances from the injection point. The research team also experimented using different colors of marked grains, to be injected at different water depths in the nearshore or for different grain sizes to assess differential transport. Almost at the same time, Portuguese investigators were testing the technique using a slightly different approach. Abecassis *et al*. (1962) tried initially to use heavy minerals and grain size trends as indicators of transport, but with scarce results, and therefore decided to employ sand marking either with fluorescent paints or using artificially tagged radioactive sands. The first method did not give good results, since natural luminescence was present in the sands. The methodology employed using fluorescent tracers was similar to that of the Russian team and they injected and collected samples on the foreshore.

In the following years, there was a boom in the use of fluorescent tracers for the study of sediment transport and investigators in the United States started to experiment with this technique. Yasso (1965) studied selective transport of different grain sizes in New Jersey; he used different colors of fluorescent paint, using a mixture of acrylic lacquer and beetle resin. Ingle (1966) undertook a study on beaches in southern California where sand samples were collected along profiles orthogonal to the coastline spacing from the foreshore to the inshore areas. He tested five marking techniques that are described in his book, probably the only published manual on the topic. Boon (1968) undertook one of the few studies that concentrated on carbonate beaches, in this case in the Bahamas, Florida. Three sand populations were considered, with different grain sizes and shapes, and marked using different colors, using fluorescent lacquer. Boon (1970) also applied his expertise on a beach in Virginia, where sand was collected from the local dunes and sieved through a series of meshes to obtain a population with a range of

0.29–0.59 mm. The sand was painted in large plastic bags, where it was mixed with acrylic lacquer, toluene, and beetle-resin.

In the 1970s, the application of tracers to measure longshore drift (see entry on *Longshore Sediment Transport*) became widespread. Empirical measurement of longshore transport to calibrate mathematical predictors for engineering studies was needed. Komar and Inman (1970) carried out several experiments on the western coast of the United States to build a database that eventually lead to their famous transport predictor. Another example of tracer application within the context of a coastal engineering project (see entry on *Engineering Applications of Coastal Geomorphology*) is that of Allen and Nordstrom (1977). In a multidisciplinary study for the assessment of beach form changes within a groin field (see entry on *Shore Protection Structures*) in New Jersey, the authors studied sediment exchange between the foreshore, the surf zone, and the bar. One of the largest experiments ever carried out on beaches is that of Chapman and Smith (1977) on the Gold Coast of Australia. Fifty tons of sand were marked and continuously injected using a dredge for about three weeks. Because the sand had a high degree of natural luminescence, the use of fluorescent paints was ruled out and a blue dye was used. Radioactive tracers were also excluded because of the large quantities involved and the subsequent environmental impact.

The fluorescent marking technique has become of interest to many European researchers in the 1990s, with the development of experiments in France (Corbau *et al*., 1994; Pedreros *et al*., 1996), Belgium (Voulgaris *et al*., 1998), and Portugal (Taborda *et al*., 1994; Ciavola *et al*., 1997a, 1998). These experiments introduced several improvements to the older methodology, in particular regarding the automatic detection of marked sand grains and the study of tracer advection in three dimensions.

Radioactive tracers

Despite the fact that radioactive tracers were at first very popular, they never became widely used, since the marking technique is complex and the method has a considerable environmental impact. Trying to compare results obtained using at the same time fluorescent and radioactive tracers, Abecassis *et al*. (1962) had already experimented with isotopes ^{110}Ag and ^{32}P, obtaining the best results with the latter. Two noteworthy field experiments using radioactive tracers were carried out by Heathershaw and Carr (1977) to assess tidally induced transport in the Severn Estuary (UK). The tracer was produced by neutron irradiation of Scandium (^{46}Sc) into glass. The glass was then sieved to obtain a population with different size classes. The detector consisted of a sodium iodide (NaI) crystal, doped with Thallium (TI) and optically coupled to a photomultiplier tube. This assembly, together with electronic components, was housed in a waterproof brass case. Measurements were made by lowering the counter on the seabed and readings were transmitted to a ship.

Clearly, the radioactive method offers many advantages such as the small quantities required, the possibility of tagging several grain size populations, the fact that the hydraulic properties of the grains are left untouched. However, although weak radioactive isotopes are used, it is most unlikely that nowadays an application for this method could be approved in the context of an environmental impact assessment.

Essential concepts for applying the fluorescent tracer method

Applicability and assumptions

The method must fulfill some basic assumptions: the marked sands should have a hydraulic behavior comparable to the unmarked ones; *advection* of the tracers should be prevalent over *diffusion* and *dispersion*; the transport system must be in equilibrium. Madsen (1987) presents an exhaustive mathematical description of the terms advection, diffusion, and dispersion.

It is no surprise that many investigators have used this method for studying sediment transport. The usage of fluorescent sands is simple, marking can be done easily and rapidly, and there is no impact on human health and the environment. Different colors can be used to tag various grain fractions, to study differential transport, and the sensitivity of the technique is on the order of 1 ppm (Ingle, 1966). The most interesting experiment on differential transport is that described by Komar (1977) on a reflective shoreface (see entry on *Reflective Beaches*) in Baja California, Mexico. A single injection of tracer took place and collection of over 200 samples was undertaken along a grid extending more than 200 m alongshore. The samples were sieved into different size fractions and the number of marked grains within each class was annotated. Later Blackley and Heathershaw (1982) revisited the issue and, in agreement with the previous author, reached the conclusion that different grain size transport was related to the transport mechanism, for example, the relationship between bedload and suspended load at a point on the foreshore. Allen and Nordstrom (1977) even used different colors to examine spatial changes of sediment exchange between the foreshore and the bar, albeit in a qualitative way.

Preparation of the tracers

Regarding this first stage of the method, an essential factor is the quantity of tracer sand to be produced. For large quantities (e.g., 1,000 kg or more), industrial preparation is probably the only feasible method, trying to use sediments with a mean grain size and density comparable to those of the natural environment. In any case, the best balance between handling during tagging and percentage of recovery during the experiment should be met. If sand is collected from the local beach, a composite sample could be obtained by mixing equal subsamples collected on the lower-, mid-, and upper-shoreface. It is important to carry out grain size analyses (see entry on *Beach Sediment Characteristics*) of each sub-environment and of the composite distribution, to compare the effects of mixing. Care should be taken to avoid local sedimentary effects due, for example, to the presence of large-scale bedforms or moribund beach cusps (see entry on *Rhythmic Patterns*).

The sand is then washed with freshwater to remove the salt and dried. Regarding the marking procedure, a number of different types of resins and paints can be used. The main requirement for the paint is to be resistant to chemical and mechanical abrasion caused by seawater. Initially, substances such as seaweed glue, bone-glue, gum, and starch were used but many authors later switched to acrylic paints, which offer better resistance to abrasion. If natural luminescence of the sediment is a problem, the solution of Chapman and Smith (1977), a blue dye dissolved in methylated spirit, can be adopted. Knoth and Nummedal (1977) marked the sand using a mixture of fluorescent paint, resin, and organic solvent. In recent experiments, fluorescent paint soluble in toluene has been widely used (Corbau *et al*., 1994; Ciavola *et al*., 1997a, 1998).

The next step is to dry the sand, minimizing the effects of aggregation. As far as the paint is maintained as thin as possible, aggregation should generally be negligible, especially if the sand is rapidly dried in the open air under sunlight. Even in the case of aggregate formation, if the sand is sieved with appropriate meshes after tagging, the mode of the populations should remain the same.

Injection of the tracer into the transport system

Injection of the sand into the transport system takes place according to the type of study being carried out. As Madsen (1987) concluded, it is possible to adopt three different techniques to analyze tracer advection. The *Time Integrated Method* (TIM) has an Eulerian nature, whereby a known quantity of tracer is released at a point and variations in tracer concentration are monitored throughout time at a location downdrift. The *Continuous Injection Method* (CIM) is similar to the previous one, with the exception that injection of the tracer is continuous at a known rate. The *Spatial Integration Method* (SIM) involves a Lagrangian approach, since it allows monitoring of tracer movement both in space and in time. Other advantages of the SIM over the previous methods is that the velocity of transport is computed referring it to the *centroid* (or center of mass) of the tracer cloud and that it is possible to calculate with confidence a recovery rate.

In the case of continuous injection on the submerged beach outside the breakers, dumping from a vessel is a possible method, while in the case of working in the breakers this may be unfeasible in terms of safety of the boat. For this reason, researchers using the TIM and CIM methods preferred injecting the tracer from several points along a transect orthogonal to the beach (Yasso, 1965; Ingle, 1966; Boon, 1970). Other experimentalists, mainly using the SIM method, placed the tracer at low tide into a shallow trench dug on the beach face, after washing it with liquid soap to avoid grain floating. There is no standard for the size and depth of the trench: the most important requirement is that all the tracer grains are removed almost instantaneously as soon as the site is covered by water. A delay in removal or burial of the tracer at the trench site could invalidate the basic assumptions of the method.

Sediment sampling

Despite the fact that many authors only worked at surface level (e.g., Ingle, 1966; Corbau *et al*., 1994; Taborda *et al*., 1994) it is preferable to collect shallow cores to assess the three-dimensional (3-D) advection of the tracer (e.g., Boon, 1970; Kraus *et al*., 1982; Ciavola *et al*., 1997a, 1998). PVC cores or other simple coring techniques are suitable for this

Figure T50 The SADAM system of Pinto *et al.* (1994) for *in situ* mapping of surface dispersal of fluorescent grains. It consists of an ATV, a dark camera with UV light, and computer with image processing software.

purpose. Inman *et al.* (1980) collected their samples according to the type of analysis to be performed: the first technique was employing a grab sampler, especially designed to collect only the first two centimeters of the surface layer and was used to carry out a spatially distributed sampling to apply the SIM. The second method was using corers that were collecting samples along a cross-shore profile at constant time intervals, for the TIM method. Duane and James (1980) adopted a similar approach for the CIM technique. Sampling was frequent along four profiles, to obtain a description of changes in concentration with time at each station. Samples were collected using a hand-held sloop, built on broad runners, that was penetrating the sand column no more than 1 cm, to avoid sampling at depths where the sand concentration was already in equilibrium. If sampling takes place on submerged sites, vaseline coated cards like those of Ingle (1966) can be used.

In case it is decided to assess surface distribution, to increase the significance of the results from the cores, it is possible to use automatic detection techniques like the system of Pinto *et al.* (1994), where a computer system in installed on an ATV (All Terrain Vehicle), to perform rapid assessments using image analysis techniques (Figure T50).

Dyed grain detection

Counting of the grains in the samples under a UV lamp can be tedious and involve several days of work. Whenever the number of tracer grains in a sample is high, automatic detection or indirect detection methods can be helpful, once the considerable calibration difficulties are overcome. In the study of Chapman and Smith (1977), where the dye was not fluorescent, counting took place following two different methodologies: photography and subsequent enlargement; affixing the samples to long strips of pressure-sensitive adhesive tape and passing the strips under a binocular microscope at an enlargement of 30–40 times to detect the grains. In both cases, the counting was undertaken using an automatic image analyzer.

At the very beginning of tracer research, Zenkovitch (1960) and Zenkovitch and Boldyrev (1965) examined the samples in the laboratory using a luminoscope. Such a piece of equipment used a UV source that stimulated fluorescence from the grains, similarly to the photometer that Yasso (1966) developed to count the number of marked grains directly on the beach. The spectrofluorimetric of Farinato and Kraus (1981) was instead based on a more original approach: the technique consisted in washing the sand samples with a solvent able to dissolve the resin and the paint covering the grains. The fluorescence of the effluent can then be measured using a spectrophotometer: the measured intensity is proportional to the number of tagged grains, the solution transmission, and the uniformity of the paint cover. The calibration of the intensity coefficient versus the number of marked grains per gram has to be undertaken according to the degree of marking, the grain size distribution, the chemical properties of the solvent and of the resin. For the method to work, all sand grains should be almost equi-dimensional: certainly in the case of a uni-modal, well-sorted sand that can be true, but as sorting becomes worse, the method looses significance. Besides, the technique assumes that the paint cover of the grains is uniform; probably this might be possible if industrially done, but since most authors mark the sands themselves to save money and time, especially when small quantities are involved, variations in color thickness must be expected.

Controversies and gaps in current knowledge

A simple conceptual model of longshore transport describes the system as two layered. The upper layer is where movement of the tracer occurs as advection longshore, while in the lower layer the sand is not activated. In order to calculate the volume of transported sand, it is necessary to calculate the *mixing depth* (see entry on *Depth of Disturbance*), that is considered equivalent to the thickness of the moving layer described above. Within this layer, grains are subjected to vertical and lateral movements caused by direct wave action and by the superimposed longshore current. There are different methods in the literature for determining the thickness of the mixing layer. While in many experiments it was simply determined in the field by digging one or more control holes, filled with marked sand, a different methodology was generally used in parallel with the previous one, considering as mixing depth the interval within the beach cores where 80% of the total mass recovered in each sample was observed (Kraus *et al.*, 1982; Kraus, 1985; Ciavola *et al.*, 1997b, 1998).

Workers using a detector at surface level may be confronted with the problem of assessing indirectly the burial depth of the tracer. Heathershaw and Carr (1977) estimated it using the *tracer balance method*, assuming that a reduction in the recovery rate of the tracer is

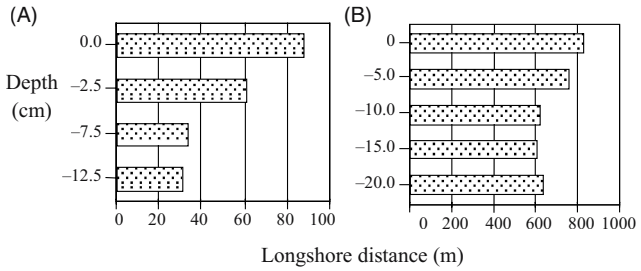

Figure T51 Vertical patterns of advection of tracer clouds from shallow beach cores: data in figure (A) was collected by Ciavola *et al.* (1997a); data in figure (B) was collected by Ciavola *et al.* (1998).

simply due to burial, and that burial can be estimated using a response function typical of the detector used. The method assumes that the tracer is uniformly distributed down to the depth of maximum burial; several field evidences points out that this might not always be true, unless total mixing is achieved, which implies that the tracer had enough time to reach equilibrium conditions. From the diagrams in Figure T51 (data from Ciavola *et al*., 1997a, 1998), it is possible to notice that the displacement of the center of mass of the tracers, and consequently its velocity, decreases with depth, becoming almost constant in proximity of the maximum depth of activation. When there is an anomalous variation with depth in the speed of displacement, this is probably related to tracer burial. In this case, it might be necessary to reject some of the core samples: simple surface studies could therefore lead to an overestimation of the speed of displacement of the center of the tracer cloud, ultimately causing a miscalculation of the volume of sediment being transported. In experiments where the tracer sampling was extended to several days (e.g., Heathershaw and Carr, 1977; Ciavola *et al*., 1997a), it was found that as time passed by, total mixing was taking place, with the whole sediment column moving almost at the same speed.

Another limitation of the method is the calculation of a significant *percentage of recovery* of the tracer. Recent experiments (Sherman *et al*., 1994; Ciavola *et al*., 1998) used grain size statistics of the tagged sediment to derive approximations for concentrations, based upon assumptions of uniform density and diameter. Estimates of total tracer recovery were made by extrapolating the point concentrations to representative control volumes, by constructing surface polygons and using tracer-depth distributions obtained from recovery depths.

Conclusions

Recently, many investigators throughout the world have been revisiting the tracer technique, especially for field measurements of longshore transport. *Tracer advection* can be measured on a 3-D basis; it is considered essential that investigators adopt such an approach if they want to obtain meaningful observations.

Most field experiments have been confined to small- to medium-scale beach studies, but tracers can be employed successfully to study transport along sandbanks and on continental shelves. In a similar fashion, the timescale of these experiments tends to be short (hours to days), because of the small quantities of tracer injected. In the past, long-term monitoring was undertaken using radioactive tracers, where a small quantity (e.g., less than 1 kg), provides enough material for a monthly exercise; however, possible negative impacts on the natural environment rule out this method. In the case of fluorescent tracers, only the usage of thousands of kilos of sand will ensure a significant recovery rate at the end of a long-term experiment. Large quantities mixed with sand during a beach recharge scheme (see entry on *Beach Nourishment*) could, for example, provide coastal managers with an independent method of assessing *where the sand is going* during monitoring activities, in addition to data for the calibration of longshore drift predictors, to decide whether further intervention is needed.

The main limitations of the method are the time and the effort required for data collection and analysis. Recent applications of automatic analyzer, particularly using image analysis methods, suffered from the cost and availability of high-resolution systems. With the recent boom of digital cameras, the power of image analysis has increased in parallel with a decrease in the costs involved, therefore a rapid development of automatic methods for grain detection and counting is likely to happen in the years to come.

Paolo Ciavola

Bibliography

Abecassis, F., Matias, M.F., Reis de Carvalho, J.J., and Vera-Cruz, D., 1962. Methods of determining sand and silt movement along the coast, in estuaries and in maritime rivers. *Laboratório Nacional de Engenharia Civil Technical Paper No. 186*. Lisbon, Portugal: Ministério das Obras Públicas.

Allen, J.R., and Nordstrom, K.F., 1977. Beach form changes in the lee of groins at Sandy Hook, New Jersey. In *Proceedings of the Coastal Sediments '77*, American Society of Civil Engineers, pp. 33–47.

Blackley, M.W.L., and Heathershaw, A.D., 1982. Wave and tidal current sorting of sand on a wide surf zone beach. *Marine Geology*, **49**: 345–356.

Boon, J.D., 1968. Trend surface analysis of sand tracer distributions on a carbonate beach, Bimini, B.W.I. *Journal of Geology*, **76**: 71–87.

Boon, J.D., 1970. Quantitative analysis of beach sand movement, Virginia Beach, Virginia. *Sedimentology*, **17**: 85–103.

Chapman, D.M., and Smith, A.W., 1977. Methodology of a large scale sand tracer experiment. In *Proceedings of the 3rd Australian Conference on Coastal and Ocean Engineering*, pp. 185–189.

Ciavola, P., Taborda, R., Ferreira, Ó., and Dias, J.A., 1997a. Field measurements of longshore sand transport and control processes on a steep meso-tidal beach in Portugal. *Journal of Coastal Research*, **13**: 1119–1129.

Ciavola, P., Taborda, R., Ferreira, Ó., and Dias, J.A., 1997b. Field observations of sand-mixing depths on steep beaches. *Marine Geology*, **141**: 147–156.

Ciavola, P., Dias, N., Ferreira, Ó., Taborda, R., and Dias, J.M.A., 1998. Fluorescent sands for measurements of longshore transport rates: a case study from Praia de Faro in southern Portugal. *Geo-Marine Letters*, **18**: 49–57.

Cooper, N.J., King, D.M., and Hooke, J.M., 1996. Collaborative research studies at Elmer Beach, West Sussex, UK. In Taussik, J., and Mitchell, J. (eds.), *Partnership in Coastal Zone Management*. Cardigan, UK: Samara Publishing Limited, pp. 369–376.

Corbau, C., Howa, H., Tessier, B., de Resseguier, A., and Chamley, H., 1994. Evaluation du transport sédimentaire sur une plage macrotidale par traçage fluorescent, Dunkerque Est, France. *Compte, Rendus Académie des Sciences de Paris*, **319**: 1503–1509.

Duane, D.B., and James, W.R., 1980. Littoral transport in the surf zone elucidated by an eulerian sediment tracer experiment. *Journal of Sedimentary Petrology*, **50**: 929–942.

Farinato, R.S., and Kraus, N.C., 1981. Spectrofluorometric determination of sand tracer concentrations. *Journal of Sedimentary Petrology*, **51**: 663–665.

Heathershaw, A.D., and Carr, A.P., 1977. Measurements of sediment transport rates using radioactive tracers. In *Proceedings of Coastal Sediments '77*, American Society of Civil Engineers, pp. 399–416.

Ingle, J.C., 1966. *The Movement of Beach Sand*. Amsterdam: Elsevier.

Inman, D.L., Zampol, J.A., White, T.E., Hanes, D.M., Waldorf, B.W., and Kastens, K.A., 1980. Field measurements of sand motion in the surf zone. In *Proceedings of the 17th International Coastal Engineering Conference*, American Society of Civil Engineers, pp. 1215–1234.

Kidson, C., and Carr, A.P., 1971. Marking beach materials for tracing experiments. In Steers, J.A. (ed.), *Introduction to Coastline Development*. Basingstoke, UK: MacMillan, pp. 69–93.

Knoth, J.S., and Nummedal, D., 1977. Longshore sediment transport using fluorescent tracers. In *Proceedings of Coastal Sediments '77*, American Society of Civil Engineers, pp. 383–398.

Komar, P.D., 1977. Selective longshore transport rates of different grain-size fractions within a beach. *Journal of Sedimentary Petrology*, **47**: 1444–1453.

Komar, P.D., and Inman, D.L., 1970. Longshore sand transport on beaches. *Journal of Geophysical Research*, **75**: 5514–5527.

Kraus, N.C., 1985. Field experiments on vertical mixing of sand in the surf zone. *Journal of Sedimentary Petrology*, **55**: 3–14.

Kraus, N.C., Isobe, M., Igarashi, H., Sasaki, T.O., and Horikawa, K., 1982. Field experiments on longshore sand transport in the surf zone. In *Proceedings of the 18th Coastal Engineering Conference*, American Society of Civil Engineers, pp. 970–988.

Madsen, O.S., 1987. Use of tracers in sediment transport studies. In *Proceedings of Coastal Sediments '87*, American Society of Civil Engineers, pp. 424–435.

Pedreros, R., Howa, H.L., and Michel, D., 1996. Applications of grain size trend analysis for the determination of sediment transport pathways in intertidal areas. *Marine Geology*, **135**: 35–49.

Pinto, J.R.C., Dias, J.M.A., Fernandes, S.P., Ferreira, Ó., Silva, A.V., and Taborda, R., 1994. Automatic system for tagged sand detection. *Gaia*, **8**: 161–164.

Sherman, D.J., Nordstrom, K.F., Jackson, N.L., and Allen, J.R., 1994. Sediment mixing-depths on a low-energy reflective beach. *Journal of Coastal Research*, **10**: 297–305.
Taborda, R., Ferreira, Ó., Dias, J.M.A., and Moita, P., 1994. Field observations of longshore sand transport in a high energy environment. In de Carvalho, S., and Gomes, V. (eds.), *Proceedings of Littoral 94*. Lisbon, Portugal: EUROCOAST Portugal, pp. 479–487.
Voulgaris, G., Simmonds, D., Michel, D., Howa, H., Collins, M.B., and Huntley, D.A., 1998. Measuring and modelling sediment transport on a macrotidal ridge and runnel beach: an intercomparison. *Journal of Coastal Research*, **14**: 315–330.
Yasso, W.E., 1965. Fluorescent tracer particle determination of the size-velocity relation for the foreshore sediment transport, Sandy Hook, New Jersey. *Journal of Sedimentary Petrology*, **34**: 989–993.
Yasso, W.E., 1966. Formulation and use of fluorescent tracers coatings in sediment transport studies. *Sedimentology*, **6**: 287–301.
Zenkovitch, V.P., 1960. Fluorescent substances as tracers for studying the movements of sand on the sea bed. *The Dock and Harbour Authority*, **40**: 280–283.
Zenkovitch, V.P., and Boldyrev, V.L., 1965. Alongshore sediment streams and methods of their study. In *Proceedings of the 11th Congress of the International Association for Hydraulic Research*, Volume 5. Leningrad, USSR: International Association for Hydraulic Research, pp. 139–148.

Cross-references

Beach and Nearshore Instrumentation
Beach Nourishment
Beach Sediment Characteristics
Depth of Disturbance
Engineering Applications of Coastal Geomorphology
Longshore Sediment Transport
Reflective Beaches
Rhythmic Patterns
Shore Protection Structures

TROTTOIRS

The term "trottoir," French for pavement, is a very imprecise one in coastal geomorphology, referring to a range of intertidal landforms formed by a variety of processes. At their simplest, they form a bioconstructional overhang perhaps a meter wide attached to steep rocky shores at about mid-tide level. Elsewhere, on less steeply sloping coastlines, erosional platforms tens of meters wide may be covered by a similar variety of calcareous algae, vermitids, and other bioconstructional organisms which, on the outer edge form a distinctive rim where wave agitation encourages more rapid accumulation. These forms are particularly prominent over calcareous substrates and in the tropics, where they cover platforms cut into raised reef limestones, may merge with the algal terraces of high-energy reef margins (Emery, 1962). In deeper water beyond the trottoirs, mushroom-shaped bosses constructed of the same organisms, may rise to the sea surface where their morphology may resemble that of coral micro-atolls.

Processes

Because of the range of morphologies which have been termed trottoirs, there are probably a number of processes involved in their formation. The simpler intertidal overhang or corniche may be entirely the result of bioconstruction. However, the protection of the coating of algae, vermitids, and other organisms give the underlying rock surface in comparison to the zones above and below this mid-tide level, where mechanical, chemical, and bio-erosional processes may be acting, can make the protuberance more prominent and give it a bedrock core. On wider rimmed platforms the paradox is that the bioconstructional layer overlies a platform which is obviously erosional which has led to contradictory hypotheses to explain the landforms' origin as either constructional or erosional (see e.g., Emery, 1962). Probably, both processes occur, either at different times or even simultaneously as many bio-erosional organisms including blue-green algae and sipunculid worms may be associated with or beneath the veneer of rock-building biota.

Organisms involved

The constructive or protective activity of many organisms is involved in the formation of trottoirs. The most ubiquitous are calcareous algae (e.g., *Neogoniolithon notarisii, Lithothamnium* sp., *Lithophyllum tortuosum, Tenarea tortuasa*), vermetid worms (e.g., *Dendropoma petraeum, Vermetus triqueter, Vermetus nigricans, Pomatocerus caeruleus*), Sabellariae (*Sabellaria kaiparaensis, Sabellaria vulgaris, Galeolaria caespitosa, Phragmatopoma iapidosa, Vermilia* sp., and oysters (*Crassostrea amasa, Crassostrea glomerata, Saxostriea* sp.) the exact combination of species depending on climate, exposure, and the environmental factors (Kelletat, 1989, 1995).

Location

Although the overall distribution, limiting factors, and importance in coastal processes are not fully investigated, trottoirs, *sensu lato* are found from northern Scotland to the tropics (Kelletat, 1989). A very wide range of forms has been described from the Mediterranean (e.g., Crete, Kelletat and Zimmerman, 1991). Rimmed platform types, are more common in warmer waters and have been described from the southern Mediterranean, the Caribbean, Micronesia, and Australia (e.g., Kelletat, 1989, 1995).

Rimmed platforms are best developed over limestone substrate and may occur closer to high tide levels than the corniche type of trottoirs, though still permanently wetted by spray even at low tide. Low to moderate tidal ranges therefore appear to be most appropriate for the development of all types of trottoirs. Moderate wave activity also appears favorable. Where too great, the amount of overhang may be limited by mechanical breakage.

Rate of growth

Trottoirs can accumulate rapidly, in tropical waters their growth rates being only a little less than those of coral reefs (Kelletat, 1989). In Crete, trottoirs of algal reefs have grown to a width of 10 m since the coastline was last uplifted 1,530 years ago representing lateral growth rates of more than 6 mm/yr. Marginal extension rates of more than 13 mm/yr and increase in thickness of 0.8 mm/yr have been reported from algal reefs in St. Croix (Adey and Vassar, 1975). Given sufficient stability, sea-level trottoirs have the ability to build significant coastal features.

David Hopley

Bibliography

Adey, W.H., and Vassar, J.M., 1975. Colonization, succession and growth rates of tropical crustose coralline algae (Rhodophyta, Cryptonemiales). *Phycologia*, **14**: 55–69.
Emery, K.O., 1962. Marine geology of Guam. *US Geological Survey Professional Paper* 403-B.
Kelletat, D., 1989. Zonality of rocky shores. In Bird, E.C.F., and Kelletat, D. (eds.), *Zonality of Coastal Geomorphology and Ecology*. *Essener Geographische Arbeiten*, **18**: 1–29.
Kelletat, D., 1995. Atlas of coastal geomorphology and zonality. *Journal of Coastal Research*, **13** (Special issue): 286pp.
Kelletat, D., and Zimmerman, L., 1991. Verbreitung und Formtypen rezenter und subrezenter organischer Gesteinsbildungen an den Küsten Kretas. *Essener Geographische Arbeiten*, **23**: 163p.

Cross-references

Algal Rims
Bioconstruction
Bioherms and Biostromes
Notches

TSUNAMIS

Introduction

The word "Tsunami" is derived from the Japanese meaning "Harbor Wave." Tsunamis are often described as tidal waves but this view is incorrect since they have nothing to do with tides. Tsunamis are generated by offshore earthquakes, submarine slides, and occasionally by subaerial landslides that enter water bodies. In each case, large-scale displacement of water takes place as a result of submarine sediment slides or from earthquakes that induce faulting of the seabed. The initial

water movement is often characterized by a rapid drawdown and a lowering of the sea surface at the coast as the water moves into the area of seabed displacement. Thereafter, large kinematic waves are propagated outwards from the zone of seabed disturbance. The waves travel across the ocean at very high velocities, often in excess of 450 km/h, and possess very long wavelengths and periods. At the coast, the tsunami flood level (runup) is partly a function of the dimensions of the propagated waves but is greatly influenced by the topography and bathymetry of the coastal zone and as such the waves can reach considerable elevations causing widespread destruction and loss of life.

Historical accounts of tsunamis

The majority of tsunamis occur around the Pacific Ocean but many are also known from other areas. The frequency of Pacific tsunamis is due to the high occurrence of severe earthquakes under or close to the seabed as a result of the subduction of oceanic crust adjacent to continental margins. Such geological processes are a characteristic feature of Japan where there is a long history of devastating earthquakes and tsunamis. Between 1596 and 1938 the Japanese islands were struck by no less than 15 major tsunamis. One of the worst of these took place on June 15, 1896 as a result of a large submarine earthquake on the ocean floor 150 km offshore. Since the epicenter of the earthquake was located beneath the ocean floor, the inhabitants on nearby coasts, although they knew that an earthquake had taken place, were unaware that a major tsunami had been generated. The following account provides a vivid description of what followed. (Myles, 1985).

> This great Sanriku tsunami came on a festival day when the townspeople were enjoying a holiday. Twenty minutes after the first shock, the sea was seen to recede, while a little past eight in the evening, noises like that of a rainstorm were heard. The tsunami was now on them—a wall of water some tens of feet high—and the holiday revellers, before they realised the awful situation, were swept away and drowned … the fishermen, who at the time were some distance out at sea, and had noticed nothing unusual, were on their way home the next morning, amazed to find the sea for miles strewn with house wreckage and floating corpses.

According to the Japanese Government, 10,617 houses were swept away, 2,456 houses were partly demolished, 27,122 persons killed, and 9,247 persons injured. Practically, every coastal town and village in the provinces of Mino and Owari on the Sanriku coast of Japan was destroyed.

One of the most severe earthquakes and tsunamis took place on the January 11, 1693 in eastern Sicily. This disastrous earthquake resulted in the loss of life of ca. 70,000 victims. A tsunami occurred at Catania and also at Augusta. According to reports, there were three withdrawals of the sea and three major waves. Similarly severe earthquakes and tsunamis took place in Calabria on February 5 and 6, 1783. At this time, a tremendous earthquake occurred in this area associated with five very strong quakes. Considerable stretches of the coastline of Calabria were badly affected by a tsunami and the sea was reported to have receded and then inundated the shore with recessions and inundations repeated at least three times at intervals of about 10 min. At Messina harbor, quays and buildings were flooded and in one area the sea withdrew for more than 7 m leaving the sea bottom dry and a lot of fish on the beach. Then suddenly the water came back surpassing the limit previously reached and flooding the coast. Local tsunamis were also produced as a result of a large earthquake-induced rockfall into the sea. The tsunami of February 6 was particularly disastrous because of the very high number of victims where many, frightened by the earthquake shocks, escaped to the beach and were drowned by waves which reached the roofs of harbor buildings. In excess of 1,500 people were drowned and the tsunami flood level was estimated to have been between 6 and 9 m. Tinti and Maramai (1996) observed that in one area the tsunami was associated with deposition of "… some sand on the ground."

A very strong earthquake and tsunami took place in the Messina Straits, Italy, on December 28, 1908. The towns of Messina and Reggio di Calabria were completely destroyed together with many neighboring villages. The area of destruction was about 6,000 km^2 and more than 60,000 people died. The earthquake produced a violent tsunami in the Straits of Messina that caused severe damage and many victims. In all places the first observed movement was the withdrawal of the sea (in some places by about 200 m). Thereafter coastal flooding took place in association with at least three large waves. According to Tinti and Maramai (1996) the tsunami lasted many hours and reached its maximum intensity along parts of the Calabrian coast and on the coast of Sicily. In some localities, the biggest wave was the first while at others it was the second. Tsunami runup was observed to decrease for increasing distances away from the epicenter but in the Messina Straits this was obscured by the effects of wave resonance. At Messina the wave height reached 3 m, numerous boats were damaged, harbor quays were destroyed, walls collapsed, and several boats were transported onshore. In certain areas the maximum level reached by the tsunami was in excess of 10 m above contemporary sea levels, resulting in the destruction of many buildings and considerable drowning (Tinti and Maramai, 1996).

Probably, the most destructive tsunami in Europe during historical times took place on November 1, 1755. An earthquake took place offshore ca. 200 km WSW of Cape St. Vincent, on the Gorringe Bank on the seafloor west of Portugal and attained a magnitude estimated at 8.5 Ms. The epicenter of the earthquake was in an area along the Azores–Gibraltar plate boundary that forms the western part of the lithosphere boundary between the Eurasian and African plates (Moreira, 1985). The eastern section of the Azores–Gibraltar plate boundary (which includes the Gorringe Bank) is a zone of active plate compression and in this area faults tend to have a large source component that results in high-magnitude and deep-seated tsunamigenic earthquakes).

The considerable destruction that took place in Lisbon, in addition to widespread fires, was mostly attributable to three tsunami waves estimated to be between 5 and 13 m high that took the lives of 60,000 people in Portugal alone. There are also numerous reports of tsunami flooding and fatalities on a large-scale along the Algarve coast and on the coastline of Morocco. In England, contemporary observations by Borlase (1755, 1758) describe the arrival of the tsunami in Mounts Bay, Cornwall. Borlase noted

> … the first and second refluxes were not so violent as the 3rd and 4th (tsunami waves) at which time the sea was as rapid as that of a mill-stream descending to an undershot wheel and the rebounds of the sea continued in their full-fury for fully 2 hours … alternatively rising and falling, each retreat and advance nearly of the space of 10 minutes until 5 and a half hours after it began.

Reconstructed tidal changes for this day for the Isles of Scilly show that the time of high tide coincided approximately with the arrival of the first tsunami wave some 5 h after the first shocks were reported on the Portuguese coast. There are no known reports of the progress of the tsunami northeast along the Channel but it is reasoned here that the coastal flooding effects must have been considerable. There is some evidence to indicate that the 1,755 Lisbon tsunami was not solely caused by a seabed fault. Recently, a large turbidite/submarine slide complex has been identified on the seafloor adjacent to the Gorringe Bank and tentatively dated to AD 1755. This discovery raises the possibility that the tsunami was partly generated by an earthquake-triggered fault on the seabed and partly by submarine sediment slumping.

Geological evidence for tsunamis in prehistory

Historical accounts of former tsunamis have particular value since they can provide information on the frequency and magnitude of events for the time period for which historical records are available. For example, in Italy the oldest historical record of a tsunami having taken place is for the AD 79 eruption of Vesuvius. Since numerous tsunamis have taken place along the coastline of Italy since then, historical accounts are a particularly valuable archive that can be used to estimate tsunami (and earthquake) recurrence. In recent years, however, geological investigations have been used to identify former tsunamis that took place in prehistory. This has proved possible owing to the recognition that, in many cases, tsunamis deposit sediment in the coastal zone (Dawson and Shi, 2000). Identification of such sediment layers in coastal sediment sequences has led to a different perspective on the past frequency and magnitude of tsunami events in different coastal regions.

Geological investigations of former tsunamis is a relatively new research area. The recognition that many tsunamis deposit sediment in the coastal zone has only become an accepted idea during the last 5–10 years. Discussion of this concept has been accompanied by a proliferation of academic papers that have described a range of sediments that have been attributed to a series of former tsunamis (Figure T52).

Unlike storm surges, tsunami runup across the coastal zone is frequently associated with the rapid lateral translation of water and suspended sediment. Thus, tsunami deposits can be used to provide an indirect record of former offshore earthquakes and underwater landslides. It is exceptionally difficult, however, if not impossible, to

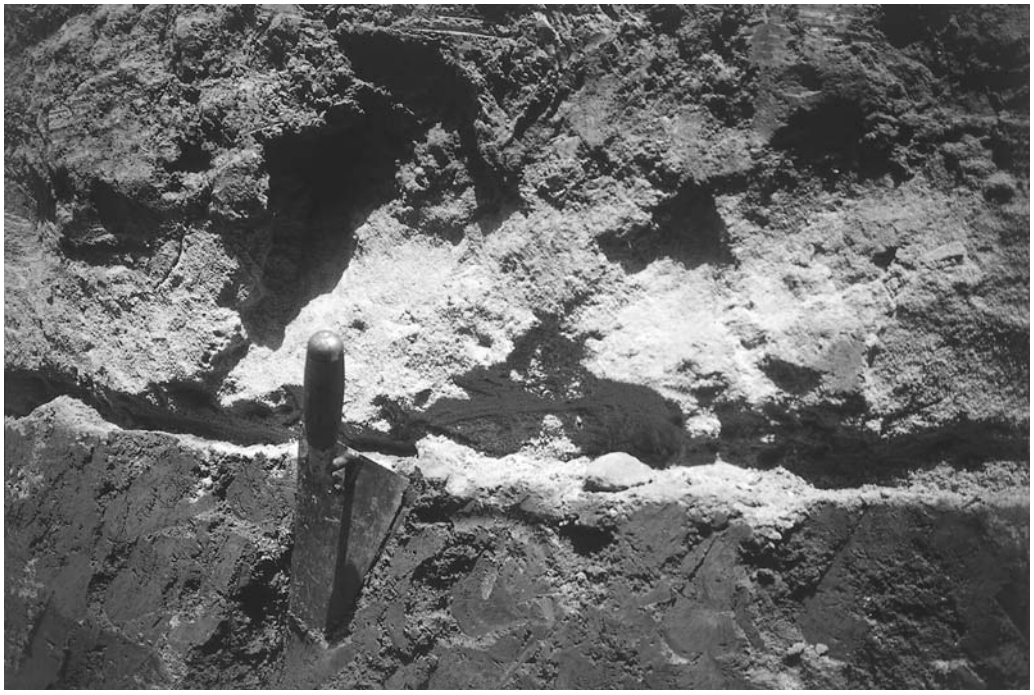

Figure T52 Sheet of sand and overlying boulders, Boco do Rio, Algarve, Portugal deposited by tsunami that accompanied the Great Lisbon earthquake of November 1, AD 1755.

differentiate tsunami deposits attributable to former submarine slides or offshore earthquakes. In particular areas of the world, especially in areas of an active plate motion where an offshore earthquake has taken place, it may be a gross oversimplification to attribute the triggering mechanism solely to earthquake-induced seabed faulting. Frequently, an offshore earthquake may also generate local submarine slides thus leading to complex patterns of tsunami flooding at the coast. In other areas (e.g., Hawaiian Islands, Norwegian Sea) submarine sediment slides may be the dominant mechanism of tsunami generation.

Tsunami deposits are distinctive. They are frequently associated with the deposition of continuous and discontinuous sediment sheets across large areas of the coastal zone. Frequently they consist of deposits of sand containing isolated boulders. On occasion, such boulders exhibit evidence of having been transported inland from the nearshore zone. In addition, microfossil assemblages of diatoms and foraminifera contained within sand sheets may provide information of onshore transport of sediment from deeper water.

Field observations of tsunami flooding usually describe the rapid lateral translation of water across the coastal zone. Frequently, the lateral water motion associated with runup is influenced by local wave resonance. Thus, the tsunami waves as they strike the coast are unlike waves associated with storm surges since not only are they associated with considerably greater wavelengths and wave periods, but they are essentially constructive as they move inland across the coastal zone. The rapid water velocities (provided that there is an adequate supply of sediment in the nearshore zone), are in most cases associated with the transport of a variety of grain size ranging from silt to boulders. Unlike storm surges individual tsunami waves reach a point of zero water velocity prior to backwash flow. At this point, large volumes of sediment may be deposited out of the water column onto the ground surface. Young and Bryant (1992) have made reference to isolated boulders in tsunami deposits in Southeast Australia. In that area, thicknesses of massive sands and silts include occasional isolated boulders, described by Young and Bryant (1992) as "boulder floats".

One of the most awkward problems in reconstructing chronologies of former tsunamis for different areas of the world is how to be able to distinguish tsunami deposits from sediments deposited as a result of hurricane-induced storm surges. For example, in coastal Alabama, USA, a series of hurricanes during historical time have resulted in the deposition of multiple sand layers in low-lying coastal wetlands. While it is accepted that storm surges result in the deposition of discrete sedimentary units, it is argued that tsunamis in contrast to storm surges, generally result in deposition of sediment sheets, often continuous over relatively wide areas and considerable distances inland. For example, sediment sheets in the Algarve, Portugal, associated with the Lisbon earthquake tsunami of 1,755 occur in excess of 1 km inland. In addition, it may be the case that tsunami deposits contain distinctive microfossil assemblages that can be differentiated from those produced by storm surges (Dawson and Shi, 2000).

Tsunamis and submarine slides

Along the coasts of the northern North Sea, Norwegian Sea, and northeastern Atlantic Ocean, a very prominent sand layer, first thought to have been deposited by a storm surge, has more recently been attributed to a large tsunami ca. 7,100 ^{14}C years ago (Figure T53). This event was generated in the Norwegian Sea as a result of the Second Storegga submarine slide. The widespread deposit is now regarded as a marker horizon against which to compare the age of related deposits and with which to more closely define patterns of land uplift.

The detail with which the tsunami is known is impressive. Several studies have examined the sedimentology of the deposit, including its particle size, microfossil content, and even the time of year it occurred. The diatom ecology of the layer has been examined and over 100 ^{14}C dates on biogenic material both within the layer and from adjacent horizons have been obtained.

Geological investigations of these tsunami deposits on the northern and eastern coastlines of Scotland as well as in uplifted lake basins along the west coast of Norway provide evidence of minimum tsunami runup. In eastern Scotland, the minimum value of runup associated with this tsunami is on the order of 4–6 m above contemporary high water mark. However, this value as stated above, should be treated with caution since tsunami flooding to higher elevations may have taken place yet did not leave a sedimentary record. Harbitz (1992) attempted to develop a numerical model of the Second Storegga submarine slide. He noted that the scale of tsunami runup along the Scottish and Norwegian coastlines very much depended upon the average landslide velocity that was used into the model. For example, he noted that an average slide velocity of 20 m/s resulted in runup values onto adjacent coastlines of between 1 and 2 m. By contrast, a modeled landslide velocity of 50 m/s resulted in runup values of between 5 and 14 m, values significantly in excess of the estimates for adjacent coastlines based on geological data. Harbitz (1992) concluded that a landslide velocity of 30 m/s provided the closest

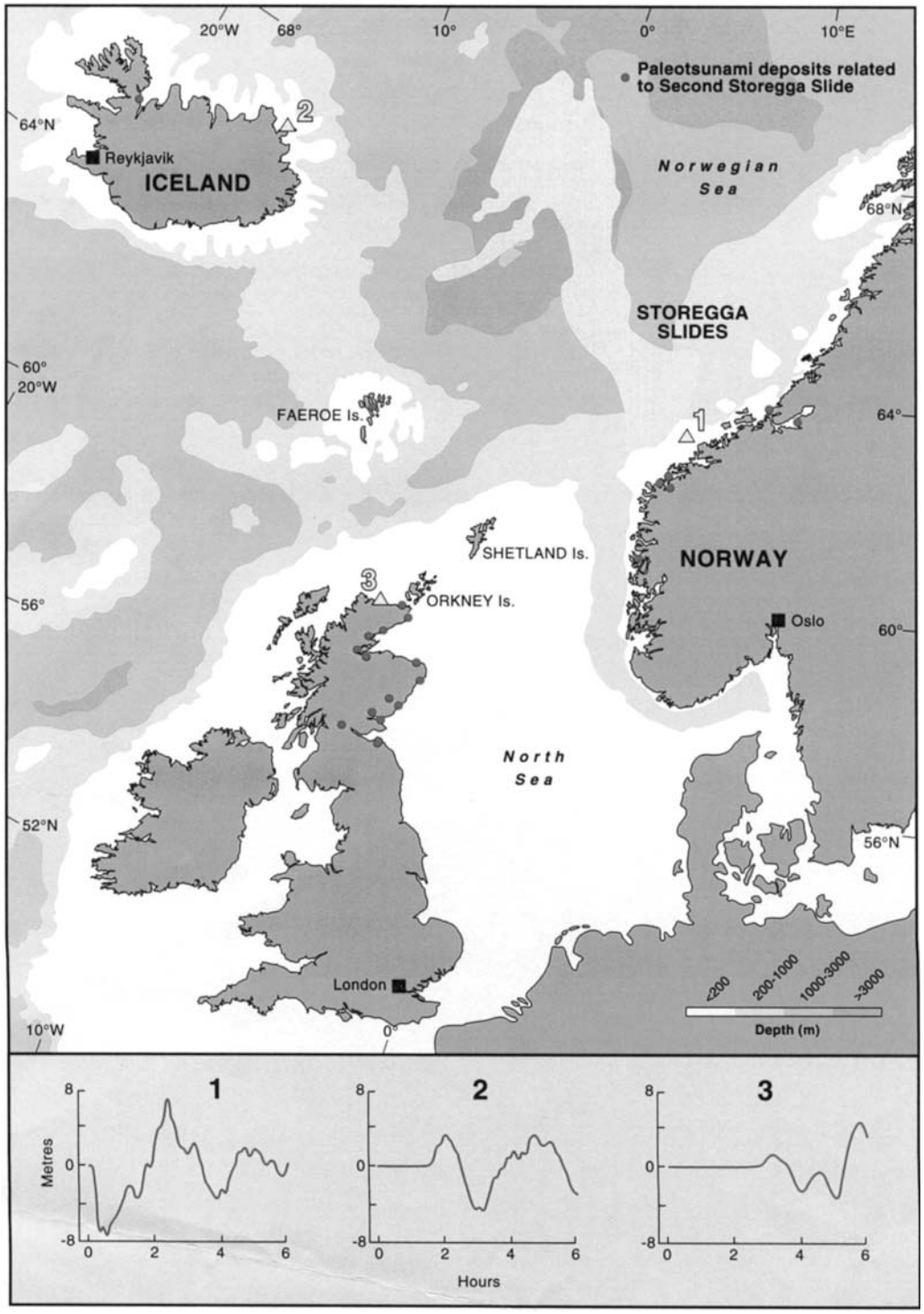

Figure T53 Map of the location of the Second Storegga slide, believed to have generated a tsunami about 7,100 ^{14}C years BP, with sites where the tsunami deposits have been found (see Dawson and Shi, 2000).

approximation to the estimated runup values based on geological data. However, the weakness in this argument is that the geological data only provide minimum estimates of likely flood runup and therefore the related numerical models of the same tsunami will always underestimate the likely average value of the submarine slide velocity.

The occurrence of this tsunami is unusual since it appears to have been generated by one of the worlds largest submarine sediment slides rather than by an earthquake. This serves to demonstrate that severe tsunamis can be generated by submarine slides in aseismic areas where there are considerable thicknesses of unconsolidated sediments on the seafloor.

Giant submarine slides and their potential to generate tsunamis are not restricted to the Norwegian Sea. Recently, Nisbet and Piper (1998) recognized a giant submarine slide occupying the majority of the seafloor of the western Mediterranean. The slide appears to have been generated in deepwater adjacent to western Sardinia and radiometric dates appear to indicate that it took place during the last glaciation of the Northern Hemisphere (probably ca. 20–30,000 years BP). At present, there is no geological evidence that this submarine slide generated a large tsunami. That such a large tsunami took place, however, can hardly be doubted. However, paleoenvironmental reconstruction of this

event appeared to indicate that the slide took place at a time when sea level in the western Mediterranean may have been at ca. −100 m below present and hence any geological record of the tsunami having taken place may lie below present sea level. Submarine slides and offshore earthquakes are not mutually exclusive, however, in their capacity to generate tsunami. For example, recent investigations have shown that the islands of Amorgos and Astipalea in the southern Aegean Sea were subject to severe tsunami flooding caused by an offshore earthquake in 1956 that simultaneously generated a major sediment slump and the two processes together acted to generate complex patterns of tsunami flooding.

Tsunami warning systems

As a result of the severe damage and loss of life caused by tsunamis, attempts have been made to develop warning systems designed to alert the public in advance of the arrival of individual tsunamis. Tsunami warning systems did not exist prior to the Aleutian Trench earthquake and tsunami of April 1, 1946. However, the destruction of the Scotch Cape Lighthouse on Uminak Island and the devastation of Hilo, Hawaii by this tsunami eventually led to vociferous calls for the establishment of a tsunami warning system designed to protect life and property.

The network was developed by the US Coast and Geodetic Survey and has its center of operations on the Island of Oahu, Hawaii. The center, known as the Pacific Tsunami Warning Center (PTWC) became operational in 1948 and was linked to over 30 seismographic stations throughout the Pacific Basin. These provide data on Pacific earthquakes whose magnitude and epicenters make them tsunamigenic (capable of producing tsunamis). When such an earthquake has taken place, the PTWC issues a tsunami watch to all receiving stations. The PTWC is also linked to over 50 tide-gauge stations located throughout the Pacific. Any tsunami that has been generated by an earthquake is automatically recorded in the tide-gauges closest to the epicenter. If a tsunami has been detected then the tsunami watch is upgraded to a tsunami warning. At this stage, the estimated times of arrival of the first waves are computed for all stations across the Pacific. Once the PTWC has issued a tsunami warning and has provided information on the times of arrival of the first waves, it is the responsibility of the local police, military, and civil defense agencies to decide on whether or not particular areas should be evacuated.

The accuracy of PTWC tsunami warnings is well-illustrated by the famous Chilean earthquake and tsunami that took place on May 21, 1960. Once the earthquake epicenter had been calculated and a brief study of local tide-gauge data had been completed, it was estimated that the velocity of the tsunami was 710 km/h and that the tsunami would reach the Hawaiian islands 14 h and 56 min after its generation off the Chilean coast. The prediction was that the first wave would strike Hilo at 9.57 p.m.—it arrived 1 min late.

In areas where the coast is located close to the epicenter of a tsunamigenic earthquake, the time that elapses between the generation of the tsunami and its arrival on the coast is often frighteningly short. For example, the first tsunami waves that struck the Chilean coast on May 21, 1960 arrived only 15 min after the main earthquake shock. Similarly, there was only a relatively short time interval between the March 27, 1964 earthquake in Alaska and the arrival of tsunami waves at the coast. In both cases, loss of life was due to the fact that the tsunamis struck coastlines long before any PTWC warning could be given.

As a result of these two great tragedies, it was realized that it was important to establish regional warning systems for Alaska (the Alaskan Regional Warning System—ARWS) and the Hawaiian Islands. In 1967, a regional center was established in Alaska at Palmer, Anchorage. The center makes use of numerous automated seismographic and tide stations and is capable of issuing tsunami watches and warnings within seconds of a particular earthquake. A regional tsunami warning center for the Hawaiian Islands was later established in 1975.

Tsunami hazards and paleoseismicity

In Europe, due to the much lower frequency of tsunamis there are almost no tsunami warning systems in place. The only one that exists has been built by Portuguese authorities who have installed seismometers and wave recorders west of Portugal with the aim of providing advance warning of any future tsunami similar to that which caused such devastation in AD 1755.

In response to the perceived hazard posed by tsunamis to European coastlines, the European Union funded a major research initiative in 1992 concerned with European tsunami risk. The Project "Genesis and Impact of Tsunamis on European Coasts (GITECs)" completed in 1998, had two principal objectives. The first was to study tsunami generation mechanisms in Europe, for example, those caused by earthquakes and by submarine or coastal landslides. The second objective is to evaluate the tsunami hazard in European seas in order to reduce tsunami risk in Europe. As part of this research effort, a unified catalog of historic and prehistoric European tsunamis has been prepared. In addition, it has proved possible to estimate tsunami frequency for selected coastal regions over long (geological) timescales. In this respect, attempts are also being made to assess tsunami hazard and the likely impact of such tsunamis for particular coastal areas. Detailed investigations have also been made to develop numerical model simulations of major European tsunamis. The project has also attempted to compare the development and implementation of two new European tsunami warning systems.

Summary

In addition to the importance of paleotsunami research in terms of coastal hazard assessment, the calculation of long-term tsunami frequency for particular coastal regions provides valuable data on the past frequency of offshore earthquake activity. In certain parts of the world (e.g., Japan), the historic frequency of offshore earthquakes and tsunamis has been so high that preparedness for future earthquakes and tsunamis is of the highest priority. By contrast, it is now known that while earthquakes have induced minor tsunamis that have struck the Portuguese coastline during the last 3,000 years, there has been only one major earthquake and one tsunami during this period that have been highly destructive. In areas where the past occurrence of tsunamis is extremely rare, a difficult problem is presented to politicians and engineers since many complex decisions have to be made in establishing appropriate coastal defenses for catastrophic marine flooding that may only take place once in several thousand years. This problem becomes more acute in areas where nuclear power plants are located close to present sea level. Sadly for most areas of the world, coastal populations have no protection from tsunamis and rely on chance that none will ever take place.

Alastair Dawson

Bibliography

Borlase, W., 1755. Letter to the Rev Charles Lytteton. *Philosophical Transaction of the Royal Society of London*, **49**: 373–378.

Borlase, W., 1758. *Observations on the Islands of Scilly*. (Reprinted 1966, Frank Graham, Newcastle upon Tyne.)

Dawson, A.G., and Shi, S., 2000. Tsunami deposits. *Pure and Applied Geophysics*, **157**: 875–897.

Harbitz, C.B., 1992. Model simulations of tsunami generated by the Storegga Slides. *Marine Geology*, **105**: 1–21.

Moreira, V.F., 1985. Seismotectonics of Portugal and its adjacent area in the Atlantic. *Tectonophysics*, **117**: 85–96.

Myles, D., 1985. *The Great Waves, Tsunami*. New York: McGraw Hill.

Nisbet, E.G., and Piper, D.J.W., 1998. Giant submarine landslides. *Nature*, **392**: 329–330.

Tinti, S., and Maramai, A., 1996. Catalogue of tsunamis generated in Italy and in Côte d'Azur, France: a step towards a unified catalogue of tsunamis in Europe. *Annali Di Geofisica*, **XXXIX**(6): 1253–1299.

Young, R.W., and Bryant, T., 1992. Catastrophic wave erosion on the southeastern coast of Australia: impact of the Lanai Tsunami ca. 105ka. *Geology*, **20**: 199–202.

Cross-references

Coastal Changes, Rapid
Coastal Sedimentary Facies
Global Vulnerability Analysis
Mass Wasting
Natural Hazards
Seismic Displacement
Storm Surge
Waves